IMMUNOMODULATION OF THE T-HELPER 17 CELL LINEAGE BY MESENCHYMAL STEM CELLS

A thesis submitted to the National University of Ireland in fulfilment of the requirements for the degree of

Doctor of Philosophy

By

Michelle M. Duffy B.Sc.

Immunology and Transplant Biology Group,
Regenerative Medicine Institute,
National Centre for Biomedical Engineering Science,
National University of Ireland, Galway.

Thesis Supervisor: Professor Matthew D. Griffin

September 2012

TABLE OF CONTENTS

ABSTRACT IV

ACKNOWLEDGEMENTS V

DEDICATIONS VI

ABBREVIATIONS VII

LIST OF FIGURES X

LIST OF TABLES XIII

CHAPTER ONE: INTRODUCTION

1.1 T-LYMPHOCYTES: COMMANDING THE ADAPTIVE ARMY 2

1.2 MESENCHYMAL STEM CELLS: KEEPING THE PEACE 13

1.3 CLINICAL RELEVANCE OF MSC THERAPY FOR TH17-MEDIATED DISEASES 21

1.4 VITAMIN D AND THE IMMUNE SYSTEM 27

1.5 AIMS AND HYPOTHESES 32

CHAPTER TWO: MESENCHYMAL STEM CELLS INHIBIT T-HELPER 17 DIFFERENTIATION FROM NAÏVE AND MEMORY $CD4^+$ T-CELL RESPONDERS IN A CELL-TO-CELL CONTACT DEPENDENT MANNER.

2.1 INTRODUCTION 34

2.2 MATERIALS AND METHODS 38

2.3 RESULTS 44

2.4 DISCUSSION 66

CHAPTER THREE: CELL-TO-CELL CONTACT INHIBITION OF T-HELPER 17 CELLS IS MEDIATED THROUGH PROSTAGLANDIN E2 *VIA* THE EP4 RECEPTOR

3.1 INTRODUCTION 73

3.2 MATERIALS AND METHODS 78

3.3 RESULTS 81

3.4 DISCUSSION 101

CHAPTER FOUR: ENHANCED SUPPRESSION OF T-HELPER 17 DIFFERENTIATION BY COMBINING PARICALCITOL AND MSCS

4.1 INTRODUCTION 109

4.2 MATERIALS AND METHODS 114
4.3 RESULTS 116
4.4 DISCUSSION 138

CHAPTER FIVE: *IN-VIVO* EFFECTS OF MSCS AND PARICALCITOL IN OBSTRUCTIVE NEPHROPATHY
5.1 INTRODUCTION 148
5.2 MATERIALS AND METHODS 154
5.3 RESULTS 159
5.4 DISCUSSION 183

CHAPTER SIX: OVERALL DISCUSSION
6.1 THE COMPLEXITY OF MSC- AND PARICALCITOL-MEDIATED EFFECTS ON NAÏVE, MEMORY AND TISSUE-ORIGINATED T-CELLS 189
6.2 DIVERSITY OF MEDIATORS AND MECHANISMS OF ACTION 190
6.3 *IN-VIVO* EFFICACY OF PARICALCITOL AND MSCS 192
6.4 CHALLENGES OF PRE-CLINICAL TO CLINICAL TRANSLATION OF MSCS 193
6.5 CONCLUSIONS 196

APPENDICES
APPENDIX ONE: PUBLICATIONS, PRESENTATIONS AND ACHIEVEMENTS 198
APPENDIX TWO: REAGENTS 201
APPENDIX THREE: ANTIBODY PREPARATIONS 204
APPENDIX FOUR: MEDIA/BUFFER FORMULATIONS 206

REFERENCES 207

ABSTRACT

T-helper 17 (Th17) cells play a pathogenic role in multiple sclerosis, inflammatory bowel disease, psoriasis, acute kidney injury, glomerulonephritis and transplant rejection. Mesenchymal stem cells (MSCs) are immunosuppressive with potential to treat inflammatory and autoimmune disease. Natural and synthetic vitamin D receptor (VDR) agonists also have direct and indirect suppressive effects on T-helper differentiation pathways including Th17. The aim of this thesis was to investigate the effects of MSCs and the VDR agonist paricalcitol alone and in combination on Th17-mediated responses *in vitro* and in a mouse model of obstructive nephropathy, characterized by maladaptive Th17 responses - unilateral ureteral obstruction (UUO).

MSCs potently suppressed naïve-phenotype responders undergoing primary Th17 differentiation but were less inhibitory towards memory-phenotype responders and had the potential to enhance IL-17A production by fully differentiated Th17 cells in the presence of IL-1 and IL-23. MSC-induced primary Th17 inhibition was mediated *via* induction of cyclooxygenase (COX)2 and subsequent prostaglandin E2 (PGE2)/EP4 signaling. This was associated with reduced expression of multiple key intracellular transcription factors including RORγt, IRF4 and Runx1. Paricalcitol-mediated suppression of Th17 differentiation occurred independently of antigen presenting cells and was associated with upregulation of the VDR.

In UUO, MSCs and paricalcitol, alone and in combination suppressed Th17 responses in terms of IL-17A expression and neutrophil recruitment. This was associated with evidence of an alteration in the balance between pro- and anti-inflammatory macrophages in addition to reduced interstitial fibrosis and tubular atrophy.

My results indicate the potential for MSCs to ameliorate tissue damage associated with maladaptive acute or chronic Th17 activation and suggest that adjunctive therapy with VDR agonists may represent a strategy for enhancing the immunosuppressive properties of MSCs.

ACKNOWLEDGEMENTS

First and foremost, to my supervisor Matt, to whom I am very grateful for giving me this fantastic opportunity. Thank you for your never ending support, advice, ideas, encouragement and generosity. Rhodri, thanks for sharing your wealth of knowledge and for being "devil's advocate". Your honesty, advice and critique throughout the years are much appreciated, not to mention the time spent teaching me FACS.

To the original "Griffin's girls" (Shirley, Jana, Michelle H. and Gudrun), thanks for all of your help and friendship. Likewise, to all the members (past and present) of the Griffin and Ceredig groups, you made working in the lab a pleasure. A special word of thanks to Bairbre, Claas and Senthil who never said 'no' and whose help was invaluable, especially in the last few months.

Thanks to my colleagues in REMEDI/NCBES who made this process so much easier. Also, to my collaborators, Cathal and Orina in UCD, the Mahon lab in Maynooth and the Fearnhead lab in NCBES, I am extremely grateful for your expertise. I would also like to thank the funding bodies that supported this thesis including Science Foundation Ireland and Abbott Laboratories.

Beyond science, a sincere thanks to Lasma, Coco, Shirley, Milo and especially Basil for providing escapism and friendship. To the Mayo girls, (Dawn, Claire, Amanda H., Annmarie, Karen, Catherine, Laura, Rachel, Lisa and Amanda Mc.), thank you for not giving up on me despite my serious lack of presence, especially in the last year. Thank you to my Galway friends (Claire, Trish, Amy, Michelle H., Marta, Claas and Lee) for all the fun and games.

Words fail to describe my gratitude to my parents, Mary and Michael, my brother, Aidan, sisters, Rosemary and Siobhán and my grandmother, Molly. Dad, you finally got a doctor in the family. Thank you all for the encouragement and support which allowed me to pursue my dreams.

Dave, I could not have done this without you. I will be forever in debt of your patience and understanding. Your ability to make me laugh even during my meltdowns surpasses me, for that and convincing me to get Basil, I will always love you!

"*Knowledge is in the end based on acknowledgement*" – Ludwig Wittgenstein

Dedicated to my parents
Michael and Mary Duffy.

ABBREVIATIONS

3,3-diaminobenzidine	DAB
Activator protein-1	AP-1
Acute kidney injury	AKI
Adipose tissue-derived MSCs	AT-MSCs
Adjuvant-induced arthritis	AIA
Alpha-smooth muscle actin	α-SMA
Analysis of variance	ANOVA
Antigen presenting cell	APC
Arachidonic acid	AA
Aryl hydrocarbon receptor	AhR
Autoimmune myasthenia gravis	AMG
Avidin-biotin complex	ABC
Becton Dickinson	BD
Blood urea nitrogen	BUN
Bone marrow	BM
Bovine serum albumin	BSA
Broncho alveolar lavage fluid	BALF
C57BL/6	B6
cAMP response element-binding	CREB
CCAAT/enhancer binding protein	C/EBP
C-C motif ligand	CCL
C-C motif receptor	CCR
C/EBP homologous protein	CHOP
c-Jun N-terminal kinase	JNK
C-X-C motif ligand	CXCL
Carboxyfluorescein diacetate succinimidyl ester	CFSE
Central nervous system	CNS
Chromatin immunoprecipitation	ChIP
Chronic kidney disease	CKD
Cluster of differentiation	CD
Collagen-induced arthritis	CIA
Complementary DNA	cDNA
Complete expansion media	CEM
Complete isolation media	CIM
Cyclic adenosine monophosphate	cAMP
Cyclooxygenase	COX
Cyclosporine A	CsA
Cytotoxic T lymphocytes	CTL
Delayed-type hypersensitivity	DTH
Dendritic cell	DC
Dextran sodium sulfate	DSS
Dimethyl sulfoxide	DMSO
Dinitrofluorobenzene	DNFB
Dulbecco’s modified Eagle’s medium	DMEM
Dulbecco’s phosphate buffered saline	D-PBS
Enzyme-linked immunosorbent assay	ELISA
Epithelial to mesenchymal transition	EMT

Experimental allergic encephalomyelitis	EAE
Experimental autoimmune prostatitis	EAP
Experimental autoimmune uveitis	EAU
Extracellular matrix	ECM
Extracellular signal-regulated kinase	ERK
Fluorescence-activated cell sorting	FACS
Fluorescence minus one	FMO
Forkhead box p3	FOXP3
Gastrointestinal	GI
GATA binding protein 3	GATA3
Gauge	G
Graft-versus-host disease	GvHD
Graft-versus-leukemia	GvL
Granulocyte-macrophage colony-stimulating factor	GM-CSF
Growth-regulated-alpha	GRO-α
Hematopoietic stem cell	HSC
Hematoxylin and eosin	H & E
Hepatocyte growth factor	HGF
Horseradish peroxidase	HRP
Human leukocyte antigen G	HLA-G
Immunoglobulin	Ig
Immunohistochemistry	IHC
Indoleamine-2,3-dioxygenase	IDO
Induced T regulatory cell	iT_{reg}
Interferon gamma	IFN-γ
Interferon regulatory factor 4	IRF4
Interleukin	IL
Interphotoreceptor retinoid-binding protein	IRBP
Intracellular adhesion molecule 1	ICAM-1
Intraperitoneal	IP
Intravenous	IV
Iscove's modified Dulbecco's medium	IMDM
Janus kinase	Jak
Knock-out	KO
Lipolysaccharide	LPS
L-NG-nitroarginine methyl ester	L-NAME
Lymph nodes	LN
Macrophage inflammatory protein 1-alpha	MIP-1α
Major histocompatibility complex	MHC
Matrix metalloproteinase	MMP
Mesenchymal stem cell	MSC
Milliliters	ml
Mitogen-activated protein kinase	MAPK
Monocyte chemotactic protein 1	MCP-1
Myelin-oligodendrocyte glycoprotein	MOG
Myxovirus resistance-1	Mx1
National Institutes of Health	NIH
Natural killer cell	NK
Naturally occurring T regulatory cell	nT_{reg}
NF-kappa B activator 1	ACT1

Nitric oxide	NO
Nitric oxide synthase	NOS
Non-obese diabetic	NOD
Non-obese diabetic – severe combined immune deficiency	NOD-SCID
Non steroidal anti-inflammatory drugs	NSAIDS
Nuclear factor kappa-light-chain-enhancer of activated B cells	NF-κB
Nuclear factor of activated T-cells	NFAT
One-way analysis of variance	ANOVA
Ovalbumin	OVA
Passage	P
Periodic Acid-Schiff	PAS
Peripheral blood mononuclear cell	PBMC
Phosphatidylinositol 3 kinase	PI3K
Phytohaemagglutinin	PHA
Platelet-derived growth factor receptor alpha	PDGFRα
Platelet endothelial cell adhesion molecule	PECAM
Programmed death ligand 1	PD-L1
Prostaglandin	PG
Prostaglandin E2	PGE2
Protein kinase A	PKA
Quantitative real time polymerase chain reaction	qRT-PCR
RAR-related orphan receptor	ROR
Regenerative Medicine Institute	REMEDI
Regulated upon activation, normal T-cell expressed and secreted	RANTES
Relative centrifugal force	RCF
Renin-angiotensin system	RAS
Retinoic acid receptor	RAR
Retinoid X receptor	RXR
Runt-related transcription factor 1	Runx1
Signal transducer and activator of transcription	STAT
Sma and Mad related protein	SMAD
Stem cell antigen-1	Sca-1
T-box 21	T-bet
T-cell receptor	TCR
Terminal deoxynucleotidyl transferase dUTP nick end labeling	TUNEL
Tetramethylbenzidine	TMB
T-helper 1 cells	Th1
T-helper 2 cells	Th2
T-helper 17 cells	Th17
T-lymphocytes	T-cells
TNF-alpha-induced protein 6	TSG-6
Transforming growth factor-beta	TGF-β
T regulatory cell	T_{reg}
Trinitrobenzene sulfonate	TNBS
Tumor necrosis factor alpha	TNF-α
Unilateral ureteral obstruction	UUO
United States	US
Vitamin D receptor	VDR
Vitamin D response element	VDRE
Wild type	WT

LIST OF FIGURES

Figure 1.1 A) T-cell development in the thymus **B)** Activation of a naïve $CD4^+$ T-cell by an APC.
Figure 1.2 The four primary $CD4^+$ T-cell subsets.
Figure 1.3 Transcription of Th17-related cytokines and transcription factors.
Figure 1.4 Effector functions of Th17 cells.
Figure 1.5 Putative mechanisms of renoprotection elicited by MSCs include transdifferentiation and production of pro-angiogenic, anti-fibrotic, anti-apoptotic and anti-inflammatory mediators.
Figure 1.6 Synthesis of metabolically active calcitriol by liver and kidney tissues or by cells of the immune system.
Figure 1.7 Summary of the immunomodulatory effects of calcitriol on the immune system.

Figure 2.1 Differentiation potential and cell surface profile of B6 BM-derived MSCs.
Figure 2.2 Inhibition of Th17 differentiation by MSCs.
Figure 2.3 IFN-γ does not enhance MSC-mediated suppression of Th17 cells.
Figure 2.4 MSC-specific inhibition of Th17 differentiation is not strain-specific.
Figure 2.5 Inhibition of Th17 cells by MSCs is limited in the absence of cell–cell contact.
Figure 2.6 Representative gating strategy for FACS experiments in which $CD4^+CD25^-CD62L^+$ naïve and $CD4^+CD25^-CD62L^-$ memory T-cells were sorted prior to co-culture with MSC.
Figure 2.7 MSCs inhibit both naïve- and memory-phenotype responders.
Figure 2.8 Cytokine and chemokine analysis.
Figure 2.9 MSC inhibition of Th17 differentiation in relation to T-cell division.
Figure 2.10 MSC-specific inhibition of Th17 differentiation.
Figure 2.11 MSC inhibition of Th17 differentiation is not dependent on APCs.
Figure 2.12 Representative gating strategy for FACS experiments in which highly purified $CD4^+CD25^-CD62L^-$ memory T-cells were sorted into $CCR6^+$ cells or $CCR6^-$ cells.
Figure 2.13 MSCs do not suppress cytokine production by highly purified $CCR6^+$ memory T-cells.
Figure 2.14 MSCs do not suppress IL-1- or IL-23-mediated enhancement of IL-17A.
Figure 2.15 MSCs have varying degrees of suppression and in some cases enhancement on Th17 cells dependent upon the state of T-cell activation and differentiation, MSC-derived mediators and soluble MSC-licensing cues in the microenvironment.

Figure 3.1 Prostaglandin production *via* COX enzymes or the alternative arachidonic acid metabolism pathway – lipoxygenase pathway.
Figure 3.2 MSC suppression of Th17 cells is COX-dependent.
Figure 3.3 Suppression of primary Th17 differentiation by MSCs is induced by cell-cell contact *via* a COX-dependent soluble factor.
Figure 3.4 Representative gating and sorting strategy and post-sort purity analysis for FACS purification of MSCs and $CD45^+$ splenocytes from individual cultures and co-cultures. FMO controls for CD45 staining of splenocytes and MSCs are shown in the bottom right panel.

Figure 3.5 COX2 is specifically upregulated in MSCs following co-culture with $CD4^+$ T-cells undergoing primary Th17 differentiation.
Figure 3.6 Reversal of MSC-mediated suppression of Th17 differentiation by selective COX2 inhibition.
Figure 3.7 PGE2 is induced in MSC/Th17 co-cultures upon cell-cell contact.
Figure 3.8 Dose-dependent suppression of primary Th17 differentiation by synthetic PGE2.
Figure 3.9 Selective reversal of MSC-mediated Th17 suppression by EP4 antagonism.
Figure 3.10 Selective EP4 agonist-mediated suppression of primary Th17 differentiation.
Figure 3.11 Outline of experiment in which Th17 cells/APCs and MSCs were separated to high purity from 18-hour co-cultures or relevant control cultures and were then re-cultured for an additional 18 hours for the purpose of analyzing PGE2 production and Th17-suppressive effects of conditioned medium from the individual cell populations.
Figure 3.12 PGE2-enriched conditioned MSC media suppresses Th17 development.
Figure 3.13 MSC-mediated inhibition of *in-vivo* derived Th17 cells.
Figure 3.14 Surface phenotype modifications of MSCs following co-culture with $CD4^+$ T-cells.
Figure 3.15 (**A**) $CD4^+$ T-cells cultured under Th17-skewed conditions in the presence of anti-CD3/anti-CD28 beads or APCs led to the production of IL-17A-producing Th17 cells. (**B**) Addition of MSCs to these cultures led to the generation of Th17 cells with suppressed CD25 expression and IL-17A production due to the induction of COX2 by MSCs following cell-cell contact with activated $CD4^+$ T-cells and subsequent PGE2 production. PGE2 engagement with the EP4 receptor led to Th17 inhibition. (**C**) Blockade of COX2 or the EP4 receptor reversed the suppressive effect of MSCs.

Figure 4.1 Dose-dependent IL-17A inhibition by paricalcitol.
Figure 4.2 Paricalcitol augments MSC-mediated inhibition of Th17 cells.
Figure 4.3 APCs are unnecessary for paricalcitol-mediated inhibition of Th17 cells.
Figure 4.4 Paricalcitol additively suppresses MSC-induced IL-17A inhibition by naïve and memory T-cells.
Figure 4.5 Paricalcitol does not inhibit *in-vivo*-derived Th17 cells.
Figure 4.6 Paricalcitol does not prevent MSC-mediated enhancement of IL-17A production in the presence of IL-1α and IL-23.
Figure 4.7 Indomethacin does not reverse paricalcitol-mediated inhibition of primary Th17 differentiation.
Figure 4.8 Paricalcitol-mediated inhibition of primary Th17 differentiation does not require COX 2 signaling.
Figure 4.9 Paricalcitol-mediated inhibition of primary Th17 differentiation does not require EP4 activation.
Figure 4.10 Paricalcitol induces upregulation of VDR.
Figure 4.11 Paricalcitol and MSCs do not target STAT3 signaling.
Figure 4.12 MSCs target the key Th17-associated transcription factor, RORγt.
Figure 4.13 Paricalcitol does not affect IRF4 or Runx1 expression.
Figure 4.14 Neither MSCs nor paricalcitol induce FOXP3 expression.

Figure 5.1 Composition of the kidney.
Figure 5.2 Pathological changes and cellular interactions between resident renal cells and infiltrating immune cells following UUO.
Figure 5.3 (A) Schematic highlighting the timeline of UUO, administration of immune modulating agents and termination of study with organ harvest. **(B)** Study design showing number of animals per group and treatment regime.
Figure 5.4 (A) Representative gating strategies of T-cell populations in control and obstructed kidneys following UUO and **(B)** representative examples of dot plots for $CD45^+$, TCR-β^+, $CD4^+$, $CD8^+$ and $CCR6^+$ populations in obstructed kidneys for each of the treatment groups.
Figure 5.5 Flow cytometric analysis of T-cell populations following UUO.
Figure 5.6 $CD3^+$ cell accumulation in the kidney following UUO.
Figure 5.7 IL-17A and FOXP3 expression following UUO.
Figure 5.8 IL-17A- and IFN-γ-producing T-cell accumulation in the kidney following UUO.
Figure 5.9 (A) Representative gating strategies of myeloid cell populations in control and obstructed kidneys following UUO and **(B)** representative examples of dot plots for $CD11b^+$ myeloid cells, $Ly6G^+$ neutrophils, $CD11c^+$ DCs, $Ly6C^+$ inflammatory monocytes and $Ly6G^-$ macrophage populations in obstructed kidneys for each of the treatment groups.
Figure 5.10 Flow cytometric analysis of myeloid populations following UUO.
Figure 5.11 Cellular infiltrate following UUO.
Figure 5.12 Dilation and atrophy of tubules following UUO.
Figure 5.13 Interstitial fibrosis following UUO.
Figure 5.14 Total histological scores following UUO.

LIST OF TABLES

Table 1.1 Summary of recent reports in which MSCs had immunomodulatory effects on Th1-mediated diseases.
Table 1.2 Summary of recent reports in which MSCs had immunomodulatory effects on Th2-mediated diseases.
Table 1.3 Summary of recent reports in which MSCs had immunomodulatory effects on T_{reg} cells *in-vivo.*
Table 1.4 Summary of current clinical trials employing MSC intervention for inflammatory bowel disease.
Table 1.5 Summary of multiple sclerosis-related clinical trials, in which the therapeutic potential of MSCs are currently being evaluated.
Table 1.6 Summary of current clinical trials employing MSC intervention for rheumatoid arthritis.
Table 1.7 Summary of clinical trials for the treatment of inflammatory kidney diseases in which the therapeutic potential of MSCs are currently being evaluated.
Table 1.8 Clinical trials employing vitamin D supplementation in diseases associated with the Th17 phenotype.

Table 2.1 Concentrations of cells and Th17-inducing factors employed in Th17 differentiation cultures.

Table 3.1 List of neutralization antibodies, blocking reagents, antagonists and agonists and the concentration of each employed in this study.

Table 4.1 Bradford protein detection assay set-up.
Table 4.2 Resolving/separating gel composition.
Table 4.3 Western Blot antibody preparations.
Table 4.4 Effects of VDR agonists on Th17-associated factors during primary Th17 differentiation *in-vitro.*
Table 4.5 Effects of MSCs or PGE2 on Th17-associated factors during primary Th17 differentiation *in-vitro.*

Table 5.1 IHC antibody preparation.
Table 5.2 Summary of *in-vivo* results.

CHAPTER ONE

INTRODUCTION

1.1 T-LYMPHOCYTES: COMMANDING THE ADAPTIVE ARMY

Adaptive immunity is unique to the individual and arises as our bodies adapt to exposure to specific pathogens. Such adaptation confers evolutionary advantage in the shape of immunological memory and exquisite specificity (Janeway, 2008). T lymphocytes (T-cells) are the primary cellular effectors of the adaptive immune system and their functional properties are central to antigen specificity and memory (Wan and Flavell, 2009).

1.1.1 T-CELL DEVELOPMENT, ACTIVATION AND DIFFERENTIATION

T -cells originate from the bone marrow (BM) from where their precursors migrate to the thymus to develop. Gene rearrangement of the T-cell receptor (TCR) leads to the generation of three T-cell lineages, natural killer (NK) T-cells, γ:δ T-cells and α:β T-cells (**Figure 1.1A)** (Janeway, 2008). Positive selection within the α:β lineage leads to the maturation of double positive T-cells into single positive cluster of differentiation (CD)4 or CD8 major histocompatibility complex (MHC)-restricted T-cells. Negative selection removes T-cells that are self-reactive. Upon maturation these naïve T-cells circulate in the bloodstream through the peripheral lymphoid organs until they encounter their corresponding antigen (Janeway, 2008). Activation and subsequent differentiation of T-cells is governed by the stimulus, the type of antigen presenting cell (APC) and the specific cytokine milieu present (Hermann-Kleiter and Baier, 2010). In addition to TCR and CD4 or CD8 co-receptor signaling with a specific antigen-MHC **(Figure 1.1B)**, full activation requires co-stimulatory signals (Hermann-Kleiter and Baier, 2010, Wan and Flavell, 2009). Constitutively expressed CD28 binds to B7-1 (CD80) and B7-2 (CD86) on the APC. This induces activation of multiple signaling pathways including nuclear factor of activated T-cells (NFAT), nuclear factor kappa-light-chain-enhancer of activated B cells (NF-κB) and activator protein-1 (AP-1). Subsequently, interleukin (IL)-2 production and CD25 (IL-2Rα) expression is induced (Hermann-Kleiter and Baier, 2010). The β and γ chains of the IL-2R are constitutively expressed by T -cells in a resting state which ligates IL-2 if present in high concentrations with low affinity. Activated T-cells express all three chains and thus bind IL-2 with very high affinity even at very low concentrations (Janeway, 2008). Engagement of IL-2 with the IL-2R activates signal transducer and

activator of transcription (STAT)5, encouraging entry into the cell cycle and thus clonal expansion (Hermann-Kleiter and Baier, 2010).

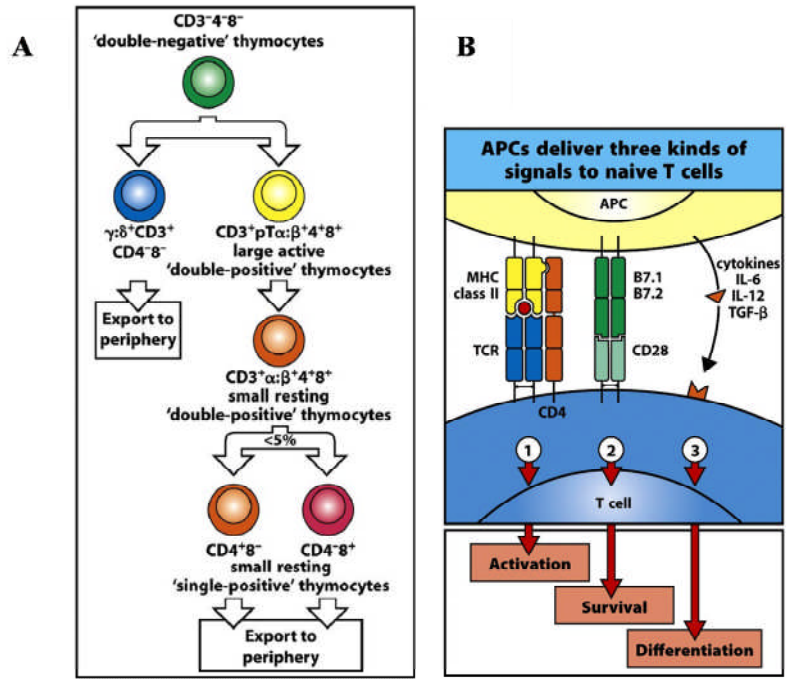

Figure 1.1 A) T-cell development in the thymus **B)** Activation of a naïve $CD4^+$ T-cell by an APC (Adapted from: Janeway's Immunobiology 7th Edition).

The range of T-cell subsets may be defined by the acquisition of characteristic cytokine secretion profiles (T-helper cells), cytolytic mechanisms (cytotoxic T lymphocytes (CTL)), or counter regulatory properties (T regulatory cells (T_{reg})) (Wan and Flavell, 2009). $CD4^+$ T-helper cells are of critical importance as they coordinate the activity of the immune response by recruiting and regulating various other immune responders. **Figure 1.2** illustrates the four main T-helper phenotypes each distinguishable by differentiation factors, transcription factors, cytokine secretion profiles and effector functions.

Small proportions of activated T-cells persist as memory cells and may retain the effector phenotype imprinted upon them during primary activation (Kaech et al., 2002, Wan and Flavell, 2009). These memory cells have the capacity to respond more rapidly and potently to secondary encounters with the same antigen without the need for co-stimulation (Kaech et al., 2002, Janeway, 2008). When these memory cells are appropriately coordinated and regulated, the diversity of T-cell effector phenotypes allows immune protection against a multitude of pathogenic microorganisms while

maintaining self-tolerance and homeostasis (Wan and Flavell, 2009). On the other hand, over exuberant pro-inflammatory T-cell responses may lead to autoimmune and allergic diseases, including multiple sclerosis, inflammatory bowel disease, type 1 diabetes mellitus, and asthma (Bai et al., 2009, Karlsson et al., 2008, Kavanagh and Mahon, 2010, Gonzalez et al., 2009). Furthermore, life-saving treatments such as allogeneic BM and solid organ transplantation may be complicated by alloantigen-specific T-cell immune responses, resulting in graft-versus-host disease (GvHD) or transplant rejection.

1.1.2 T-HELPER PHENOTYPES

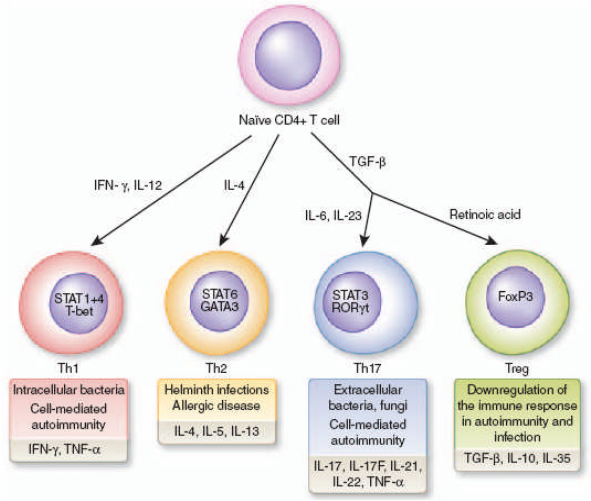

Figure 1.2 The four primary $CD4^+$ T-cell subsets (From: Turner et al., 2010).

T-HELPER 1 CELLS

In 1989 Mosmann and Coffman described two subsets of T-helper cells based on their cytokine secretion profiles, T-helper 1 (Th1) and T-helper 2 (Th2) (Mosmann and Coffman, 1989). Th1 cells secrete interferon (IFN)-γ and tumor necrosis factor (TNF)-α. Th1 induction requires the presence of IL-12 and IFN-γ (Hermann-Kleiter and Baier, 2010). IL-12 is synthesized primarily by dendritic cells (DCs) as well as monocytes and macrophages while IFN-γ is produced by already differentiated Th1 cells in addition to NK cells and NKT cells (Hermann-Kleiter and Baier, 2010). TCR-induced transcription factors (NF-κB, AP-1 and NFAT) along with STAT1 which is activated by IFN-γ, induce the expression of the transcription factor T-box 21 (T-bet) (Hermann-Kleiter and Baier, 2010). Known effector functions of Th1 cells include

activation and recruitment of macrophages to sites of inflammation and induction of immunoglobulin (Ig)G2a production by B-cells (Wan and Flavell, 2009). Th1 cells are responsible for the clearance of intracellular pathogens and delayed-type hypersensitivity (DTH) reactions by amplifying cellular immunity (Hermann-Kleiter and Baier, 2010). Delayed-type hypersensitivity reactions are mediated by both Th1 cells and CTLs (Lim et al., 2010), and, through their role as coordinators of this form of immune response, Th1 cells have the capacity to cause maladaptive tissue damage. Th1-mediated inflammatory and autoimmune diseases include type 1 diabetes mellitus and Crohn's disease (Gonzalez et al., 2009).

T-HELPER 2 CELLS

Th2 cells produce the cytokines IL-4, IL-5, IL-9, IL-10, and IL-13 (Wan and Flavell, 2009, Hermann-Kleiter and Baier, 2010). Th2 differentiation occurs in the presence of notch ligands and IL-4. Interleukin-4 is produced by differentiated Th2 cells in addition to mast cells, basophils, eosinophils and NKT cells (Hermann-Kleiter and Baier, 2010, Janeway, 2008). Ligation of the IL-4R by IL-4 activates STAT6 and its downstream target, the transcription factor GATA binding protein 3 (GATA3) (Hermann-Kleiter and Baier, 2010). The role of Th2 cells in adaptive immunity is linked to host defense against extracellular parasites, antibody class switching to IgG1 and IgE in B cells, and recruitment of eosinophils (Coffman, 2010, Hermann-Kleiter and Baier, 2010, Wan and Flavell, 2009). Dysregulated Th2 cell responses are associated with allergic diseases such as asthma (Kavanagh and Mahon, 2010).

REGULATORY T CELLS

A subset of $CD4^+$ T-cells has also been identified as having regulatory (suppressor) functions that are essential for the prevention of autoimmunity and the resolution of inflammatory processes. T_{regs} are best characterized by surface expression of CD25 and, more specifically, by intracellular expression of the transcription factor forkhead box p3 (FOXP3). They can be further subdivided into naturally occurring T_{reg} (nT_{reg}) that develop in the thymus or induced T_{reg} (iT_{reg}) that differentiate from naïve peripheral $CD4^+$ T-cells in the presence of transforming growth factor (TGF)-β1 (Wan and Flavell, 2009). TGF-β1 is an abundant cytokine produced by DCs and epithelial cells in the absence of infection and thus favours the induction of T_{regs} while the environment is free from pro-inflammatory cytokines (Janeway, 2008). T_{regs} may

negatively regulate the activation of each of the major T-helper cell subtypes as well as other immune and inflammatory cells (Wan and Flavell, 2009).

1.1.3 T-HELPER 17 CELLS

The work described in this thesis relates to a fourth subset of T-helper cells. The description of this additional subset, termed T-helper 17 (Th17) cells, has added further complexity to our understanding of cellular adaptive immunity. Th17 cells are distinguished by production of the characteristic cytokine IL-17A. Despite the cloning of IL-17A in 1993 (Rouvier et al., 1993), Th17 cells were not described until a decade later most notably by the Cua Laboratory. Murphy et al. described a pro-inflammatory role for the IL-12 family cytokine IL-23 in collagen-induced arthritis (CIA) (Murphy et al., 2003). IL-23 shares a common p40 subunit with IL-12 however they differ by p19 and p35 subunits respectively. IL-23p19 knock-out (KO) mice displayed reduced Th17 responses while maintaining Th1 responses. These mice did not develop CIA or experimental autoimmune encephalomyelitis (EAE) (Murphy et al., 2003, Cua et al., 2003, Langrish et al., 2005).

TH17 DIFFERENTIATION

Th17 differentiation is dependent on a wide variety of cytokines, transcription factors and signaling pathways. TGF-β1, IL-6, IL-23 and IL-1 are critical players in the induction and expansion of mouse Th17 cells from naïve $CD4^+$ precursors (Wan and Flavell, 2009).

Signaling of TGF-β1 *via* a heteromeric TGF-βR1/TGF-βR2 complex leads to the activation of Sma and Mad related protein (SMAD)2 and SMAD3 with subsequent dimerization with SMAD4. This complex binds to SMAD-binding elements in target genes however the exact mechanism whereby TGF-β1 signaling induces Th17 differentiation remains unclear (Hwang, 2010). TGF-β1 may suppress the expression of T-bet and GATA3 in Th1 and Th2 cells respectively thus playing an indirect role in Th17 development (Hirahara et al., 2010). Lu et al. demonstrated that pharmacological inhibition of TGF-βR2 in the presence of exogenous IL-6 and TGF-β1 prevented the development of Th17 cells from naïve $CD4^+$ precursors while promoting the induction of Th1 cells. These findings were independent of SMAD2 or SMAD3 (Lu et al., 2010). Extracellular signal-regulated kinase (ERK), p38 and c-Jun

N-terminal kinase (JNK) signaling pathways are mitogen-activated protein kinase (MAPK) members associated with mediating alternative non-SMAD responses to TGF-β. Indeed inhibition of p38 and JNK suppressed Th17 development highlighting the importance of SMAD-independent TGF-β1 signaling pathways notably MAPK signaling in Th17 development (Lu et al., 2010). ERK1/2 on the other hand has been shown to negatively regulate Th17 differentiation (Tan and Lam, 2010).

IL-6 is produced by multiple cell types including endothelial cells, fibroblasts, mast cells, B-cells, monocytes, macrophages and DCs. Engagement of IL-6 with the IL-6R activates Janus kinase (Jak)1 and Jak2 leading to phosphorylation of the IL-6R and recruitment of STAT3 to the receptor complex (O'Shea et al., 2009). Interferon regulatory factor 4 (IRF4) together with STAT3 phosphorylation leads to the activation of the downstream master regulator of the Th17 subset, retinoic acid receptor (RAR)-related orphan receptor (ROR)γt (Hermann-Kleiter and Baier, 2010). RORγt is a member of the nuclear hormone receptor family and is encoded by the *RORC* gene (Ivanov et al., 2007). RORγt, in addition to various other transcription factors and co-activators, binds to the IL-17 promoter region to induce its transcription while suppressing FOXP3 expression (Hermann-Kleiter and Baier, 2010). RORα may synergize with RORγt to augment Th17 differentiation (O'Shea et al., 2009). Th17 cells also express the aryl hydrocarbon receptor (AhR) and mice that lack AhR are resistant to EAE. Additionally, mice that lack IRF4 are resistant to EAE (O'Shea et al., 2009). **Figure 1.3** illustrates the plethora of transcription factors and transactivators known to be associated with transcription of Th17-related cytokines and transcription factors. Certain transcription factors may also silence the actions of competing regulators. An example of this is T-bet. This Th1 inducing-transcription factor binds to runt-related transcription factor 1 (Runx1) in unprimed T-helper cells preventing it from transactivating RORγt and thus suppressing Th17 differentiation (Lazarevic et al., 2011).

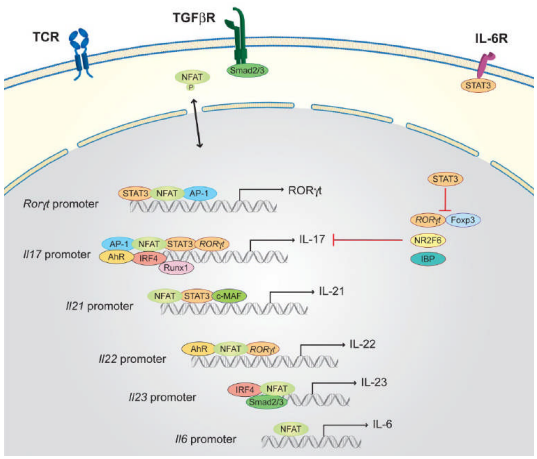

Figure 1.3 Transcription of Th17-related cytokines and transcription factors (From: Hermann-Kleiter and Baier, 2010).

IL-23 is produced by DCs and macrophages. It is a member of the IL-6 superfamily. It contains two subunits p40 shared by IL-12 and a unique p19 subunit. Similarly the IL-23R shares a common IL-12Rβ1 chain with the IL-12R and a unique IL-23R chain. IL-23 signaling involves STAT3 activation. The IL-23R is expressed by DCs, macrophages, NKT cells and memory T-cells (Paust et al., 2009). Naïve T-helper cells express little or no IL-23R thus IL-23 is not necessary for the differentiation of Th17 cells rather is required for expansion and maintenance of Th17 cells *in-vivo*. Following infection with various strains of fungi, IL-23p19 KO mice displayed limited Th17 responses associated with reduced fungal clearance (Espinosa and Rivera, 2012). Additionally, IL-23p19 KO mice were protected from CIA while IL-12p35 KO mice had exacerbated severity (Murphy et al., 2003).

IL-1α and IL-1β are proinflammatory cytokines in the IL-1 superfamily. The eleven member family also contains a naturally occurring antagonist IL-1RA, IL-18 and IL-33. Both IL-1α and IL-1β have been shown to augment IL-23-induced IL-17 production from $CD4^+$ T-cells. Similarly IL-1RI KO mice had lower incidence of EAE than wild type (WT) mice (Sutton et al., 2006). Chung et al. demonstrated a critical role for IL-1 in early Th17 differentiation, in induction of Th17-mediated EAE and, in maintenance of the Th17 phenotype (Chung et al., 2009). Furthermore, renal DC- and monocyte-derived IL-1 enhances Th17 activation in a mouse model of obstructive nephropathy (Pindjakova et al., 2012).

Early studies of human-derived Th17 cells suggested phenotypic discrepancies between Th17 cells originating from human and mouse. A number of key differences were noted. Human Th17 cells co-expressed RORC (ortholog of RORγt) and T-bet in addition to IL-17A and IFN-γ. Subset plasticity has only recently been described for mouse Th17 cells with multiple laboratories now reporting shifts from Th17 to T_{reg} or Th1 phenotypes (Annunziato and Romagnani, 2011, Esplugues et al., 2011). Another source of controversy is TGF-β1 which is dispensable for human Th17 differentiation. Early studies in mouse described TGF-β1 as a critical co-factor along with IL-6 for Th17 differentiation while IL-23 and/or IL-1 amplified Th17 responses. Refined probing in the mouse system by Chung et al. revealed IL-17A- and IL-17F-producing Th17 cells that differentiate in the presence of IL-6 with high concentrations of TGF-β1. In keeping with human Th17 cells, the combination of IL-6, IL-1 and IL-23 in the absence of high concentrations of TGF-β1, can also induce mouse Th17 cells that produce comparable levels of IL-17A and IL-17F to the IL-6/TGF-β1 induction system but with large quantities of IL-22 (Chung et al., 2009). The functional relevance of these two distinct mouse Th17 phenotypes remains to be defined. Moreover, studies of human Th17 differentiation in serum-free conditions have indicated that low concentrations of TGF-β1 play a role (Mills, 2008).

EFFECTOR FUNCTIONS OF TH17 CELLS

The Th17 effector phenotype is defined by preferential secretion of IL-17A along with other cytokines and chemokines, including IL-17F, IL-21, IL-22, TNF-α and C-C motif ligand (CCL)20 (Turner et al., 2010a, O'Connor et al., 2010). In addition to IL-17A the IL-17 family also includes IL-17B, IL-17C, IL-17D, IL-17E (IL-25) and IL-17F. These cytokines exert their actions as homodimers (Kolls and Linden, 2004) while IL-17A and IL-17F may also form heterodimers (Gaffen, 2009). The IL-17 family also contains 5 receptors IL-17RA, IL-17RB, IL-17RC, IL-17RD and IL-17RE.

IL-17A signals *via* a heteromeric IL-17RA-IL-17RC complex (Turner et al., 2010a) and exerts its actions by engaging the NF-κB activator 1 (ACT1) adaptor. Pathways that become activated include NF-κB, MAPK and CCAAT/enhancer binding protein (C/EBP) (Gaffen, 2009). IL-17A stimulates epithelial cells and fibroblasts to produce

the chemokines IL-8, C-X-C motif ligand (CXCL)1, CXCL2, CCL2, CCL3, and CCL20 which lead to the recruitment of neutrophils, monocytes and Th1 cells (Turner et al., 2010a, Ouyang et al., 2008). Stimulation of granulocyte-macrophage colony-stimulating factor (GM-CSF) and G-CSF production locally by IL-17A activates and expands the recruited cells while IL-6 and prostaglandin E2 (PGE2) contribute to the inflammatory environment (Aggarwal and Gurney, 2002). IL-17A induces macrophage production of pro-inflammatory TNF-α and IL-1β (Kitching and Holdsworth, 2011). IL-17A is also produced by $CD8^+$ T-cells, γ:δ T-cells, NK cells and NKT cells (O'Connor et al., 2010).

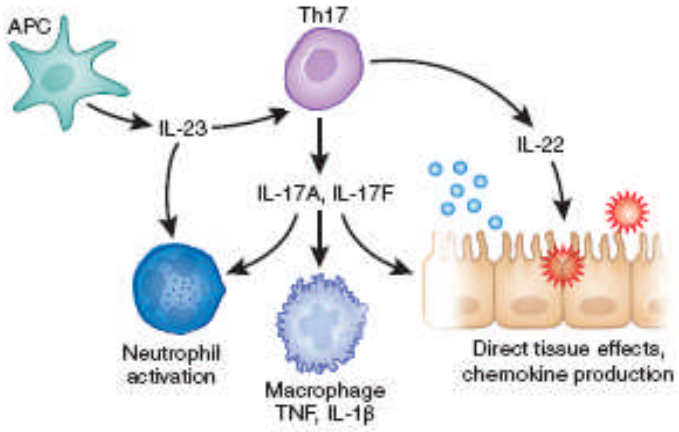

Figure 1.4 Effector functions of Th17 cells (From: Kitching and Holdsworth, 2011).

Th17 cells express CD146 and C-C motif receptor (CCR)6 for trafficking (Kitching and Holdsworth, 2011, O'Connor et al., 2010, Flanagan et al., 2012). CD146 is expressed by both mouse and human Th17 cells and has been shown to be responsible for Th17 infiltration into the central nervous system (CNS) in EAE *via* the ligand, laminin-411. Blockade of CD146 inhibited Th17 infiltration and ameliorated EAE (Flanagan et al., 2012).The CCR6/CCL20 axis is also involved in limiting Th17 responses. Following TCR stimulation, Th17 cells generated in the periphery are recruited to the duodenum (Esplugues et al., 2011). Intestinal epithelial cells up-regulate CCL20 in response to IL-17 signaling and thus recruit Th17 cells which are subsequently controlled by acquisition of an IL-10-producing regulatory phenotype in the intestine or are removed *via* the intestinal lumen (Esplugues et al., 2011).

PATHOGENICITY OF TH17 CELLS IN KIDNEY DISEASE

Th17 cells have been shown to have an important role in immunological diseases including rheumatoid arthritis, multiple sclerosis, inflammatory bowel disease, cystic fibrosis, psoriasis and kidney disease (Awasthi and Kuchroo, 2009, Kitching and Holdsworth, 2011, McAllister et al., 2005). The work described in this thesis focused on Th17 pathogenicity in the context of acute kidney injury. IL-17-producing T-cells play a pathogenic role in multiple forms of kidney disease including obstructive nephropathy, glomerulonephritis, lupus nephritis and systemic lupus erythematosus (Turner et al., 2010a). In a mouse model of obstructive nephropathy, Dong et al. demonstrated the accumulation of activated memory phenotype Th17 cells following 72 hours of unilateral ureteral obstruction (UUO). Clodronate depletion of renal DCs prevented this accumulation (Dong et al., 2008). Deeper probing led to the identification of IL-1 as the Th17-enhancing factor (Pindjakova et al., 2012). Paust et al. detected Th17 accumulation in nephrotoxic serum nephritis, a mouse model of glomerulonephritis (Paust et al., 2009). IL-23p19 KO mice had ameliorated renal dysfunction and significantly reduced clinical scores. Similarly IL-17 KO mice displayed attenuated disease as characterized by reduced cellular infiltrate and crescent formation of the glomeruli (Paust et al., 2009). Moreover, the Kitching laboratory demonstrated amelioration of accelerated autologous-phase anti-glomerular basement membrane glomerulonephritis in RORγt KO mice (Steinmetz et al., 2010).

PROTECTIVE ROLE FOR TH17 CELLS

Despite evidence pointing towards a pathogenic role for Th17 cells, their primary function is in protection against extracellular pathogens such as fungi, mycobacteria and Gram-positive and Gram-negative bacteria *via* recruitment of neutrophils (Awasthi and Kuchroo, 2009). IL-17A protects from lethal doses of *Candida albicans* when administered to WT mice. Wild-type mice are less susceptible to infection with *Candida albicans* than IL-17RA KO mice. IFN-γ-producing Th1 cells are protective in *Mycobacterium tuberculosis* infections. However, the recruitment of Th1 cells is dependent upon IL-17-mediated chemokine production. *Mycoplasma pneumoniae* infections of the respiratory tract are cleared by neutrophils that are recruited *via* Th17-derived IL-17A and IL-17F. IL-17A KO, IL-17R KO and IL-23p19 KO mice are particularly susceptible to infection with *Klebsiella pneumoniae* due to reduced neutrophil recruitment (Korn et al., 2009).

Thus, the multifaceted Th17 subset, when appropriately coordinated and regulated, maintains homeostasis by controlling infections. However, over-exuberant Th17 responses, primed by pro-inflammatory IL-23 and/or IL-1, may drive autoimmune and inflammatory diseases.

1.2 MESENCHYMAL STEM CELLS: KEEPING THE PEACE

The osteogenic potential of a population of BM stromal cells was first described in the 1960s by Friedenstein and colleagues (Friedenstein et al., 1966). In the years that followed we were to learn that what are now termed mesenchymal stem cells (MSCs) may also differentiate into various other mesodermal cell lineages including adipocytes and chondrocytes under controlled culture conditions (**Figure 1.2A**) (Barry and Murphy, 2004). This heterogeneous population of self-renewing fibroblast-like progenitor cells may be isolated readily by adherence to plastic and expanded from BM, umbilical cord, fat, gingiva, and other tissues (Barry and Murphy, 2004). The primary role of MSCs in the BM is to provide trophic cues and components of the extracellular matrix to support hematopoietic stem cells (HSCs). Recent findings suggest that subpopulations of BM-MSCs play specific functional roles. Park et al. demonstrated that $CD105^{+}CD140a^{+}$ myxovirus resistance-1 (Mx1) promoter-induced MSCs display multi-lineage potential *in-vitro* yet are limited to the osteocyte lineage *in-vivo* (Park et al., 2012). Moreover, proliferating Mx1-osteogenic progenitors were the primary source of osteoblasts following a fracture injury model in mice and did not contribute to the formation of new cartilage (Park et al., 2012). Morikawa et al. demonstrated that a subpopulation of MSCs that express stem cell antigen-1 (Sca-1) and platelet-derived growth factor receptor alpha (PDGFRα) reside in the arterial perivascular space and function as a haematopoeitic niche (Morikawa et al., 2009). Furthermore, Mendez-Farrer et al. showed that $nestin^{+}$ MSCs are also niche cells spatially related in the perivascular region to HSCs and expressing HSC maintenance factors CXCL12, IL-7 and osteopontin (Mendez-Ferrer et al., 2010). Despite much work in this field to identify distinct subpopulations of MSCs with specific functional properties, there are currently no MSC-specific cell surface markers. MSCs may be defined by the presence of a combination of cell surface markers including CD29, CD44, CD73, CD90, CD105 and Sca-1 and the absence of CD11b, CD14, CD19, CD34 and CD45 (English et al., 2010). Species differences exist between human and mouse cell surface markers and even between mouse strains with CD73, CD90 and CD105 being dispensable for some strains of mouse MSCs including C57BL/6 (B6) (Bouffi et al., 2010).

1.2.1 IMMUNOMODULATORY PROPERTIES OF MSCS

In the past two decades, MSCs have garnered considerable attention for their potential use as regenerative therapeutic agents in a range of acute and chronic diseases (English et al., 2010, Griffin et al., 2010, Barry and Murphy, 2004, Caplan, 2009). Mechanistically, the beneficial effects of MSC therapies have been more frequently linked to their 'trophic' (paracrine) effects rather than their ability to transdifferentiate (Caplan, 2009). MSCs themselves demonstrate a lack of stimulatory capacity towards immune cells (Batten et al., 2006, Rasmusson et al., 2007). Specifically, MSCs are now viewed as having potent anti-inflammatory and immune-modulating properties.

Reported roles for both cell-cell contact and release of soluble factors in MSC-mediated suppression are evident throughout the literature and numerous candidate mediators have been reported: PGE2, indoleamine-2,3-dioxygenase (IDO), nitric oxide (NO), IL-27, TGF-β, monocyte chemotactic protein 1 (MCP-1/CCL2), human leukocyte antigen G (HLA-G), intracellular adhesion molecule 1 (ICAM-1), and TNF-α-induced protein 6 (TSG-6) among others (English et al., 2009, Tatara et al., 2011, Wang et al., 2008a, Zhao et al., 2008, Ren et al., 2010, Griffin et al., 2010, Lee et al., 2009). This topic shall be discussed in more detail in chapter 3 however the abundance of mediators identified to date suggests that MSCs exploit different immunosuppressive mechanisms under different disease conditions.

MSC-specific modulatory effects in the innate immune system are very well described (Le Blanc and Mougiakakos, 2012). Natural killer cells possess cytotoxic activity and play a pivotal role in GvHD and graft-versus-leukemia (GvL) by containing tumour growth (Pradier et al., 2011). MSCs inhibited proliferation and pro-inflammatory cytokine secretion by naive NK cells while they had no effect on the cytotoxic activity of previously activated NK cells (Pradier et al., 2011). This is of importance in GvL for the prevention of reactivation of resting malignancies and to ensure that tumour cells do not evade immune surveillance. Another phenomenon associated with MSCs is reprogramming of inflammatory monocytes/macrophages to IL-10-secreting anti-inflammatory macrophages (Nemeth et al., 2009). Neutrophils are protected from undergoing apoptosis with preservation of chemotactic and phagocytic activity by MSCs (Raffaghello et al., 2008). In the context of this thesis I am focusing on MSC-

specific modulation of the adaptive immune system with particular emphasis on the Th17 subset of helper T-cells.

1.2.2 MESENCHYMAL STEM CELL MODULATION OF T-HELPER CELL MEDIATED IMMUNE RESPONSES

The T-cell suppressive effects of MSCs were initially described over a decade ago (Bartholomew et al., 2002) and have since been reported consistently for both T-helper cells and CTLs (English et al., 2010, Caplan, 2009, Gieseke et al., 2010). Suppression of T cells by MSCs may be direct or may occur indirectly *via* modulatory effects on APCs such as DCs, resulting in altered cytokine expression and impaired antigen presentation (Cutler et al., 2010, Wang et al., 2008b, English et al., 2009). MSC therapy has been successful in a range of disease models and some clinical conditions known to be associated with damaging effector T-cell responses or failure of T_{reg}-mediated counter-regulation or both (Bai et al., 2009, Kavanagh and Mahon, 2010, Wang et al., 2008a, Lim et al., 2010, Ge et al., 2010, Casiraghi et al., 2008). In many studies MSCs have been shown to be associated with inhibition of effector T-cell activation with or without a concomitant increase in regulatory T-cell numbers (Bai et al., 2009, Kavanagh and Mahon, 2010).

MODULATION OF TH1 CELLS

The literature to date indicates that MSCs exert primarily suppressive effects on Th1 cell differentiation and effector function, and evidence favors predominantly indirect mechanisms. *In vitro*, the generation of Th1 cells is reduced in mixed lymphocyte cultures containing MSCs or MSC-conditioned medium, likely due to inhibition of Th1 cell stimulating properties of DCs (Aksu et al., 2008). The immunomodulatory effects of MSCs on Th1 cells in the *in vivo* setting are highlighted in **Table 1.1** below. These examples from the recent literature indicate that, in clinically relevant disease settings, MSCs consistently suppress harmful autoimmune Th1 cell responses by predominantly indirect mechanisms, including modulation of antigen-presenting DCs and promotion of FOXP3-expressing T_{reg}.

Table 1.1 Summary of recent reports in which MSCs had immunomodulatory effects on Th1-mediated diseases

Animal model - disease relevance	MSC effects
Cutaneous delayed-type hypersensitivity in mice (Lim et al., 2010)	Disease attenuated - reduced infiltration of $CD4^+$ and $CD8^+$ T-cells at the challenge site and increased apoptosis of activated T-cells in the draining lymph nodes (LN) - MSCs found close to the germinal centre and paracortical region of LN – modulation of immune response in area where DCs activate T-cells.
Trinitrobenzene sulfonate (TNBS)-induced colitis in mice – animal model of Crohn's disease (Gonzalez et al., 2009)	Dose-dependent xenogenic, allogenic, and autologous adipose tissue-derived MSCs (AT-MSCs) ameliorated disease activity - reduced IFN-γ-producing Th1 cells and increased $FOXP3^+$ T-cells.
Dextran sodium sulfate (DSS)- and TNBS-induced colitis in mice – animal models of Crohn's disease (Duijvestein et al., 2011)	MSCs pre-treated with IFN-γ had enhanced migration potential to sites of inflammation within the colitic colon and increased potential to suppress Th1-mediated responses.
Streptozotocin-treated rats - diabetes mellitus (Boumaza et al., 2009)	Increased IL-10 and IL-13 expression by T-cells and increased frequencies of both $CD4^+$ and $CD8^+$ $FOXP3^+$ T-cells with a direct reduction of IFN-γ-producing-T-cells.
Non-obese diabetic (NOD) mice - diabetes mellitus (Madec et al., 2009)	A single MSC injection minimized beta-cell destruction following transfer of diabetogenic T-cells. Protection was associated with MSC migration to pancreatic LNs and induction of IL-10-producing $FOXP3^+$ $T_{reg.}$
Lipolysaccharide (LPS)-induced acute lung injury in mice (Sun et al., 2011)	Intrapulmonary transplanted human umbilical cord MSCs ameliorated acute lung injury *via* induction of T_{reg} with a reduction in IFN-γ and TNF-α.

MODULATION OF TH2 CELLS

In the *in-vitro* setting, Batten and colleagues describe the use of human BM-derived MSCs for tissue engineering of a heart valve (Batten et al., 2006). $CD4^+$ T cells co-cultured with MSCs expressed lower levels of IL-1-α and -β, TNF and IFN-γ but higher levels of IL-5, IL-8 and IL-13 in response to allogeneic peripheral blood mononuclear cells suggesting the induction of a Th2 phenotype (Batten et al., 2006). Very few studies have examined MSC effects on immune-mediated diseases in which Th2 cell responses are dominant. The immunomodulatory effects of MSCs on Th2 cells in the *in vivo* setting are highlighted in **Table 1.2** below. The experimental evidence to date suggests that MSCs suppress effector function of Th2 cells in Th2

cell-predominant inflammation. In other T-cell-mediated immunological disorders, however, predominant MSC suppression of the Th1 and Th17 cell pathways may result in a relative skewing toward less damaging Th2 and T_{reg} phenotypes. Whether MSCs actively induce the differentiation and expansion of Th2 cells during antigen-specific immune responses has not been well tested but appears less likely.

Table 1.2 Summary of recent reports in which MSCs had immunomodulatory effects on Th2-mediated diseases

Animal model - disease relevance	MSC effects
Mouse model of ovalbumin (OVA)-induced airway inflammation - asthma (Kavanagh and Mahon, 2010)	Allogeneic MSCs suppressed allergen-specific Th2 responses *via* induction of T_{reg} - reduced numbers of infiltrating eosinophils, suppressed IgE induction and inhibited IL-13 and IL-4 production with increased IL-10 and FOXP3 expression.
OVA-induced allergic airway inflammation in mice (Goodwin et al., 2011, Ou-Yang et al., 2011)	MSCs migrated to site of inflammation *via* CXCR4. Protective effect associated with shift from Th2-mediated inflammation to Th1-mediated immune responses.
Sclerodermatous chronic GvHD in humans (Zhou et al., 2010)	Clinical improvement with a reduction in IL-4- and IL-10-producing T-cells and a concomitant increase in IL-2- and IFN-γ-producing cells.
Relapsing-remitting and chronic EAE in mice - multiple sclerosis (Bai et al., 2009)	Neurological improvement was associated with reduced $CD45^+$ leukocytic infiltration of the brain and spinal cord, with increased levels of Th2 cell-related cytokines IL-4 and IL-5, and with potent reduction in IL-17, IFN-γ, TNF, and IL-12. following administration of human-MSCs.
Experimental autoimmune type 1 diabetes (Fiorina et al., 2009)	Shift in Th1/Th17 cell balance toward Th2 cells following allogeneic MSC administration to NOD mice.

MODULATION OF T_{REG} CELLS

There has been a consistent theme among many *in vitro* and *in vivo* studies in support of MSC enhancement of T_{reg} number and activity (Griffin et al., 2010). In the *in-vitro* setting, English and colleagues (English et al., 2009) showed that human $FOXP3^+CD25^{high}$ T_{reg} were induced upon co-culture of allogeneic MSCs and $CD4^+$ T-cells and exerted suppressive activity when re-purified and added to a newly initiated mixed lymphocyte culture. Additional studies to those mentioned in **Tables 1.1** and **1.2** summarizing the immunomodulatory effects of MSCs on T_{reg} cells in the *in vivo* setting are summarized in **Table 1.3**.

Table 1.3 Summary of recent reports in which MSCs had immunomodulatory effects on T_{reg} cells *in-vivo*

Animal model - disease relevance	MSC effects
Rheumatoid arthritis (Gonzalez-Rey et al., 2010)	Human adipose tissue-derived MSCs reduced IL-17, TNF, and IFN-γ production and induced IL-10-producing, $FOXP3^+$ T_{reg} *in vitro* among collagen-specific peripheral blood T-cells. Upon re-isolation, T_{reg} generated in the presence of MSCs had the capacity to inhibit IFN-γ production and proliferation of a subsequent collagen-stimulated T-cell culture.
Kidney, liver and heart allotransplantation (Ge et al., 2010, Casiraghi et al., 2008, Wang et al., 2009)	Protective effects observed with MSC therapy linked directly to the presence of $T_{reg.}$ Graft rejection occurs following T_{reg} depletion.

MODULATION OF TH17 CELLS

This thesis specifically studies the modulation of Th17 cells by MSCs. At the initiation of this project in September 2008, there were a very limited number of publications in relation to MSC-specific regulation of Th17 cells (Zhao et al., 2008). During the course of this project, we and a number of other research groups have examined MSC effects on the Th17 differentiation pathway in mice and humans. Ghannam and colleagues (Ghannam et al., 2010) observed that human MSCs induce regulatory characteristics in Th17 cells in an inflammatory environment by down-regulating the Th17 cell-specific transcription factor RORγt and up-regulating FOXP3. Moreover, when re-purified, these regulatory-phenotype Th17 cells suppressed proliferation of newly initiated $CD4^+$ T cells (Ghannam et al., 2010). *In vivo*, MSC administration has been shown to suppress the development of EAE *via* a reduction in IL-17 production in the central nervous system along with reduced IFN-γ, TNF and IL-23 and increased TGF-β1 and IL-4 (Wang et al., 2008a). Oh and colleagues demonstrated that 5-fluorouracil-resistant MSCs remitted myelin-oligodendrocyte glycoprotein (MOG)-induced EAE, mediated *via* a combination of reduced IL-17A with increased Th2-related cytokines, IL-10, PGE2 and IL-1RA (Oh et al., 2012). Inhibition of Th17 cell activity in EAE has also been reported by Zappia and colleagues (Zappia et al., 2005) and Rafei and colleagues (Rafei et al., 2009) although the studies to date have identified different mechanisms for the MSC anti-Th17 cell effect, including IL-27 (Wang et al., 2008a), IL-10, IL-1RA and PGE2 (Oh

et al., 2012) alternatively cleaved MCP-1 (Rafei et al., 2009), and induction of a state of T-cell anergy (Zappia et al., 2005).

Although these studies indicate that MSCs have the potential to suppress Th17 cell-mediated immunity and may do so by several mechanisms, some evidence for a Th17 cell-promoting effect of MSCs also exists. For example, Carrión and colleagues (Carrion et al., 2010) observed that MSCs promoted Th17 cells while inhibiting Th1 cells *in vitro* if their addition to mouse T-cell differentiation cultures was delayed by 3 days. Similarly, Darlington and colleagues (Darlington et al., 2010) observed that MSC-conditioned medium suppressed human Th1 cells *in vitro* while having an opposing effect on Th17 cells. In the same study, MSC conditioned medium was found to reduce numbers of IL-17/IFN-γ double-expressing $CD4^+$ T cells; this finding may have clinical implications for patients with multiple sclerosis as this subset was recently described in immune-mediated demyelinating disease (Darlington et al., 2010).

Whether MSCs inhibit or enhance disease associated Th17 cells *in vivo* is less well understood, although Ghannam and colleagues (Ghannam et al., 2010) observed that MSCs suppressed the production of IL-17 and IL-22 by established human Th17 cell clones with a paradoxical increase in IL-10-producing cells. Furthermore, Rafei and colleagues (Rafei et al., 2009) demonstrated amelioration of EAE and inhibition of Th17 cell activity when MSCs were first administered 1 week after the onset of neurological signs of disease, suggesting the inhibition of established T-cell effector responses. Inhibition of Th17 cell-mediated inflammation and autoimmunity by MSC administration has also been reported in models of type 1 diabetes mellitus, CIA and experimental autoimmune myasthenia gravis in association with shifts toward increased Th2 or T_{reg} activity or both (Zhao et al., 2008, Bouffi et al., 2010, Kong et al., 2009, Zhou et al., 2011, Liang et al., 2011, Park et al., 2011).

Overall, a significant amount of evidence for specific effects of MSCs on the Th17 cell effector pathway has emerged. These effects appear to be suppressive under diverse conditions but with the potential to enhance Th17 cell activity under some circumstances. In this regard, it is worth noting that MSCs may act as a source of IL-6, which is one of the primary mediators of Th17 cell differentiation (Chen et al.,

2010a). The role of MSC-produced IL-6 is likely to be more complex, however, as MSCs derived from IL-6-deficient mice were less effective than wild-type MSCs in suppressing inflammation associated with CIA in a study by Bouffi and colleagues (Bouffi et al., 2010).

The body of work associated with this thesis has added to the current understanding and growing appreciation of the field in which Th17 cells display maladaptive hallmarks and are also targets of MSC therapy.

1.3 CLINICAL RELEVANCE OF MSC THERAPY FOR TH17-MEDIATED DISEASES

The work described in this thesis focused on the pathogenicity of Th17 cells in the context of acute kidney injury. Th17 cells are also pathogenic in multiple autoimmune and inflammatory diseases including inflammatory bowel disease, rheumatoid arthritis, multiple sclerosis, psoriasis and transplant rejection (Awasthi and Kuchroo, 2009, Kitching and Holdsworth, 2011) therefore my results will additionally be of relevance to other diseases in which Th17 cells are known to play a role.

Given the complex nature of many of these autoimmune and inflammatory diseases, MSCs appear to be a very attractive alternative therapy to conventional approaches due to their multimodal immunomodulatory effects on a wide variety of immune populations. Specifically, a large literature related to the T-cell suppressive effects of MSCs has accumulated over the last decade. The clinical relevance of which has been demonstrated by the beneficial effects of MSCs in multiple Th17-mediated pre-clinical studies including colitis, EAE and CIA as discussed in section 1.2.2.

Inflammatory bowel disease which includes ulcerative colitis and Crohn's disease is a chronic inflammatory condition of the gastrointestinal (GI) tract. Ulcerative colitis is restricted to the colon while Crohn's disease may affect any part of the GI tract. The Centre for Disease Control and Prevention estimate that 1.4 million Americans suffer from inflammatory bowel disease. Surgery is a necessity for 66-75% of Crohn's patients as current treatments become ineffective over time. Therapies for ulcerative colitis are unsuccessful in 25-33% of cases thus colectomy may be required (www.cdc.gov/ibd). Preemptive therapies to attenuate inflammatory bowel disease or to induce long-lasting remission are a must therefore. Th17 cells play a critical role in multiple forms of inflammatory bowel disease (Abraham and Cho, 2009). Successful preclinical models provide a strong impetus for translating MSC therapy to widespread clinical use for a range of common, Th17-mediated inflammatory diseases including inflammatory bowel disease. **Table 1.4** summarizes clinical trials associated with inflammatory bowel disease which are currently active, recruiting participants, not yet recruiting participants or enrolling participants by invitation and, in which MSC interventions are employed (www.clinicaltrials.gov).

Table 1.4 Summary of current clinical trials employing MSC intervention for inflammatory bowel disease.

Clinical trial	Th17-mediated disease	Sponsor	Phase	NCT number
Umbilical cord MSC infusion for ulcerative colitis	Ulcerative colitis	Qingdao University, China	1/2	NCT01221428
Treatment of fistulous Crohn's disease by implant of autologous MSCs derived from adipose tissue	Crohn's disease	Clinica Universidad de Navarra, Spain	1/2	NCT01157650
MSC therapy for the treatment of severe or refractory inflammatory and/or autoimmune disorders	Crohn's disease	University Hospital of Liege, Belgium	1/2	NCT01540292
Dose-escalating therapeutic study of allogeneic BM-MSCs for the treatment of fistulas in patients with refractory perianal Crohn's disease	Crohn's disease	Leiden University Medical Center, Netherlands	1/2	NCT01144962
Evaluation of PROCHYMAL® for treatment-refractory moderate-to-severe Crohn's disease	Crohn's disease	Osiris Therapeutics, US	3	NCT01233960
AT-MSCs for induction of remission in perianal fistulizing Crohn's disease	Crohn's disease	Cellerix, Spain	3	NCT01541579
Safety and treatment outcome study of PROCHYMAL® (Remestemcel-L) intravenous infusion in subjects with treatment-resistant Crohn's disease	Crohn's disease	Osiris Therapeutics, United States (US)	-	NCT01510431
Evaluation of PROCHYMAL® adult human stem cells for treatment-resistant moderate-to-severe Crohn's disease	Crohn's disease	Osiris Therapeutics, US	3	NCT00482092

Multiple sclerosis is a demyelinating disease of the CNS. The Multiple Sclerosis Foundation estimates that 2.5 million people are living with multiple sclerosis worldwide (www.msfocus.org). There is currently no cure for multiple sclerosis however, IFN-β therapy has been proven to limit the number and severity of attacks. Durelli et al. demonstrated that Th17 cells are selective targets for IFN-β treatment as the Th17 cell population specifically expands in active multiple sclerosis and expresses increased IFN-αR1 compared to Th1 cells. Additionally IFN-β treatment of $CD4^+$ T-cells from multiple sclerosis patients resulted in reduced frequencies of Th17 cells (Durelli et al., 2009). Treatments including IFN-β have potential adverse side effects however. In addition to the beneficial effects of MSCs observed in animal models of multiple sclerosis, the ever increasing number of clinical trials employing

MSCs for the treatment of multiple sclerosis **(Table 1.5)** highlights the therapeutic potential of these cells as replacements for or in combination with traditional agents (www.clinicaltrials.gov).

Table 1.5 Summary of multiple sclerosis-related clinical trials, in which the therapeutic potential of MSCs are currently being evaluated.

Clinical trial	Th17-mediated disease	Sponsor	Phase	NCT number
Evaluation of autologous MSC transplantation (effects and side effects) in multiple sclerosis	Multiple sclerosis	Royan Institute, Iran	1/2	NCT01377870
Safety and efficacy of umbilical cord MSC therapy for patients with progressive multiple sclerosis and neuromelitis optica	Multiple sclerosis	Shenzhen Beike Bio-technology Co. Ltd., China	1/2	NCT01364246
Autologous AT-MSCs in patients with secondary progressive multiple sclerosis	Multiple sclerosis	Fundacion Progreso Y Salud, Spain	1/2	NCT01056471
MSC transplantation in multiple sclerosis	Multiple sclerosis	Hospital Clinic of Barcelona, Spain	2	NCT01228266
Autologous MSC transplantation in multiple sclerosis	Relapsing-remitting multiple sclerosis	The Cleveland Clinic, US	1	NCT00813969
Stem cells in rapidly evolving active multiple sclerosis	Multiple sclerosis	Imperial College London, United Kingdom (UK).	1/2	NCT01606215

Rheumatoid arthritis is a chronic autoimmune disease most commonly affecting synovium, cartilage and bone. The National Institute of Arthritis and Musculoskeletal and Skin Diseases at the National Institutes of Health (NIH) state that in the US alone, 1.3 million people are estimated to be suffering from rheumatoid arthritis. Current treatments often involve use of analgesics, corticosteroids and non steroidal anti-inflammatory drugs (NSAIDS). More recently biologic response modifiers have been employed in the treatment of rheumatoid arthritis including TNF inhibitors (Etanercept™) and IL-1 inhibitors (Anakinra™) however, such agents often require daily injections and have multiple side effects (www.niams.nih.gov). McGovern et al. recently demonstrated that T_{reg} from patients with rheumatoid arthritis who respond to anti-TNF therapy with adalimumab suppressed Th17 responses by inhibiting monocyte-derived IL-6 (McGovern et al., 2012), highlighting the importance of the Th17 phenotype in rheumatoid arthritis. While IL-6 plays a proinflammatory role in driving Th17 differentiation it also has anti-inflammatory properties. MSCs reduced

the clinical manifestations of CIA *via* IL-6-dependent PGE2 production (Bouffi et al., 2010). Encouraging results from animal models are a driving force for progression to clinical trials to evaluate the potential benefits of MSC therapy in rheumatoid arthritis (**Table 1.6**) (www.clinicaltrials.gov).

Table 1.6 Summary of current clinical trials employing MSC intervention for rheumatoid arthritis.

Clinical trial	Th17-mediated disease	Sponsor	Phase	NCT number
Safety and efficacy study of umbilical cord-derived MSCs for rheumatoid arthritis	Rheumatoid arthritis	Alliancells Bioscience Corporation Ltd., China	1/2	NCT01547091

Psoriasis is an inflammatory skin disorder involving the proliferation of keratinocytes that affects more than 5 million adults in the US alone. Some forms of psoriasis are unresponsive to light therapy or topical treatments while systemic treatments, retinoids for example, can have multiple side effects including birth defects. Leonardi et al. demonstrated improved clinical symptoms of chronic plaque psoriasis with anti-IL-17 monoclonal antibody in an Eli Lilly-funded clinical trial however, long-term safety studies are required as 63% of participants experienced adverse effects (Leonardi et al., 2012). There are currently no registered clinical trials for psoriasis with MSC interventions although MSC therapy may prove to be a safer alternative to currently approved treatments.

A number of pre-clinical studies have also highlighted the beneficial effects of MSCs in inflammatory and fibrotic kidney disease. Bi et al. demonstrated that intravenous (IV)- and intraperitoneal (IP) BM-MSCs and AT-MSCs, in addition to MSC conditioned media, improved survival rate, tubular cell apoptosis and renal function as measured by blood urea nitrogen (BUN) and creatinine levels in mice following cisplatin-induced renal failure (Bi et al., 2007). Male IV- and IP-administered MSCs were undetectable in female cisplatin-treated mice further suggesting that the renoprotective effects of MSCs are paracrine in nature (Bi et al., 2007). In contrast, Morigi et al. showed that the same dose of IV-injected MSCs localized to the tubular epithelial lining suggesting some level of engraftment (Morigi et al., 2004). Furthermore, human MSCs administered to non-obese diabetic – severe combined

immune deficiency (NOD-SCID) mice following cisplatin treatment minimized tubular damage and reduced mortality (Morigi et al., 2008).

MSCs administered *via* the carotid artery were detected in the capillaries of glomeruli in rats subjected to bilateral ischemia reperfusion injury. This was associated with improved renal function and reduced tubular damage (Lange et al., 2005). Herrera et al. demonstrated that MSCs home to the injured kidney *via* CD44 (Herrera et al., 2007).

A limited number of studies have examined the effects of MSCs in obstructive nephropathy. Liu et al. demonstrated that IV administered, adenovirus-hepatocyte growth factor (HGF)–transfected MSCs (Ad-HGF-MSCs) were only detectable in tubular epithelial cells in the outer medulla of obstructed kidneys of rats subjected to UUO. Both untransfected MSCs and Ad-HGF-MSCs suppressed the activation of myofibroblasts suggesting that this treatment may prevent epithelial to mesenchymal transition (EMT) and fibrosis in obstructive nephropathy (Liu et al., 2011). Human MSCs administered immediately prior to UUO *via* the renal artery in rats migrated to the cortical tubules and interstitium of obstructed kidneys (Asanuma et al., 2011). Moreover, the MSC-treated group was protected from tubulointerstitial fibrosis and EMT (Asanuma et al., 2011). Liu et al. showed that MSCs significantly reduced tubular damage on days 3 and 7 following administration *via* the inferior vena cava however, by day 14 MSCs were unable to confer protection (Liu et al., 2012). This was associated with reduced $ED1^+$ macrophage infiltration and renal IFN-γ expression and increased T_{reg} accumulation at day 3 and 7 (Liu et al., 2012) suggesting that MSCs provide beneficial immunomodulatory effects early during the course of UUO.

Recently, MSC-derived microvesicles have been reported to attenuate multiple forms of kidney disease (He et al., 2012, Bruno et al., 2012, Bruno et al., 2009). The protective effects of MSCs are well reported in diverse animal models of kidney disease, as are the potential mechanisms of action as illustrated in **Figure 1.5**. MSC-specific modulation of kidney disease has also translated to clinical trials (**Table 1.7**) (www.clinicaltrials.gov).

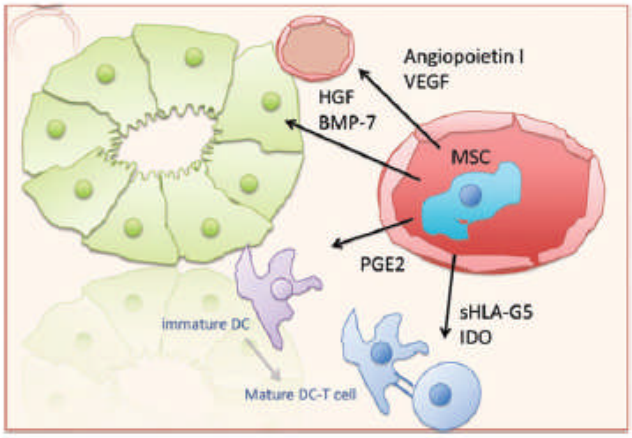

Figure 1.5 Putative mechanisms of renoprotection elicited by MSCs include transdifferentiation and production of pro-angiogenic, anti-fibrotic, anti-apoptotic and anti-inflammatory mediators (From: Reinders et al., 2010).

Table 1.7 Summary of clinical trials for the treatment of inflammatory kidney diseases in which the therapeutic potential of MSCs are currently being evaluated.

Clinical trial	Th17-mediated disease	Sponsor	Phase	NCT number
Phase 2 study of human umbilical cord derived MSCs for the treatment of lupus nephritis	Lupus nephritis	CytoMed & Beike	2	NCT01539902
MSC transplantation for refractory systemic lupus erythematosus	Refractory systemic lupus erythematosus	Nanjing Medical University, China	1/2	NCT00698191
MSCs In cisplatin-induced acute renal failure in patients with solid organ cancers	Acute kidney injury	Mario Negri I.P.R., Italy	1	NCT01275612
A study to evaluate the safety and efficacy of AC607 for the treatment of kidney injury in cardiac surgery subjects	Acute kidney injury	AlloCure Inc., US	2	NCT01602328

1.4 VITAMIN D AND THE IMMUNE SYSTEM

In year four of this thesis, the effects of a vitamin D receptor (VDR) agonist alone and in combination with MSCs on Th17 immune responses were examined. Vitamin D plays a pivotal role in bone mineralization and homeostasis of calcium and phosphorus (Griffin et al., 2003). Vitamin D deficiency is associated with rickets in children and with osteomalacia in adults. Furthermore, active vitamin D is used clinically to treat secondary hyperparathyroidism associated with chronic kidney disease. Limitations associated with active vitamin D including excessive calcemia and phosphatemia led to the formulation of synthetic analogues of vitamin D and VDR agonists with structural modifications aimed at reducing these adverse side effects while retaining the ability to suppress parathyroid hormone levels (Brown et al., 2002). Paricalcitol (19-nor-1alpha, 25-dihydroxyvitamin D2), for example, is a VDR agonist developed for this purpose and currently marketed by Abbott Laboratories as Zemplar™.

The most common form of vitamin D in mammals is vitamin D_3 (cholecalciferol). The natural source of vitamin D_3 is synthesis in the skin following metabolism of sterol 7-dehydrocholesterol by ultraviolet light. Vitamin D may also be obtained from a limited number of foods including salmon, mackerel, tuna, egg yolk and beef livers. Hepatocyte 25-hydroxylase induces hydroxylation of cholecalciferol into calcidiol (25-hydroxycholecalciferol/25(OH)D_3) (Campbell et al., 2010). In proximal renal tubules, 1α-hydroxylase further hydroxylates calcidiol to calcitriol (1α 25-dihydroxycholecalciferol/1α,25-$(OH)_2$ D_3) (Campbell et al., 2010). This is the most biologically active form of the hormone. In addition to the liver and kidneys, certain immune cells can also metabolize vitamin D including T-cells, B-cells, macrophages and DCs as illustrated in **Figure 1.6** (Mora et al., 2008).

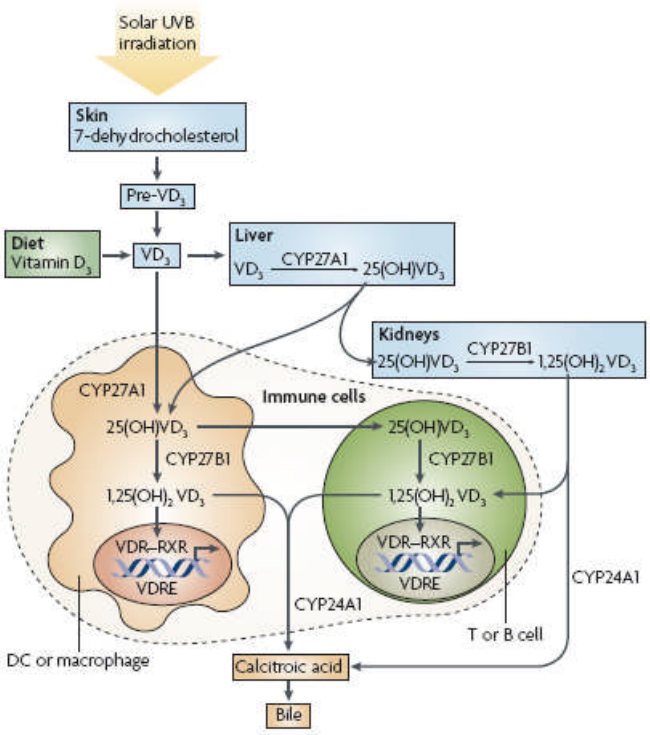

Figure 1.6 Synthesis of metabolically active calcitriol by liver and kidney tissues or by cells of the immune system (From: Mora et al., 2008).

The VDR is expressed by T-cells, B-cells, monocytes, macrophages and DCs and, can be cytoplasmic or nuclear (Mora et al., 2008, Campbell et al., 2010). Engagement of calcitriol with the VDR leads to the formation of a heterodimer with a retinoid X receptor (RXR) isoform which can then engage vitamin D responsive elements (VDRE) in target gene promoter regions (Campbell et al., 2010). Vitamin D specifically influences the immune system as illustrated in **Figure 1.7**. (Mora et al., 2008, Griffin et al., 2003). Calcitriol has been shown to inhibit the expression of maturation and co-stimatory markers by DCs, induce tolerogenic DCs, inhibit proinflammaotry cytokine producion by monocytes and macrophages, suppress antibody production and plasma cell differentiation and suppress Th1 and, to a lesser extent, Th17 responses while promoting Th2 and T_{reg} responses (Mora et al., 2008).

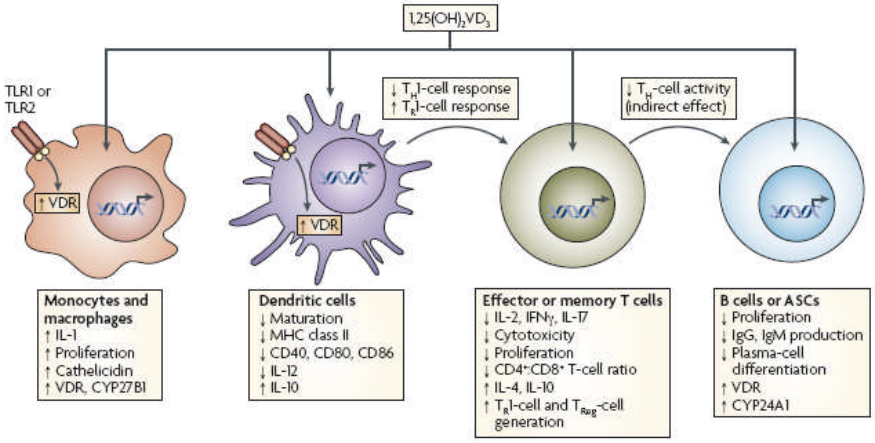

Figure 1.7 Summary of the immunomodulatory effects of calcitriol on the immune system (From: Mora et al., 2008).

These immunomodulatory properties have raised substantial interest in the use of VDR agonists to treat and prevent a variety of immune-mediated diseases including multiple sclerosis, type I diabetes mellitus, rheumatoid arthritis and inflammatory bowel disease (Szodoray et al., 2008). Mayne et al. demonstrated that mice that were fed a diet supplemented with calcitriol displayed delayed onset and reduced incidence of MOG-induced EAE by over 50% (Mayne et al., 2011). Resistance was dependent on the expression of VDR by cells of the hematopoietic lineage in particular pathogenic $CD4^+$ T-cells (Mayne et al., 2011). Consistent with the findings of Mayne et al., Chang et al. also demonstrated that orally administered calcitriol conferred resistance to MOG-induced EAE which was associated with reduced frequency of Th17 cells in the spleen and with lack of accumulation of Th17 cells in the CNS (Chang et al., 2010a). Similarly, this study also showed dependence on VDR expression by $CD4^+$ T-cells. Colin et al. demonstrated that calcitriol synergizes with dexamethasone by reducing IL-17A production by peripheral blood mononuclear cells (PBMCs) from patients who have not received any treatment for early rheumatoid arthritis (Colin et al., 2010). Furthermore, calcitriol suppressed IL-17A, IL-17F and IL-22 production by $CD4^+CD45RO^+$ memory T-cells abundant in patients with early rheumatoid arthritis (Colin et al., 2010). Calcitriol and synthetic VDR agonists have beneficial effects in multiple forms of kidney disease. Cyclosporine A (CsA) is used as an immunosuppressant following solid organ transplantation however, it is also associated with nephrotoxic effects characterized by progressive interstitial fibrosis and tubular atrophy. Park et al. demonstrated that paricalcitol attenuated renal

interstitial fibrosis, tubular atrophy and dilation, tubular epithelial apoptosis and macrophage infiltration associated with CsA-induced kidney injury in rats (Park et al., 2010a). Furthermore, the same laboratory showed attenuated gentamicin-induced nephropathy following paricalcitol treatment in rats (Park et al., 2010b). In streptozotocin-induced diabetic nephropathy in rats, Sanchez-Nino demonstrated reduced renal pro-inflammatory IL-6, IL-8, MCP-1 and TNF-α together with reduced NF-κB activation, collagen deposition and glomerulus cell apoptosis (Sanchez-Nino et al., 2012). The Liu laboratory in Pennsylvania, USA has been successful in demonstrating attenuated obstructive nephropathy in mice that underwent unilateral ureteral obstruction using paricalcitol treatment. This was associated with reduced interstitial fibrosis, tubular cell EMT (Tan et al., 2006) and $CD3^+$ T-cell and $F4/80^+$ macrophage infiltration (Tan et al., 2008). Moreover, paricalcitol and trandolapril displayed additive renal protection. Trandolapril is an angiotensin-converting enzyme inhibitor used for the treatment of chronic kidney disease. Induction of renin is a limitation of its use as renin can exacerbate renal injury. Of clinical relevance, paricalcitol reversed the induction of renin associated with trandolapril (Tan et al., 2009).

CLINICAL RELEVANCE OF VDR AGONISTS

Vitamin D receptor agonists have been shown to exert beneficial effects in pre-clinical studies of multiple sclerosis, rheumatoid arthritis, inflammatory bowel disease and multiple forms of kidney disease. Encouraging results observed in animal models are a strong force for clinical translation. **Table 1.8** summarizes clinical trials associated with Th17-mediated diseases with vitamin D interventions which are currently active, recruiting participants, not yet recruiting participants or enrolling participants by invitation (www.clinicaltrials.gov). Clinical trials associated with vitamin D interventions in which outcome measures do not encompass inflammatory parameters have been excluded. Vitamin D interventions may involve supplementation of vitamin D or pharmacotherapeutic intervention of active vitamin D.

Table 1.8 Clinical trials employing vitamin D supplementation in diseases associated with the Th17 phenotype.

Clinical trial	Th17-mediated disease	Sponsor	Phase	NCT number
Vitamin D treatment in ulcerative colitis	Ulcerative colitis	University of Chicago, US	-	NCT01640496
Vitamin D supplementation in Crohn's patients	Crohn's disease	Penn State University, US	1	NCT00742781
Vitamin D supplementation in adult Crohn's disease	Crohn's disease	Trinity College Dublin, Ireland	4	NCT01369667
Safety and immunologic effect of low dose versus high dose vitamin D3 in multiple sclerosis	Multiple sclerosis	Johns Hopkins University, US	1	NCT01024777
The effects of IFN-β combined with vitamin D on relapsing remitting multiple sclerosis patients	Multiple sclerosis	Carmel Medical Center, Israel	4	NCT01005095
Vitamin D and fish oil for autoimmune disease, inflammation and knee pain	Rheumatoid arthritis	Brigham and Women's Hospital, US	4	NCT01351805
Prospective intervention study on vitamin D in patients with cystic fibrosis	Cystic fibrosis	Karolinska Institutet, Sweden	2	NCT01321905
Vitamin D for enhancing the immune system in cystic fibrosis	Cystic fibrosis	Emory University, US	3	NCT01426256
Metabolic effects of paricalcitol	Chronic kidney disease	University of Washington, US	2	NCT01003275

Putative mechanisms of action for MSC modulation of T-cells to date include both cell-cell mediated and paracrine factors while VDR agonist modulation of immune populations is mediated through genomic effects of the VDR. Therefore, there is potential for paricalcitol to augment MSC therapy *via* complementary immunosuppressive/anti-inflammatory mechanisms. Additionally, VDR agonist immune modulation has been shown to be additive to or synergistic with the immune suppressive effects of other therapeutic agents (Deb et al., 2010, Tan et al., 2009). This thesis will therefore explore the possibility of using paricalcitol as an adjunt to stem cell therapy.

1.5 AIMS AND HYPOTHESES

Overall, it is now very well established that MSCs exert diverse and potent modulatory effects on the T-cell compartment of the immune system, most of which are suppressive in nature and of potential therapeutic value. Nevertheless, some significant controversies and a basic lack of information regarding the range of effects that MSCs have on naïve versus memory T-cells particularly within the Th17 compartment remain. Vitamin D, in addition to its traditional effects on bones and mineral homeostasis, modulates the immune system *via* direct effects through the VDR. Therefore, in the context of this study, my overarching goal was to elucidate the therapeutic potential of MSCs alone and in combination with the VDR agonist paricalcitol to favourably modulate maladaptive Th17-mediated immune responses.

Chapter 2 aim: Determine the effects of mouse MSCs on $CD4^+$ T-cells undergoing primary Th17 differentiation and re-activation of Th17-skewed cells *in-vitro.*
Chapter 2 hypothesis: MSCs potently suppress $CD4^+$ T-cells undergoing primary Th17 differentiation.

Chapter 3 aim: Determine the mechanism of MSC-mediated Th17 modulation.
Chapter 3 hypothesis: MSC-mediated inhibition of primary Th17 differentiation requires cell-cell contact.

Chapter 4 aim: Determine the effects of paricalcitol alone and in combination with MSCs on the primary activation and secondary reactivation of Th17 cells *in-vitro.*
Chapter 4 hypothesis: Paricalcitol augments MSC-mediated inhibition of primary Th17 differentiation.

Chapter 5 aim: Determine the effects of paricalcitol and MSCs alone and in combination in a mouse model of kidney disease characterized by abnormal Th17 immune responses, unilateral ureteral obstruction.
Chapter 5 hypotheses: Inflammatory kidney disease characterised by activation of IL-17-producing $CD4^+$ T-cells are ameliorated by combined administration of paricalcitol and autologous MSCs.

CHAPTER TWO

MESENCHYMAL STEM CELLS INHIBIT T-HELPER 17 DIFFERENTIATION FROM NAÏVE AND MEMORY $CD4^+$ T-CELL RESPONDERS IN A CELL-TO-CELL CONTACT DEPENDENT MANNER.

2.1 INTRODUCTION

At the initiation of this study only a small number of studies had addressed the interaction between MSCs and Th17 cells. Conflicting evidence emerged for both suppressive and augmenting effects of MSCs on this Th cell differentiation pathway (Rafei et al., 2009, Wang et al., 2008a, Zhao et al., 2008, Guo et al., 2009, Kong et al., 2009).

Rafei et al. demonstrated that mouse B6 MSC conditioned media (20 X concentrated) potently suppressed IL-17A production and STAT3 phosphorylation *ex-vivo* by MOG-specific $CD4^+$ T-cells which was dependent upon a matrix metalloproteinase (MMP)-processed form of CCL2/MCP-1 (Rafei et al., 2009). Furthermore, WT MSCs significantly ameliorated EAE compared with CCL2 KO MSCs. In *ex-vivo* recall experiments, EAE mice treated with WT MSCs displayed reduced IL-17A production by $CD4^+$ T-cells (Rafei et al., 2009). This study indicated that the MSC-derived soluble factor CCL2 was responsible for suppression of IL-17A-producing T-cells at least in response to MOG.

In rats with MBP68-86 peptide-induced EAE, MSCs delayed the onset of disease and lowered the clinical score (Wang et al., 2008a). This was associated with reduced IL-17A expression and cellular infiltrate in the spinal cords. Serum levels of IL-17A, IL-23, TNF-α and IFN-γ were reduced while IL-27 and TGF-β were increased. Blockade of IL-27 *in-vitro* in EAE-LN mononuclear cell co-cultures with MSCs enhanced IL-17A production. Furthermore, MBP68-86 peptide-specific T-cells co-cultured with MSCs under IL-27 blockade induced more severe adoptive transfer-EAE with increased levels of circulating IL-17A and increased expression in the spinal cords than MBP68-86 peptide-specific T-cells co-cultured with MSCs without IL-27 blockade. This study also demonstrated that MSCs suppress Th17 responses in EAE albeit by a different mechanism to that identified by Rafei and colleagues.

In an experimental rat model of autoimmune myasthenia gravis (AMG), Kong et al. showed that MSCs attenuated the severity of the disease – an effect which was characterized by a shift from IL-17A- and IFN-γ-producing $CD4^+$ T-cells to IL-4-producing T-cells and $FOXP3^+$ T_{regs} (Kong et al., 2009). Furthermore, MSCs

suppressed the proliferation and IL-17A production by acetylcholine receptor (AMG autoantigen)-specific T-cells *in-vitro* which was partially reversed in the presence of an IDO inhibitor (Kong et al., 2009).

Zhao et al. showed that MSCs also have beneficial effects in NOD mice with type I diabetes (Zhao et al., 2008). In this system, islets of MSC-treated mice had reduced inflammatory lesions and IL-17A expression. Serum IL-17A was also reduced while TGF-β increased. Blockade of TGF-β in *in-vitro* co-cultures of MSCs and lymphocytes reversed the suppressive effect on IL-17A production (Zhao et al., 2008).

Human AT-MSCs suppressed IL-17A production *in-vitro* from collagen type-II-specific T-cells isolated from patients with rheumatoid arthritis (Gonzalez-Rey et al., 2010). In this study a requirement for cell-cell contact was observed as inhibition of IL-17A production was significantly reduced in transwell cultures (Gonzalez-Rey et al., 2010).

The studies described above demonstrated that the suppressive effects of MSCs on Th17 cells occured across species and in diverse autoimmune diseases. Experimental evidence also pointed towards diverse MSC-derived mediators of Th17 suppression under specific conditions. At the same time however, a contrasting report emerged that MSCs actually augment Th17 responses. The study by Guo et al. introduced the first evidence of MSC-enhancement of the Th17 lineage (Guo et al., 2009). MSCs were derived from bone marrow of human fetuses. Peripheral blood mononuclear cells or $CD4^+$ T-cells cultured in the presence of MSCs with phytohaemagglutinin (PHA) and IL-2 had higher expression of IL-17A than cells cultured in the absence of MSCs. The authors found increased IL-6 in their co-cultures which, when added exogenously to T-cell cultures, enhanced Th17 differentiation. IL-1 was also enhanced in co-cultures. Separate blockade of IL-6 and IL-1 partially reversed the augmentation of human IL-17-producing T-cells.

This collection of studies from 2008 to early 2009 demonstrated that MSCs were primarily suppressive of Th17 cells originating from antigen-specific animal models and patients which were re-challenged *ex-vivo* however; under specific culture

conditions MSCs expanded Th17 cells. Thus, major gaps remained in the literature at the initiation of my project. The effects of MSCs had not been investigated on $CD4^+$ T-cells undergoing primary Th17 differentiation under standard Th17 culture conditions in the presence of IL-6 and TGF-β with blockade of IL-4 and IFN-γ.

Furthermore, the effects of MSCs on naïve T-cells undergoing primary Th17 differentiation had not been compared to memory T-cell responders undergoing the same process. T-cells are considered naïve in nature (inactivated and undifferentiated) prior to a primary encounter with a compatible antigen. Following the clearance of infection, the majority of $CD4^+$ T-cells die *via* apoptosis however a proportion remain as memory T-cells (Janeway, 2008). Due to their capacity to respond to secondary re-encounter with the same antigen more rapidly and potently and their ability to retain effector function in the case of effector memory T-cells, memory T-cell responses may not be suppressed by MSCs to the same extent as naïve T-cell responses. One study from the group of Krampera and Dazzi demonstrated that both naïve and memory T-cells were subject to MSC-mediated suppression (Krampera et al., 2003). In this system, T-cells with a transgenic HY (male antigen)-specific TCR were stimulated in the presence or absence of MSCs with syngeneic splenocytes pulsed with HY peptides and used as a source of naïve T-cells. Memory cells originated from female mice transplanted with male cells which were re-stimulated *in-vitro* with male splenocytes in the presence or absence of MSCs. The cells were subsequently re-stimulated after 7 days with HY peptide-pulsed female splenocytes. The authors demonstrated dose-dependent suppression of T-cell proliferation in the presence of MSCs in addition to reduced frequency of cytotoxic IFN-γ-producing $CD8^+$ T-cells. In this study however, $CD4^+$ T-cell responses were not investigated (Krampera et al., 2003). The possibility remained at the onset of my project that the relative effects of MSCs on naive T-cells undergoing primary Th17 differentiation differed for those of previously activated, or memory-phenotype T-cells. Furthermore, effector memory T cells have been implicated in non-antigen-specific forms of tissue injury such as ischemia-reperfusion (Dong et al., 2008, Ysebaert et al., 2004) and the effects of MSCs on Th17 cells from non-antigen specific forms of inflammation were unknown.

Controversy also existed over the putative mediator of MSC-induced Th17 suppression with some groups demonstrating a requirement for cell-cell contact

(Gonzalez-Rey et al., 2010) with others reporting roles for various soluble factors including CCL2, IL-27, IDO and TGF-β (Rafei et al., 2009, Wang et al., 2008a, Kong et al., 2009, Zhao et al., 2008). A report by Sheng et al. showed that T-cell-produced IFN-γ induced programmed death ligand 1 (PD-L1) up-regulation on MSCs which was responsible for the suppressive effect observed on $CD4^+$ T-cell proliferation in co-cultures with MSCs (Sheng et al., 2008). Under these culture conditions, cell-cell contact was also necessary for inhibition of proliferation. Therefore, under proinflammatory conditions, certain cytokines may prime MSCs to become immunosuppressive. Furthermore, Wang et al. showed that MSCs indirectly inhibited T-cell proliferation and induced IL-4-producing T-cells over IFN-γ-producing T-cells by impairing DC maturation, antigen presentation and co-stimulation of T-cells (Wang et al., 2008b). Based on this evidence, a wide range of potential mediators and mechanisms of suppression existed at the onset of my project. Further investigation was clearly necessary to interpret such a multifaceted response by MSCs.

Therefore, specific aims for chapter 2 were to:

1. Determine whether MSCs suppress $CD4^+$ T-cells undergoing primary Th17 differentiation *in-vitro*.
2. Determine the requirement for cell-cell contact in MSC effects on Th17 differentiation.
3. Ascertain whether MSCs affect naïve and memory $CD4^+$ T-cells equally during primary Th17 differentiation.
4. Clarify the divergent suppressive and augmenting effects of MSCs on Th17 responses.

2.2 MATERIALS AND METHODS

2.2.1 ANIMAL STRAINS AND ETHICAL APPROVAL

Eight- to 12-week-old female B6 and BALB/c mice were purchased from Harlan Laboratories UK (Bicester, UK) or Charles Rivers Laboratories (Margate, UK). Experimental animals were housed in a specific pathogen-free facility and fed a standard chow diet. All animal procedures were carried out under license from the Irish Department of Health and Children by procedures approved by the NUI Galway Animal Care Research Ethics Committee.

2.2.2 MSC ISOLATION

B6 mouse MSCs were isolated from BM according to the method described by Peister et al. by our colleagues in NUI, Maynooth (Peister et al., 2004). BALB/c and DBA MSCs were isolated according to a similar protocol by researchers in the Regenerative Medicine Institute (REMEDI) in NUI, Galway. A brief methodology for the isolation of mouse MSCs is as follows. On day 0, femurs and tibias from 6-8 week old mice were removed and excess tissue cut away. Marrow was flushed from the bones using a 27 gauge (G) needle filled with complete isolation media (CIM) (see appendix 4 for details of media and buffer compositions). An 18G needle was used to break up clumps. Centrifugation was performed at 600 x relative centrifugal force (RCF) for 5 minutes. Passage (P) 0 cells were counted and plated at 20 x 10^6/T25 vented flask in 8 milliliters (ml) CIM. Non-adherent cells were removed on day 1. The attached cells were washed with sterile Dulbecco's phosphate buffered saline (D-PBS) (see appendix 2 for list of reagents and suppliers). Fresh pre-warmed CIM was added and changed every 3-4 days. Cells were split after 4 weeks using 0.25% trypsin/EDTA for 2 minutes at 37°C. Cells were neutralized with CIM and centrifuged at 600 x RCF for 5 minutes. P1 cells were counted and plated at 1 x 10^6/T25 in CIM. Media was exchanged every 3-4 days for 2 weeks. Cells were split and re-plated at 1 x 10^6/T25 or 5 x 10^6/T75 in 8 ml or 15 ml respectively in complete expansion media (CEM). P2 cells were expanded to P5 and frozen down in freezing media or used experimentally.

2.2.3 MSC CULTURE CONDITIONS

All experiments were carried out with passage 5-9 MSCs grown to 80% confluence in supplemented Iscove's modified Dulbecco's medium (IMDM).

2.2.4 MSC CHARACTERISATION

Tri-lineage differentiation capacity was determined using well described chondrogenic, adipogenic and osteogenic differentiation assays (English et al., 2007) by Georgina Shaw in REMEDI. The cell surface profile of MSCs was extensively characterised by flow cytometry. B6 MSCs expressed CD29, CD44^{low}, CD80, CD106^{low}, MHC-I^{low} and Sca-1 but, similar to B6 MSCs employed in other studies, did not express CD73, CD90 or CD105 (Bouffi et al., 2010) or any hematopoietic cell markers (**Figure 2.1**) (see appendix 3 for list of antibodies employed in this study).

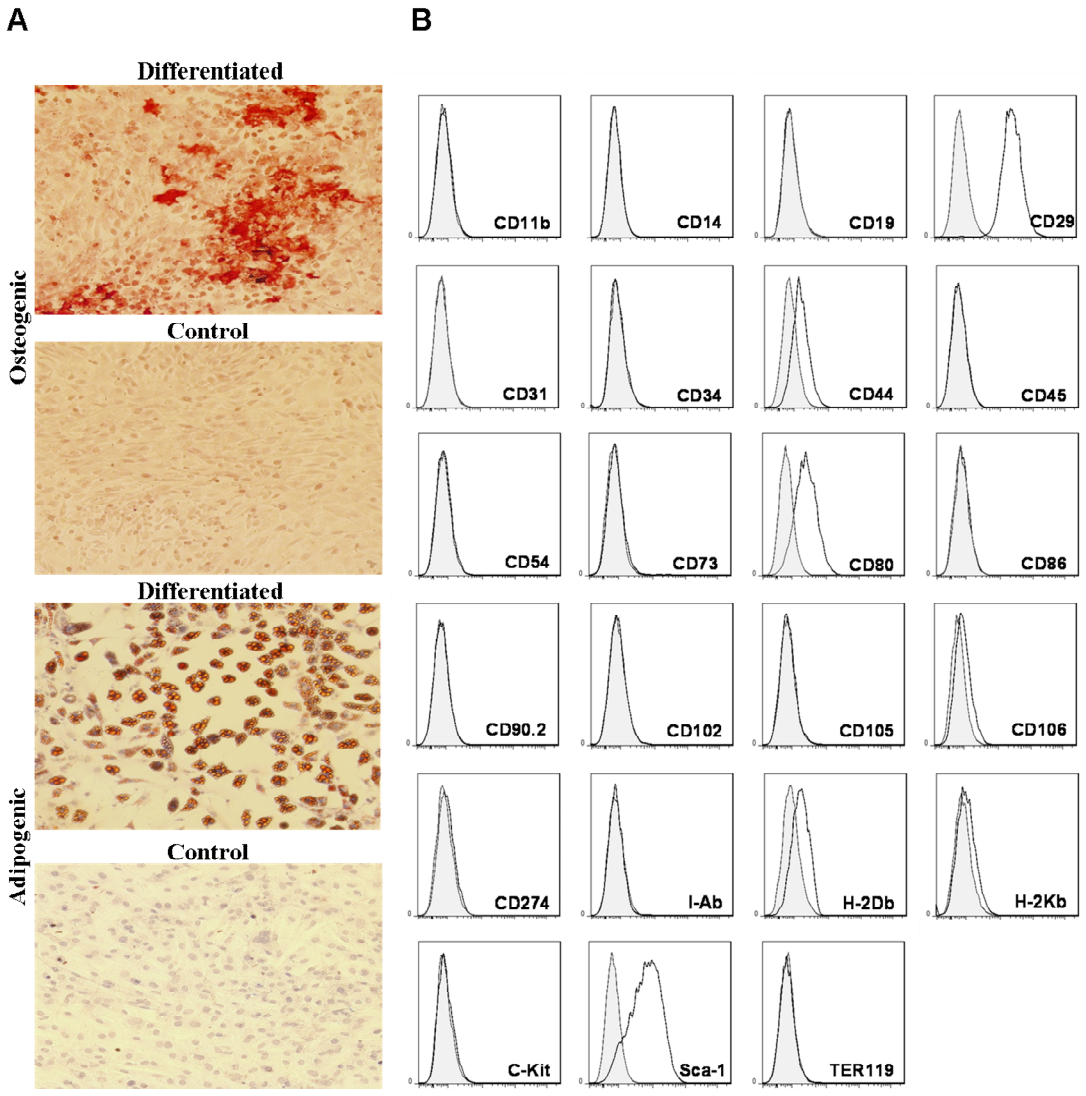

Figure 2.1 Differentiation potential and cell surface profile of B6 BM-derived MSCs. MSCs were subjected to osteogenic (upper A) and adipogenic (lower A) or control differentiation media followed by Alizarin Red S staining (upper A) and Oil Red O staining (lower A). Chondrogenic pellet cultures yielded GAG/DNA ratio > 4 µg/µg. MSCs (open histograms) did not express hematopoietic markers while they expressed CD29, CD44^{low}, CD80, CD106^{low}, MHC-I^{low} and Sca-1. Shaded histograms represent specific isotype controls.

2.2.5 FIBROBLAST ISOLATION

Primary renal cortical fibroblasts were prepared according to the protocol of Alvarez (Alvarez et al., 1992). Briefly, cortex of kidneys from healthy adult mice was diced and forced through a series of mesh screens (230mM, 104mM and 74mM) using a glass pestle. Cells were washed with Hank's Balanced Salt Solution. The resulting cell suspensions were re-suspended in F-12 Nutrient mixture mixed 1:1 with supplemented Dulbecco's modified Eagle's medium (DMEM). The cultured cells were allowed to form colonies in 6-well plates for 7 days. Cells were lifted using 0.2% disodium EDTA, reseeded into T75 flasks at 1 x 10^6/flask and cultured for a further 7 days before use in co-culture experiments.

2.2.6 TH17 DIFFERENTIATION CULTURE

Th17 cell culture was carried out in supplemented DMEM. Single cell suspensions were prepared from mouse spleen and lymph nodes by mechanical disruption and filtering through 150μM Sefar Nitex ribbon mesh (Sefar Ltd., Lancashire, UK). The resulting cell suspension was subjected to erythrocyte lysis in ammonium chloride lysis buffer for 2 minutes at room temperature. Cell suspensions were incubated with anti-mouse CD4 microbeads for 20 minutes at 4°C, washed in MACS buffer and separated using MS columns and an OctoMACS® separator according to manufacturer's instructions (Miltenyi Biotec. Inc., Auburn, CA, USA). $CD4^+$ fractions were washed in MACS buffer, re-suspended in culture medium and used as responders in activation cultures. $CD4^-$ fractions were depleted of remaining T-cells using anti-CD90.2 microbeads by the same protocol and were used as APCs. For Th17 differentiation, $CD4^+$ T-cells and APCs were cultured for 4-5 days in 96-well round bottomed plates or for 3 days in the lower compartment of Corning® HTS Transwell® 96-well permeable supports (Sigma-Aldrich, St. Louis, USA) according to the specifications in **Table 2.1**. In some experiments, $CD4^+$ T-cells were cultured at 1 x 10^6/ml with 1:1 mouse CD3/CD28 T-cell expander beads (Dynabeads®). Other reagents were added as described for individual experiments.

Table 2.1 Concentrations of cells and Th17-inducing factors employed in Th17 differentiation cultures.

Th17 differentiation factors	Concentration
$CD4^+$ T-cells	1 x 10^6/ml
$CD90.2^-$ APCs	2 x 10^6/ml
Anti-CD3ε	1 µg/ml
Anti-IFN-γ	5 µg/ml
Anti-IL-4	4 µg/ml
IL-6	25 ng/ml
TGF-β1	5 ng/ml

For co-culture experiments, MSC or fibroblasts were re-suspended in Th17 culture media and added in graded numbers to the wells of 96-well round-bottom plates. MSCs were allowed to adhere for 4 hours prior to the addition of $CD4^+$ T-cells/APCs or $CD4^+$ T-cells/Dynabeads®. For re-stimulation cultures, Th17-skewed T-cells from primary cultures and co-cultures were subjected to magnetic separation using anti-CD4 microbeads with positive column fractions saved. The resulting re-purified $CD4^+$ T-cells were re-plated at 0.5 x 10^6/ml in fresh medium containing 1:1 Dynabeads® with no other additions in 96-well round-bottom plates for a further 24 hours. Cell culture supernatants were stored at -20°C prior to analysis.

2.2.7 Carboxyfluorescein diacetate succinimidyl ester (CFSE) labelling

For some experiments, $CD4^+$ T-cells were labeled for analysis of proliferation by flow cytometry using CellTrace CFSE cell proliferation kit® (Invitrogen, Paisley, UK). $CD4^+$ T-cells were counted and re-suspended in pre-warmed 0.1% bovine serum albumin (BSA)/PBS (1 x 10^6 cells /ml). Dimethyl sulfoxide (DMSO) was used to reconstitute the CFSE. CFSE was added to the cells (2 µl/1 x 10^6 cells). Cells were incubated at 37°C in a water bath for 10 minutes. Ice-cold 10% serum-supplemented media was added to the cells (twice the volume of BSA/PBS solution). Cells were centrifuged at 400 RCF and washed twice more. Cells were re-counted prior to experimentation.

2.2.8 Flow cytometry, intracellular staining, and fluorescence-activated cell sorting (FACS)

For flow cytometry experiments, cells were suspended in FACS buffer at 5 x 10^6/ml. Cells were incubated with various combinations of fluorochrome-labeled antibodies for 20 minutes at 4°C (see appendix 3 for list of antibody preparations). Cells were

washed and re-suspended in FACS buffer prior to being analysed using a Becton Dickinson (BD) Biosciences FACSCanto® cytometer (San Jose, CA, USA) and FlowJo® software (TreeStar Inc., Olten, Switzerland). For intracellular staining, brefeldin A (GolgiPlug® 1 µl/ml, BD Biosciences) was added to cultures for 8 hours prior to analysis. Surface staining was performed prior to intracellular staining using Cytofix/Cytoperm® reagents (BD Biosciences). For FACS experiments, magnetic column-enriched $CD4^+$ T-cells were incubated for 20 minutes in FACS sorting buffer at 4°C with combinations of fluorochrome-labeled antibodies. Cells were washed and re-suspended in FACS sorting buffer prior to being sorted using a BD FACSAriaII®.

2.2.9 Enzyme-linked immunosorbent assay (ELISA)

Supernatants from cultures and co-cultures were analysed by ELISA using DuoSet® ELISA Development Systems (R&D Systems, Minneapolis, MN, USA.) for IL-17A, IFN-γ and TGF-β1. Briefly, flat-bottomed 96-well plates were coated with capture antibody diluted in PBS overnight. The following morning, plates were washed in 0.05% Tween 20®/PBS. Plates were blocked in 1%BSA/PBS for 1 hour prior to being washed in 0.05% Tween 20®/PBS. Standards and pre-diluted samples were added to the plate for 2 hours. Plates were washed in 0.05% Tween 20®/PBS followed by coating with biotin-labeled detection antibody diluted in 1% BSA/PBS for 2 hours. Plates were washed in 0.05% Tween 20®/PBS prior to the addition of streptavidin-horseradish peroxidase (HRP) diluted in 1%BSA/PBS for 20 minutes in the dark. Plates were washed in 0.05% Tween 20®/PBS. Tetramethylbenzidine substrate was added for 20 minutes. Stop solution (2 M sulphuric acid) was added and the absorbance was read at 450 nm on a Wallac 1420 Victor3™ Multilabel Counter plate reader (Perkin Elmer, Waltham, MA, USA).

2.2.10 Bio-Plex® analysis of culture supernatnants

A multi-plex murine cytokine kit (Biorad, Hercules, CA, USA) was employed to quantify multiple different analytes simultaneously in the same sample. Briefly, a 96-well filter assay plate was pre-wet with assay buffer and vacuum-filtered. Antibody-coupled beads were added to the plate. Each bead contained a unique spectral signature of 2 fluorescent dyes specific for a particular analyte. Two vacuum-filtered washes were performed. An 8-point broad range cytokine standard curve and pre-diluted samples were added to the plate for 30 minutes. Three vacuum-filtered washes

were performed. Biotinylated detection antibody was added to the plate for 30 minutes. Three vacuum-filtered washes were performed. Streptavidin-PE was added for 10 minutes. Three vacuum-filtered washes were performed. The beads were re-suspended in the plate which was analyzed on a Bio-Plex® 200 suspension array system (Biorad). The constituents of each well were drawn up into the flow-cell where the fluorescent dyes embedded in the beads were excited by the red laser whilst the PE reporter dye in the reaction mixture was excited by the green laser. Specific cytokines were identified by detection of the specific fluorescent spectral signature of each bead. Quantification of individual cytokines was performed by measuring the fluorescence intensity of the streptavidin-PE. Unknown cytokine concentrations were automatically calculated by the Bio-Plex Manager™ software using the standard curve derived from the recombinant cytokine standard.

2.3 RESULTS

2.3.1 MSCs INHIBIT THE PRIMARY DIFFERENTIATION OF TH17 CELLS

In initial experiments I elected to co-culture MSCs with $CD4^+$ T-cells undergoing Th17 induction to determine the effects of MSCs on primary differentiating Th17 cells. B6 MSCs were co-cultured for 4 days with autologous $CD4^+$ T-cells during primary activation with anti-CD3ε and APCs under Th17-skewed conditions at MSC:$CD4^+$ T-cell ratios of 1:2000–1:20. In these cultures, the day 4 concentration of IL-17A was significantly different between the groups [$p\ (1,5) = <0.0001$; $F = 189.2$] as deduced by one-way analysis of variance (ANOVA) (**Figure 2.2A**). Post hoc analysis using Tukey's multiple comparison test showed that the control with 0 MSCs had significantly greater IL-17A accumulation on day 4 than all other groups with the exception of the lowest grade of MSCs (1:2000). IL-17A sequentially decreased with increasing numbers of MSCs.

CD25 is the IL-2R α chain and a marker of T-cell activation. Surface expression level of CD25 by $CD4^+$ T-cells was reduced in a dose-dependent manner in the presence of MSCs and significantly different between the groups [$p\ (1,5) = <0.0001$; $F = 406.3$] (**Figure 2.2B**).

When re-stimulation of equal numbers of $CD4^+$ cells retrieved from the cultures was carried out using anti-CD3/anti-CD28 beads, IL-17A production was significantly different between the groups [$p\ (1,5) = <0.0001$; $F = 121.5$]. Concentrations of IL-17A were dose-dependently lower for cells generated in the presence of MSCs (**Figure 2.2C**). In multiple experiments, inhibition was consistently observed at MSC:$CD4^+$ T-cell ratios as low as 1:400.

This series of experiments demonstrated that Th17-skewed culture conditions yielded high levels of IL-17A and T-cell activation. $CD4^+$ T-cells re-stimulated under non-skewed conditions retained the Th17 phenotype. Furthermore, MSCs potently suppressed Th17 responses in terms of IL-17A production in the primary culture in addition to IL-17A production by CD4+ T-cells re-stimulated in the absence of MSCs under non-Th17 skewed conditions. Moreover, MSCs prevented the upregulation of CD25 expression by $CD4^+$ T-cells.

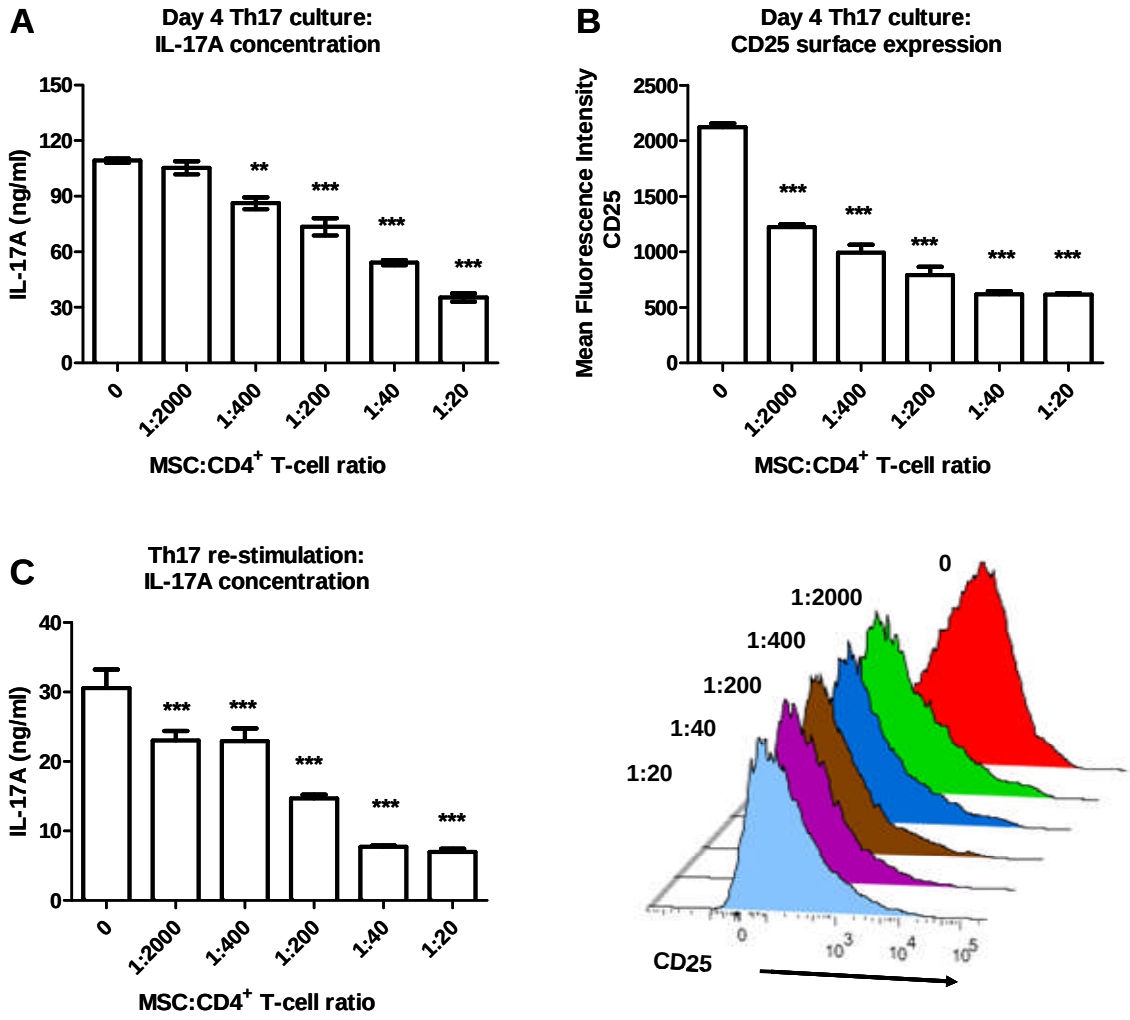

Figure 2.2 Inhibition of Th17 differentiation by MSCs: $CD4^+$ T-cells were cultured under Th17-skewed conditions with anti-CD3ε and APCs with graded concentrations of autologous MSCs for 4 days. (**A**) Concentration of IL-17A in supernatants at day 4 as measured by ELISA, (**B**) surface expression level of CD25 on $CD4^+$ T-cells at day 4 (**Below**: examples of anti-CD25 histograms with cells gated on $CD4^+$ cells) as measured by flow cytometry, and (**C**) IL-17A concentrations in supernatants of repurified $CD4^+$ T-cells re-stimulated for 24 hours with anti-CD3/anti-CD28-coated beads. Data are represented as mean +/-standard deviations and are representative of five individual experiments (** p = < 0.01, *** p = <0.001 compared with 0 MSC control, Tukey's multiple comparison test).

2.3.2 PRIMING OF MSCS BY IFN-γ IS UNNECESSARY FOR SUPPRESSION OF TH17 DIFFERENTIATION.

Under Th17-skewed conditions, blockade of IFN-γ is necessary to prevent the induction of Th1 cells. Experiments to date have demonstrated that MSCs potently suppress Th17 differentiation in the presence of IFN-γ blockade. IFN-γ has, however, been reported to be necessary for triggering of maximal T-cell inhibitory effects of MSCs under some conditions (Krampera et al., 2006, Ryan et al., 2007). Therefore, in this series of experiments I sought to determine whether omission of anti-IFN-γ from the primary co-cultures was associated with more potent MSC-mediated Th17 suppression.

The importance of the presence of anti-IFN-γ in Th17 cultures was highlighted by limited Th17 responses in its absence (**Figure 2.3A**). The absence of anti-IFN-γ did not significantly alter CD25 surface expression (**Figure 2.3B**) while the concentration of IL-17A in re-stimulated culture supernatants remained lower for cells generated in the presence of MSCs regardless of the anti-IFN-γ status (**Figure 2.3C**).

I observed inhibition of Th17 differentiation to occur despite the presence of anti-IFN-γ however, omission of anti-IFN-γ resulted in less effective Th17 differentiation. Nonetheless, a comparable suppressive effect of MSCs was observed in the presence and absence of IFN-γ blockade in terms of CD25 expression and IL-17A production in re-stimulated cultures. Therefore, IFN-γ priming of MSCs is unnecessary for MSC-mediated inhibition of Th17 induction.

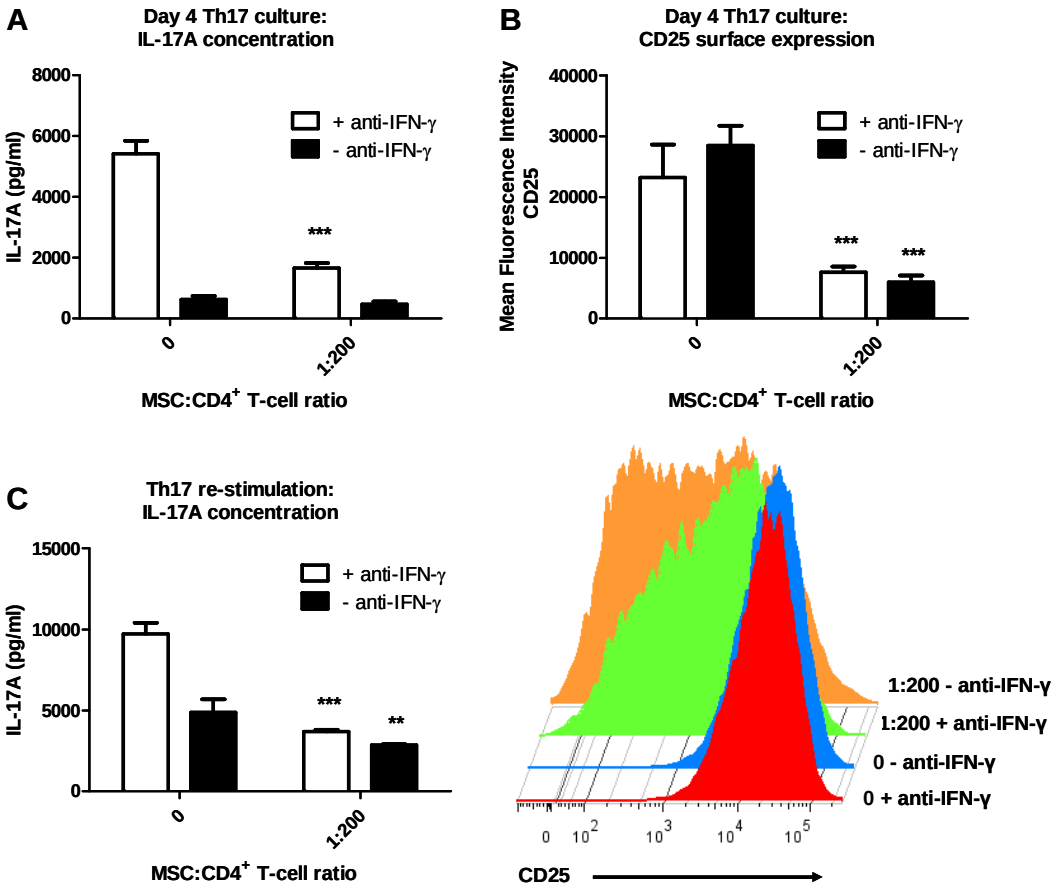

Figure 2.3 IFN-γ does not enhance MSC-mediated suppression of Th17 cells: $CD4^+$ T-cells were cultured in the presence or absence of anti-IFN-γ with anti-CD3/anti-CD28-coated beads, anti-IL-4, IL-6 and TGF-β1 with 1:200 MSC:$CD4^+$ T-cell cell ratio for 4 days. (**A**) Concentration of IL-17A in supernatants at day 4 as measured by ELISA, (**B**) surface expression level of CD25 on $CD4^+$ T-cells at day 4 (**Below**: examples of anti-CD25 histograms with cells gated on $CD4^+$ cells) as measured by flow cytometry, and (**C**) IL-17A concentration following overnight stimulation of re-purified $CD4^+$ T-cells Data are represented as mean +/-standard deviations and are representative of triplicate samples from one experiment (** p = < 0.01, *** p = <0.001 compared with 0 MSC control, Bonferroni posttest).

2.3.3 MSC-SPECIFIC INHIBITION OF TH17 CELLS IS NOT STRAIN-SPECIFIC

Different strains of mice exhibit different characteristics in terms of MSC biology in particular in relation to cell surface marker expression and differentiation potential (Bouffi et al., 2010). These experiments were designed to determine whether MSCs from different strains of mice were capable of suppressing Th17 cells from allogeneic counterparts.

The inhibitory effect of MSCs on primary Th17 activation was not strain-specific being demonstrable in an allogeneic cross-over experiment in which BALB/c MSCs inhibited IL-17A production by B6 $CD4^+$ T-cells following overnight re-stimulation of equal numbers of $CD4^+$ T-cells retrieved from primary Th17 induction co-cultures (**Figure 2.4A**). The level of suppression was comparable to that of B6 MSC-mediated suppression of BALB/c $CD4^+$ T-cells (**Figure 2.4B**). One-way ANOVA revealed significant differences between the groups [p (1,5) = <0.0001; F = 65.72] and [p (1,5) = <0.0001; F = 75.89], **Figures 2.4A** and **2.4B** respectively. Furthermore, DBA MSCs also displayed immunosuppressive characteristics (data not shown).

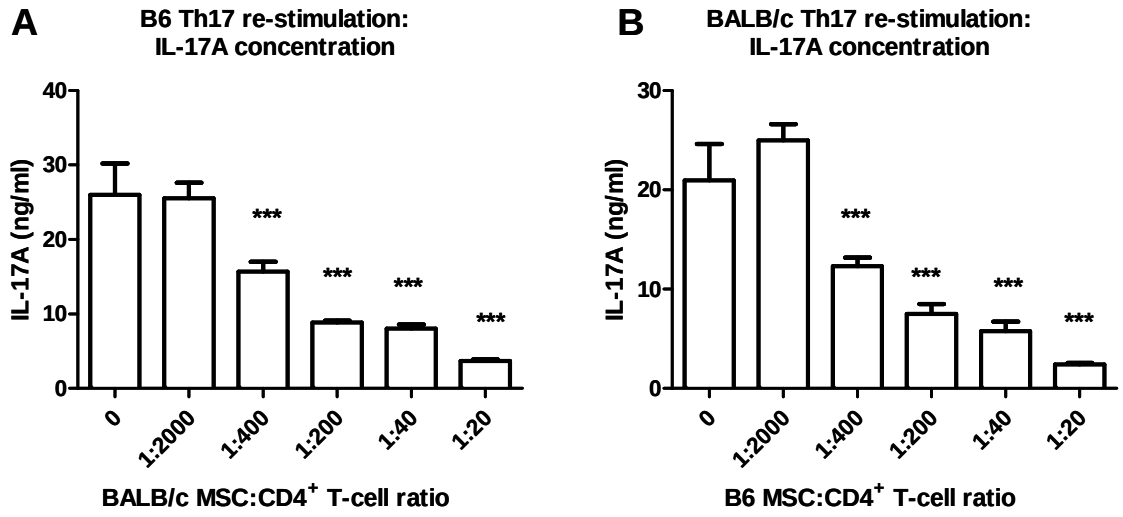

Figure 2.4 MSC-specific inhibition of Th17 differentiation is not strain-specific: B6 $CD4^+$ T-cells were cultured for 5 days under Th17-skewed conditions with anti-CD3ε and autologous APCs and graded numbers of BALB/c MSCs while BALB/c $CD4^+$ T-cells were also cultured for 5 days under Th17-skewed conditions with anti-CD3ε and autologous APCs and graded numbers of B6 MSCs. $CD4^+$ cells were repurified by MACS and re-stimulated overnight with anti-CD3/anti-CD28-coated beads. (**A**) IL-17A concentration following overnight stimulation of re-purified B6 $CD4^+$ T-cells. (**B**) IL-17A concentration following overnight stimulation of re-purified BALB/c $CD4^+$ T-cells. Data are represented as mean +/-standard deviations and are representative of triplicate samples from one experiment (*** p = <0.001 compared with 0 MSC control, Tukey's multiple comparison test).

2.3.4 MSC INHIBITION OF TH17 CELLS REQUIRES CELL-CELL CONTACT

A requirement for initial cell–cell contact was examined using Transwell cultures in which $CD4^+$ T cells undergoing primary Th17 induction in the presence of APCs and anti-CD3ε in the lower compartment, were separated from MSCs in the upper compartment.

One-way ANOVA revealed significant differences between the groups [p (1,5) = 0.0003; F = 11.48]. However, in these experiments, the concentration of IL-17A in culture supernatants at day 3 was not reduced in the presence of MSCs (**Figure 2.5A**).

Similarly, significant differences were detected between the groups in terms of CD25 expression [p (1,5) = 0.0002; F = 12.3]. In this case, a modest reduction in the surface level of CD25 on $CD4^+$ T cells was observed at the highest MSC:T-cell ratios of 1:60 and 1:30 (**Figure 2.5B**).

Significant differences also occurred in the re-stimulation cultures [p (1,5) = <0.0001; F = 21.84]. Reduction in IL-17A production following re-stimulation occurred only at the highest MSC:T-cell ratio of 1:30 (**Figure 2.5C**). Consistently, comparable degrees of Th17 inhibition in cultures lacking direct T-cell/MSC contact required >ten-fold greater MSC numbers than direct contact co-cultures. Therefore, cell-cell contact was a key component of the suppressive nature of MSCs directed towards primary differentiating Th17 cells.

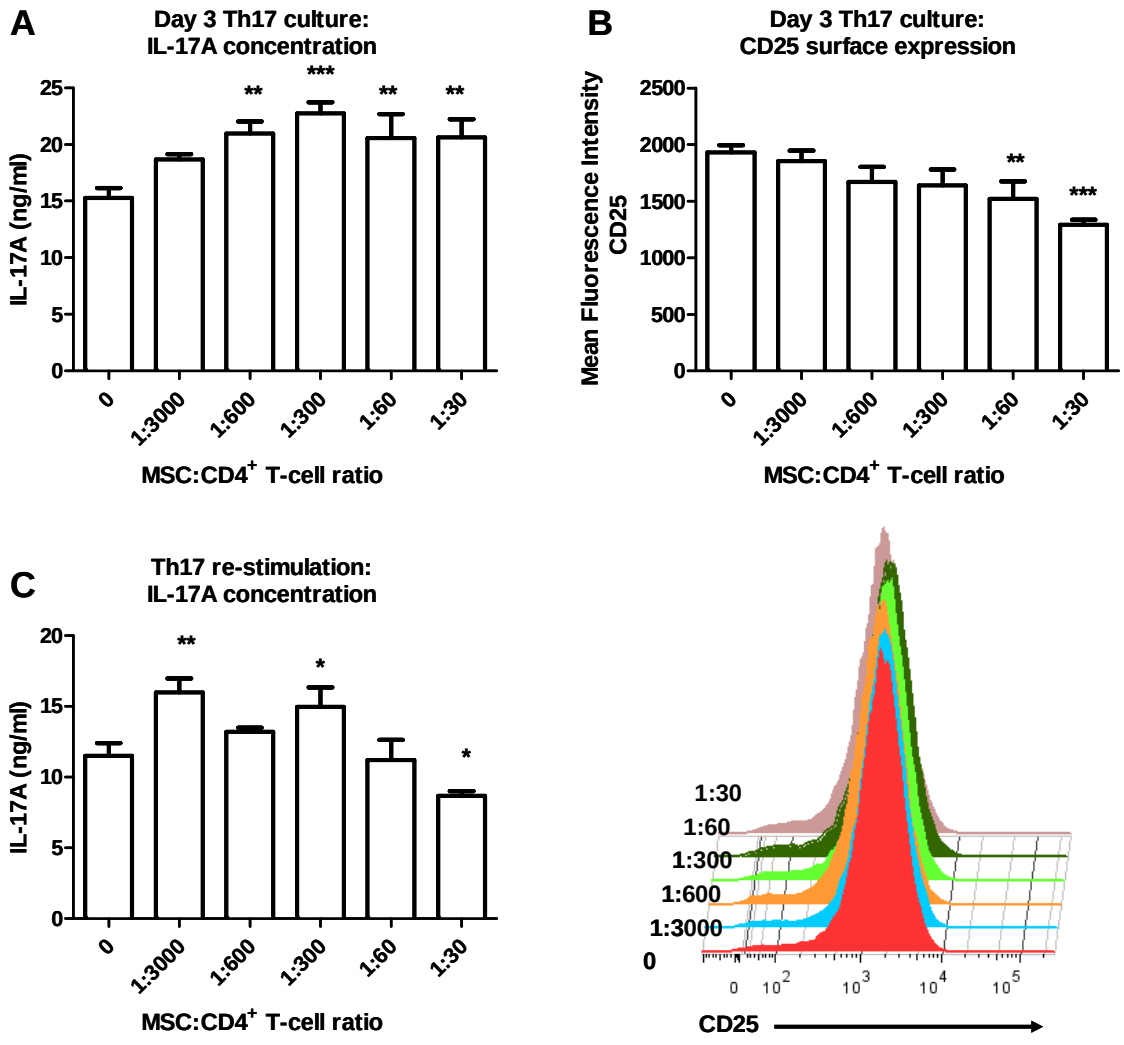

Figure 2.5 Inhibition of Th17 cells by MSCs is limited in the absence of cell–cell contact: $CD4^+$ T-cells were activated with anti-CD3ε and APCs under Th17-skewed conditions separated from B6 MSCs at the indicated ratios in Transwell® plates. (**A**) Concentration of IL-17A in supernatants at day 3 as measured by ELISA. (**B**) Surface expression of CD25 on $CD4^+$ T cells at day 3, as measured by flow cytometry (**Below**: examples of anti-CD25 histograms with cells gated on $CD4^+$ cells). (**C**) IL-17A concentrations in supernatants of re-purified $CD4^+$ T-cells re-stimulated for 24 hours with anti-CD3/anti-CD28-coated beads, as measured by ELISA. Data are represented as mean +/-standard deviations and are representative of 3 individual experiments (* p = <0.05, ** p = <0.01, *** p = <0.001 compared with 0 MSC control, Tukey's multiple comparison test).

2.3.5 Inhibition of primary Th17 differentiation by MSCs occurs with both naïve- and memory-phenotype responders

Phenotypic differences exist between naïve- and memory-phenotype $CD4^+$ T-cells including the loss of migration and adhesion markers (CD62L) by memory T-cells and increased potency with more rapid responses to secondary re-encounter with corresponding antigens. It was of interest therefore, to determine whether MSCs may have diverse effects on naïve- and memory-phenotype responders undergoing primary Th17 differentiation.

Experiments thus far were performed on bulk MACS-enriched $CD4^+$ T-cells. Additional experiments were carried out to investigate the effects of MSCs on highly purified naïve- and memory-phenotype-responders. MACS-enriched $CD4^+$ T cells were therefore further purified by FACS. Cells were gated on viable $CD4^+$ cells following doublet discrimination and sorted into naïve- ($CD25^-/CD62L^{high}$) and memory- ($CD25^-/CD62L^{low}$) phenotype populations (**Figure 2.6**). Post sort purity was consistently greater than 90%.

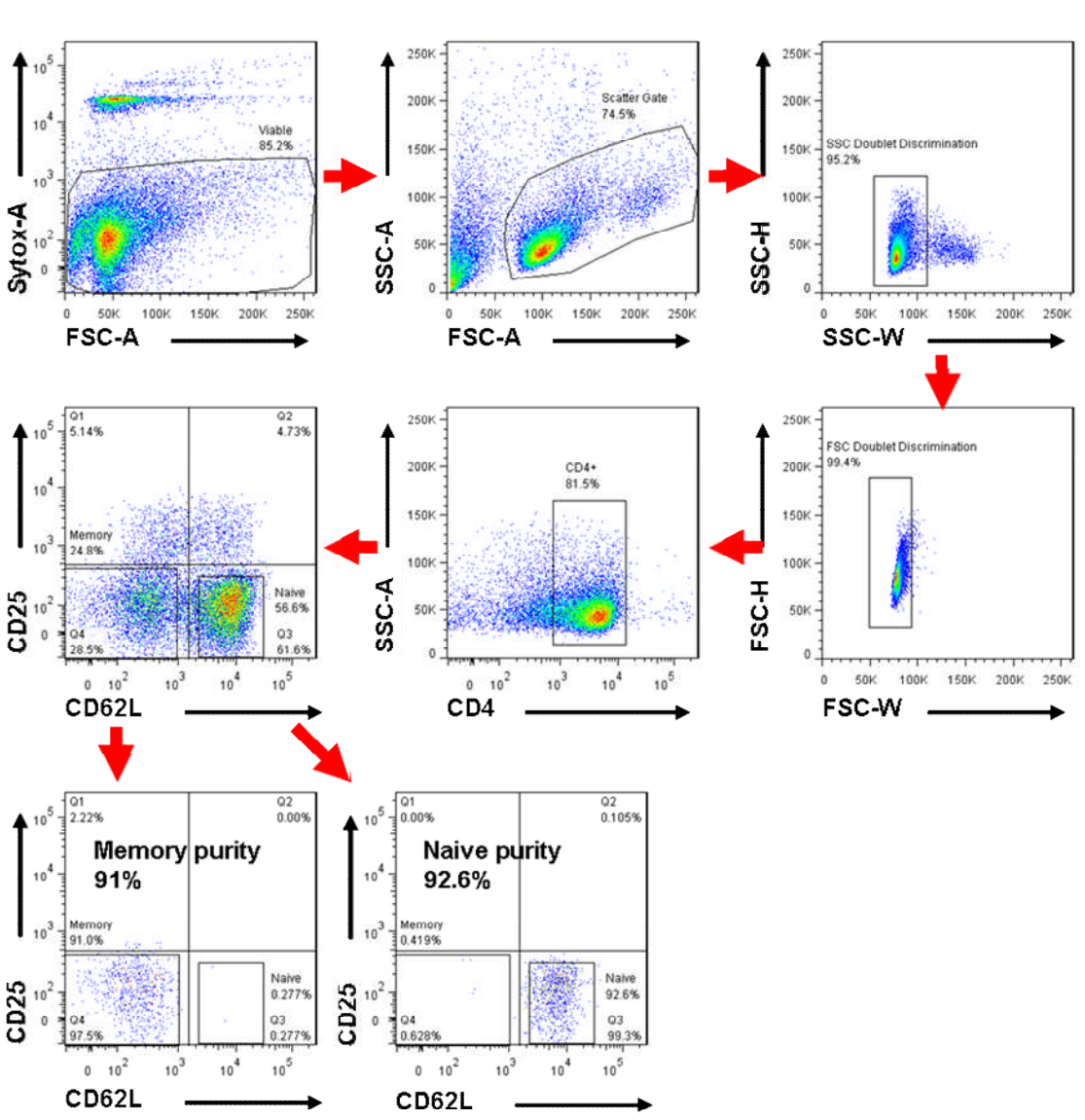

Figure 2.6 Representative gating strategy for FACS experiments in which $CD4^{+}CD25^{-}CD62L^{+}$ naïve and $CD4^{+}CD25^{-}CD62L^{-}$ memory T-cells were sorted prior to co-culture with MSC.

Naïve and memory-phenotype responders were separately activated under Th17-skewed conditions in the presence or absence of MSCs. For both responder populations, co-culture with low numbers of MSCs (MSC:T-cell ratio 1:400) was associated with reduced IL-17A accumulation in culture supernatants at day 4 (**Figure 2.7A**). MSCs also significantly inhibited CD25 up-regulation on both naïve and memory T-cells on day 4 of co-culture (**Figure 2.7B**).

IL-17A production upon re-stimulation was reduced in both naïve and memory T-cells following Th17 differentiation in the presence of MSCs (**Figure 2.7C**). Qualitatively similar results were observed in a total of five similar experiments with

median proportionate inhibition of IL-17A production following re-stimulation of 26% (range 13–66%) for memory-phenotype responders and 66% (range 33–80%) for naïve-phenotype responders.

This series of experiments demonstrated that memory cells produced more IL-17A than naïve cells and that MSCs displayed proportionately less overall suppression of the Th17 phenotype when co-cultured with memory-phenotype responders.

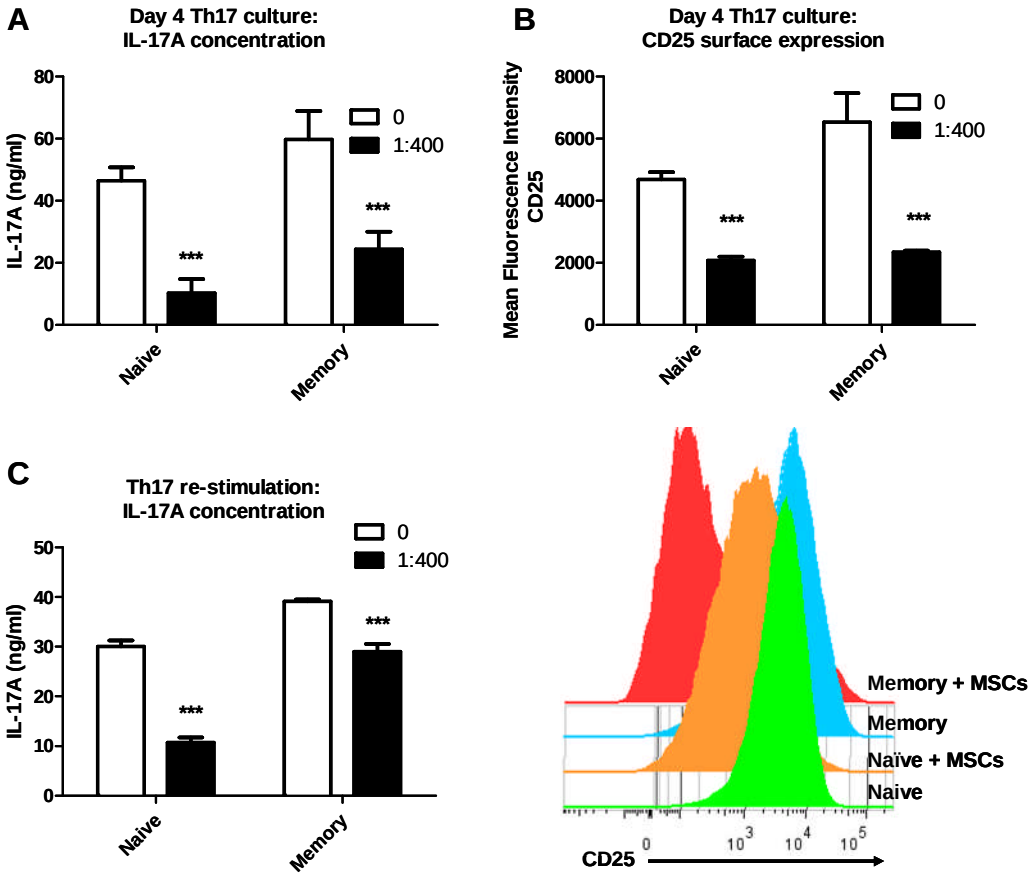

Figure 2.7 MSCs inhibit both naïve- and memory-phenotype responders: FACS-purified naïve ($CD4^+CD62L^+CD25^-$) and memory ($CD4^+CD62L^-CD25^-$) T-cells were separately activated under Th17-skewed conditions in the presence or absence of MSCs for 4 days. (**A**) Concentration of IL-17A in supernatants at day 4 as measured by ELISA. (**B**) Surface expression of CD25 on $CD4^+$ T cells at day 4, as measured by flow cytometry (**Below**: examples of anti-CD25 histograms with cells gated on $CD4^+$ cells). (**C**) IL-17A concentrations in supernatants of re-purified $CD4^+$ T-cells re-stimulated for 24 hours with anti-CD3/anti-CD28-coated beads, as measured by ELISA. Data are represented as mean +/-standard deviations and are representative of 3 individual experiments for **A/B** and 5 individual experiments for **C** (*** p = <0.001 compared with 0 MSC control, Bonferroni posttest).

Furthermore, in addition to IL-17A, I elected to quantify other cytokines and growth factors secreted in MSC co-cultures with both naïve- and memory-phenotype $CD4^+$ T-cells undergoing primary Th17 differentiation in the presence of APCs and anti-CD3ε.

A multi-plex murine cytokine kit was used to analyze multiple different analytes in the same sample on a Bio-Plex® 200 suspension array system. This technology employs a dual laser flow cytometer, fluorescently labeled beads and a digital signal processor in which quantification of analytes is achieved using the principle of sandwich immunoassay. Additionally, TGF-β1 was measured using a standard Duoset® ELISA kit from R&D Systems.

Supernatants from both naïve and memory $CD4^+$ T-cells co-cultured with MSCs under Th17-skewed conditions in the presence of APCs contained minimal concentrations of Th1-associated IFN-γ (< 15 pg/ml) and Th2-associated IL-4 (< 10 pg/ml) demonstrating the effectiveness of IFN-γ and IL-4 blockade in these cultures (**Figure 2.8A/B**). The T-cell growth factor IL-2 was predominantly produced in naïve T-cell cultures and was increased in the presence of MSCs (**Figure 2.8A**). The Th17-inducing factor TGF-β1 was significantly increased in both naïve and memory T-cell co-cultures with MSCs while IL-6 was specifically increased in memory T-cell/MSC co-cultures (**Figure 2.8C**). IL-1α and IL-1β concentrations were both reduced in the presence of MSCs (**Figure 2.8C**). The chemokines CCL2/MCP-1 (monocyte chemotaxis) and CXCL1/growth-regulated-α (GRO-α) (neutrophil chemoattractant and melanoma growth factor) were increased in both naïve and memory T-cell cultures in the presence of MSCs (**Figure 2.8D**). However, CCL3/macrophage inflammatory protein 1-α (MIP-1α), CCL4/MIP-1β and CCL5/regulated upon activation, normal T-cell expressed and secreted (RANTES) were selectively produced in memory T-cell cultures. Furthermore, all 3 chemokines were significantly suppressed in the presence of MSCs (**Figure 2.8D**).

Overall, supernatants from both naïve and memory T-cell co-cultures with MSCs contained reduced concentrations of pro-inflammatory IL-1α, IL-1β, IL-12p70, IFN-γ, and TNF-α in addition to anti-inflammatory IL-10. In contrast TGF-β1, MCP-1 and CXCL1 were increased in the presence of MSCs. Furthermore, memory T-cell co-cultures with MSCs contained reduced concentrations of pro-inflammatory MIP-1α, MIP-1β and RANTES. These results highlight the complexity of the interactions between MSCs & $CD4^+$ T-cells, particularly in the presence of APCs.

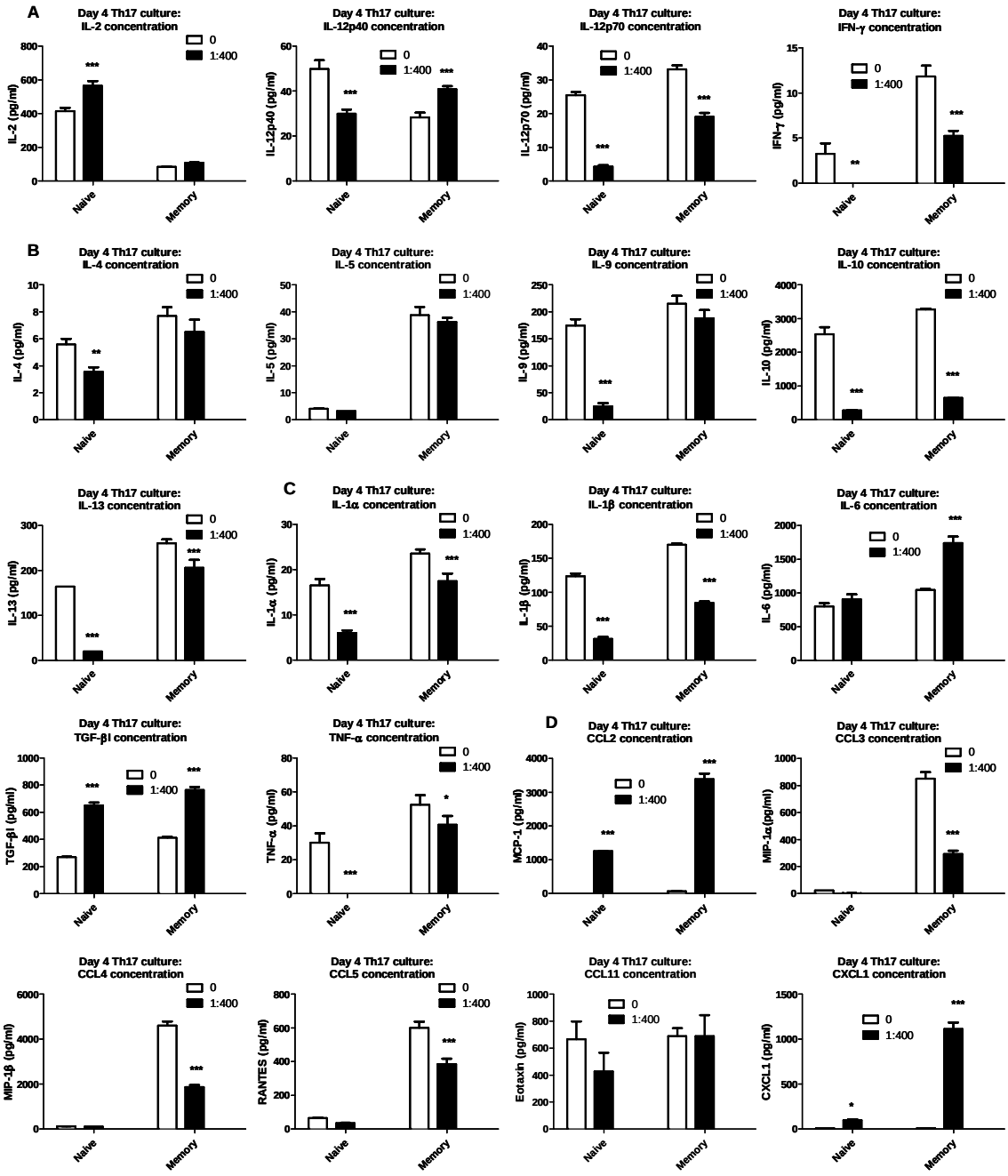

Figure 2.8 Cytokine and chemokine analysis: FACS-purified naïve and memory T-cells were separately activated under Th17-skewed conditions in the presence or absence of MSCs for 4 days. Supernatants were subjected to a BioPlex® 200 immunoassay or ELISA (TGF-β1) (**A**) Concentration of Th1-related cytokines. (**B**) Concentration of Th2-related cytokines. (**C**) Concentration of Th17-inducing cytokines and factors produced by Th17 cells. (**D**) Concentration of chemokines. Data are represented as mean +/-standard deviations and are representative of triplicate samples from 1 experiment (* p = <0.05, ** p = <0.01, *** p = <0.001 compared with appropriate 0 MSC control, Bonferroni posttest).

2.3.6 MSC INHIBITION OF TH17 CELLS IS ASSOCIATED WITH MODERATE ANTI-PROLIFERATIVE EFFECT BUT POTENT SUPPRESSION OF IL-17A

MSCs have been reported to have potent anti-proliferative effects on multiple T-cell lineages (Bartholomew et al., 2002, Di Nicola et al., 2002). It was possible therefore that the suppressive effect observed on IL-17A production in experiments thus far was solely a consequence of inhibition of $CD4^+$ T-cell proliferation. For this reason experiments were designed to determine whether the suppression of IL-17A production by Th17 cells was entirely explained by MSC-mediated inhibition of T-cell proliferation or whether MSCs specifically prevent IL-17A production independent of inhibition of T-cell proliferation. CFSE-labeling in combination with intracellular IL-17A staining by flow cytometry was employed.

Both naïve- and memory-phenotype $CD4^+$ T-cells co-cultured with MSCs retained the capacity to proliferate. Co-culture with a low ratio of MSCs (1:200 MSC:$CD4^+$ T-cell) was associated with a moderate anti-proliferative effect under Th17-skewed conditions using CFSE labeling (**Figure 2.9A**). A reduced proportion of IL-$17A^+$ cells were detected in the presence of MSCs within each generation of cell division using intracellular staining for IL-17A (**Figure 2.9A/B**).

This series of experiments demonstrated two discrete properties of MSC-modulation of Th17 cells: (A) Moderate inhibition of T-cell proliferation and (B) potent suppression of IL-17A production in divided cells.

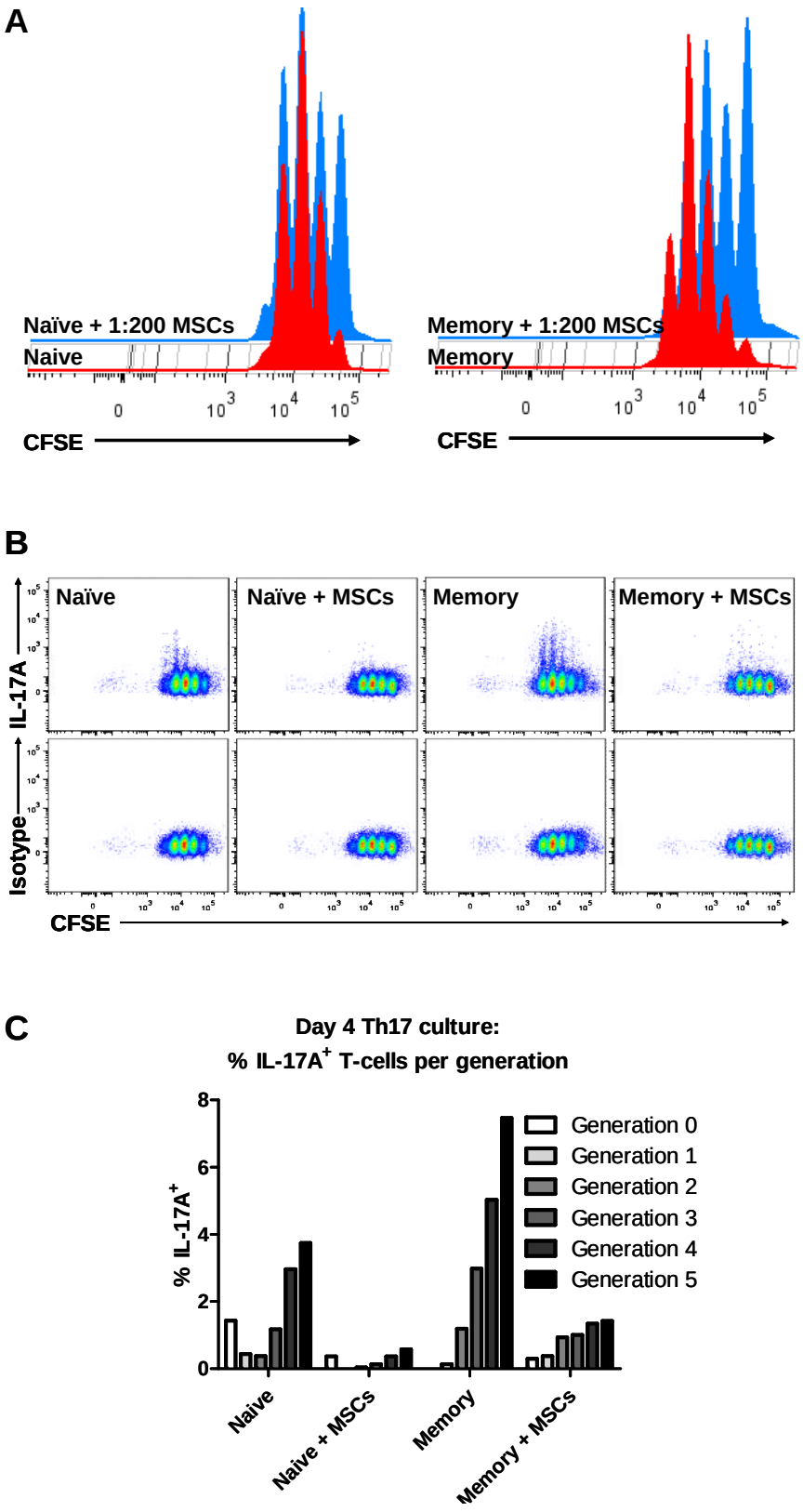

Figure 2.9 MSC inhibition of Th17 differentiation in relation to T-cell division: FACS-purified naïve- and memory-phenotype $CD4^+$ T-cells were CFSE-labeled and activated with anti-CD3ε plus APCs under Th17-skewed conditions with 1:200 MSC:$CD4^+$ T-cells. (**A**) CFSE dye dilution histograms illustrating $CD4^+$ T-cell proliferation at day 4. (**B**) Representative dot plots showing intracellular IL-17A staining relative to CFSE dilution in $CD4^+$ T-cells at day 4. (**C**) Graphic representation of the proportions of each generation that were IL-$17A^+$. Data are representative of three individual experiments.

2.3.7 Th17 suppression of both naïve and memory $CD4^+$ T-cells is MSC specific

The specificity of MSC suppression of Th17 differentiation was demonstrated in experiments in which the effects of primary mouse fibroblasts were compared to those of MSCs. Inhibition of Th17 responses was not apparent following co-culture with primary renal cortical fibroblasts. MSCs consistently suppressed IL-17A production by Th17-skewed naïve- and memory-phenotype $CD4^+$ T-cells to a much greater extent than fibroblasts in both day 4 culture supernatants and in re-stimulation cultures (**Figure 2.10A/C**). In contrast to MSCs, the presence of fibroblasts in Th17 cultures did not alter CD25 surface expression compared to 0 MSC/fibroblast control (**Figure 2.10B**).

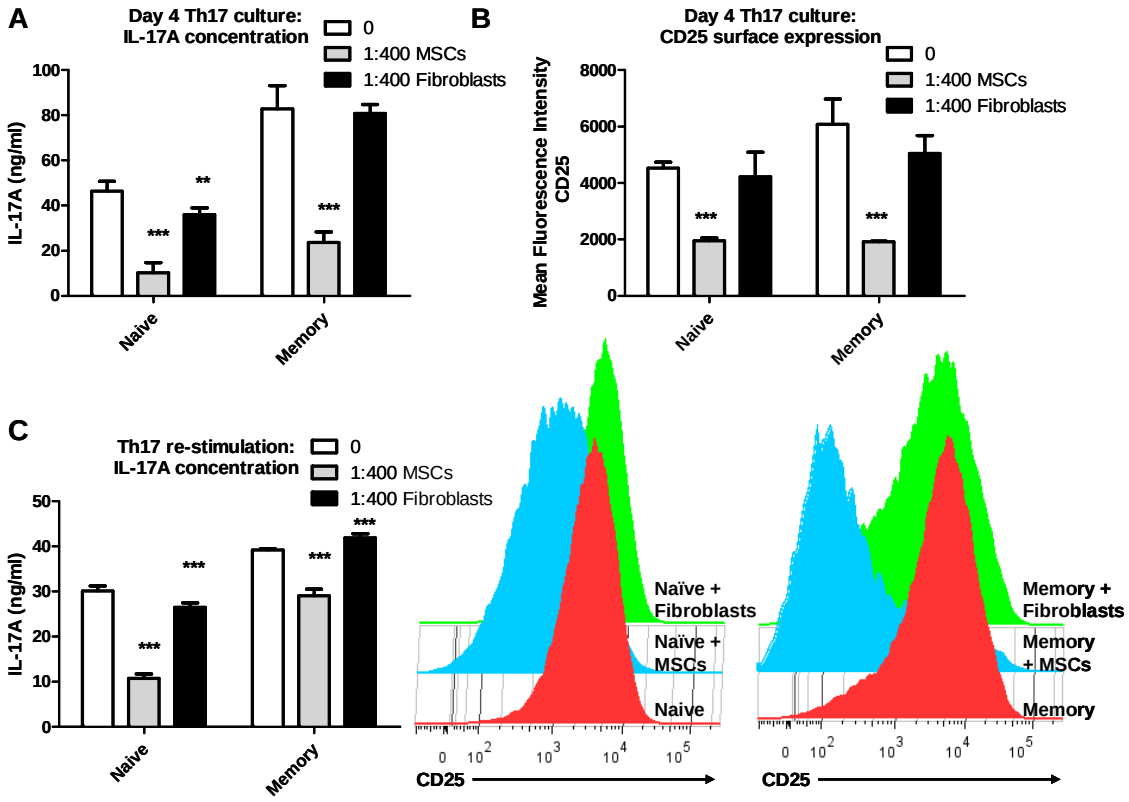

Figure 2.10 MSC-specific inhibition of Th17 differentiation: FACS-purified naïve and memory T-cells were separately activated under Th17-skewed conditions in the presence or absence of MSCs or renal cortical fibroblasts for 4 days. (**A**) Concentration of IL-17A in supernatants at day 4 as measured by ELISA. (**B**) Surface expression of CD25 on $CD4^+$ T cells at day 4, as measured by flow cytometry (**Below**: examples of anti-CD25 histograms with cells gated on $CD4^+$ cells). (**C**) IL-17A concentrations in supernatants of re-purified $CD4^+$ T-cells re-stimulated for 24 hours with anti-CD3/anti-CD28-coated beads, as measured by ELISA. Data are represented as mean +/-standard deviations and are representative of 2 individual experiments for (** p = <0.01, *** p = <0.001 compared with 0 MSC/fibroblast control, Bonferroni posttest).

2.3.8 MSC-SPECIFIC INHIBITION OF TH17 DIFFERENTIATION IS NOT DEPENDENT ON APCS

MSCs have been reported to impair antigen presentation, cytokine production and maturation of APCs including DCs (Cutler et al., 2010) raising the possibility that the suppressive effects I observed on primary Th17 differentiation may be an indirect result of MSC effects on APC populations in the primary Th17 differentiation cultures. The direct nature of MSC suppression of Th17 differentiation was demonstrated in an APC-free system.

The possibility that monocyte/macrophages or DCs were responsible for indirectly mediating MSC suppressive effects on naïve and memory T-cell responders was eliminated by experiments in which primary $CD4^+$ T-cell/MSC co-cultures were initiated with anti-CD3/anti-CD28-coated beads rather than APCs. In this case, the Th17-suppressive effect of MSCs for both naïve and memory $CD4^+$ T-cells persisted (**Figure 2.11**). The concentration of IL-17A in day 4 supernatants and in re-stimulated cultures in addition to CD25 surface expression was significantly reduced in the presence of MSCs. Similar to experiments carried out in the presence of APCs, MSC effects on memory-phenotype $CD4^+$ T-cells undergoing primary Th17 differentiation were not as potent as those of naïve-phenotype responders.

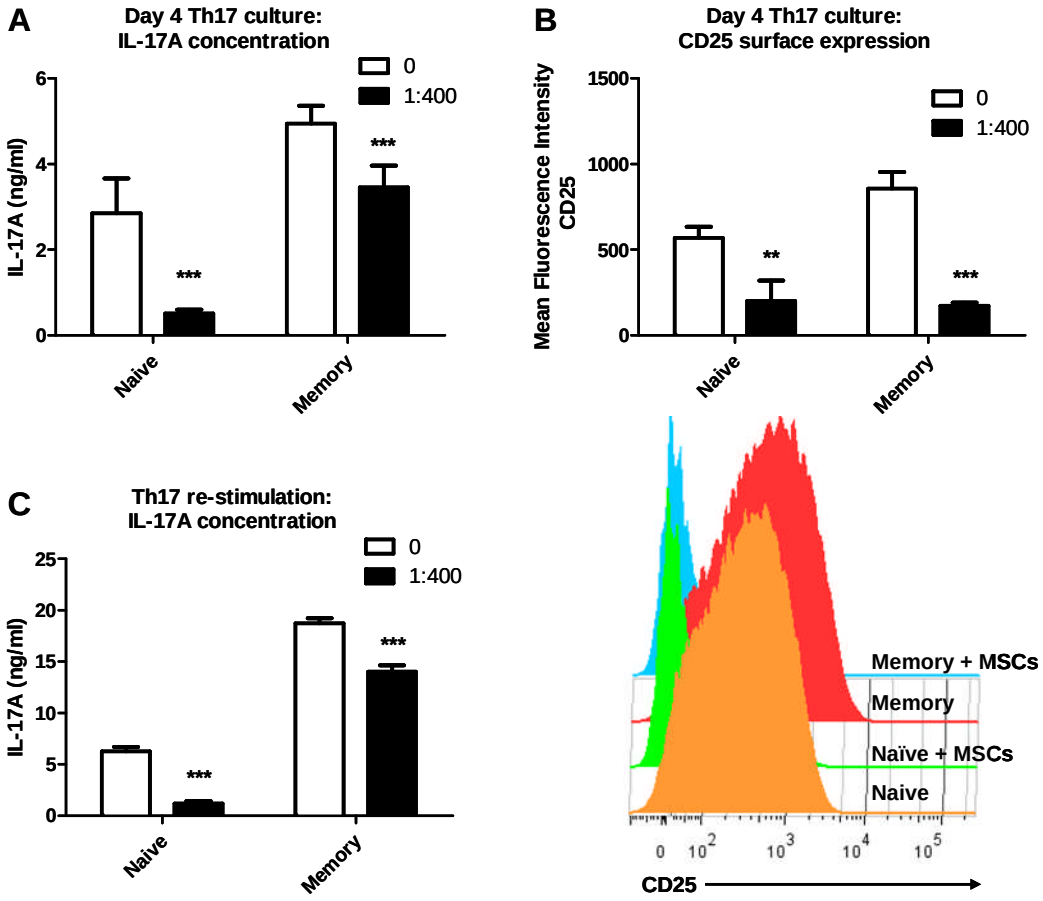

Figure 2.11 MSC inhibition of Th17 differentiation is not dependent on APCs: FACS-purified naïve and memory T-cells were separately activated by anti-CD3/anti-CD28-coated beads under Th17-skewed conditions in the presence or absence of MSCs for 4 days. (**A**) Concentration of IL-17A in supernatants at day 4 as measured by ELISA. (**B**) Surface expression of CD25 on $CD4^+$ T cells at day 4, as measured by flow cytometry (**Below**: examples of anti-CD25 histograms with cells gated on $CD4^+$ cells). (**C**) IL-17A concentrations in supernatants of re-purified $CD4^+$ T-cells re-stimulated for 24 hours with anti-CD3/anti-CD28-coated beads, as measured by ELISA. Data are represented as mean +/- standard deviations and are representative of 2 individual experiments for (** p = <0.01, *** p = <0.001 compared with 0 MSC control, Bonferroni posttest).

2.3.9 MSCs DO NOT SUPPRESS IL-17A PRODUCTION BY PRIMARY $CCR6^+$ MEMORY T-CELLS FROM SPLEEN

Only a proportion of total cells expressed IL-17A even under Th17-skewed conditions as illustrated by intracellular IL-17A and CFSE staining (**Figure 2.9B/C**). Th17 cells have been reported to express the chemokine receptor CCR6 *in-vitro* and *in-vivo* (Pindjakova et al., 2012). This expression has been associated with migration of Th17 cells during inflammation (Turner et al., 2010b, Esplugues et al., 2011). I therefore elected to use CCR6 as a surrogate marker to enrich for primary IL-17A-producing $CD4^+$ T-cells among splenic memory T-cells.

To further tease out the effect of MSCs on memory T-cells, a population of highly purified $CCR6^+$ memory cells was isolated by FACS. Following doublet discrimination, viable $CD4^+CD25^-CD62L^-$ memory T-cells were separated into $CCR6^{high}$ T-cells (0.1-0.2% of the total splenocyte population) or $CCR6^{low}$ T-cells (0.5-0.8% of the total splenocyte population) (**Figure 2.12**). Due to the narrow spread of CCR6 staining post sort purity was 42.4% for the $CCR6^-$ population and 66.7% for the $CCR6^+$ population.

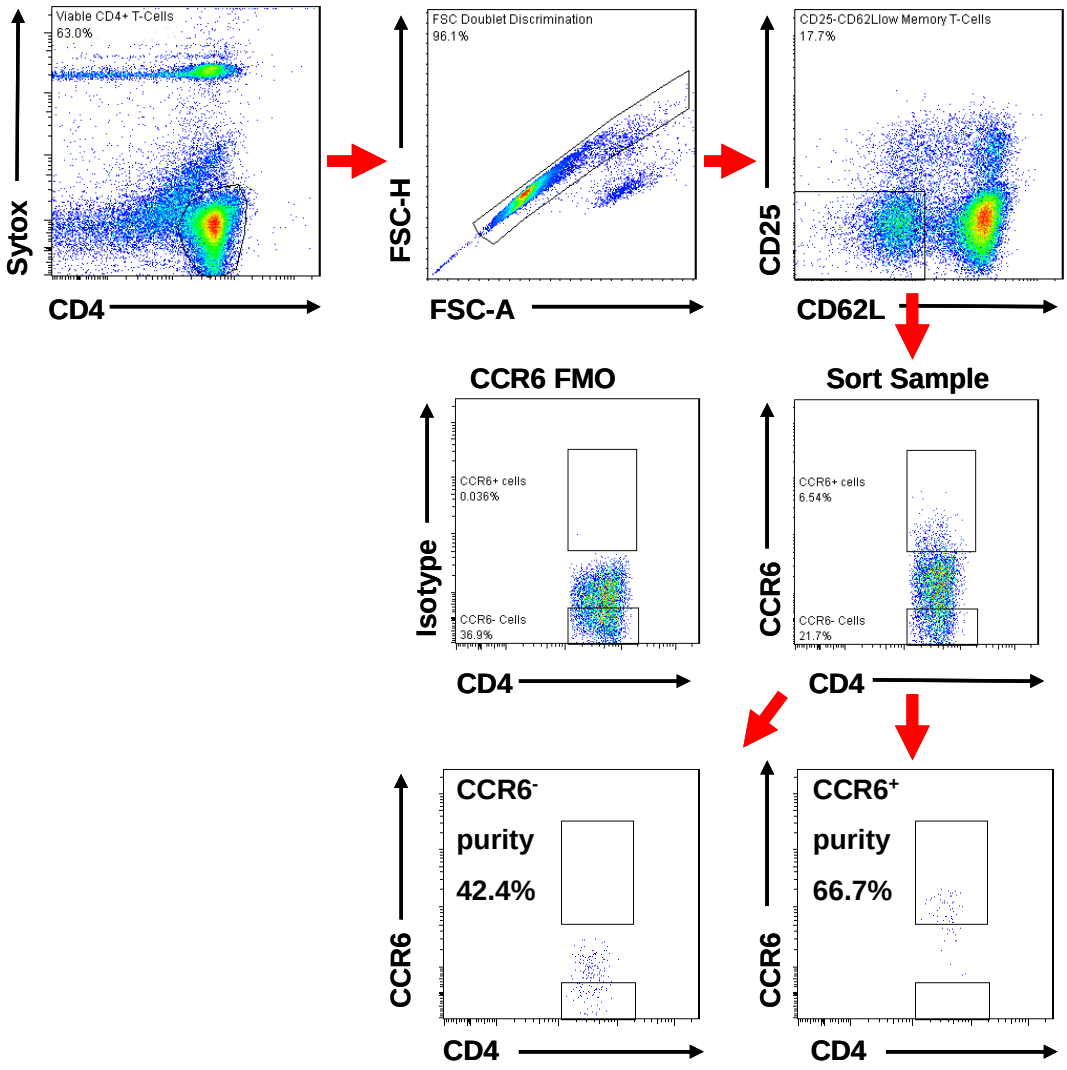

Figure 2.12 Representative gating strategy for FACS experiments in which highly purified $CD4^{+}CD25^{-}$ $CD62L^{-}$ memory T-cells were sorted into $CCR6^{+}$ or $CCR6^{-}$ cells.

$CCR6^{+}$ and $CCR6^{-}$ cells were separately activated with anti-CD3/anti-CD28-coated beads for 36 hours. Cytokine analysis at 36 hours showed that the $CCR6^{+}$ population produced significantly more IL-17A and less IFN-γ than the $CCR6^{-}$ population (**Figure 2.13A**). In a total of 4 individual sorts, $CCR6^{+}$ cells produced limited amounts of IFN-γ demonstrating the selective nature of this population. However, for both responder populations, co-culture with low numbers of MSCs (MSC:T-cell ratio 1:200) did not result in reduced IL-17A or IFN-γ at 36 hours (**Figure 2.13 B/C**).

The inability of MSCs to reduce IL-17A production by $CCR6^{+}$ memory T-cells was my first experimental indication of the limitations of MSC suppression of Th17 cells. This generated an interest in whether MSCs could interfere with Th17 cells in an

inflammatory environment containing the Th17-enhancing factors IL-1 and IL-23 (Pindjakova et al., 2012, Chung et al., 2009).

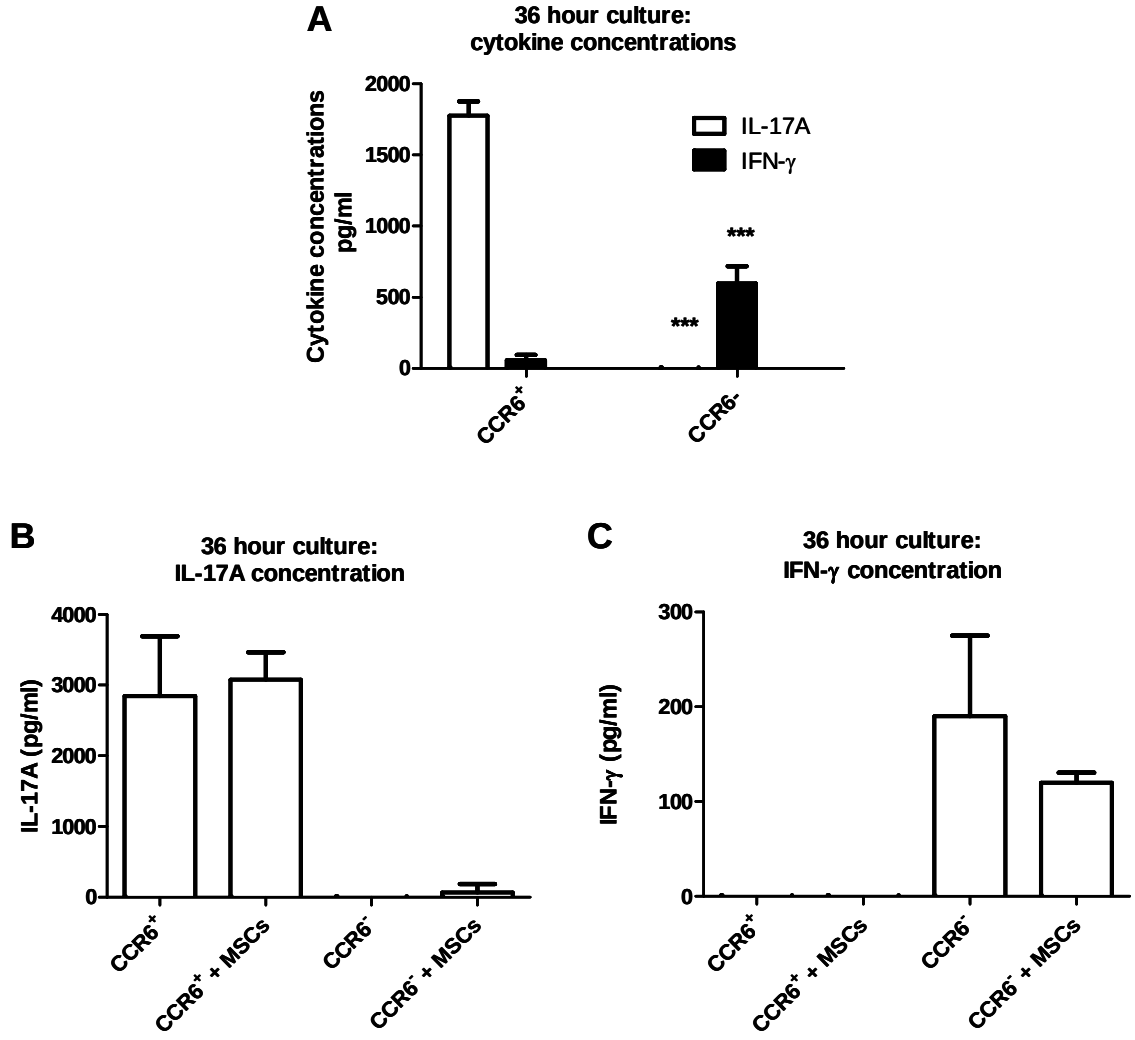

Figure 2.13 MSCs do not suppress cytokine production by highly purified CCR6$^+$ memory T-cells: CD4$^+$CD25$^-$CD62L$^-$CCR6$^+$ memory T-cells and CD4$^+$CD25$^-$CD62L$^-$CCR6$^-$ memory T-cells were separately activated with anti-CD3/anti-CD28-coated beads for 36 hours in the absence or presence of MSCs (1:200). (**A**) Concentrations of IL-17A and IFN-γ in supernatants at 36 hours as measured by ELISA. (**B**) Concentrations of IL-17A in supernatants at 36 hours as measured by ELISA. (**C**) Concentrations of IFN-γ in supernatants at 36 hours as measured by ELISA. Data are represented as mean +/-standard deviations and are representative of 4 individual experiments for (*** p = <0.001 compared with equivalent CCR6$^+$ population, Bonferroni posttest (**A**) and compared with 0 MSC control, Tukeys multiple comparison test (**B/C**)).

2.3.10 MSCs DO NOT SUPPRESS IL-1- AND IL-23-MEDIATED ENHANCEMENT OF IL-17A

Thus far, I observed that MSCs potently suppress $CD4^+$ T-cells undergoing primary activation and Th17 differentiation *in-vitro*. However, MSCs did not suppress IL-17A production by highly purified $CD4^+$ $CCR6^+$ memory T-cells from spleen.

In this experiment, the modulatory effects of MSCs on tertiary-re-activated Th17 cells were investigated. MACS-enriched $CD4^+$ T-cells were cultured for 6 days under Th17-skewed conditions with anti-CD3ε and APCs. $CD4^+$ T-cells were re-stimulated after 6 days with freshly isolated APCs and anti-CD3ε for a further 4 days under Th17-skewed conditions. $CD4^+$ T-cells were finally re-stimulated with anti-CD3ε with or without IL-1α (0.5 ng/ml) and IL-23 (5 ng/ml) for 24 hrs in the presence or absence of MSCs.

In the absence of IL-1α or IL-23, MSCs did not significantly reduce IL-17A production by these Th17 cells generated by prolonged differentiation culture (**Figure 2.14 bars 1-2**). Furthermore, MSCs significantly augmented IL-1α- and IL-23-mediated enhancement of IL-17A production by differentiated Th17 cells undergoing tertiary re-activation (**Figure 2.14 bars 3-8**).

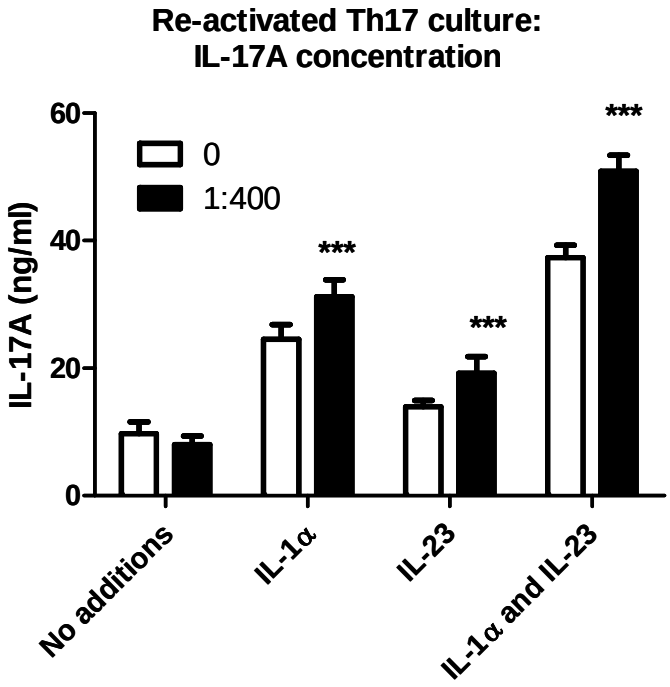

Figure 2.14 MSCs do not suppress IL-1- or IL-23-mediated enhancement of IL-17A: $CD4^+$ T-cells were cultured for 6 days under Th17-skewed conditions prior to re-stimulation with freshly isolated APCs and anti-CD3ε for a further 4 days under Th17-skewed conditions. $CD4^+$ T-cells were re-stimulated with anti-CD3ε with or without IL-1α and IL-23 for 24 hours in the presence or absence of 1:400 MSC:$CD4^+$ T-cells. Graphical representation of the concentrations of IL-17A in culture supernatants following 24 hour tertiary stimulation of Th17 cells in the presence or absence of MSCs. Data are represented as mean +/-standard deviations and are representative of 6 replicates from 1 individual experiment (*** p = <0.001 compared with equivalent 0 MSC control, Bonferroni posttest)

Experimental evidence from chapter 1 has revealed that MSCs suppress naïve and memory $CD4^+$ T-cells undergoing primary Th17 differentiation independent of IFN-γ and APCs. The suppressive effect was clearly dependent upon cell-cell contact. Renal cortical fibroblasts were unable to replicate the MSC-specific immunomodulatory effects which were not stain specific. In contrast, MSCs did not suppress IL-17A production by directly purified $CCR6^+$ memory T-cells or by Th17 cells polarized through prolonged differentiation culture. Furthermore, MSCs augmented IL-1- and IL-23-enhancement of IL-17A production by pre-polarized Th17 cells. Therefore MSCs have differential effects on Th17 responses under diverse conditions with evidence pointing towards suppression of $CD4^+$ T-cells undergoing primary differentiation but opposing effects on previously differentiated Th17 cells.

2.4 DISCUSSION

In chapter 2, I have demonstrated that low numbers of MSCs are capable of suppressing *de novo* Th17 differentiation in mouse through a mechanism that is initiated most potently by MSC/$CD4^+$ T-cell contact (**Figures 2.2 and 2.5**). In contrast to other reported T-cell inhibitory phenomena, I found that IFN-γ-mediated triggering of MSCs was not necessary for Th17 suppression (**Figure 2.3**). I demonstrated suppression by MSCs of Th17 differentiation from both naïve- and memory-phenotype precursors (**Figure 2.7**). However, I also observed that MSCs augmented IL-23- and IL-1α-mediated enhancement of IL-17A production when added to cultures of fully differentiated Th17 cells (**Figure 2.14**).

2.4.1 INHIBITION OF PRIMARY TH17 DIFFERENTIATION BY MSCS

My initial observations of MSC effects on *in vitro* generated Th17 cells from mouse both confirmed and extended results recently reported by Ghannam et al. for human cells (Ghannam et al., 2010). In agreement with this study, I observed that mouse MSCs inhibited the primary differentiation of Th17 cells from naïve precursors and that MSC co-culture resulted in reduced IL-17A production by T-cells during MSC-free re-stimulation (**Figure 2.2**). Ghannam and colleagues observed that human naïve cord blood-derived $CD4^+$ T-cells co-cultured with human BM-MSCs produced significantly less IL-17A, IL-22 and CCL20 (Ghannam et al., 2010). This was associated with increased Th2-related cytokines IL-4, IL-5 and IL-13 and T_{reg}–associated IL-10 and FOXP3. Contrary to this finding, I observed a reduction in these cytokines in mouse MSC/naïve and memory $CD4^+$ T-cells co-cultures (**Figure 2.8**) suggesting that mechanistic differences may exist across species. Additionally, Tatara et al. confirmed that mouse MSCs suppressed Th17 differentiation from splenic bulk $CD4^+$ T-cells and FACS-purified naïve $CD4^+CD25^-CD62L^+CD44^-$ T-cells (Tatara et al., 2011). My study has added to the field of MSC-mediated modulation of Th17 differentiation by additionally describing (a) the dose-dependent inhibition of T-cell activation using flow cytometry to analyze CD25 surface expression (**Figure 2.2**), (b) the specificity (**Figure 2.10**) and non MHC-restricted nature of MSC-mediated suppression of Th17 differentiation (**Figure 2.4**) and (c) the inhibition of IL-17A production independent of suppression of T-cell proliferation (**Figures 2.9**).

2.4.2 SUPPRESSION OF MEMORY-PHENOTYPE RESPONDERS BY MSCS

From a clinical perspective, it is important to consider the degree to which Th17 suppression by MSCs applies to pre-activated T-cells and T-cells with pre-existing Th17 imprinting. The results I present here for purified memory-phenotype $CD4^+$ T cells indicate suppression of IL-17A secretion (**Figure 2.7**). MSC contact was also associated with inhibition of proliferation and of CD25 up-regulation. These results are in-line with the *in vitro* and *in vivo* findings of Rafei et al. for MSC effects on MOG-specific Th17 cells in mouse EAE (Rafei et al., 2009). Furthermore, in agreement with Rafei at al., I detected increased CCL2 in Th17 cultures in the presence of MSCs (**Figure 2.8**). In addition, MSC-mediated suppression of Th17 responses has been reported for antigen-specific Th17 cells in rat EAE and autoimmune myasthenia gravis and in established autoimmune diabetes mellitus in NOD mice as described in the introduction to this chapter (Zhao et al., 2008, Wang et al., 2008a, Kong et al., 2009). Furthermore, Ghannam et al. showed that under non-Th17-skewed conditions, MSCs suppressed IL-17A and IL-22 production by differentiated Th17 cell clones (Ghannam et al., 2010). This was associated with a concomitant increase in IL-10-producing and IL-10/IL-17A double-producing T-cells. When Th17 cells re-purified from MSC co-cultures were added to freshly isolated $CD4^+$ T-cells cultures they displayed anti-proliferative properties suggesting that there was an induction of Th17 cells with regulatory activity (Ghannam et al., 2010).

During the course of this thesis a number of additional groups have demonstrated the beneficial effects of MSCs in animal models associated with maladaptive Th17 immune responses. Zhou et al. reported that human AT-MSCs displayed both preventative and therapeutic properties in CIA of mice by administering MSCs before and after the induction of CIA. This was associated with reduced circulating levels of IL-17A and expression of IL-17A in joint extracts (Zhou et al., 2011). Similarly, human umbilical cord-derived MSCs ameliorated TNBS-induced colitis in mice in association with suppressed levels of IL-17A in serum and colonic extracts (Liang et al., 2011). In a rat model of experimental autoimmune uveoretinitis induced by interphotoreceptor retinoid-binding protein (IRBP), both autologous and allogeneic MSCs ameliorated the disease. The authors also demonstrated reduced IL-17A production by IRBP-specific T-cells from MSCs treated mice re-challenged *ex-vivo* compared with non-treated control mice (Zhang et al., 2011). In Th17-mediated EAE,

administration of conditioned media generated from human MSCs resulted in lower clinical scores than PBS treatment. In this study, the beneficial effect was mediated by HGF (Bai et al., 2012).

2.4.3 Potential for enhancement of Th17 responses by MSCs

Interestingly, however, evidence for enhancement of Th17 differentiation and IL-17A production by MSCs and fibroblasts has also been presented in a small number of studies (Schirmer et al., 2010, Carrion et al., 2010, Darlington et al., 2010, Guo et al., 2009). Schirmer et al. demonstrated that skin fibroblasts indirectly enhanced IL-17 production from human $CD4^+$ T-cells *via* induction of IL-23 by DCs which, when blocked, reversed the enhancing effect (Schirmer et al., 2010).

Darlington and colleagues showed suppression of Th1 development from PHA-activated PBMCs with an increase in Th17 differentiation in the presence of conditioned media generated from human MSCs (Darlington et al., 2010). In this study, however, the effects of MSCs on Th1 differentiation were examined under neutral culture conditions while Th17 differentiation was carried out in the presence of IL-23. Indeed, my own work has shown that MSCs enhance IL-23-induced IL-17A production (**Figure 2.14**) suggesting that these authors should also investigate the effects of human MSCs on Th17 differentiation from PBMCs in the absence of IL-23. Carrion et al. confirmed that MSCs potently suppressed IL-17A production in primary cultures if added at day 0 but, when added on day 3 of Th17 differentiation, MSCs augmented IL-17A production (Carrion et al., 2010). Guo et al. additionally confirmed potent MSC suppression of the Th1 lineage from PHA-activated PBMCs (Guo et al., 2009) whereas IL-17A was enhanced in the presence of MSCs – an effect that was partially reversed by anti-IL-6. I have also confirmed increased production of IL-6 by MSCs co-cultured with activated memory T-cells (**Figure 2.8**). Furthermore, I found that the proportionate inhibition of IL-17A production following re-stimulation of $CD4^+$ T-cells re-purified from co-cultures was lower for memory-phenotype responders than for naïve-phenotype responders. This reduced potency of suppression could reflect the effect of MSC-derived IL-6 as multiplex analysis of primary culture supernatants revealed higher IL-6 levels in co-cultures of MSCs with memory-phenotype but not naïve-phenotype responders (**Figure 2.8**). Furthermore, I found increased TGF-β1 in both co-culture systems (**Figure 2.8**). Therefore, in TGF-

β1-predominant naïve co-cultures, MSCs readily suppress Th17 differentiation however, in memory co-cultures in which TGF-β1 and IL-6 are increased, MSCs may not be as potent.

2.4.4 PRIMING OF MSCS

In relation to IFN-γ-priming of MSCs, I found that IFN-γ was unnecessary for the suppressive effects observed in Th17/MSC co-cultures (**Figure 2.3**). Indeed when IFN-γ blockade was omitted, Th17 responses were very poor. This may be due to the induction of high levels of TGF-β1 by MSCs as demonstrated by Ryan et al. in human MSCs treated with exogenous IFN-γ (Ryan et al., 2007). Svobodova and colleagues demonstrated that MSC conditioned media inhibited IL-17A production by allogeneic-activated splenocytes. The suppressive effect on IL-17A production was reversed by blockade of MSC-derived TGF-β1 in the conditioned media (Svobodova et al., 2011). Moreover, IL-1α pretreated MSC conditioned media enhanced IL-17A production in addition to RORγt expression. IL-1α-pre-treated MSC conditioned media was found to contain high levels of IL-6 with lower levels of TGF-β1, favouring Th17 induction. Indeed blockade of IL-6 reversed the induction of Th17 expansion (Svobodova et al., 2011). This enhancement of IL-17A production by MSCs pre-treated with IL-1α corresponds with my finding that MSCs augmented IL-1α-enhancement of IL-17A production (**Figure 2.14**). Future experiments may involve the measurement and blockade of IL-6 to investigate whether IL-1α induces MSCs to produce IL-6 in my culture system thereby enhancing IL-17 production.

Although priming of MSCs by IFN-γ was redundant in my culture system, other pro-inflammatory cytokines produced in MSC/Th17 co-cultures may play a role in enhancing the suppressive nature of MSCs. TNF-α for example is produced by Th17 cells which was shown by English et al. to induce MSCs to upregulate cyclooxygenase 2 (COX2) and subsequently PGE2 production (English et al., 2007). Ghannam et al. demonstrated that blockade of PGE2 partially reversed MSC-specific suppression of Th17 responses (Ghannam et al., 2010). I clearly demonstrated in transwell cultures that cellular cross talk was indispensable for MSC suppression of Th17 cells as did Ghannam and colleagues (Ghannam et al., 2010). This topic shall be discussed in detail in chapter 3. Therefore, while priming of MSCs by pro-inflammatory factors may alter their expression of immune modulatory factors which

may suppress or in some cases enhance Th17 responses, my experiments would suggest that it is not the primary mechanism of Th17 inhibition by MSCs. Indeed priming of MSCs *in-vivo* may not be beneficial despite efficacy *in-vitro*. Papadopoulou and colleagues reported that MSCs were ineffective in adjuvant-induced arthritis (AIA) in rats unless administered prior to disease induction (Papadopoulou et al., 2012). However, bortezomib (proteasome inhibitor) and MSC double-treated animals exhibited improved AIA and severe spontaneous erosive arthritis compared with single agent controls (Papadopoulou et al., 2012). Bortezomib altered the inflammatory milieu prior to administration of MSCs, restoring efficacy to MSC therapy (Papadopoulou et al., 2012). Therefore, certain inflammatory microenvironments may silence the immunosuppressive properties of MSCs as demonstrated in this study and it may be important to understand the cytokine milieu present at individual sites of tissue injury prior to MSC infusion.

2.4.5 DIRECT EFFECTS OF MSCS ON TH17 CELLS

Regarding the question of whether MSC suppressive effects are exerted directly upon $CD4^+$ T cells undergoing Th17 differentiation, experiments in an APC-culture system effectively rule out an intermediary role for DCs, macrophages or other accessory cells (**Figure 2.11**). As only a fraction of the $CD4^+$ T-cells within primary cultures were IL-$17A^+$ by intracellular staining at a given time (**Figure 2.9**), I cannot definitively rule out a role for an additional T-cell population in suppressing the Th17 differentiation program. Nonetheless, cross-regulation by Th1 or Th2 effectors during primary Th17 induction cultures is highly unlikely given the continuous blockade of IFN-γ and IL-4. Furthermore, and in contrast to the findings of Ghannam et al., I did not detect induction of $FOXP3^+$ or IL-10^+ T-cells in experiments carried out using FACS-purified, naïve-phenotype $CD4^+$ T-cells co-cultured with MSCs under Th17-skewed conditions (data not shown). In addition to the lack of T_{reg} induction in my mouse Th17 cultures in the presence of MSCs, I also ruled out the possibility that T_{reg} present in bulk T-cell cultures were responsible for the suppressive effects by FACS-purifying $CD25^-$ naive and memory T-cells (**Figure 2.6**) thereby preventing the introduction of T_{reg} to the primary cultures.

2.4.6 SUMMARY

To the best of my knowledge, this is the first study in which the traditional approach of analysing bulk $CD4^+$ T-cells was combined with intricate FACS-techniques to isolate highly pure naïve and memory $CD4^+$ T-cell responders and $CCR6^+$ memory T-cells to compare how MSCs relatively affect specific populations of $CD4^+$ T-cells undergoing primary Th17 differentiation. Additionally, the modulatory effects of MSCs on primary Th17 differentiation were compared to fully differentiated Th17 cells under the influence of inflammatory mediators IL-1α and IL-23. I demonstrated that MSCs have potent effects on bulk MACS-enriched $CD4^+$ T-cells undergoing primary activation and Th17 differentiation in addition to FACS-purified $CD4^+CD25^-CD62L^+$ naïve-phenotype responders undergoing similar differentiation protocols. MSCs also suppressed $CD4^+CD25^-CD62L^-$ memory-phenotype responders, albeit to a lesser extent. MSCs did not suppress $CCR6^+$ memory T-cells and even enhanced IL-17A production by fully differentiated Th17 cells in the presence of IL-1α and IL-23. Therefore, the potency of MSC suppression on Th17 cells is limited by factors including the state of activation and differentiation of the responder cell. The balance of MSC effects on Th17 cells may also be influenced by MSC-derived IL-6 and TGF-β1 and by environmental factors produced by other cell types including IL-1 and IL-23 (**Figure 2.15**).

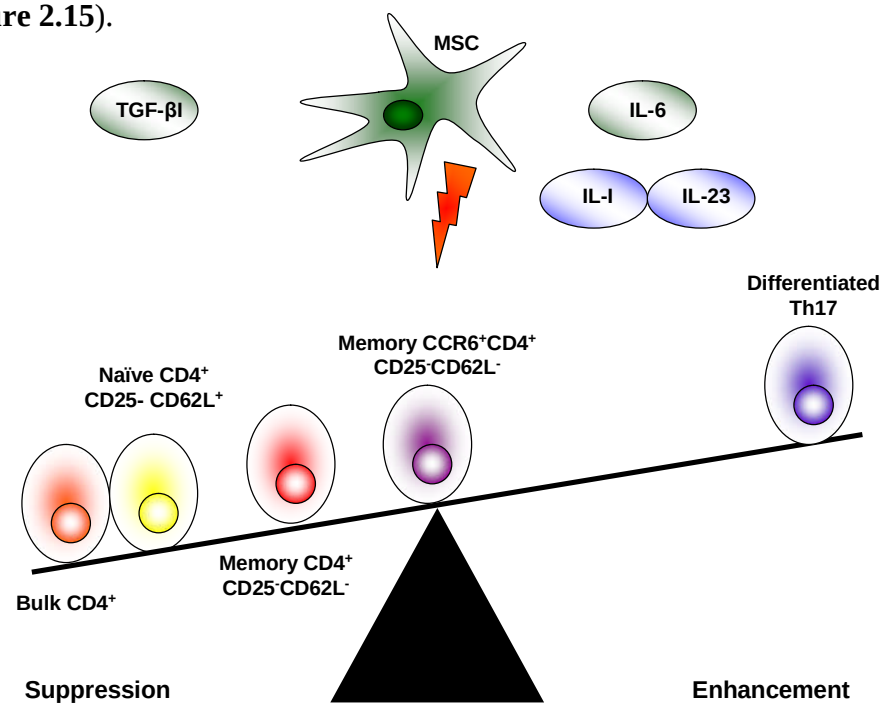

Figure 2.15 MSCs have varying degrees of suppression and in some cases enhancement on Th17 cells dependent upon the state of T-cell activation and differentiation, MSC-derived mediators and soluble MSC-licensing cues in the microenvironment.

CHAPTER THREE

CELL-TO-CELL CONTACT INHIBITION OF T-HELPER 17 CELLS IS MEDIATED THROUGH PROSTAGLANDIN E2 *VIA* THE EP4 RECEPTOR

3.1 INTRODUCTION

As described in chapter 2, a number of mediators of MSC-induced suppression of Th17 responses were described at the initiation of this thesis including TGF-β1, IL-27, CCL2 and IDO (Zhao et al., 2008, Wang et al., 2008a, Rafei et al., 2009, Kong et al., 2009). Zhao and colleagues described a role for MSC-derived TGF-β1 in ameliorating type I diabetes (Zhao et al., 2008) while IDO production by MSCs was implicated in the amelioration of autoimmune myasthenia gravis (Kong et al., 2009). Wang et al. reported that IL-27 suppressed EAE following administration of MSCs (Wang et al., 2008a) however, Rafei and colleagues showed amelioration of EAE *via* MSC-derived alternatively cleaved CCL2 (Rafei et al., 2009). English et al. reported that IFN-γ induced functional IDO production by mouse MSCs while PGE2 was induced by TNF-α in addition to IFN-γ. This was essential for inhibition of alloantigen-specific proliferation (English et al., 2007). Initial experiments for this chapter pointed strongly to the COX pathway as a key mediator of MSC-associated inhibition of primary Th17 differentiation.

PGE2 is a prostanoid product of the COX pathway of eicosanoid metabolism (Miller, 2006). The other pathway is the lipoxygenase pathway of which the leukotrienes and lipoxins are members. In addition to PGE2, PGD2, PGF2, and PGI2, the prostanoid family also contains platelet-derived thromboxane and endothelial cell-derived prostacyclin. Prostaglandins (PGs) are unsaturated fatty acids derived from arachidonic acid metabolism. Erythrocytes are the only cell type which does not synthesise PGs. As a result, PGs are ubiquitous to most cell membranes (Miller, 2006).

Arachidonic acid (AA) is released from phospholipids in the cell membrane by calcium-dependent phospholipase-A2 or –C following certain stimuli (inflammation, collagen, hormones and physical disruption of cell membranes). COX enzymes convert AA to PGG2 and subsequently PGH2. Depending on the particular end product, different enzymes convert PGH2 to diverse PGs (Miller, 2006). PGs differ from one another by substitutions to a cyclopentane ring in their prostanoic acid structure. Once synthesised, PGs are released into the extracellular space, act locally and are rapidly catabolised to inactive forms. PGE2 is catabolised to 13,14-dihydro-

15-keto PGE2 by prostaglandin 15-dehydrogenase and has a half life of only 30 seconds in the circulation. PGE2 is more stable *in vitro* (Miller, 2006).

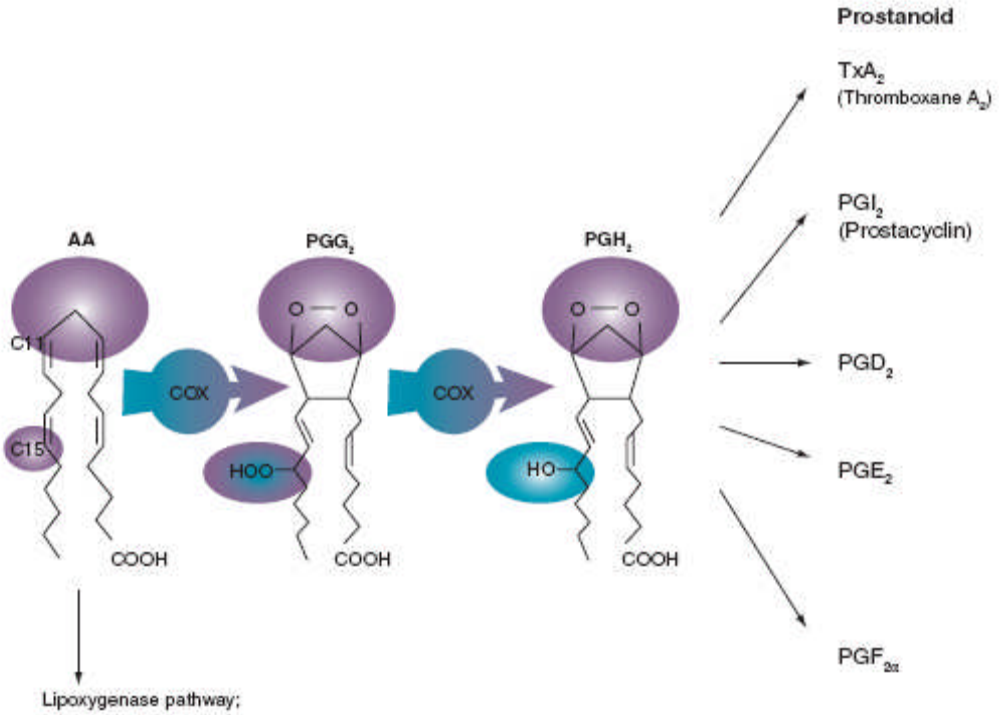

Figure 3.1 Prostaglandin production *via* COX enzymes or the alternative arachidonic acid metabolism pathway – the lipoxygenase pathway (Adapted from: Rajakariar et al., 2006)

Three isoforms of COX enzymes exist. COX1 synthesises low levels of PGs and is mostly constitutive in nature with induction under diverse circumstances. It is involved in the maintenance of and homeostasis of physiological functions in organ systems. In contrast, COX2 is strongly inducible by pro-inflammatory cytokines, growth factors and mitogens in addition to being expressed constitutively in discrete cell types of the kidney and brain. COX2 was originally thought to be entirely proinflammatory however this hypothesis has been challenged. Both COX1 and COX2 are now known to possess proinflammatory functions while COX2 has also been reported to be anti-inflammatory under some conditions. COX3 is a variant of COX1 and is encoded by the same gene. It is expressed in the brain and heart but its functions remain largely unknown (Rajakariar et al., 2006).

PGE2 is a vasodilator in many organ systems including the cardiovascular system, respiratory system and reproductive system. PGE2 is synthesised in the collecting ducts and interstitial cells of the renal medulla where it increases blood flow, inhibits sodium transport into the interstitium from the ascending loop of Henle, prevents

reabsorption of sodium and urea from collecting ducts and also decreases water permeability in the collecting ducts (Miller, 2006). PGE2 is cytoprotective in the GI tract by inhibiting secretion of gastric acid, stimulating bicarbonate and mucus secretion and increasing blood flow. PGE2 also affects bone formation and resorption and is involved in uterine muscle contractions during child birth (Miller, 2006).

PGE2 acts by engaging one of four G-protein-coupled receptors (EP1 through EP4) which activate different signalling pathways (Kalinski, 2012). Both human and mouse $CD4^+$ T-cells express EP2 and EP4 (Boniface et al., 2009). Both EP2 and EP4 ligation are reported to induce cyclic adenosine monophosphate (cAMP) which in turn activates protein kinase A (PKA) and subsequent transactivation of the cAMP response element-binding (CREB) transcription factor. EP4 additionally activates the phosphatidylinositol 3 kinase (PI3K)-dependent ERK 1/2 pathway leading to NF-κB activation (Sreeramkumar et al., 2011, Kalinski, 2012). Reported roles for both anti-inflammatory and pro-inflammatory functions of PGE2 appear to be related to the concentration of PGE2 in the system, duration of exposure to PGE2, PGE2 signalling *via* different EP receptors and activation of different signalling pathways and/or the presence of environmental/proinflammatory stimuli.

In relation to Th17 cells specifically, Chen et al. demonstrated that 0.01-1 μM PGE2 dose-dependently inhibited IL-17A production and RORγt expression by mouse $CD4^+CD62L^+$ MACS-enriched naïve T-cells activated with soluble anti-CD28 and plate-bound anti-CD3ε for 3 days under Th17-skewed conditions (Chen et al., 2009). Yao et al. confirmed the finding of dose-dependent inhibition of primary Th17 differentiation from $CD4^+CD62L^+$ naïve T-cells by PGE2 in the range of 0.1-100 nM (Yao et al., 2009). *In-vivo,* Kabashima et al. reported that a PGE2 analogue reversed indomethacin enhancement of DSS-induced colitis (Kabashima et al., 2002). Furthermore, EP4 KO mice and EP4 antagonist-treated WT mice developed severe colitis. In contrast, WT mice treated with an EP4 agonist displayed ameliorated colitis (Kabashima et al., 2002).

In contrast, a number of studies reported that PGE2 enhanced Th17 responses predominantly *via* indirect effects on APCs. Khayrullina et al. showed that BM-DCs activated in the presence of GM-CSF with PGE2 for 7-8 days, enriched for CD11c by

MACS and stimulated by LPS for 24 hours produced increased levels of IL-1β, IL-6, IL-10, IL-23, IL-27, TNF-α and TGF-β compared to non-PGE2 cultured DCs (Khayrullina et al., 2008). When co-cultured with $CD4^+$ T-cells, PGE2-DCs enhanced IL-17A production but suppressed IFN-γ and IL-4 – an effect which was reversed by addition of a combination of anti-IL-6, anti-p19 (IL-23), anti-TGF-β and recombinant IFN-γ (Khayrullina et al., 2008). The same laboratory reported that analogues of PGE2 augmented TNBS-induced colitis and collagen-induced arthritis in association with increased DC-derived IL-23 and T-cell-derived IL-17 (Sheibanie et al., 2007b, Sheibanie et al., 2007a). Yao et al. demonstrated that anti-CD40-activated splenic $CD11c^+$ DCs produced IL-23 and that this effect was augmented in the presence of PGE2 or a selective EP4 agonist. Moreover, PGE2 enhanced IL-23-induced Th17 development (Yao et al., 2009). When these findings were applied in-vivo, EP4 antagonism suppressed EAE and dinitrofluorobenzene (DNFB)-induced contact hypersensitivity – characterised by reduced Th17 responses (Yao et al., 2009).

PGE2 also enhanced exogenous IL-1β- and/or IL-23-induced IL-17A production by human naïve and memory T-cells (Boniface et al., 2009). In the mouse system, PGE2 added to re-stimulated cultures of differentiated Th17 cells augmented IL-1β- and IL-23-induced IL-17A production (Boniface et al., 2009). This was confirmed by Chizzolini and colleagues (Chizzolini et al., 2008). One study reported direct enhancing effects of PGE2 on human memory Th17 cells (Napolitani et al., 2009). IL-1β, IL-23 and PGE2 (0.5 μM) enhanced IL-17A production by PBMCs activated with toxic shock syndrome toxin 1. Addition of anti-IL-23 and anti-IL-1 neutralization antibodies to PGE2-treated cultures did not affect IL-17A production. These results suggested that the inducing effect of PGE2 on IL-17A was independent of IL-23 and IL-1 and occurred as a result of a direct effect of PGE2 on T-cells, however the authors did not employ isotype controls or a positive control for the neutralization antibodies employed in this study (Napolitani et al., 2009). The authors showed PGE2 also increased IL-17A production by anti-CD3/anti-CD28-activated $CD4^+CD45RA^-CD25^-$ memory T-cells.

Thus, the interaction between PGE2 and differentiating Th17 cells is complex in nature and certainly warranted further investigation. The majority of reports investigating PGE2 effects on Th17 cells focused on indirect PGE2 modulation of

APC-derived or exogenous IL-1 and/or IL-23 induced Th17 responses. In contrast, the direct effects of PGE2 on primary differentiating Th17 cells were not well studied. Specifically, the direct effects of MSC-derived PGE2 had not been examined on $CD4^+$ T-cells undergoing primary Th17 differentiation.

Therefore, specific aims for charter 3 were to:

1. Determine the mechanism of MSC-mediated inhibition of primary Th17 differentiation.
2. Investigate the effect of PGE2 on primary Th17 differentiation.
3. Determine a role for PGE2/EP receptor signalling in Th17 induction.

3.2 MATERIALS AND METHODS

3.2.1 NEUTRALIZATION AND BLOCKING REAGENTS

Table 3.1 List of neutralization antibodies, blocking reagents, antagonists and agonists and the concentration of each employed in this study

Reagent	Concentration(s)	Reference
Anti-CCL2 neutralization antibody	5 μg/ml	(Rafei et al., 2009)
L-NAME	1 mM	(Bouffi et al., 2010)
Indomethacin	5 μM	(Ghannam et al., 2010)
COX2 inhibitor NS-398	0.1-1 μM	(Lee et al., 2010)
Purified PGE2	0.02-100 nM	(Chen et al., 2009)
EP1 antagonist SC-51322	1 μM	(Foudi et al., 2008)
EP2 antagonist AH-6809	1 μM	(Woodward et al., 1995)
EP4 antagonist L-161,982	0.01-10 μM	(Takayama et al., 2002)
EP4 agonist L-902,688	0.01-10 nM	(Foudi et al., 2008)

3.2.2 PARAMETER™ PGE2 COMPETITIVE ASSAY

This assay was performed according to the manufacturer's instructions (R&D Systems). Standards and pre-diluted samples were added to a 96-well microplate coated with goat anti-mouse polyclonal antibody. Mouse monoclonal anti-PGE2 was added to the plate which was incubated for 1 hour on a microplate shaker at room temperature. PGE2-HRP was added to the plate for 2 hours. The plate was washed after which substrate solution was added for 30 minutes. The absorbance was read on a Victor3™ 1420 Multilabel Counter plate reader at 450 nm and 550 nm following addition of stop solution.

3.2.3 FACS OF MSCS AND IMMUNE CELLS FROM CO-CULTURES

In some experiments, MSCs were re-purified from co-cultures by FACS based on CD45 surface expression and then subjected to Western Blot, quantitative RT-PCR or re-cultured to generate conditioned media. Sorted cells were re-analysed to ensure high purity. Dead cells were excluded using Sytox® dead-cell stain. Splenocytes and MSCs were gated separately based on their forward and side scatter profiles in both control cultures and co-cultures. Each population was then subjected to rigorous doublet discrimination gating after which the resulting populations of cells were separately analysed for CD45. A fluorescence-minus-one (FMO) control was employed to discriminate between CD45 positive and negative cells.

3.2.4 qRT-PCR for COX1 and COX2

Quantitative (Real Time) RT-PCR was performed by a collaborator, Dr. Cathal McCarthy in the Conway Institute, University College Dublin, for murine COX1 and COX2 using SYBR® Green primer pairs and SYBR® Green PCR Master Mix (Qiagen, Valencia, CA, USA) with 18S rRNA as a normalization control. Samples were amplified on a Prism 7900HT Real-time PCR System (Applied Biosystems, Carlsbad, CA, USA). Relative quantification was performed using the comparative CT method with results expressed as fold difference relative to the MSCs alone sample.

COX1 (forward primer sequence ACC TAC GTC TAC GCC AAA GG, reverse primer sequence GTG GTT TCC AAC CAA GAT CA).
COX2 (forward primer sequence AGC CCA CCC CAA ACA CAGT, reverse primer sequence AAA TAT GAT CTGGAT GTC AGC ACA TATT).

3.2.5 Western Blot for COX1 and COX2

FACS-purified MSCs were incubated for 1 hour on ice in complete lysis buffer A. The protein concentration was determined using a BCA Protein Assay Kit (Fisher Scientific Ireland, Dublin 15, Ireland) and proteins were separated on 4–20% Precise™ Protein Gels (Fisher Scientific Ireland) in a Mini-Protean® Tetra Cell (Bio-Rad). Electro-transfer to Immobilon® P PVDF membranes (Millipore, Billerica, MA, USA) was performed prior to blocking for 1 hour at room temperature in 5% w/v skimmed milk powder. Membranes were incubated with anti-mouse COX1 (1:200), anti-mouse COX2 (1:200) or anti-β-actin (1:50,000) overnight at 4°C followed by washing in TBST, incubation for 1 hour at room temperature with goat anti-rabbit IgG-HRP (1:5000), development using Immobilon® Western Chemiluminescent HRP substrate and imaging on a Kodak® Image Station 4000MM Pro (Eastman Kodak Company, Rochester, NY, USA).

3.2.6 Mouse UUO and preparation of single cell suspensions from kidneys

Mice were anaesthetized with ketamine/xylazine following which a 1cm incision was made in the left abdominal wall and peritoneum, the left ureter was identified and ligated mid-way between the kidney and bladder with two 4-0 silk sutures (Johnson and Johnson, New Brunswick, NJ, USA). The abdominal incision was closed with

absorbable 5-O chromic catgut (Johnson and Johnson) using interrupted stitches. Seventy two hours later mice were euthanized and the left (obstructed) and right (control) kidneys were dissected, diced with a scalpel and reduced to single cell suspensions by collagenase/DNase I digestion. Briefly, chopped pieces of kidney were incubated for 30 minutes in a solution of collagenase (0.4 mg/ml) and DNase I (0.2 mg/ml) at 37°C. The sample was vortexed every 10 minutes during the incubation. Remaining clumps were crushed with a sterile pestle and the suspension pipetted until smooth. The enzymes were neutralized with DMEM and washed. The sample was re-suspended in DNase I (0.2 mg/ml) for 15 minutes at room temperature followed by washing. The sample was re-suspended in DMEM and allowed to settle for 15 minutes. The lower 30% of the solution was discarded with the upper 70% being subjected to filtration and red cell lysis. Leukocyte-enriched fractions were prepared from kidney cell suspensions by positive magnetic selection using anti-CD45 microbeads (Miltenyi Biotec). $CD45^+$ cells (1×10^6/ml) were cultured for 24–48 hours in 96-well round bottom plates with 0.01 µg/ml anti-CD3ε with graded numbers of MSCs and other reagents as described for individual experiments.

All other methods for this chapter are as described in section 2.2.

3.3 RESULTS

3.3.1 MSC SUPPRESSION OF PRIMARY TH17 INDUCTION IS MEDIATED IN A COX-DEPENDENT MANNER

At the onset of this thesis, reported mediators of Th17 suppression by MSCs included TGF-β1, CCL2, IDO and IL-27 (Kong et al., 2009, Wang et al., 2008a, Zhao et al., 2008, Rafei et al., 2009). In order to identify potential mediators of MSC-induced Th17 suppression in this system, experiments were carried out in which FACS-purified naïve $CD4^+$ T-cells were Th17-skewed with anti-CD3ε and APCs in the presence or absence of MSCs (1:400 ratio) with or without blocking/inhibiting factors for candidate mediators. I initially inhibited CCL2 using an anti-mouse neutralization antibody (5 μg/ml) previously validated by Rafei et al. (Rafei et al., 2009) due to the abundance of this molecule in both naïve- and memory-phenotype $CD4^+$ T-cell co-cultures with MSCs. As shown in chapter 2, of the 21 factors measured in these co-cultures, CCL2 was most potently induced (**Figure 2.8**). Additionally, CCL2 was recently reported as an MSC-derived mediator of Th17 suppression (Rafei et al., 2009).

Analysis of CD25 surface expression by flow cytometry revealed that the suppressive effect of MSCs on this parameter was not reversed in the presence of CCL2 blockade (**Figure 3.2A**). Furthermore, IL-17A production was the same for naïve $CD4^+$ T-cells cultured in the presence of MSCs as for those cultured in the presence of MSCs with CCL2 neutralization as detected by intracellular flow cytometric analysis (**Figure 3.2B**). Thus, MSC suppression of primary Th17 induction in this culture system was not mediated by CCL2.

After ruling out a role for CCL2 in MSC-mediated suppression of Th17 development, I elected to block two well reported MSC-associated mediators - PGE2, *via* non-selective inhibitor of COX enzymes using indomethacin (5 μM) and, NO, *via* inhibition of nitric oxide synthases (NOS) using L-NG-nitroarginine methyl ester (L-NAME) (1 mM). The vehicle control for both of these compounds was DMSO.

A simple CD25 surface expression assay was employed to identify potential mediators prior to extensive characterization. As illustrated in **Figure 3.2C**, minimal

though statistically significant reversal of CD25 suppression by MSCs was detected in the presence of L-NAME. In contrast, indomethacin completely reversed CD25 inhibition. Thus, based on this assay, I hypothesized that the primary mediator of MSC-specific modulation of Th17 differentiation was COX-dependent in this culture system. This was further characterized in the following experiments.

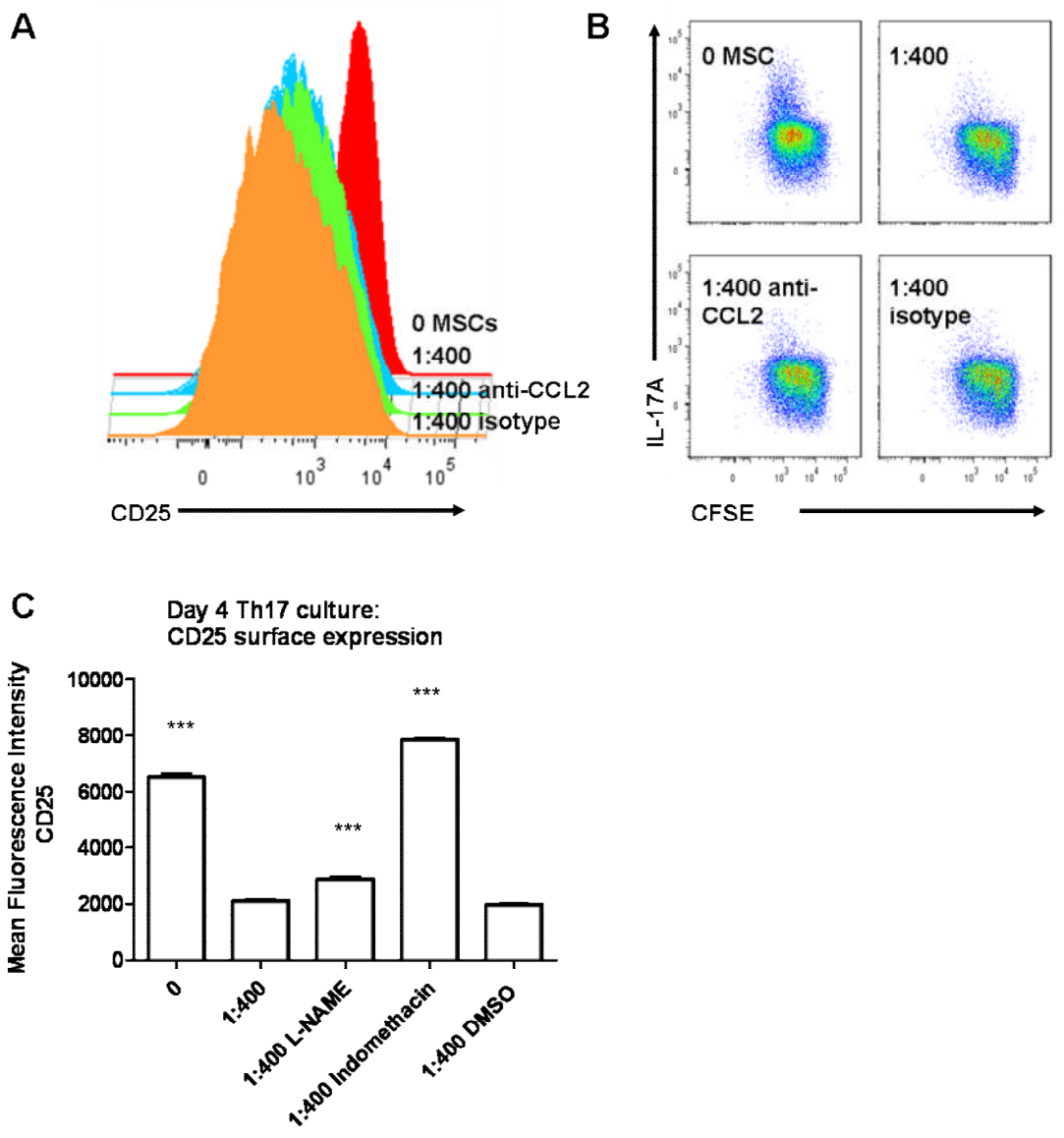

Figure 3.2 MSC suppression of Th17 cells is COX-dependent: FACS-purified naïve $CD4^+$ T-cells were cultured for 4 days under Th17-skewed conditions with anti-CD3ε and APCs in the presence of MSCs (1:400 MSC:$CD4^+$ T-cell ratio). Blocking reagents and equivalent concentrations/volumes of isotype or vehicle controls were additionally added. (**A**) Representative CD25 histograms of naïve $CD4^+$ T-cells cultured in the presence or absence of MSCs with or without anti-CCL2 neutralizing antibody or equivalent isotype control. (**B**) Representative intracellular staining for IL-17A on the same cells. (**C**) Surface expression level of CD25 on $CD4^+$ T-cells at day 4 following culture in the presence or absence of MSCs with or without blocking reagents for NO and PGE2 or equivalent vehicle control. Data are presented as mean +/-standard deviations and are representative of 2 individual experiments (*** p = <0.001 compared with 1:400 MSC:$CD4^+$ T-cell ratio, Tukey's multiple comparison test).

3.3.2 Production of a soluble prostanoid mediator is due to direct contact between MSCs and activated $CD4^+$ T-cells.

In order to confirm a direct role for COX-associated factors in MSC-mediated suppression of primary Th17 differentiation, experiments were carried out in which FACS-purified naïve $CD4^+$ T-cells were Th17-skewed in APC-free culture (anti-CD3/anti-CD28 beads) in the presence or absence of MSCs with or without indomethacin. Day 4 culture supernatants were recovered and stored at -20°C for the conditioned media experiment described below. Therefore, the primary experimental read-outs were $CD4^+$ T-cell expression of CD25 on day 4 and secretion of IL-17A following overnight stimulation of equal numbers of re-purified $CD4^+$ T-cells. As shown in **Figure 3.3A**, indomethacin reversed the MSC suppressive effect and, in some experiments, was associated with a paradoxical increase in IL-17A production. Surface expression of CD25 was also restored in the presence of indomethacin (**Figure 3.3B**).

The observation was consistent with induction, *via* $CD4^+$ T-cell–MSC contact, of a COX-dependent soluble mediator. To test this further, culture supernatants were removed from 4-day, APC-free Th17 cultures generated with and without indomethacin in the presence or absence of MSCs. These supernatants were applied to newly initiated Th17 cultures along with unconditioned medium and MSC-conditioned medium containing equivalent concentrations of Th17 inducing factors with and without indomethacin. $CD4^+$ T-cells were then re-purified from each culture and stimulated overnight, after which IL-17A production was measured by ELISA. As shown in **Figure 3.3C**, MSC-conditioned medium was associated with a modest reduction in IL-17A compared with unconditioned medium. In contrast, medium from MSC/Th17 co-cultures resulted in substantially greater reduction of IL-17A as well as strong inhibition of CD25 up-regulation (**Figure 3.3D**). These effects were entirely or predominantly absent for media derived from indomethacin-containing cultures. Addition of medium from Th17 cultures lacking MSCs had no suppressive effect and was not influenced by indomethacin.

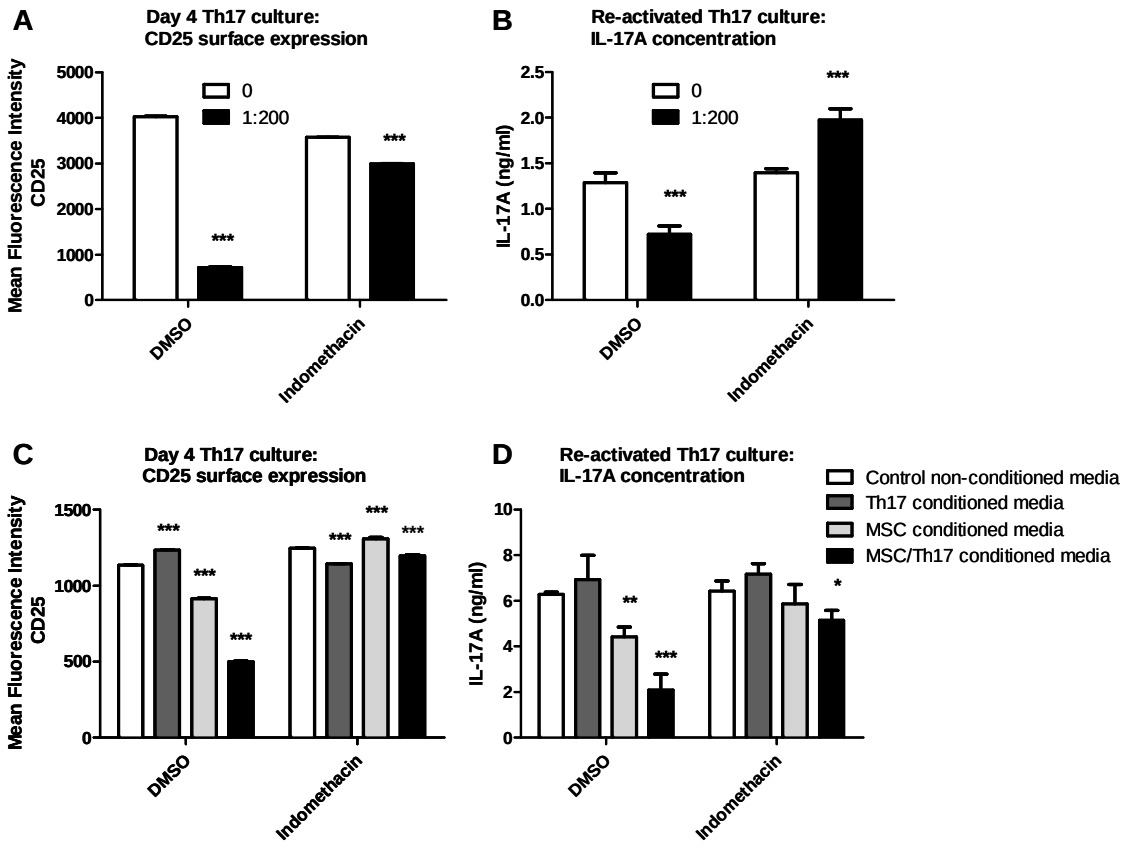

Figure 3.3 Suppression of primary Th17 differentiation by MSCs is induced by cell-cell contact *via* a COX-dependent soluble factor: (A) CD25 surface expression on FACS-purified, naïve-phenotype $CD4^+$ T-cells activated for 4 days with anti-CD3/anti-CD28 beads under Th17-skewed conditions in the presence or absence of 1:200 MSC:$CD4^+$ T-cell ratio with vehicle (DMSO) or 5 μM indomethacin. (**B**) IL-17A production by $CD4^+$ T-cells re-purified and stimulated overnight in equal numbers. (**C**) CD25 surface expression on $CD4^+$ T-cells stimulated for 4 days by anti-CD3/anti-CD28 beads under Th17-skewed conditions with the addition of various conditioned media. (**D**) IL-17A production by $CD4^+$ T-cells re-purified and stimulated overnight in equal numbers. Data are represented as mean +/-standard deviations and are representative of 4 individual experiments for **A/B** and 2 individual experiments for **C/D** (* p = <0.05, ** p = <0.01, *** p = <0.001 compared with equivalent 0 MSC control for **A/B** and equivalent non-conditioned control media for **C/D**, Bonferroni posttest).

3.3.3 Up-regulation of COX2 in MSCs following direct contact between MSCs and activated $CD4^+$ T-cells

Next, MSCs were FACS-purified from 4-day Th17 co-cultures. I used the common leukocyte antigen CD45 to discriminate between MSC and splenocytes as illustrated in detail in **Figure 3.4**. As expected, splenocytes demonstrated universal high-level staining for CD45. In contrast, MSC did not express CD45 – i.e. their CD45 profile did not change when compared to the CD45 FMO control (although MSC were more auto-fluorescent on this channel compared to splenocytes as shown in the bottom right

panels). The sorted fractions were subjected to qRT-PCR and Western Blot using COX1 and COX2-specific reagents.

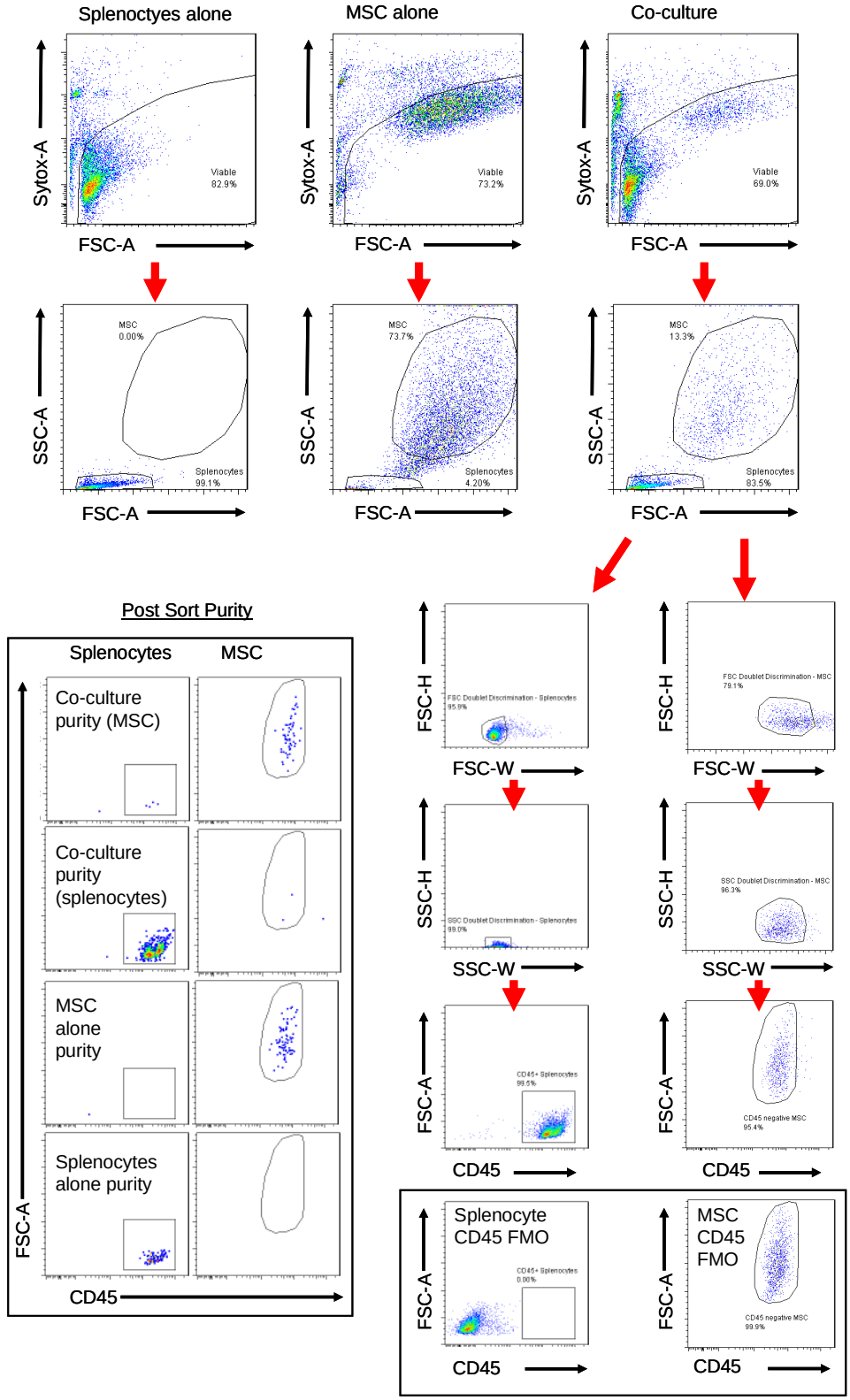

Figure 3.4 Representative gating and sorting strategy and post-sort purity analysis for FACS purification of MSCs and CD45$^+$ splenocytes from individual cultures and co-cultures. FMO controls for CD45 staining of splenocytes and MSCs are shown in the bottom right panel.

As shown in **Figure 3.5**, specific up-regulation of COX-2 in MSCs co-cultured with $CD4^+$ T-cells under Th17-skewed conditions was observed at mRNA and protein level.

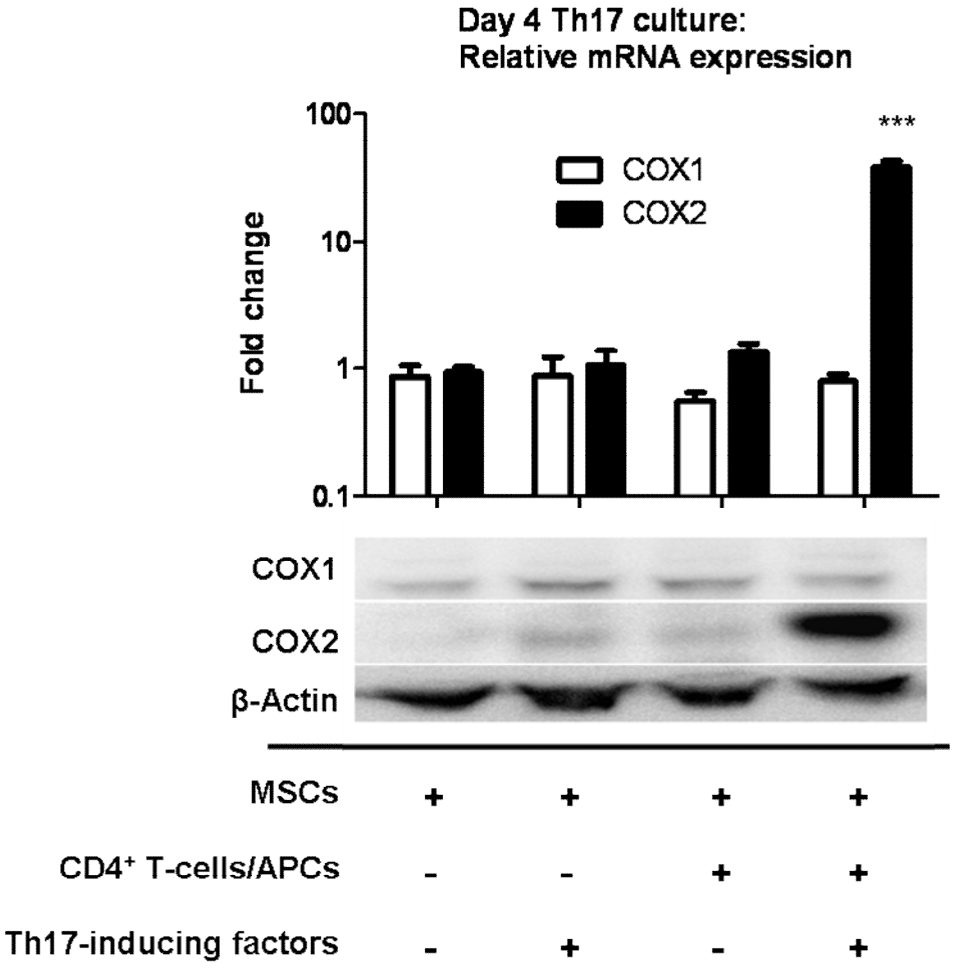

Figure 3.5 COX2 is specifically upregulated in MSCs following co-culture with $CD4^+$ T-cells undergoing primary Th17 differentiation: MSCs were cultured for 4 days alone, in the presence of Th17-inducing agents (anti-IL-4, anti-IFN-γ, TGF-β1, IL-6 and anti-CD3ε), in the presence of $CD4^+$ T-cells and APCs or with a combination of Th17-inducing agents and $CD4^+$ T-cells and APCs. MSCs were re-purified by FACS and subjected to RT-PCR and Western Blot. Top: relative mRNA expression of COX1 and COX2 in MSCs. Bottom: Western blots for COX1, COX2 and β-actin of FACS-purified MSCs. Results are representative of 2 individual experiments and are presented as mean +/-standard deviations. (*** p = <0.001 compared with equivalent MSCs alone control).

3.3.4 MSC-MEDIATED SUPPRESSION OF PRIMARY TH17 DIFFERENTIATION IS REVERSED BY SELECTIVE COX2 INHIBITION

Blocking experiments to date were performed with indomethacin which is a non-selective inhibitor of COX thereby blocking COX1 and COX2. In order to confirm that COX2 was specifically involved in MSC-mediated suppression of primary Th17 differentiation, I employed a selective COX2 inhibitor, NS-398 (Sigma-Aldrich) (Lee et al., 2010). In these experiments, $CD4^+$ T-cells were stimulated for 4 days by anti-CD3/anti-CD28 beads under Th17-skewed conditions with 1:200 MSC:$CD4^+$ T-cell ratio in the presence of low dose (0.1 μM) or high dose (1.0 μM) NS-398 or equivalent volumes of vehicle then re-purified and stimulated overnight in equal numbers. Reversal of the MSC suppressive effect on primary Th17 differentiation was demonstrated using NS-398. As shown in **Figure 3.6A**, NS-398 restored CD25 expression to $CD4^+$ T-cells co-cultured with MSCs under Th17-skewed conditions in a dose-dependent manner. More strikingly, selective COX2 inhibition (1 μM NS-398) completely reversed the suppressive effect on IL-17A production following overnight culture of equal numbers of re-purified $CD4^+$ T-cells in the absence of MSCs in non-Th17 skewed conditions (**Figure 3.6B**).

Thus, these experiments supported a conclusion that the primary mechanism of Th17 suppression from $CD4^+$ T-cells was the production of a prostanoid mediator due to induced up-regulation of COX2 in MSCs following direct contact between MSCs and activated T-cells.

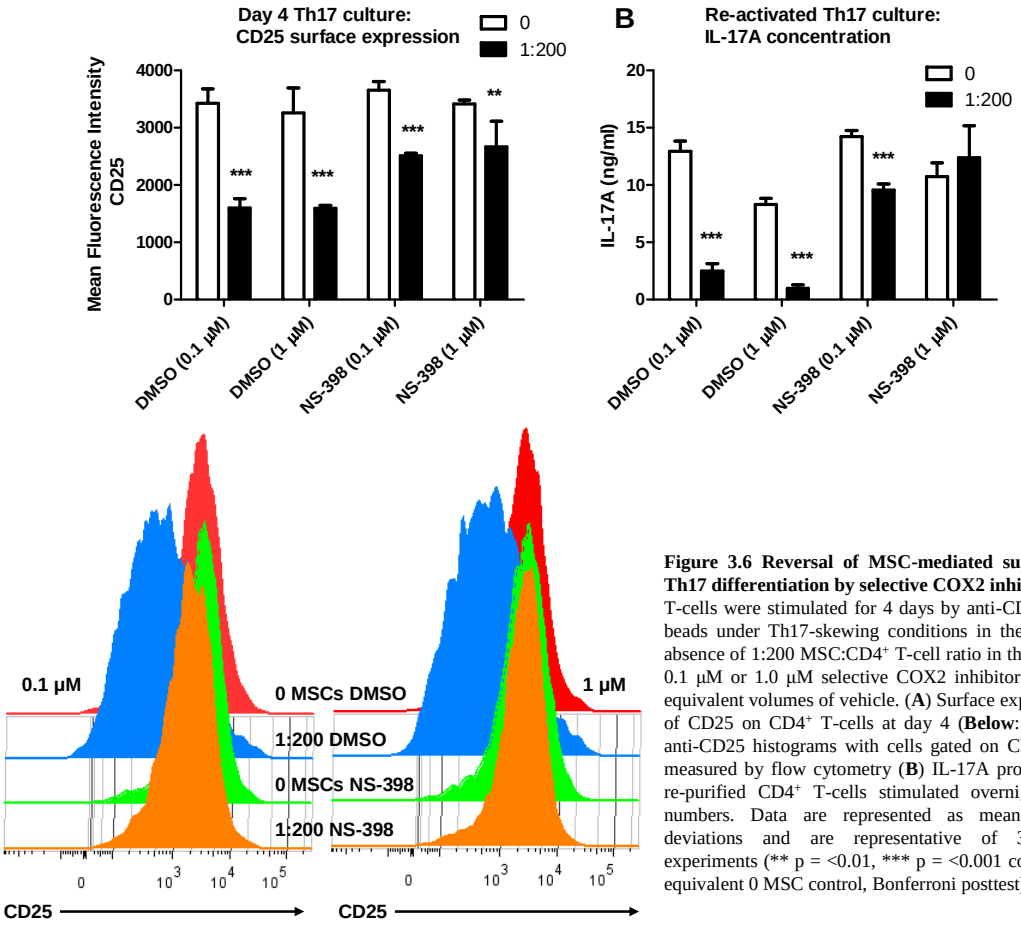

Figure 3.6 Reversal of MSC-mediated suppression of Th17 differentiation by selective COX2 inhibition: $CD4^+$ T-cells were stimulated for 4 days by anti-CD3/anti-CD28 beads under Th17-skewing conditions in the presence or absence of 1:200 MSC:$CD4^+$ T-cell ratio in the presence of 0.1 µM or 1.0 µM selective COX2 inhibitor (NS-398) or equivalent volumes of vehicle. (**A**) Surface expression level of CD25 on $CD4^+$ T-cells at day 4 (**Below**: examples of anti-CD25 histograms with cells gated on $CD4^+$ cells) as measured by flow cytometry (**B**) IL-17A production from re-purified $CD4^+$ T-cells stimulated overnight in equal numbers. Data are represented as mean +/-standard deviations and are representative of 3 individual experiments (** p = <0.01, *** p = <0.001 compared with equivalent 0 MSC control, Bonferroni posttest).

3.3.5 PGE2 IS INDUCED IN MSC/TH17 CO-CULTURES

As PGE2 has been reported to mediate multiple immune suppressive effects of MSCs (Ghannam et al., 2010, Nemeth et al., 2009, English et al., 2009), supernatants from MSC/Th17 co-cultures of 6–72 hour duration were analyzed for PGE2 concentration with relevant controls. Neither MSCs cultured alone nor $CD4^+$ T-cells/APCs cultured with or without Th17-activating/inducing reagents generated high PGE2 levels (**Figure 3.7A**). In contrast, MSC/$CD4^+$ T-cell/APC co-cultures under Th17 differentiating conditions had significant accumulation of PGE2 over 12–72 hours. Interestingly, increased PGE2 production was also observed from 6 to 24 hours in MSC/$CD4^+$ T-cell/APC co-cultures lacking Th17-activating/inducing factors but levels declined again between 48 and 72 hours (**Figure 3.7A**). These findings were reproduced in APC/anti-CD3ε-free culture conditions in which $CD4^+$ T-cells were activated with anti-CD3/anti-CD28 coated beads (data not shown).

In additional experiments, PGE2 concentrations in supernatants from 4 day fibroblast/Th17 co-culture supernatants were shown to be no different to those of control Th17 cultures (**Figure 3.7B**). Additionally, PGE2 concentration increased in a dose-dependent manner in Th17 cultures involving direct contact with MSCs but not in transwell co-cultures at the same MSC:$CD4^+$ T-cell ratios (**Figure 3.7C**).

Thus, in keeping with a mechanism whereby a soluble prostanoid mediator was induced upon cell-cell contact, PGE2 was induced in MSC/Th17 co-cultures as early as 12 hours following cellular cross talk and was not evident in fibroblast/Th17 cultures.

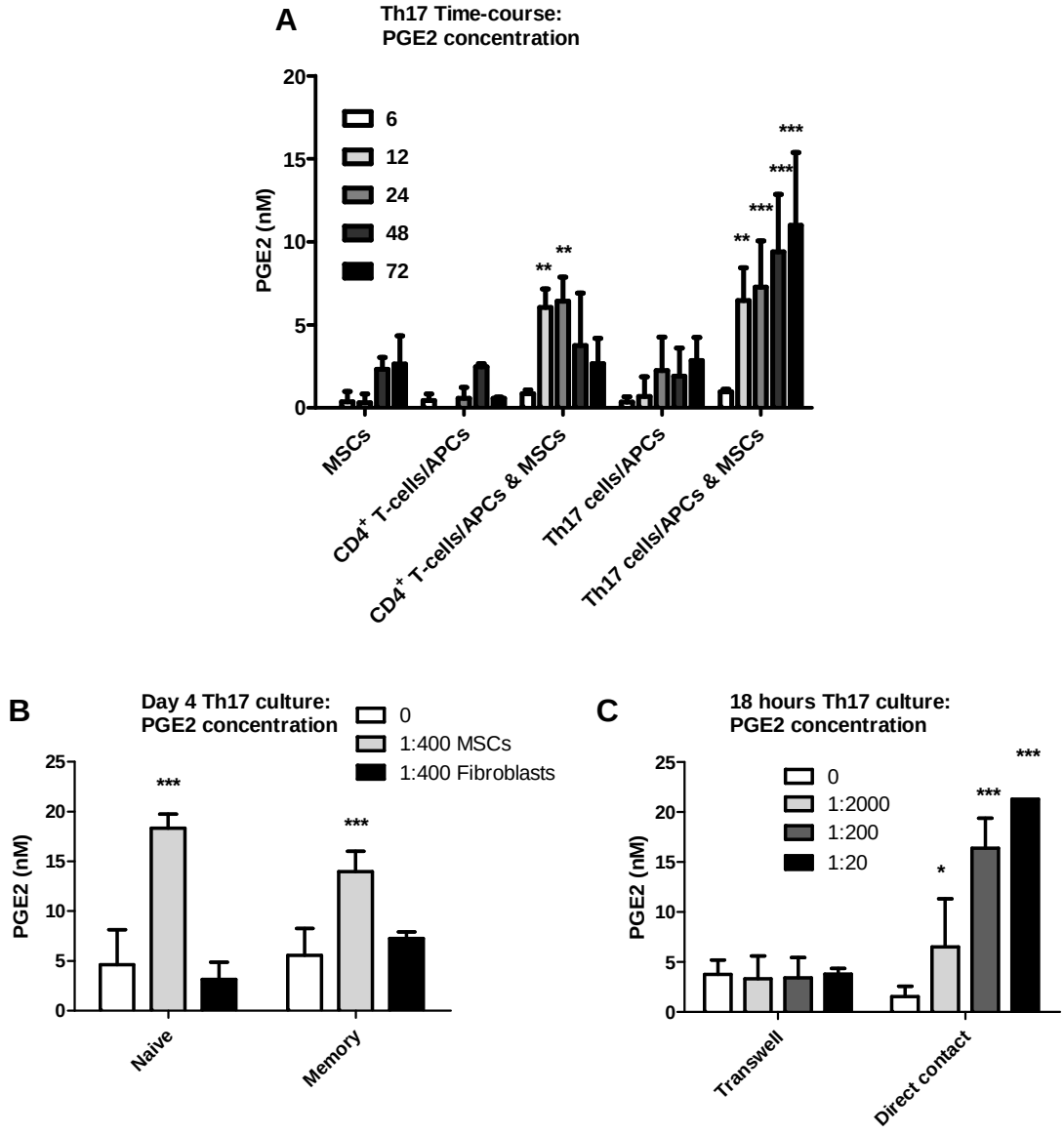

Figure 3.7 PGE2 is induced in MSC/Th17 co-cultures upon cell-cell contact: (**A**) $CD4^+$ T-cells were cultured with APCs or with APCs and Th17 inducing factors (anti-IL-4, anti-IFN-γ, IL-6, TGF-β & anti-CD3ε) in the presence or absence of MSCs (1:200 ratio) for 6-72 hours. Culture supernatants were analyzed for PGE2 at various time-points. (**B**) Concentration of PGE2 in 4 day culture supernatants of naïve- and memory-phenotype $CD4^+$ T-cells cultured in the presence or absence of MSCs or renal cortical fibroblasts under Th17-skewed conditions. (**C**) Concentration of PGE2 at 18 hours following $CD4^+$ T-cell culture under Th17-skewed conditions in the absence or presence of varying ratios of MSCs in transwell or direct contact. Data are represented as mean +/-standard deviations and are representative of 5 individual experiments for **A** and 1 individual experiment each for **B/C** (* p = <0.05, ** p = <0.01, *** p = <0.001 compared with equivalent 6 hour control for **A** & 0 MSC control for **B/C**, Bonferroni posttest).

3.3.6 Dose-dependent inhibition of Th17 differentiation by synthetic PGE2

It was next determined whether MSC suppressive effects on primary Th17 cultures were mediated by PGE2. MACS-enriched $CD4^+$ T-cells were cultured under Th17 skewed conditions for 4 days with anti-CD3/anti-CD28 coated beads. Addition of

purified PGE2 (Cayman Chemical Company) was associated with a potent dose-dependent inhibition of IL-17A at day 4 (**Figure 3.8A**). Furthermore, in 3 individual experiments I observed dose-dependent suppression of CD25 surface expression (**Figure 3.8B/C**), $CD4^+$ T-cell proliferation (**Figure 3.8D**) and IL-17A production (**Figure 3.8E**) by flow cytometry following re-stimulation of equal numbers of $CD4^+$ T-cells for 8 hours in the presence of anti-CD3/antiCD28 coated beads and brefeldin A. Inhibition occurred between 2 and 20nM PGE2 – within the range observed by 12 h in MSC/Th17 co-cultures.

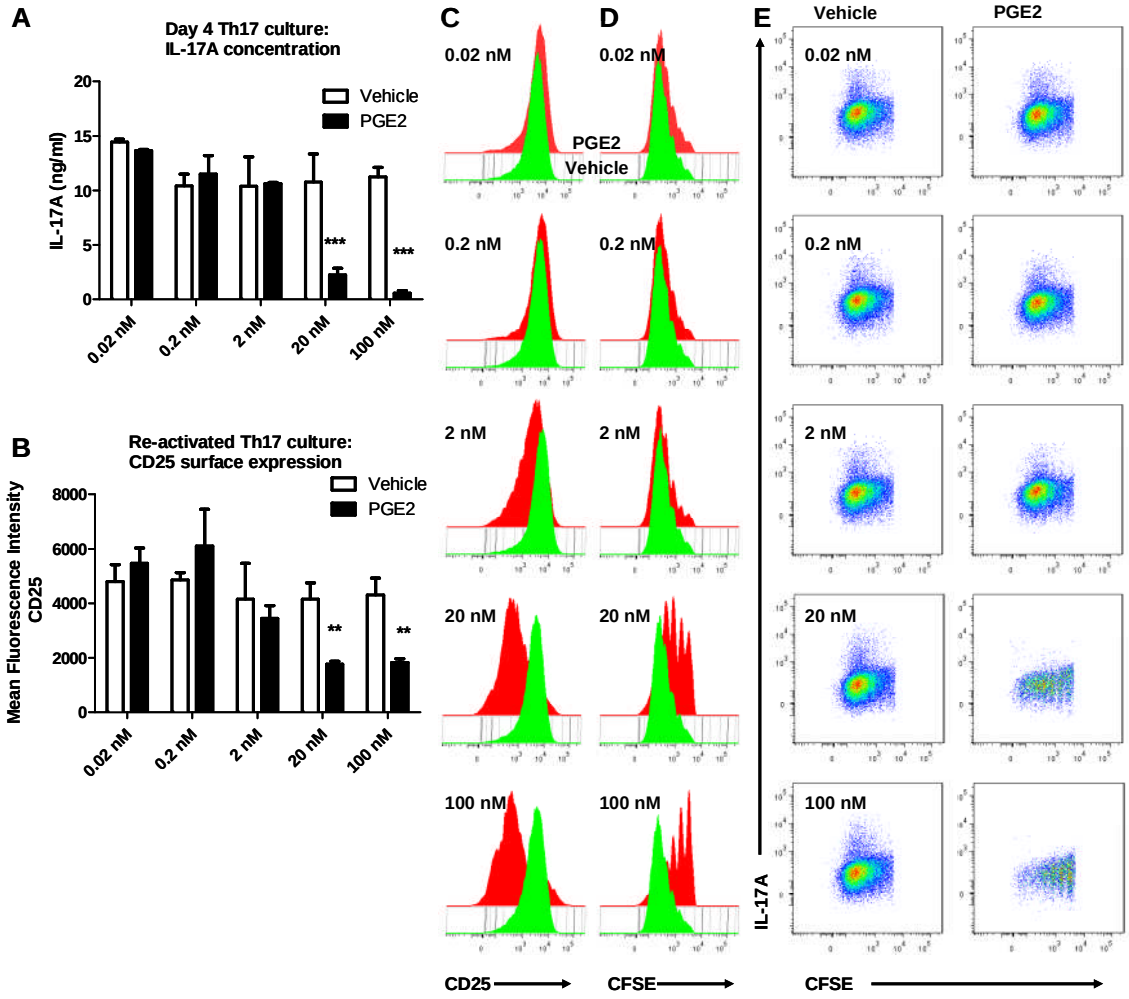

Figure 3.8 Dose-dependent suppression of primary Th17 differentiation by synthetic PGE2: $CD4^+$ MACS-enriched T-cells were activated with anti-CD3/anti-CD28 coated beads for 4 days under Th17 skewed conditions in the presence of graded concentrations of PGE2 or equivalent volumes of vehicle (ethanol). Cells were then re-stimulated for 8 hours with anti-CD3/anti-CD28 beads under non-Th17-skewed conditions. (**A**) Concentration of IL-17A in culture supernatants at day 4. (**B**) Surface expression of CD25 on re-stimulated $CD4^+$ T-cells. (**C**) Representative examples of CD25 histograms following re-stimulation. (**D**) Representative CFSE histograms following re-stimulation. (**E**) Representative intracellular staining for IL-17A following re-stimulation. Data are represented as mean +/-standard deviations and are representative of 3 individual experiments (** p = <0.01, *** p = <0.001 compared with equivalent vehicle control, Bonferroni posttest).

3.3.7 MSCs SUPPRESS TH17 DIFFERENTIATION BY PGE2 *VIA* THE EP4 RECEPTOR

As shown in **Figure 3.8**, purified PGE2 suppressed primary Th17 differentiation in a dose-dependent manner. The role of PGE2 in mediating MSC suppressive effects on Th17 differentiation cultures was confirmed by addition of specific antagonists and agonists for candidate PGE2 receptors.

As shown in **Figure 3.9A**, addition of selective EP4 antagonist (L-161,982 Cayman Chemical Company) to co-cultures of MSCs and $CD4^+$ T-cells activated with anti-CD3/anti-CD28 beads under Th17 skewed conditions restored CD25 surface expression to the T-cells. Experiments carried out with antagonists of the EP1 and EP2 receptors (SC-51322 and AH-6809 respectively) yielded negative results. Indeed, selective inhibition of EP1 in Th17 cultures in the absence of MSCs also had a negative effect.

To further investigate the effect of EP4 antagonism on MSC/Th17 co-cultures, the EP4 antagonist L-161,982 was added in graded concentrations to primary cultures. CD25 surface expression on $CD4^+$ T-cells at day 4 (**Figure 3.9B**) and IL-17A secretion by $CD4^+$ T-cells re-purified from MSC/Th17 co-cultures and re-stimulated overnight in equal numbers was dose-dependently restored to the same level as that of control Th17 cultures (**Figure 3.9C**) by the EP4 receptor antagonist.

The results are consistent with a conclusion that PGE2 is induced in MSC/Th17 co-cultures and suppresses primary Th17 differentiation *via* the EP4 receptor.

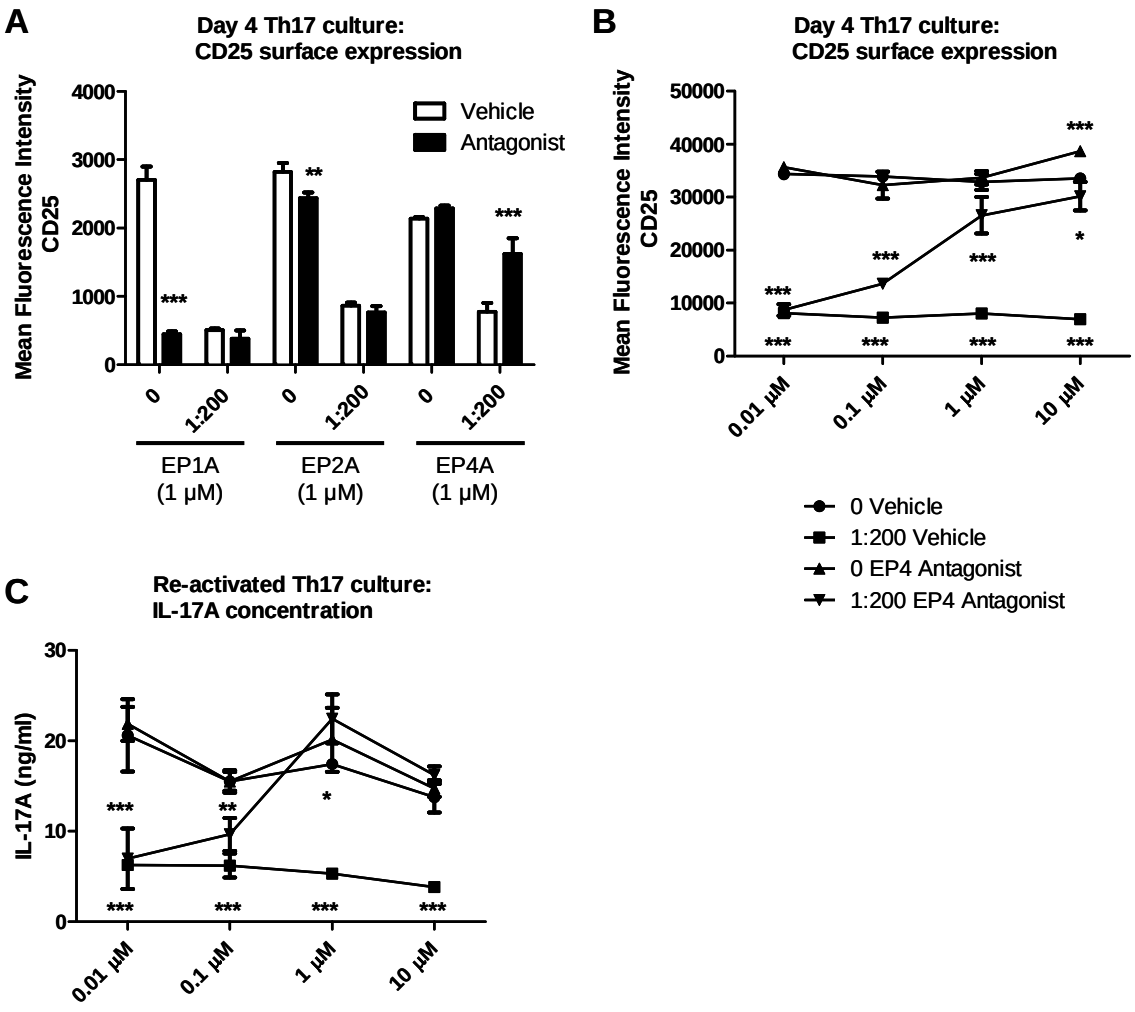

Figure 3.9 Selective reversal of MSC-mediated Th17 suppression by EP4 antagonism: $CD4^+$ T-cells were activated by anti-CD3/anti-CD28 coated beads under Th17 skewed conditions in the presence or absence of 1:200 MSC:$CD4^+$ T-cell ratio with varying concentrations of selective EP antagonists or equivalent volumes of vehicles (DMSO) for 4 days prior to re-stimulation overnight of equal numbers of re-purified $CD4^+$ T-cells with anti-CD3/anti-CD28 beads. (**A**) CD25 surface expression by $CD4^+$ T-cells at day 4. (**B**) CD25 surface expression by $CD4^+$ T-cells at day 4 following co-culture with varying concentrations of EP4 antagonist in the presence or absence of MSCs. (**C**) Concentration of IL-17A following overnight stimulation of equal numbers of $CD4^+$ T-cells re-purified from **B**. Data are represented as mean +/-standard deviations and are representative of 2 individual experiments for **A** and 4 individual experiments for **B/C** (* p = <0.05, ** p = <0.01, *** p = <0.001 compared with equivalent vehicle control, Bonferroni posttest).

As further evidence of a specific role for PGE2/EP4, the EP4 agonist L-902,688 (Cayman Chemical Company) was shown to mediate dose-dependent inhibition of the primary induction of Th17 cells. MACS-enriched $CD4^+$ T-cells were anti-CD3/anti-CD28 bead activated under Th17 skewed conditions in the presence or absence of varying concentrations of L-902,688 or equivalent volumes of ethanol vehicle. As shown in **Figure 3.10A**, surface expression of CD25 by T-cells was suppressed in a dose-dependent manner. Furthermore, IL-17A production by re-purified T-cells was

inhibited by nanomolar concentrations of the EP4 receptor agonist (**Figure 3.10B**) confirming that signaling *via* the EP4 receptor was directly responsible for suppression of primary Th17 differentiation.

This series of experiments provided compelling evidence of induction of COX2 in MSCs following cell-cell contact with activated $CD4^+$ T-cells undergoing primary Th17 differentiation. MSC-mediated suppression of Th17 differentiation was reversed by indomethacin, selective COX2 inhibition and the EP4 receptor antagonist L-161,982. The suppressive effects were mimicked by purified PGE2 and the EP4 agonist L-902,688. High levels of PGE2 were detected in MSC/Th17 co-culture thus, the next set of experiments were designed to determine which cell type produced the PGE2.

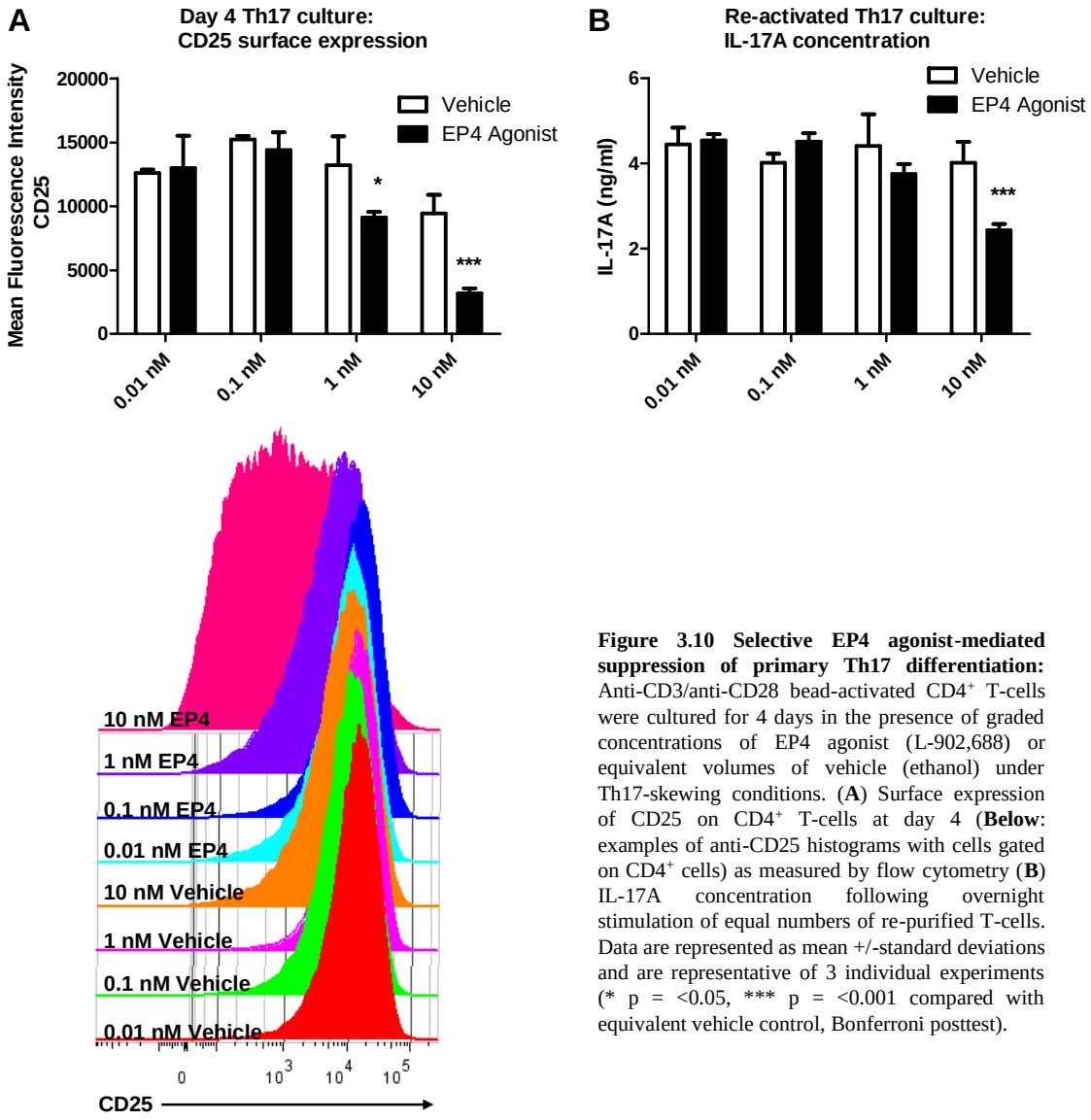

Figure 3.10 Selective EP4 agonist-mediated suppression of primary Th17 differentiation: Anti-CD3/anti-CD28 bead-activated $CD4^+$ T-cells were cultured for 4 days in the presence of graded concentrations of EP4 agonist (L-902,688) or equivalent volumes of vehicle (ethanol) under Th17-skewing conditions. (**A**) Surface expression of CD25 on $CD4^+$ T-cells at day 4 (**Below**: examples of anti-CD25 histograms with cells gated on $CD4^+$ cells) as measured by flow cytometry (**B**) IL-17A concentration following overnight stimulation of equal numbers of re-purified T-cells. Data are represented as mean +/-standard deviations and are representative of 3 individual experiments (* p = <0.05, *** p = <0.001 compared with equivalent vehicle control, Bonferroni posttest).

3.3.8 MSCs ARE THE PRIMARY PRODUCERS OF PGE2

In order to definitively prove which cells produced PGE2 in MSC/Th17 co-cultures, I sorted individual cell populations following 18 hours of co-culture then re-plated them for an additional 18 hours and quantified PGE2 concentration in the resulting supernatants. The experimental design is illustrated in **Figure 3.11**.

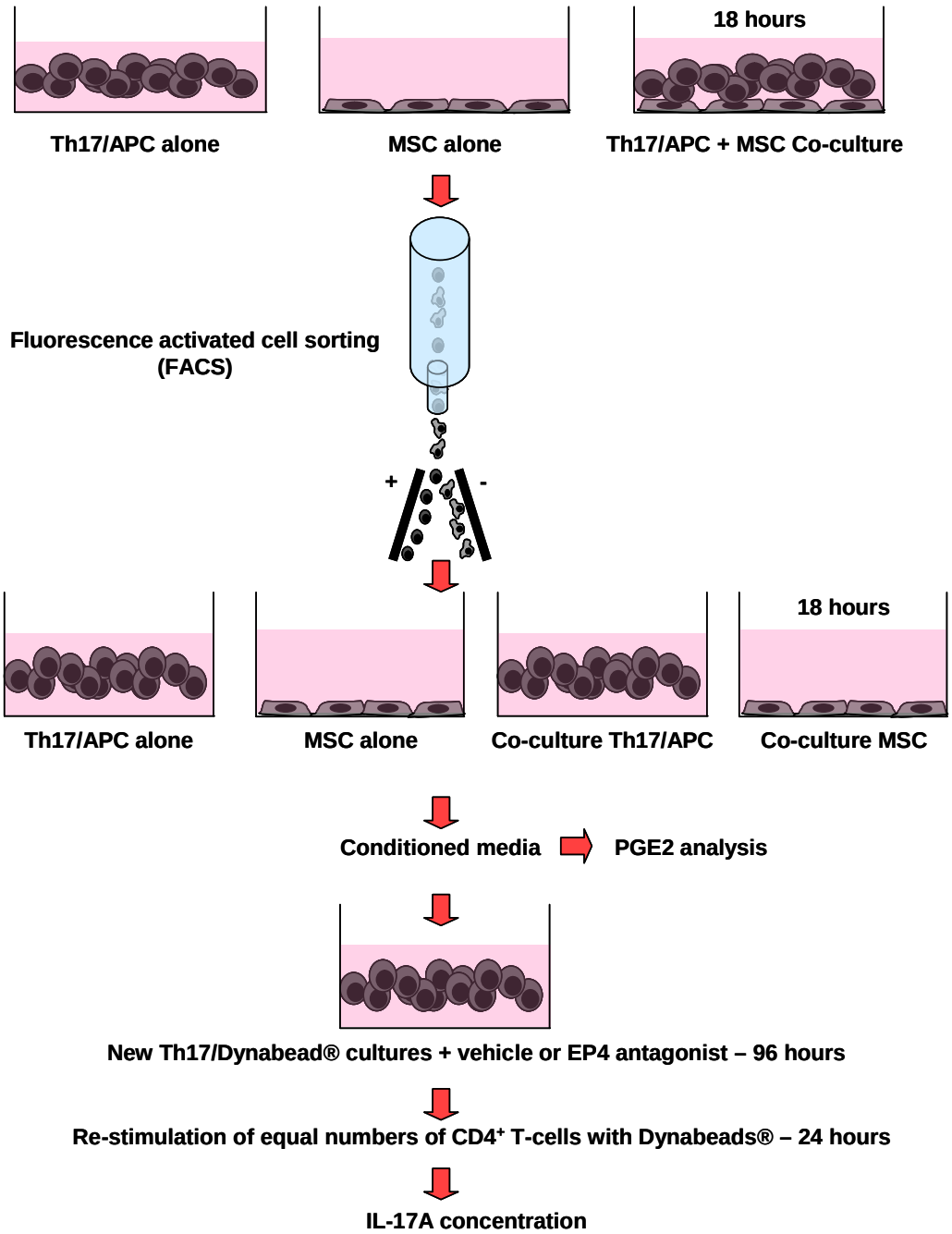

Figure 3.11 Outline of experiment in which Th17 cells/APCs and MSCs were separated to high purity from 18-hour co-cultures or relevant control cultures and were then re-cultured for an additional 18 hours for the purpose of analyzing PGE2 production and Th17-suppressive effects of conditioned medium from the individual cell populations.

Representative gating and sorting strategy and post-sort purity analysis for FACS purification of MSCs and $CD45^+$ immune cells from individual cultures and co-cultures are shown in **Figure 3.4**. By this strategy MSCs were formally confirmed to be the predominant source of PGE2 in MSC/Th17 co-cultures (**Figure 3.12B**). Low level PGE2 was also detected in Th17/APC cultures post sort (**Figure 3.12B**) although this may have been due to a small number of contaminating MSCs as shown in the post sort purity panel in **Figure 3.4**.

That the observation of inhibition of primary Th17 differentiation was specifically attributable to PGE2 produced by MSCs during co-culture was confirmed by transfer of conditioned media from FACS-sorted co-culture populations and relevant controls to fresh Th17 cultures in the presence or absence of EP4 antagonist as illustrated in **Figure 3.11**. In this case, only medium conditioned by MSCs sorted from Th17/MCS co-cultures transferred a Th17 suppressive effect that was reversible by EP4 antagonism (**Figure 3.12B**).

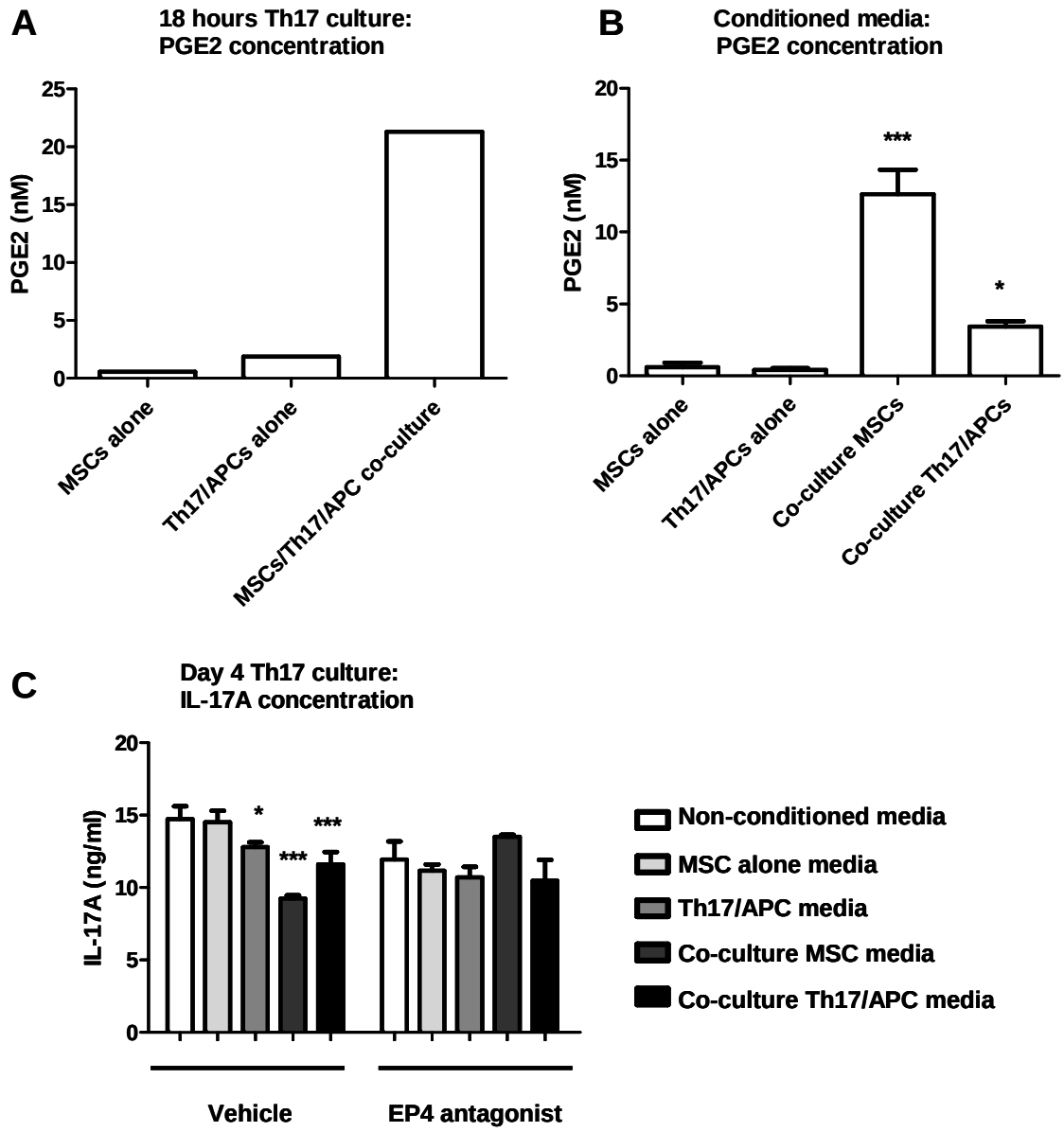

Figure 3.12 PGE2-enriched conditioned MSC media suppresses Th17 development: $CD4^+$ T-cells were cultured with anti-CD3ε and APCs under Th17-skewed conditions for 18 hours in the presence or absence of MSCs. Immune cells and MSCs were sorted by FACS into individual populations and cultured separately for an additional 18 hours. Culture supernatants were analyzed for PGE2 or applied to newly initiated Th17 cultures activated with anti-CD3/anti-CD28 beads in the presence or absence of the EP4 antagonist L-161,982 for 4 days to determine the suppressive nature of the conditioned media. (**A)** PGE2 concentration in original 18 hour supernatant prior to FACS. (**B**) PGE2 concentration in conditioned media and **(C)** IL-17A concentration following 24 hour stimulation of $CD4^+$ T-cells re-purified from varying conditions with DMSO vehicle or EP4 antagonist and conditioned media. Data are represented as mean +/-standard deviations and are representative of 2 individual experiments (* $p = <0.05$, ** $p = <0.01$, *** $p = <0.001$ compared with MSC alone control for **B** and equivalent non-conditioned media for **C**, Tukey's multiple comparison test (**B**) Bonferroni posttest (**C**)).

3.3.9 MSCs SUPPRESS DE-NOVO IL-17A PRODUCTION BY EFFECTOR-MEMORY TH17 CELLS FROM OBSTRUCTED KIDNEY

Up to this point, the experiments were carried out exclusively with primary naïve and/or memory $CD4^+$ T-cells undergoing activation *in vitro* under short-term Th17-skewed conditions. Making use of a unilateral ureteral obstruction (UUO) model in which intra-renal accumulation of effector-memory phenotype Th17 cells has been reported (Dong et al., 2008, Pindjakova et al., 2012), it was determined whether MSCs exert a mechanistically-similar suppressive effect on the re-activation of committed Th17 cells from an area of ongoing tissue inflammation. As shown in **Figure 3.13A**, B6 mice underwent UUO for 72 hours following which $CD45^+$ cells were enriched from obstructed and contra-lateral (non-obstructed) kidneys and briefly stimulated through the TCR in the absence or presence of MSCs. Anti-CD3e-stimulation was associated with robust secretion of IL-17A by cells from obstructed kidneys (**Figure 3.13B**). The presence of MSCs was associated with dose-dependent reduction in IL-17A concentration following either 24 or 48 hours culture periods (**Figure 3.13B/C**). Qualitatively similar results were observed in a total of seven similar experiments with median proportionate inhibition of IL-17A production being 56% (range 19–69%) at MSC:$CD45^+$ cell ratio of 1:20. IL-17A secretion was absent from stimulated cultures of $CD45^+$ cells from non-obstructed kidneys (**Figure 3.13B**). The suppressive effect of MSCs was reversed by indomethacin (**Figure 3.13D**). Thus, effector-memory Th17 cells from a site of inflammation undergoing activation through the TCR signaling complex are amenable to suppression by MSCs *via* a similar COX2-dependent mechanism.

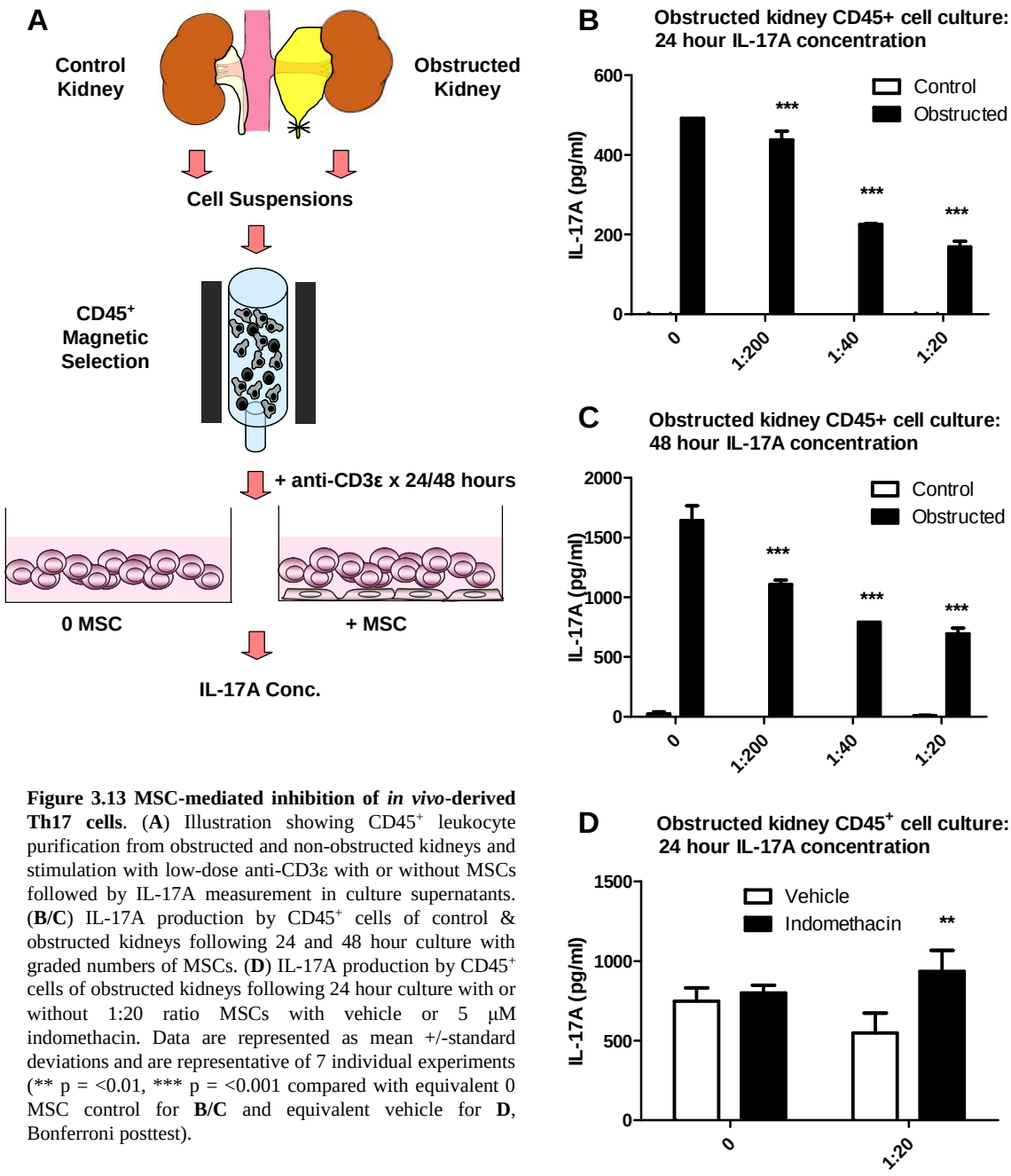

Figure 3.13 MSC-mediated inhibition of *in vivo*-derived Th17 cells. (**A**) Illustration showing $CD45^+$ leukocyte purification from obstructed and non-obstructed kidneys and stimulation with low-dose anti-CD3ε with or without MSCs followed by IL-17A measurement in culture supernatants. (**B/C**) IL-17A production by $CD45^+$ cells of control & obstructed kidneys following 24 and 48 hour culture with graded numbers of MSCs. (**D**) IL-17A production by $CD45^+$ cells of obstructed kidneys following 24 hour culture with or without 1:20 ratio MSCs with vehicle or 5 μM indomethacin. Data are represented as mean +/-standard deviations and are representative of 7 individual experiments (** p = <0.01, *** p = <0.001 compared with equivalent 0 MSC control for **B/C** and equivalent vehicle for **D**, Bonferroni posttest).

In summary, experimental evidence from chapter 3 demonstrated induction of COX2 in MSCs following co-culture with Th17 cells which, when blocked, reversed the suppressive effects. Furthermore, MSC-derived PGE2 was specifically upregulated in MSC/Th17 co-cultures and suppressed Th17 induction *via* the EP4 receptor.

3.4 DISCUSSION

3.4.1 SUPPRESSION OF PRIMARY TH17 DIFFERENTIATION BY MSC-DERIVED PGE2

From a mechanistic perspective, I provided compelling evidence in chapter 3 that the induced production of PGE2 by MSCs (**Figure 3.12A/B**) in direct contact with $CD4^+$ T-cells undergoing primary activation (**Figure 3.7**) was chiefly responsible for suppressive effects on Th17 cells *in vitro* (**Figure 3.3, 3.6, 3.10**) as well as on *in vivo*-derived effector-memory Th17 cells stimulated through the TCR (**Figure 3.13**).

This is consistent with the report of Ghannam et al., in which indomethacin reversed MSC-mediated suppression of Th17 differentiation from human naïve, cord blood $CD4^+$ T-cells as well as IL-17A production by Th17 clones (Ghannam et al., 2010). The observation of reversal of MSC suppression of Th17 differentiation by indomethacin (**Figure 3.3**) was also confirmed by Tatara et al. in the mouse system (Tatara et al., 2011). Bouffi et al. additionally reported that PGE2 is a potent immunosuppressive agent in MSC/splenocyte co-cultures (1:20 ratio). The authors correlated PGE2 induction with IL-6 secretion (Bouffi et al., 2010) however this was not the case in my culture system. IL-6 was not increased in naïve Th17/MSC co-cultures while it was increased in memory Th17/MSC co-cultures (**Figure 2.8**) yet more potent suppression was observed on naïve cells co-cultured with MSCs rather than memory cells as described in chapter 2. Furthermore, I demonstrated that PGE2 was dose-dependently induced in Th17/MSC direct contact co-cultures but that this was not the case when the cells were separated in transwell cultures (**Figure 3.7**). This indicated that cell-cell contact was necessary for PGE2 induction in my culture system rather than IL-6 as reported by Bouffi and colleagues.

By utilizing FACS to re-purify MSCs (**Figure 3.4**), I convincingly demonstrated up-regulation of COX2 (**Figure 3.5**) and production of PGE2 (**Figure 3.7A**) by these cells within 12–24 hours of placement in Th17-skewed cultures. I also confirmed the role of COX2 using the selective inhibitor NS-398 (**Figure 3.6**) and illustrated the participation of an induced soluble mediator by medium transfer experiments (**Figure 3.3 and 3.12**). Furthermore, I demonstrated that inhibition of Th17 cell proliferation, CD25 up-regulation and IL-17A-secreting capacity are reproducible by synthetic PGE2 (**Figure 3.8**) at comparable concentrations to those observed in Th17/MSC co-

cultures (**Figure 3.7A**). My findings have added to the field by providing further insight into how MSC-derived PGE2 suppresses Th17 differentiation as initially described by the laboratories of Ghannam, Bouffi and Tatara (Ghannam et al., 2010, Bouffi et al., 2010, Tatara et al., 2011). Results obtained with selective antagonists (**Figure 3.9**) and agonists (**Figure 3.10**) for the EP4 receptor in APC-free cultures indicate a previously unreported direct suppressive action of MSC produced PGE2 on $CD4^+$ T-cells *via* this receptor.

3.4.2 Effects of PGE2 on Th17 responses

Of relevance to this study, it is clear from a number of recent reports that the interplay between PGE2, the EP4 receptor and immunological processes, including the Th17 differentiation pathway, is an important but complex one. Xiao et al. demonstrated that both PGE2 and EP4 agonists protect the heart from ischemia reperfusion injury *via* EP4 (Xiao et al., 2004). Additionally, Kabashima et al. reported, in a mouse model of colitis, that EP4-deficient mice develop more severe disease compared with mice deficient in other prostanoid receptors. Complementary results were obtained in animals treated with EP4 antagonist and the effects were associated with increased activation of T-cells in the colon of treated animals (Kabashima et al., 2002). *In-vitro*, Valdez et al. recently confirmed suppression of Th17 development from naïve $CD4^+$ T-cells in the presence of PGE2 *via* EP2/EP4 signaling and cAMP activation. Downstream, the Th17 transcription factors IRF4, AhR, RORγt and RORα were suppressed in the presence of PGE2 (Valdez et al., 2012). *Cryptococcus neoformans* produce PGE2 which inhibits IL-17A production by $CD4^+$ T-cells undergoing Th17 differentiation. Administration of indomethacin to mice with *Cryptococcus neoformans* infection improved survival of the mice, reduced the number of colony formation units in total homogenized lungs at 1 week and increased IL-17A production by $CD4^+$ T-cells in broncho-alveolar lavage fluid (BALF) at 1 week and in the spleen at 13 days. Furthermore, depletion of $CD4^+$ T-cells using an anti-CD4 antibody or neutralization of IL-17 reversed the protective effect of indomethacin in this model (Valdez et al., 2012).

In contrast however, Yao et al. reported that PGE2 enhanced expansion of Th17 cells *in vitro* and *in vivo* through PGE2-EP4 signaling. This effect was mediated indirectly through IL-23 and, consistent with my findings, PGE2 was also shown to dose-

dependently suppress Th17 differentiation from naïve $CD4^+$ T cells in an APC-free culture system (Yao et al., 2009). Nonetheless, enhancement of Th17-mediated immune responses by PGE2/EP4 signaling has also been described in other experimental settings. For instance it has been reported that fibroblast-derived PGE2 stimulation of IL-23 secretion by APCs is responsible for enhanced IL-17A production (Schirmer et al., 2010). To further complicate the matter, Esaki et al. demonstrated that EP4 KO mice displayed ameliorated EAE compared to WT, EP1 KO, EP2 KO and EP3 KO mice (Esaki et al., 2010). This was confirmed by administration of EP4 antagonist to WT mice during MOG immunization – characterized by suppressed MOG-specific Th1 and Th17 generation. However, if administered at the onset of EAE, the EP4 antagonist did not confer protection. In contrast, an EP4 agonist prevented inflammatory cell infiltration into the CNS and inhibited myelin degeneration when administered at the onset of EAE (Esaki et al., 2010) suggesting that PGE2/EP4 signaling facilitated Th17 cell generation following MOG administration but prevented Th17 entry into the CNS and subsequent demyelination at the onset of EAE. In a study by Chen et al., EP4 antagonism suppressed CIA and IL-17A production in mice. The authors also demonstrated that an EP3/4 agonist induced IL-23 production by human DCs stimulated with TLR4/7, GM-CSF and IL-4. Furthermore, PGE2 enhanced IL-17A production by murine $CD4^+$ T-cells cultured with IL-23 and anti-CD3/anti-CD28. However, in this study, PGE2 did not induce IL-17A production in the presence of IL-6 and TGF-β (Chen et al., 2010b) further supporting the notion that PGE2 enhancement of Th17 responses is indirect *via* induction of IL-23. Of interest, Valdez et al. reported that PGE2 suppressed primary Th17 differentiation but enhanced IL-17A production from secondary re-activated Th17 cells with or without IL-23 (Valdez et al., 2012). This is in keeping with my finding from chapter 2, in which MSCs potently suppressed primary Th17 differentiation but enhanced IL-17A production by fully differentiated Th17 cells re-activated in the presence of IL-1, IL-23 and MSCs (**Figure 2.16**). This may explain the paradoxical increase in IL-17A by fully differentiated Th17 cells in the presence of MSCs.

Given the pleiotropic effects and diverse cellular targets of PGE2 *in vivo*, it appears unlikely that the inhibitory effects of MSCs on Th17 cell differentiation and activation can be selectively reproduced in an active disease setting by administration of COX2

inhibitor or EP4 agonist. Rather, the combined effects of PGE2 and other MSC-associated mediators may be necessary to additionally regulate the production of Th17-promoting factors (IL-1 & IL-23) by ancillary cell populations such as dendritic cells and monocyte/macrophages. Thus, it is important to consider that MSC inhibition of Th17 cell differentiation and activation, while potent, is conditional, being dependent upon opportune MSC/T-cell contact and inducible factors which, when absent or subject to blockade, may unmask a paradoxical capacity for enhancement of Th17 activity.

3.4.3 OTHER IMMUNOMODULATORY MEDIATORS

These results highlight the broad role that has been reported for PGE2 in mediating various immune suppressive effects of MSCs while also emphasizing the fact that high-level production of this and other soluble mediators is dependent upon an initial, contact-dependent cross-talk between MSCs and target cells. Additional mediators of MSC inhibition of Th17 cells have been reported, primarily in the context of rodent models of tissue-specific autoimmunity, including alternatively cleaved CCL2, IDO, IL-27, TGF-β1 (Kong et al., 2009, Zhao et al., 2008, Wang et al., 2008a, Rafei et al., 2009) and more recently IL-10 (Qu et al., 2012). As described in chapter 2, in my culture system, IL-10 was lower in MSC/Th17 co-cultures at 1:200 ratio than in Th17 cultures in the absence of MSCs (**Figure 2.8**) suggesting that IL-10 was not responsible for the suppressive effects observed. Qu et al. employed 1:10 MSC:$CD4^+$ T-cell ratio (Qu et al., 2012). At higher MSC:$CD4^+$ T-cell ratios, it is possible that IL-10 may be induced. Ghannam et al. showed in the human system that MSCs induce IL-10-producing T-cells with a regulatory phenotype at 1:40 ratio however the suppressive effects of MSCs on Th17 differentiation were attributable to PGE2 and not IL-10 (Ghannam et al., 2010). Furthermore, the likelihood of $CD4^+$ T-cells interacting with high numbers of MSCs *in-vivo* is marginal. For this reason, I feel that co-culture of $CD4^+$ T-cells with low numbers of MSCs is a more appropriate experimental approach. In the co-culture system reported in this thesis, significant reversal of MSC-mediated Th17 suppression was not observed with blocking/inhibiting agents for CCL2 or NO (**Figure 3.2**) in keeping with the report of Tatara and colleagues (Tatara et al., 2011).

Inhibition of COX2 was consistently associated with complete or almost complete reversal of suppression in my culture system. Nonetheless, given the diversity of MSC-associated suppressive mediators that have been identified to date, it appears likely that additional direct and indirect mechanisms of Th17 inhibition participate under different conditions.

3.4.4 CONTACT-DEPENDENT SIGNALS

I propose that further characterization of the interactions between Th17 cells and MSCs, including the nature of the contact-dependent signal responsible for COX-2 up-regulation, will identify additional opportunities for manipulation of the Th17 differentiation program. Although there was not time to pursue this during the course of my Ph.D., experiments in which I co-cultured MSCs for 24 hours with $CD4^+$ T-cells and APCs with or without TCR stimulus revealed a potential candidate mediator. MSCs were examined by flow cytometry for cell surface markers and potential contact ligands. Cells were gated on $CD45^-$ to identify MSCs in co-cultures. PD-L1 and MHC-I were specifically upregulated on MSCs following co-culture with activated $CD4^+$ T-cells (**Figure 3.14**). This is consistent with the report of Sheng et al. who demonstrated that IFN-γ induced PD-L1 expression on MSCs and that this was a necessary component of MSC-induced immunosuppression (Sheng et al., 2008). Furthermore, Schurger et al. reported that IL-17 synergized with IFN-γ to enhance PD-L1 expression (Schurgers et al., 2010). Although IFN-γ is not necessary for MSC-induced suppression of primary Th17 differentiation, it is possible that IL-17A may also synergize with other pro-inflammatory cytokines to induce PD-L1 expression. Fiorina et al. reported that BALB/c MSCs had 4 fold higher expression of PD-L1 than MSCs generated from NOD mice which was further induced following culture in the presence of pro-inflammatory IL-1β for 48 hours (Fiorina et al., 2009). Subsequently, BALB/c MSCs delayed diabetes onset and reversed hyperglycemia in NOD mice which was not evident with NOD-MSCs (Fiorina et al., 2009). Moreover, Augello and colleagues reported that MSCs suppressed T-cell proliferation *via* engagement of PD-1 by PD-L1 and PD-L2 (Augello et al., 2005). Therefore, it would be of interest to determine whether the cell-cell contact signal required for MSC-mediated suppression of primary Th17 differentiation involves the PD-1/PD-L1 pathway.

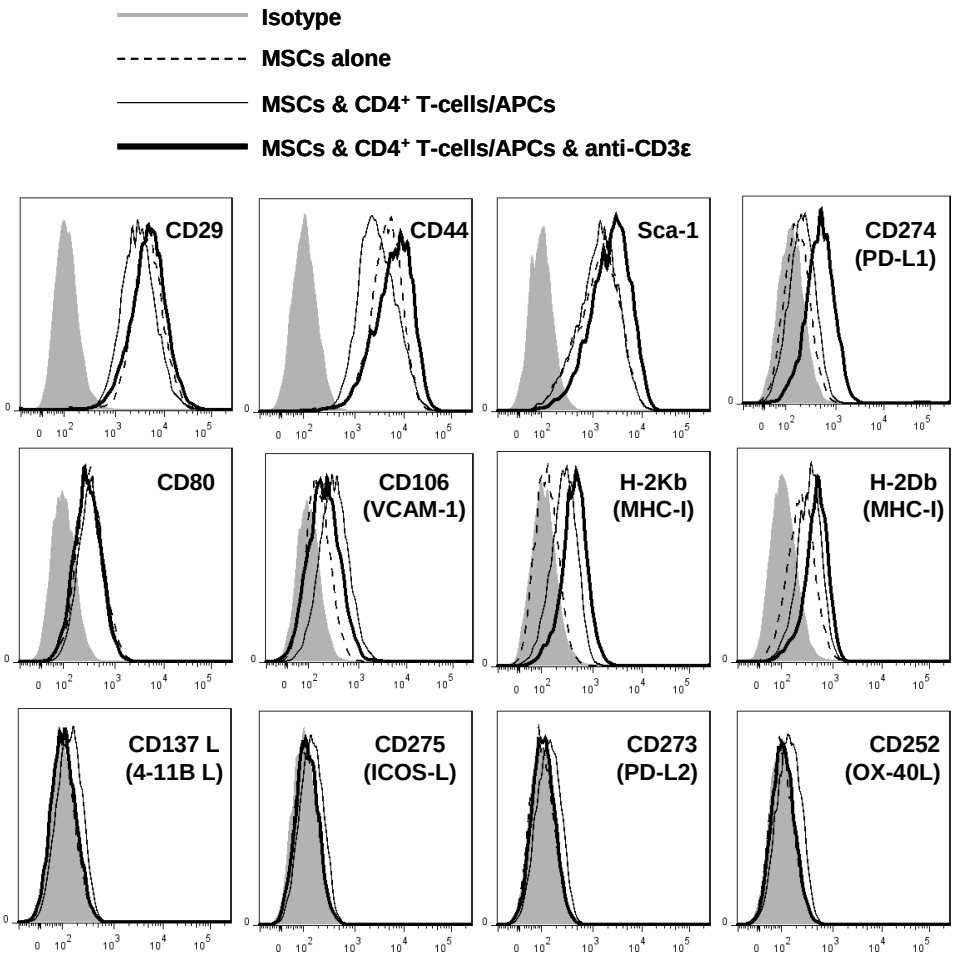

Figure 3.14 Surface phenotype modifications of MSCs following co-culture with CD4$^+$ T-cells: MSCs were cultured for 24 hours in the presence or absence of CD4$^+$ T-cells, APCs and anti-CD3ε prior to analysis of cell surface markers by flow cytometry.

3.4.5 SUMMARY

In conclusion, this study provides novel evidence that MSC-derived PGE2 is highly induced in Th17-MSC co-cultures and mediates a potent suppressive effect on primary and secondary Th17 induction *via* the EP4 receptor as illustrated in **Figure 3.15**. Furthermore, suppression of IL-17A production by effector-memory Th17 cells derived from a site of ‘‘sterile inflammation’’ indicates the potential for MSCs to ameliorate tissue damage associated with maladaptive acute or chronic Th17 activation if delivered in the correct context.

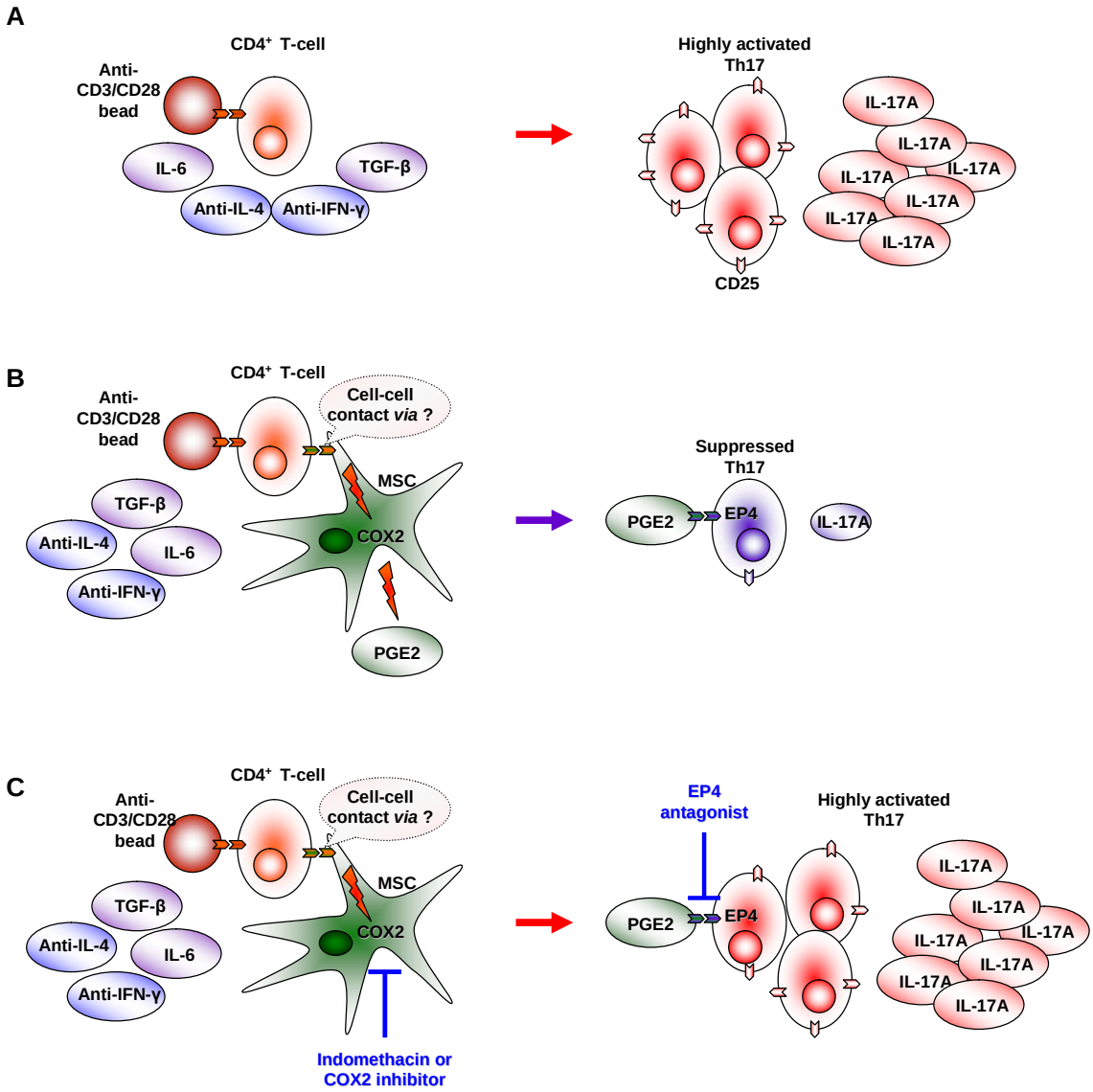

Figure 3.15 (**A**) $CD4^+$ T-cells cultured under Th17-skewed conditions in the presence of anti-CD3/anti-CD28 beads or APCs led to the production of IL-17A-producing Th17 cells. (**B**) Addition of MSCs to these cultures led to the generation of Th17 cells with suppressed CD25 expression and IL-17A production due to the induction of COX2 by MSCs following cell-cell contact with the activated $CD4^+$ T-cells and subsequent PGE2 production. PGE2 engagement with the EP4 receptor led to Th17 inhibition. (**C**) Blockade of COX2 or the EP4 receptor reversed the suppressive effect of MSCs.

CHAPTER FOUR

ENHANCED SUPPRESSION OF T-HELPER 17 DIFFERENTIATION BY COMBINING PARICALCITOL AND MSCS

4.1 INTRODUCTION

MSCs have unique suppressive effects on T-cell activation and differentiation (Uccelli et al., 2008). The clinical relevance of these effects has been well demonstrated in preclinical models of autoimmune and inflammatory diseases (Caplan, 2009). The immune system is also specifically influenced by VDR agonists such as calcitriol *via* genomic effects of the VDR itself (Griffin et al., 2003, Mora et al., 2008). Calcitriol is the most biologically active form of vitamin D_3 and is synthesized in the kidney or by various cells of the immune system (Mora et al., 2008). A number of studies have highlighted the potential of calcitriol or analogues of calcitriol to synergize or have additive effects with other therapies (Deb et al., 2010, Tan et al., 2009, Daniel et al., 2008). The experiments described in this chapter are novel in that they represent the first study to examine the combined immunomodulatory effects of a VDR analogue and a stem cell population. At the onset of this body of work in September 2011, the role of calcitriol in suppressing Th1 differentiation and promoting Th2 and T_{reg} differentiation was well described (Mora et al., 2008). A small number of laboratories had also described a suppressive role for calcitriol in Th17 cell differentiation *in-vitro* (Ikeda et al., 2010, Chang et al., 2010b, Tang et al., 2009).

Chang and colleagues reported that the VDR is expressed by mouse Th2 and Th17 cells but not by naïve $CD4^+$ T-cells or Th1 cells (Chang et al., 2010b). VDR was induced in naïve $CD4^+CD25^-CD62L^+CD44^-$ cells following 3 days in culture under Th17 differentiation conditions. Calcitriol suppressed IL-17A, IL-17F and IL-22 production by Th17 cells. Suppression was dependent upon VDR signaling as cytokine production was not affected in VDR KO T-cells in response to calcitriol (Chang et al., 2010b).

In another study, naïve ($CD4^+CD62L^+CD44^-CD25^-$) T-cells cultured under Th17-skewed conditions with calcitriol produced significantly less IL-17A as measured by ELISA and intracellular flow cytometry (Tang et al., 2009). Furthermore, memory ($CD4^+CD62L^-CD44^+$) T-cells cultured under neutral and Th17-polarized conditions also produced significantly less IL-17A in the presence of calcitriol (Tang et al., 2009)

Ikeda et al. reported that calcitriol inhibited the numbers of both OVA-stimulated DO11.10 and anti-CD3/anti-CD28/OVA-stimulated OT-II TCR transgenic IL-17A-producing $CD4^+CD45RB^+$ naïve T-cells after 6 days under Th17-skewed culture conditions. The vitamin A metabolite, all-trans retinoic acid, synergized with calcitriol to further inhibit the frequency of $CD4^+$ IL-17-producing cells (Ikeda et al., 2010). Moreover, calcitriol reduced ear swelling in DNFB-induced contact hypersensitivity in mice in association with reduced frequencies of IL-17A-producing $CD4^+$ and $CD8^+$ T-cells in the draining lymph nodes. Calcitriol suppressed the production of IL-17A, IL-21, IL-1R1, IL-21R, IL-23, RORC and AhR by human naïve ($CD4^+CD45RA^+$) T-cells cultured under Th17-skewed conditions. Furthermore, memory ($CD4^+CD45RO^+$) T-cells cultured for 6 days under Th17-skewed conditions had reduced expression of IL-17A and IL-22 (Ikeda et al., 2010).

A number of laboratories also reported beneficial effects in pre-clinical animal models using calcitriol to treat Th17-mediated diseases (Daniel et al., 2008, Penna et al., 2006, Tang et al., 2009, Chang et al., 2010a, Colin et al., 2010). Penna and colleagues were the first to report significantly less IL-17A production *ex-vivo* by anti-TCR-stimulated popliteal LN cells from elocalcitol (vitamin D agonist)-treated NOD mice with prostatein-induced experimental autoimmune prostatitis (EAP) (Penna et al., 2006). Elocalcitol-treated mice also showed reduced numbers and proliferation of cellular infiltrate but increased apoptosis of intraprostatic infiltrate. Furthermore, adoptive transfer of splenic $CD4^+$ T-cells from elocalcitol-treated NOD mice to NOD-SCID mice resulted in impaired type 1 diabetes and EAP (Penna et al., 2006).

In a mouse model of TNBS-induced colitis, Daniel et al. demonstrated significant reduction in the severity of colitis using calcitriol as measured by hyperemia scores, inflammation, colonic necrosis, cellular infiltrate and fibrosis. This effect was further enhanced in combination therapy with dexamethasone. Furthermore, in established colitis in which calcitriol and dexamethasone were not administered until day 3 after induction of colitis, calcitriol resulted in less overall loss of body weight and mice had longer colons which weighed less than their non-treated counterparts by day 5 (Daniel et al., 2008). Further improvements were observed with dual treatment of calcitriol and dexamethasone. Mechanistically, the authors convincingly showed a reduction in Th1-associated IFN-γ and T-bet and in Th17-associated IL-23 and IL-17 expression.

These effects were accompanied by a concomitant increase in Th2-associated IL-4 and GATA3 and T_{reg}-associated IL-10, TGF-β1 and FOXP3 expression in colonic protein extracts from calcitriol-treated mice compared with control TNBS-induced colitis animals (Daniel et al., 2008).

In IRBP-induced experimental autoimmune uveitis (EAU), calcitriol prevented EAU if administered 6 days prior to administration of IRBP and attenuated, albeit not significantly, EAU if administered 7 days post IRBP administration (Tang et al., 2009). DTH reactions were also significantly reduced following re-challenge with IRBP on day 21 as measured by ear swelling. Re-challenge of draining LN cells *ex-vivo* resulted in reduced IL-17A, IL-6, MIP-1α and MIP-2. Administration of anti-IL-17 systemically, significantly reduced EAU scores however, anti-IFN-γ did not (Tang et al., 2009) thus, highlighting the importance of the Th17 cell population in EAU.

Calcitriol potently attenuated MOG-induced EAE in association with reduced frequency of double positive CD3/CD4 cells in the CNS in addition to reduced frequency of splenic IL-17A- and FOXP3-expressing $CD4^+$ T-cells (Chang et al., 2010a). IFN-γ-expressing cells were not affected by calcitriol. Re-challenge of $CD4^+$ T-cells *ex-vivo* with MOG, also resulted in reduced frequencies of T_{regs} and Th17 cells in the presence of calcitriol. The suppressive effect was not antigen specific being demonstrable in OVA-specific T-cells also (Chang et al., 2010a). Addition of exogenous IL-2 reversed the suppressive effect on FOXP3 expression but not IL-17A. IL-27 is known to inhibit Th17 responses *via* STAT1 activation however suppression of IL-17A by calcitriol was also independent of STAT1 and IL-10 (Chang et al., 2010a).

Patients with rheumatoid arthritis have a higher frequency of IL-17A- and IL-22-producing cells among the $CD45RO^+$ memory population than healthy controls (Colin et al., 2010). Calcitriol inhibited IL-17A, IL-17F and IL-22 production by these memory-phenotype cells. Furthermore, PBMCs from untreated patients recently diagnosed with rheumatoid arthritis produced significantly lower levels of IL-17A and IFN-γ but higher levels of IL-4 in response to calcitriol following 72 hours *in-vitro* activation with anti-CD3/anti-CD28.

Calcitriol reportedly exerts genomic effects on cells of the immune system by directly modulating transcription through the VDR. Following engagement of the VDR by calcitriol, VDR-RXR heterodimers bind to VDREs in promoters of target genes thus modulating gene transcription by preventing DNA-binding proteins from accessing their genomic targets (Carlberg et al., 2012). In a study by Chang and Kweon, the suppressive effect of calcitriol was dependent upon VDR expression by $CD4^+$ T-cells as VDR KO $CD4^+$ T-cells activated by WT APCs under Th17-polarized conditions produced similar amounts of IL-17A in the presence or absence of calcitriol while WT $CD4^+$ T-cells activated by VDR KO APCs produced significantly less IL-17A in response to IL-17A (Chang et al., 2010a). A number of studies have shown that upon interaction with calcitriol, VDR-RXR complexes bind to VDREs in the promoter regions of both IFN-γ and IL-2 thereby mediating transcriptional repression. In the case of IL-2, the formation of NFAT/AP-1 transcription factor complexes was prevented thus transcriptional activators of IL-2 were inhibited (Mora et al., 2008, Alroy et al., 1995).

In contrast, the laboratory of Chang and Dong reported that calcitriol-mediated inhibition of primary Th17 differentiation occurred at the post-transcriptional level as mRNA for IL-17A, IL-17F, IL-22, RORC, RORα and IL-23R were unaltered but protein levels of IL-17A, IL-17F and IL-22 were suppressed in the presence of calcitriol (Chang et al., 2010b). This was confirmed by Tang et al. who demonstrated that while protein levels of IL-17A were suppressed by calcitriol, RORγt mRNA was not affected by calcitriol. The authors also showed that calcitriol did not affect protein levels of phosphorylated STAT3 which is upstream of RORγt (Tang et al., 2009).

Chang and Dong also demonstrated that calcitriol suppressed IL-17A production by induction of C/EBP homologous protein (CHOP) (Chang et al., 2010b). CHOP is also called growth-arrest and DNA damage-inducible gene 153 (GADD153). It is induced following severe endoplasmic reticulum stress and attenuation of translation. It is associated with arrest of the cell cycle and apoptosis (Oyadomari and Mori, 2004). Calcitriol dose-dependently induced CHOP expression in naïve T-cells cultured under Th17-skewed conditions. Furthermore, retroviral over-expression of CHOP by $CD4^+$ T-cells was associated with reduced expression of IL-17A, IL-17F and IL-22

compared to non-transduced $CD4^+$ T-cells under the same Th17 differentiation culture conditions (Chang et al., 2010b).

Thus, at the initiation of this study, the suppressive effects of calcitriol on naïve and memory $CD4^+$ T-cells undergoing Th17 differentiation *in-vitro* from both human and mouse were well documented. Combined administration of calcitriol and other immune modulating agents including vitamin A metabolites and dexamethasone was shown to be beneficial in a number of studies. Beneficial effects of calcitriol were also reported in a number of Th17-mediated disease models including EAU, EAE, EAP and colitis. However, the effects of the calcitriol analogue paricalcitol on primary Th17 differentiation had not been investigated nor had the combined effects of calcitriol or calcitriol analogues and cell based therapies been examined *in-vitro* or *in-vivo*. Furthermore, controversy remained over the mechanistic effects of calcitriol with some laboratories reporting transcriptional repression while others suggested that post-transcription regulation was key to calcitriol-mediated inhibition of primary Th17 differentiation.

In this thesis, the individual and combined effects of MSCs and paricalcitol were examined. Paricalcitol is a synthetic analogue of calcitriol with reduced calcemic properties (Brown et al., 2002). It is clinically available and used to treat secondary hyperparathyroidism associated with chronic kidney disease.

Therefore, specific aims for chapter 4 were to:

1. Determine the effects of paricalcitol on the primary differentiation of Th17 cells.
2. Determine whether paricalcitol augments MSC-induced inhibition of primary Th17 differentiation.
3. Determine the individual and combined effects of paricalcitol and MSCs on expression of key intracellular mediators of Th17 differentiation.

4.2 MATERIALS AND METHODS

4.2.1 WESTERN BLOT

Th17 cell cultures were set up for 3 days as per section 2.2 with the exception of lower anti-CD3ε stimulation (0.1 μg/ml) in 6-well plates in the presence or absence of MSCs (1:200 ratio) and/or paricalcitol (10 nM). $CD4^+$ T-cells were re-purified by MACS following co-culture. Pellets were re-suspended in complete lysis buffer B (5 μl/1 x 10^6 T-cells and 5 μl/1 x 10^5 MSCs) overnight at -20°C. A portion of the sample (5 μl) was left on ice for a Bradford® protein detection assay. Boiling 2 X Laemmli buffer was added to the lysed sample the following morning and vortexed for 30 seconds. The sample was boiled at 95°C for 5 minutes and then stored at -20°C.

Lysed samples (2 μl) were added to a 96-well flat bottomed plate in duplicate. Bradford® reagent (198 μl) was added to the wells to bring the volume up to 200 μl. A 5-point standard curve was constructed according to **Table 4.1** below. The absorbance was read at 595 nm on a Victor3™ 1420 Multilabel Counter plate reader after 5-10 minutes incubation.

Table 4.1 Bradford protein detection assay set-up

Final protein concentration (μg/ml)	Volume of 1 mg/ml BSA (μl)	Volume of Bradford reagent (μl)	Volume of lysis buffer (μl)
0	0	198	2
10	2	196	2
20	4	194	2
30	6	192	2
40	8	190	2
50	10	188	2

Resolving/separating gels were prepared according to the molecular weight of the protein of interest (**Table 4.2**). Equal amounts of protein (10 μg) diluted in 1 X Laemmli buffer were loaded into the wells. Proteins were separated by electrophoresis in a Mini-Protean® Tetra Cell (Bio-Rad) for ~ 1 hour at 150 volts (V). Electro-transfer to Immobilon® P PVDF membranes (Millipore) was performed for 1 hour at room temperature at 100 V on a magnetic stirrer with an ice block inside the Tetra Cell.

Table 4.2 Resolving/separating gel composition

SDS-PAGE gel (10ml)	8% (120-200 kDa) (ml)	10% (80-120 kDa) (ml)	12% (30-100 kDa) (ml)	15% (6-60 kDa) (ml)	Stacking (4ml)
dH_20	4.62	3.96	3.29	2.29	2.74
30% acrylamide	2.67	3.33	4	5	0.68
1.5 M Tris-HCl pH 8.8	2.5	2.5	2.5	2.5	-
1 M Tris-HCl pH 6.8	-	-	-	-	0.5
10% Sodium Dodecyl Sulfate	0.1	0.1	0.1	0.1	0.04
10% Ammonium persulfate	0.1	0.1	0.1	0.1	0.04
TEMED	0.01	0.01	0.01	0.01	0.004

The membrane was stained with Ponceau S solution followed by 3 X 5 minute washes in TBST buffer. The membrane was placed in blocking buffer (5% w/v milk powder in TBST) on a rocker at 4°C overnight. Membranes were incubated with primary antibodies diluted according to **Table 4.3** in 5% w/v milk powder in TBST overnight at 4°C on a rocker followed by washing in TBST. Membranes were then incubated for 1 hour at room temperature with HRP-linked secondary antibody diluted in 5% w/v milk powder in TBST with Streptactin®-HRP (1/30,000) for detection of the chemiluminescent ladder. Membranes were washed in TBST. Development was achieved using Immobilon® Western Chemiluminescent HRP substrate and imaged on a Fluorochem™ chemiluminescent imaging system.

Table 4.3 Western Blot antibody preparations

Name	Dilution	Details	kDa	Secondary
VDR	1/2000	Rabbit monoclonal	48	Goat anti-rabbit (1/5000)
FOXP3	1/2000	Anti-mouse/rat purified	50	Goat anti-rat (1/5000)
RORγt	1/2000	Anti-mouse purified	56-58	Goat anti-rat (1/5000)
Runx1	1/2000	Rabbit polyclonal	55	Goat anti-rabbit (1/5000)
IRF4	1/2000	Rabbit polyclonal	50	Goat anti-rabbit (1/5000)
STAT3 total	1/2500	Rabbit polyclonal	79, 86	Goat anti-rabbit (1/5000)
STAT3 phosphorylated Tyr	1/2500	Rabbit polyclonal	79, 86	Goat anti-rabbit (1/5000)
β-actin	1/20,000	Mouse Monoclonal	42	Goat anti-mouse (1/5000)

All other methods for this chapter are as described in sections 2.2 and 3.2.

4.3 RESULTS

4.3.1 DOSE-DEPENDENT INHIBITION OF IL-17A PRODUCTION BY PARICALCITOL

In-vitro findings suggest that under certain proinflammatory conditions, MSCs may enhance Th17 responses *via* predominantly indirect effects, such as induction of IL-23 by APCs. Therefore, I elected to combine MSCs with another immunosuppressive agent, paricalcitol in an attempt to augment the suppressive effects observed on Th17 development with MSCs alone.

In order to determine the effect of paricalcitol alone on primary Th17 differentiation, MACS-enriched $CD4^+$ T-cells were cultured with APCs under Th17-skewed conditions for 3 days in the presence of varying concentrations of paricalcitol (10^{-7}-10^{-12} M) or equivalent volumes of ethanol control. Cells were re-stimulated for 8 hours with anti-CD3/anti-CD28 coated-beads with brefeldin A in order to perform intracellular staining for IL-17A.

As shown in **Figure 4.1A**, paricalcitol was associated with dose-dependent inhibition of IL-17A at day 3 which was not evident with the vehicle control. Following re-stimulation for 8 hours under non-Th17 skewed conditions, $CD4^+$ T-cells cultured in the presence of paricalcitol had a lower frequency of IL-17A-producing cells as measured by intracellular IL-17A flow cytometric staining (**Figure 4.1B/C**). The suppressive effect on IL-17A production was particularly evident at 10^{-8} M (10 nM) therefore all experiments carried out after this point employed 10 nM concentration of paricalcitol.

In contrast to the potent suppression of IL-17A, paricalcitol had a mild effect on proliferation of $CD4^+$ T-cells (**Figure 4.1D**) and did not suppress CD25 surface expression (**Figure 4.1E**) at all. This suggests that paricalcitol specifically targets the Th17 differentiation pathway as opposed to broad-spectrum suppression on $CD4^+$ T-cell activation. I therefore hypothesized that the combination of MSCs and paricalcitol would further dampen Th17 responses *via* differential mechanisms.

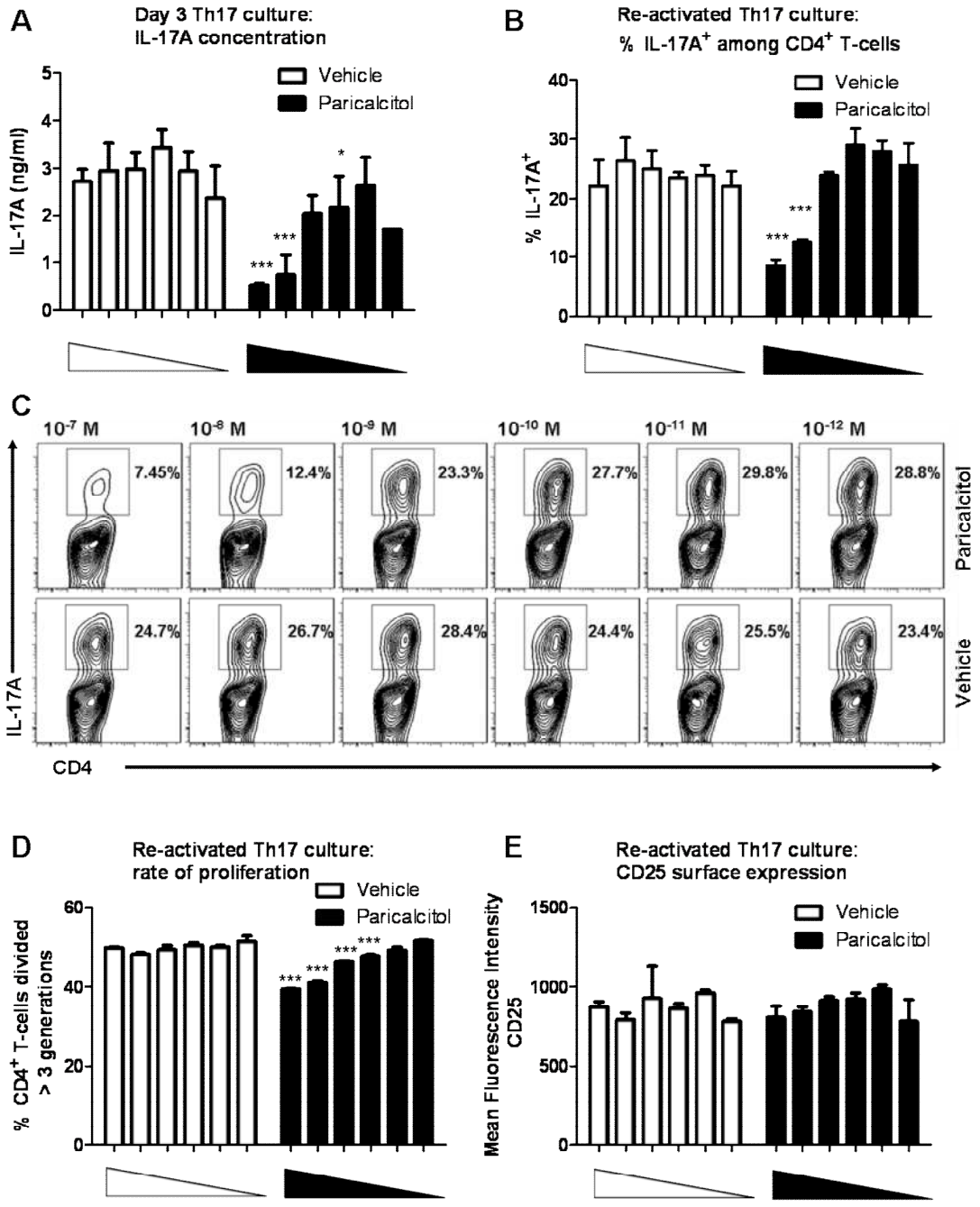

Figure 4.1 Dose-dependent IL-17A inhibition by paricalcitol: $CD4^+$ T-cells were cultured for 3 days under Th17-skewed conditions in the presence of APCs and graded concentrations of paricalcitol (10^{-7} M–10^{-12} M) or equivalent volumes of vehicle (ethanol) prior to 8 hour re-stimulation with anti-CD3/anti-CD28 beads. (**A**) Concentration of IL-17A in day 3 culture supernatants. (**B**) Flow cytometric analysis of the % of $IL\text{-}17A^+$ cells among cells gated on $CD4^+$ following re-stimulation. (**C**) Representative examples of contour plots of intracellular IL-17A staining of re-stimulated $CD4^+$ T-cells. (**D**) Graphical representation of the % of $CD4^+$ T-cells that underwent 3 or more cell divisions. (**E**) Surface expression of CD25 on $CD4^+$ T-cells following re-stimulation. Data are represented as mean +/-standard deviations and are representative of 2 individual experiments (* p = <0.05, *** p = <0.001 compared with equivalent vehicle control, Bonferroni posttest).

4.3.2 Enhanced suppression of Th17 responses by combining MSCs with paricalcitol

A number of studies have reported beneficial synergistic effects by combining paricalcitol with other agents (Deb et al., 2010, Tan et al., 2009). In this study, the combined effects of paricalcitol (10 nM) and MSCs (1:400 MSC:$CD4^+$ T-cell ratio) were examined on $CD4^+$ T-cells undergoing primary Th17 differentiation.

As shown in **Figure 4.2A**, IL-17A was reduced in cultures containing MSCs alone and paricalcitol alone compared to control cultures containing vehicle with no MSCs. The combination of MSCs and paricalcitol further reduced IL-17A production by $CD4^+$ T-cells. Similar results were detected in re-stimulated Th17 cultures by intracellular IL-17A staining (**Figure 4.2C/D**).

Consistent with results from **Figure 4.1**, paricalcitol had a mild suppressive effect on T-cell proliferation (**Figure 4.2B**). MSCs were more potent inhibitors of T-cell proliferation than paricalcitol however additive effects were observed by combining the two treatments. Surface expression of CD25 on $CD4^+$ T-cells was significantly suppressed in the presence of MSCs (**Figure 4.2E**). In contrast, paricalcitol did not affect the expression of CD25 and there was no significant difference between vehicle and paricalcitol treated $CD4^+$ T-cells in the presence or absence of MSCs.

CCR6 is highly expressed by Th17 cells and is an important determinant of Th17 migration *in-vivo* in response to CCL20 (Pindjakova et al., 2012, Chang et al., 2010a). Paricalcitol additively suppressed CCR6 surface expression on $CD4^+$ T-cells in the presence of MSCs (**Figure 4.2F**).

Based on these experiments, I concluded that paricalcitol and MSCs additively inhibit proliferation, IL-17A production and CCR6 expression by Th17 cells, however CD25 surface expression is not affected by paricalcitol.

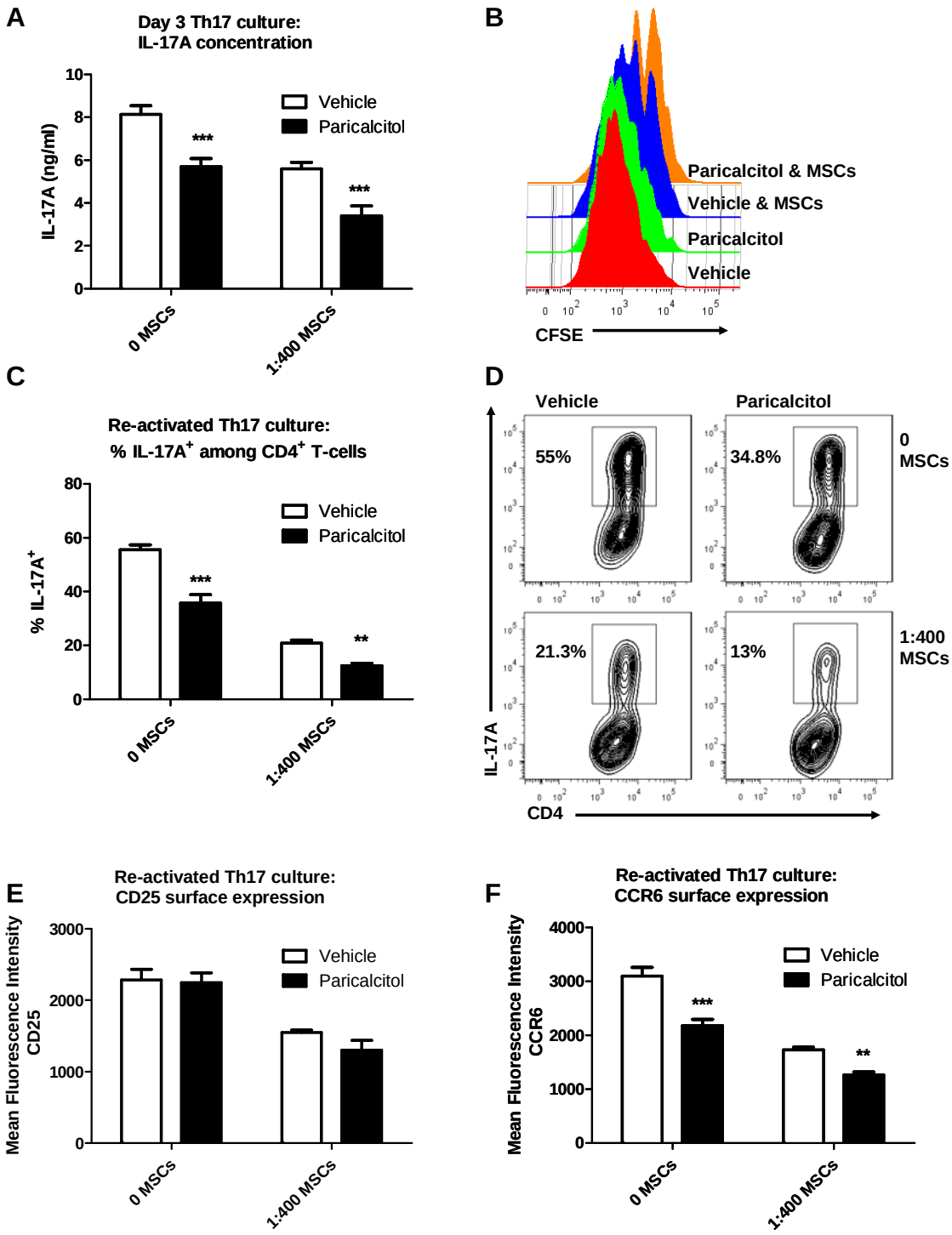

Figure 4.2 Paricalcitol augments MSC-mediated inhibition of Th17 cells: $CD4^+$ T-cells were cultured for 3 days under Th17-skewed conditions in the presence of APCs and paricalcitol (10^{-8} M) or equivalent volume of vehicle with or without MSCs prior to 8 hour re-stimulation with anti-CD3/anti-CD28 beads. (**A**) Concentration of IL-17A in day 3 culture supernatants. (**B**) Representative histograms of CFSE staining of re-stimulated $CD4^+$ T-cells (**C**) Flow cytometric analysis of the % of $IL\text{-}17A^+$ cells among cells gated on $CD4^+$ following re-stimulation. (**D**) Representative examples of contour plots of intracellular IL-17A staining of re-stimulated $CD4^+$ T-cells. (**E**) Surface expression of CD25 on $CD4^+$ T-cells following re-stimulation. (**F**) Surface expression of CCR6 on $CD4^+$ T-cells following re-stimulation. Data are represented as mean +/- standard deviations and are representative of 4 individual experiments (** p = <0.01, *** p = <0.001 compared with equivalent vehicle control, Bonferroni posttest).

4.3.3 APCs ARE UNNECESSARY FOR PARICALCITOL-MEDIATED INHIBITION OF TH17 CELLS

In addition to the suppressive effects on T-cells, calcitriol has been reported to inhibit APC maturation, antigen presentation and cytokine production (Griffin et al., 2003). In order to determine whether paricalcitol suppresses primary Th17 differentiation indirectly *via* inhibition of APCs, I elected to differentiate $CD4^+$ T-cells into Th17 cells in an APC-free culture system.

MACS-enriched $CD4^+$ T-cells were cultured under Th17-skewed conditions for 3 days in the presence of anti-CD3/anti-CD28 coated beads. IL-17A was measured in the supernatant at day 3. The cells were re-stimulated for 8 hours for intracellular IL-17A staining.

Consistent with my findings in chapter 2, Dynabead®-activated Th17 cells produce less IL-17A than APC-activated Th17 cells (**Figure 4.3**). Nonetheless, paricalcitol significantly inhibited IL-17A production in the absence of APCs. Furthermore, the combination of MSCs and paricalcitol further suppressed IL-17A production compared to MSCs and vehicle (**Figure 4.3B/C**). Therefore, from a mechanistic point of view, paricalcitol-mediated inhibition of primary Th17 differentiation occurred independent of APCs.

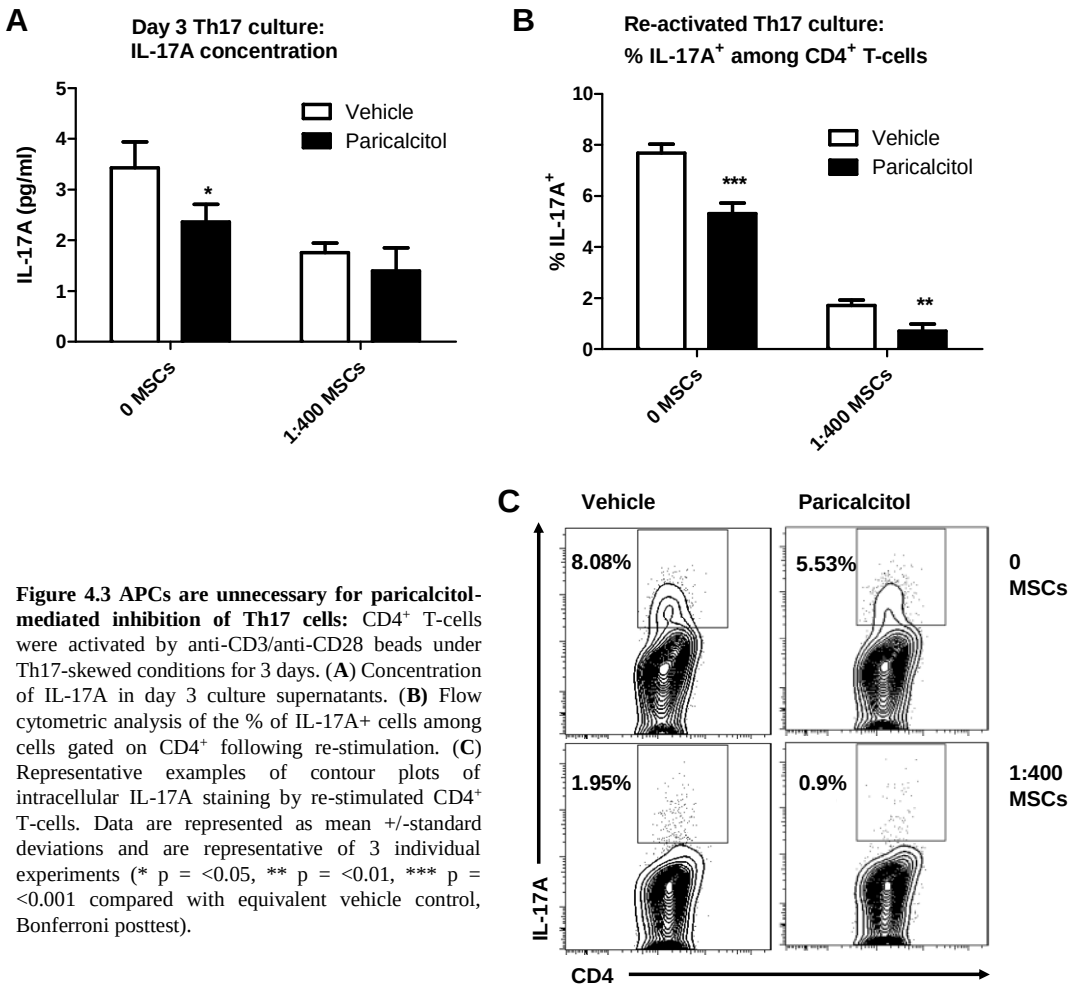

Figure 4.3 APCs are unnecessary for paricalcitol-mediated inhibition of Th17 cells: $CD4^+$ T-cells were activated by anti-CD3/anti-CD28 beads under Th17-skewed conditions for 3 days. (**A**) Concentration of IL-17A in day 3 culture supernatants. (**B**) Flow cytometric analysis of the % of IL-17A+ cells among cells gated on $CD4^+$ following re-stimulation. (**C**) Representative examples of contour plots of intracellular IL-17A staining by re-stimulated $CD4^+$ T-cells. Data are represented as mean +/-standard deviations and are representative of 3 individual experiments (* p = <0.05, ** p = <0.01, *** p = <0.001 compared with equivalent vehicle control, Bonferroni posttest).

4.3.4 ADDITIVE INHIBITION OF BOTH NAÏVE- AND MEMORY-PHENOTYPE RESPONDERS:

My results from chapter 2 demonstrated potent inhibition of naïve-phenotype $CD4^+$ T-cells undergoing primary Th17 differentiation by MSCs while memory-phenotype responders were not as efficiently suppressed. In fact, MSCs were unable to modulate $CCR6^+$ memory-phenotype T-cells at all and actually enhanced Th17 responses by fully differentiated Th17 cells in the presence of IL-1 and IL-23. An experiment was designed, therefore, to determine whether paricalcitol enhances MSC-mediated suppression of Th17 cells particularly within the memory-phenotype compartment.

Naïve- and memory-phenotype responders were FACS purified as per **Figure 2.6** and separately activated under Th17-skewed conditions in the presence of paricalcitol or vehicle with or without MSCs for 3 days after which IL-17A was measured in supernatants by ELISA. Cells were re-stimulated for 8 hours under non-Th17 skewed conditions with anti-CD3/anti-CD28 beads for intracellular IL-17A staining.

As shown in **Figure 4.4**, memory-phenotype responders produced more IL-17A under Th17-skewed conditions than their naïve counterparts. Paricalcitol alone significantly inhibited IL-17A production in primary and re-stimulated cultures of naïve- and memory-phenotype responders ($p = <0.001$). The combination of MSCs and paricalcitol further suppressed IL-17A production in naïve cultures (primary culture $p = <0.05$, re-stimulated culture $p = <0.001$) (**Figure 4.4A/B/C**).

Paricalcitol-mediated suppression of memory-phenotype responders undergoing primary Th17 differentiation *in-vitro* was significantly less potent than naïve-phenotype responders. Qualitatively similar results were observed in a total of three similar experiments with median proportionate inhibition of IL-17A production following re-stimulation of 9% (range 2-17%) for memory-phenotype responders and 45% (range 34-44%) for naïve-phenotype responders.

Nonetheless, the combination of MSCs and paricalcitol further suppressed IL-17A production in memory cultures (primary culture $p = <0.01$, re-stimulated culture $p = <0.001$). Therefore, paricalcitol alone potently suppresses IL-17A production by naïve-phenotype responders. Paricalcitol and MSCs additively suppress both naïve- and memory-phenotype responders undergoing primary Th17 differentiation.

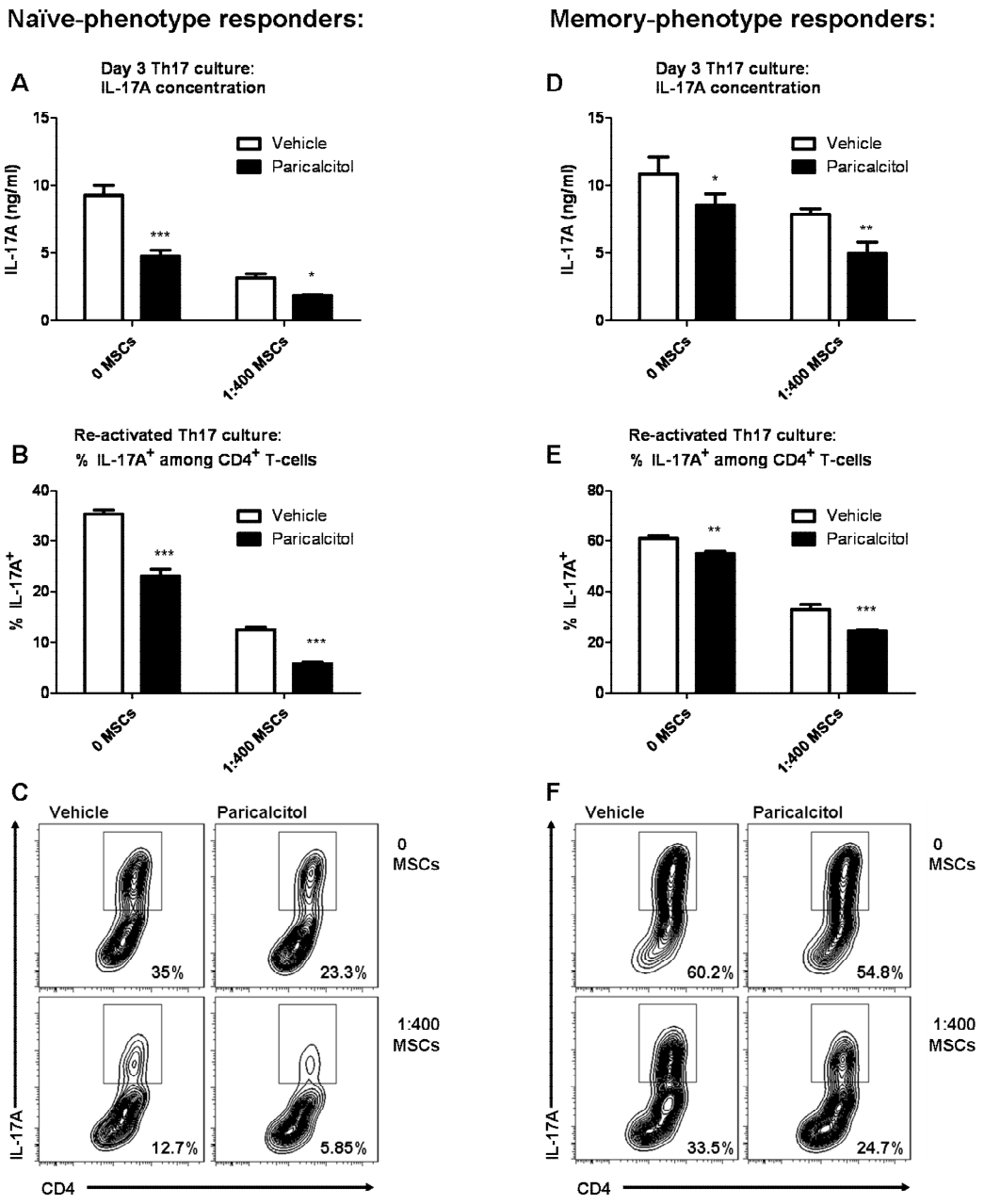

Figure 4.4 Paricalcitol additively suppresses MSC-induced IL-17A inhibition by naïve and memory T-cells: MACS-enriched $CD4^+$ T-cells were further purified by FACS into naïve ($CD25^-$ $CD62L^+$) and memory ($CD25^-CD62L^-$) T-cells. T-cells were separately activated under Th17-skewed conditions for 3 days in the presence of paricalcitol (10 nM) or equivalent volume of vehicle with or without MSCs (1:400 ratio). Cells were re-stimulated for 8 hours with anti-CD3/anti-CD28 beads. (**A/D**) Concentrations of IL-17A in day 3 culture supernatants. (**B/E)** Flow cytometric analysis of the % of $IL\text{-}17A^+$ cells among cells gated on $CD4^+$ following re-stimulation. (**C/F**) Representative examples of contour plots of intracellular IL-17A staining by re-stimulated $CD4^+$ T-cells. Data are represented as mean +/-standard deviations and are representative of 3 individual experiments (* p = <0.05, ** p = <0.01, *** p = <0.001 compared with equivalent vehicle control, Bonferroni posttest).

4.3.5 INHIBITION OF IN-VIVO-DERIVED TH17 CELLS

In order to determine the effect of paricalcitol on Th17 cells derived *in-vivo* from a site of sterile inflammation, UUO was performed on mice for 72 hours after which control and obstructed kidneys were harvested. Single cell suspensions were prepared and anti-CD3ε-activated $CD45^+$ leukocytes were cultured for 3 days in the presence or absence of MSCs and/or paricalcitol.

MSCs significantly suppressed both IL-17 and IFN-γ production by $CD45^+$ cells compared to equivalent vehicle treated 0 MSC controls ($p = <0.05$ for IL-17 and $p = <0.001$ for IFN-γ) (**Figure 4.5)**. In contrast, paricalcitol did not significantly inhibit IL-17A or IFN-γ production in the absence of MSCs. Despite a trend towards reduced cytokine production in double-treated conditions, the combination of paricalcitol and MSCs did not significantly suppress cytokine production compared to the equivalent MSC single-treated control. A significant reduction in both IL-17A and IFN-γ was detected in double-treated conditions compared to paricalcitol alone ($p = <0.01$ for IL-17 and $p = <0.001$ for IFN-γ). These results suggest that although MSCs suppress IL-17A and IFN-γ by $CD45^+$ cells from an obstructed kidney, the addition of paricalcitol did not confer further suppressive effects.

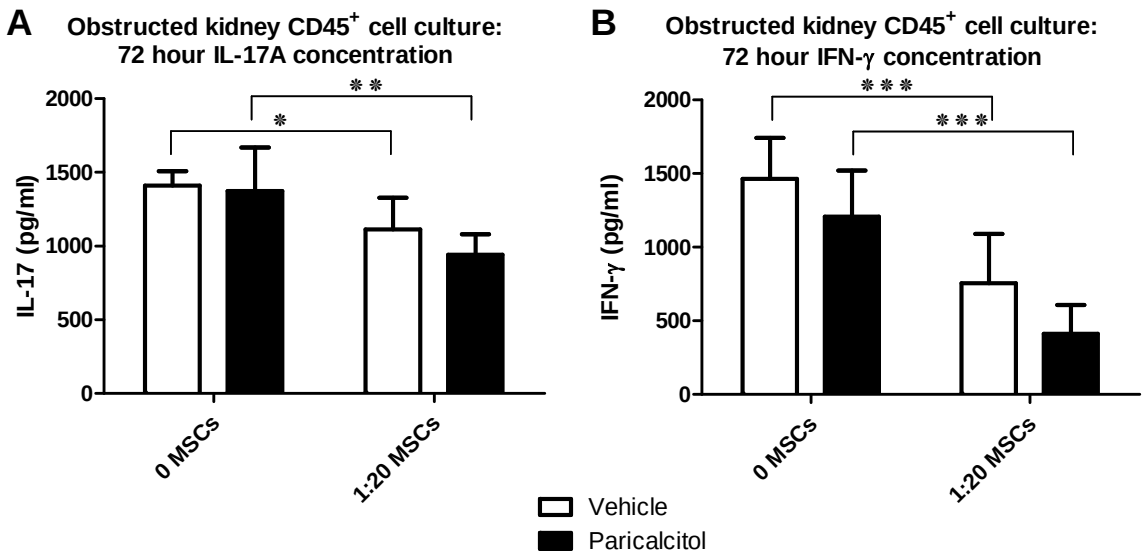

Figure 4.5 Paricalcitol does not inhibit *in-vivo*-derived Th17 cells: $CD45^+$ cells isolated from obstructed kidneys were anti-CD3ε-stimulated for 3 days with or without MSCs and/or paricalcitol. (**A**) Concentration of IL-17A and (**B**) concentration of IFN-γ in culture supernatants. Data are represented as mean +/-standard deviations and are representative of 3 individual experiments (Bonferroni posttest, * = compared with equivalent vehicle control, * = compared with 0 MSCs control).

4.3.6 PARICALCITOL DOES NOT RESCUE MSC-MEDIATED ENHANCEMENT OF IL-1- AND IL-23-MEDIATED IL-17A PRODUCTION BY DIFFERENTIATED TH17 CELLS

Results from chapter 2 demonstrated that MSCs enhance IL-1α- and/or IL-23-mediated induction of IL-17A by fully differentiated Th17 cells. These experiments were designed to determine whether paricalcitol prevents MSC-mediated enhancement of IL-17 production by fully differentiated Th17 cells in the presence of IL-1α and/or IL-23.

MACS-enriched $CD4^+$ T-cells were cultured for 6 days under Th17-skewed conditions with anti-CD3ε and APCs. $CD4^+$ T-cells were then re-stimulated with freshly isolated APCs & anti-CD3ε for a further 4 days under Th17-skewed conditions. $CD4^+$ T-cells were finally re-stimulated with anti-CD3ε with or without IL-1α (0.5 ng/ml) & IL-23 (5 ng/ml) for 24 hrs in the presence or absence of MSCs with or without paricalcitol (10 nM) or equivalent volume of vehicle control.

As shown in **Figure 4.6**, paricalcitol significantly suppressed IL-17A production by Th17 cells re-stimulated in the presence of paricalcitol alone for the final 24 hour re-stimulation compared to Th17 cells re-stimulated in the presence of vehicle alone ($p = <0.01$). MSCs did not inhibit IL-17 production. Furthermore, the combination of paricalcitol and MSCs did not result in IL-17A suppression.

Th17 cells re-stimulated in the presence of IL-1α for the final 24 hour re-stimulation produced more IL-17A than Th17 cells re-stimulated in the absence of IL-1α for the final 24 hour re-stimulation (**Figure 4.6**). Paricalcitol alone significantly suppressed IL-17A production in the presence of IL-1α ($p = <0.01$) however MSCs enhanced IL-17A production and addition of paricalcitol did not prevent this effect.

Likewise, Th17 cells re-stimulated in the presence of IL-23 for the final 24 hour re-stimulation produced more IL-17A than Th17 cells re-stimulated in the absence of IL-23 (**Figure 4.6**). Paricalcitol alone did not suppress IL-17A production in the presence of IL-23. MSCs enhanced IL-17A production in the presence of IL-23. The combination of MSCs and paricalcitol prevented the significant induction of IL-17A in the presence of IL-23 observed in MSC cultures with vehicle (**Figure 4.6**).

Addition of IL-1α and IL-23 to Th17 cells for the final 24 hour re-stimulation additively enhanced IL-17A production compared to Th17 cells re-stimulated in the absence of both IL-1α and IL-23. Paricalcitol did not suppress this additive effect (**Figure 4.6**). MSCs enhanced IL-1α and IL-23-mediated induction of IL-17A. Paricalcitol did not prevent MSC-induced IL-17A in the presence of IL-1α and IL-23.

To summarise these results, in a simulated pro-inflammatory environment containing both IL-1α and IL-23, MSCs augment IL-17A production by Th17 cells through a mechanism that is not inhibited by paricalcitol.

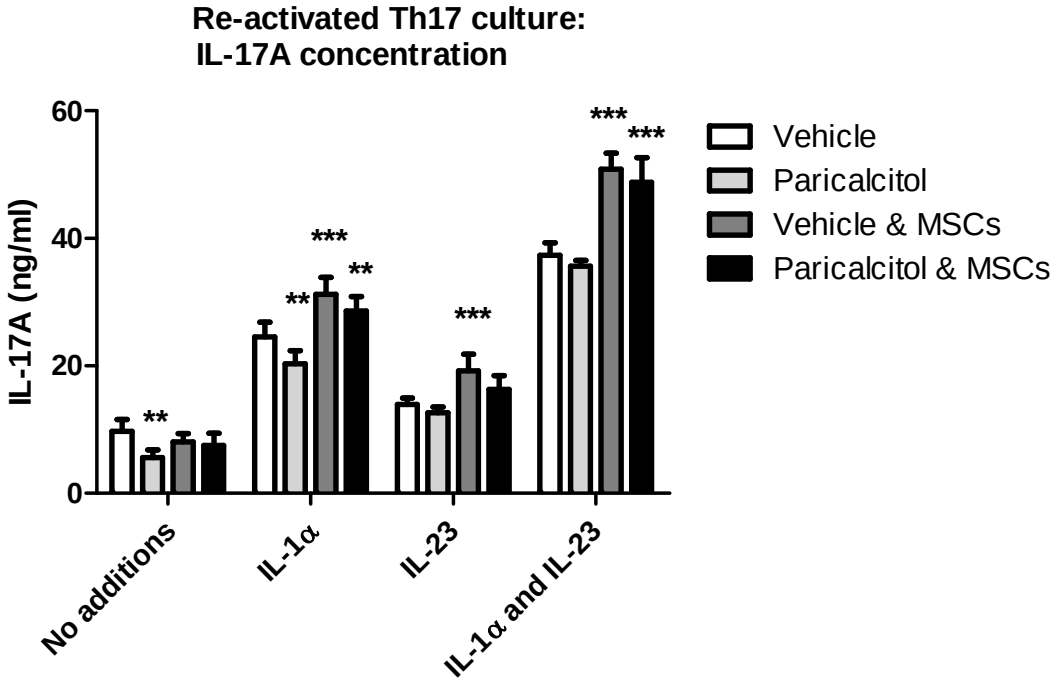

Figure 4.6 Paricalcitol does not prevent MSC-mediated enhancement of IL-17A production in the presence of IL-1α and IL-23: $CD4^+$ T-cells were cultured for 6 days under Th17-skewed conditions prior to re-stimulation with freshly isolated APCs & anti-CD3ε for a further 4 days under Th17-skewed conditions. $CD4^+$ T-cells were re-stimulated with anti-CD3ε with or without IL-1α & IL-23 for 24 hrs in the presence or absence of 1:400 MSC:$CD4^+$ T-cells and/or paricalcitol (10 nM). Graphical representation of the concentrations of IL-17A in culture supernatants. Data are represented as mean +/-standard deviations and are representative of 6 replicates from 1 individual experiment (** p = <0.01, *** p = <0.001 compared with equivalent vehicle/0 MSC control, Bonferroni posttest)

4.3.7 PARICALCITOL DOES NOT SUPPRESS TH17 CELLS *VIA* COX2 SIGNALING

Experiments from chapter 3 demonstrated the requirement for COX induction and PGE2 production in MSC-mediated suppression of primary Th17 differentiation. Based on differential CD25 surface expression by T-cells in the presence of MSCs or paricalcitol, I hypothesized that paricalcitol inhibited the induction of Th17 cells from $CD4^+$ precursors *via* distinct mechanisms compared to those of MSCs. In order to determine whether any of the observed effects of paricalcitol were dependent on COX induction to suppress Th17 differentiation, experiments were carried out in the presence of the non-selective COX inhibitor, indomethacin.

As shown in **Figure 4.7**, indomethacin significantly reversed MSC-induced inhibition of IL-17A in day 3 culture supernatants however paricalcitol-mediated inhibition of IL-17A was unaffected by indomethacin

Following re-stimulation of T-cells for 8 hours in the presence of anti-CD3/anti-CD28 beads, the frequency of IL-17A-producing $CD4^+$ T-cells that were originally cultured in the presence of MSCs and vehicle was significantly lower than in the vehicle alone control condition. Addition of indomethacin to MSC/Th17 co-cultures reversed this suppressive effect. The frequency of IL-17A-producing $CD4^+$ T-cells was comparable to control conditions in the absence of MSCs. In agreement with ELISA results, intracellular flow cytometry revealed that indomethacin was not associated with a paradoxical reversal of IL-17A production when $CD4^+$ T-cells were cultured with paricalcitol alone (**Figure 4.7 B/C**).

In order to confirm this finding, similar experiments were set up using NS-398, a selective COX 2 inhibitor and L-161, 982, a selective EP4 antagonist, both of which were previously shown to prevent MSC-mediated inhibition of primary Th17 differentiation in chapter 3.

Figures 4.8 and **4.9** provide further evidence that MSC-mediated inhibition of $CD4^+$ T-cells undergoing primary Th17 differentiation is dependent upon COX2 and EP4. In contrast, paricalcitol-induced suppression of Th17 differentiation occurs independently of COX2/PGE2.

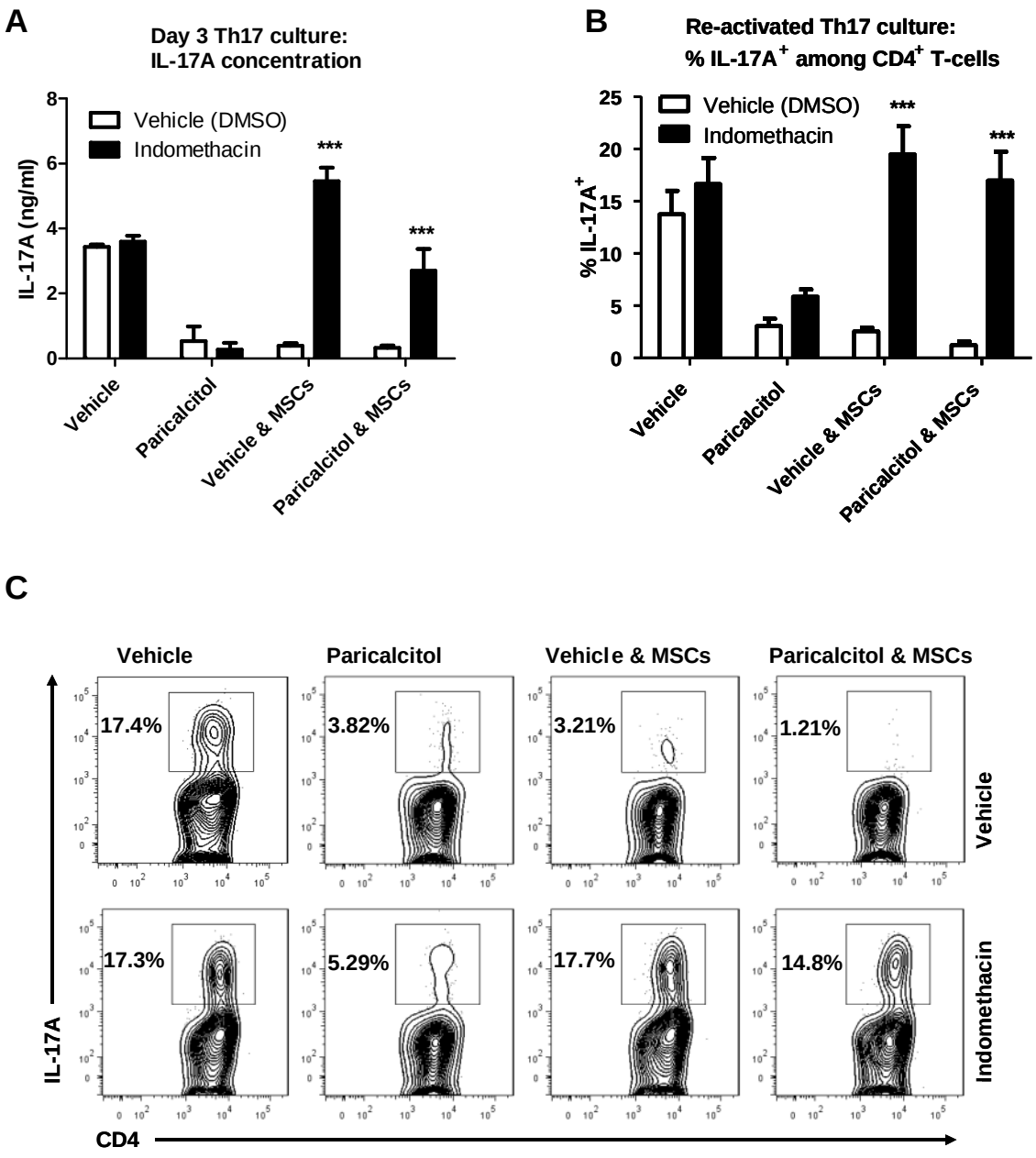

Figure 4.7 Indomethacin does not reverse paricalcitol-mediated inhibition of primary Th17 differentiation: $CD4^+$ T-cells were MACS-enriched and cultured for 3 days under Th17-skewed conditions in the presence of APCs with or without MSCs and/or paricalcitol. Indomethacin (5 μM) was added to the primary culture or equivalent volume of DMSO vehicle. (**A**) Concentration of IL-17A in supernatant at day 3. (**B**) Graphical representation showing the frequency of $IL\text{-}17A^+$ cells among cells gated on $CD4^+$. (**C**) Representative contour plots of intracellular IL-17A staining following re-stimulation for 8 hours Data are represented as mean +/-standard deviations and are representative of 2 individual experiments (*** p = <0.001 compared with equivalent vehicle (DMSO) control, Bonferroni posttest).

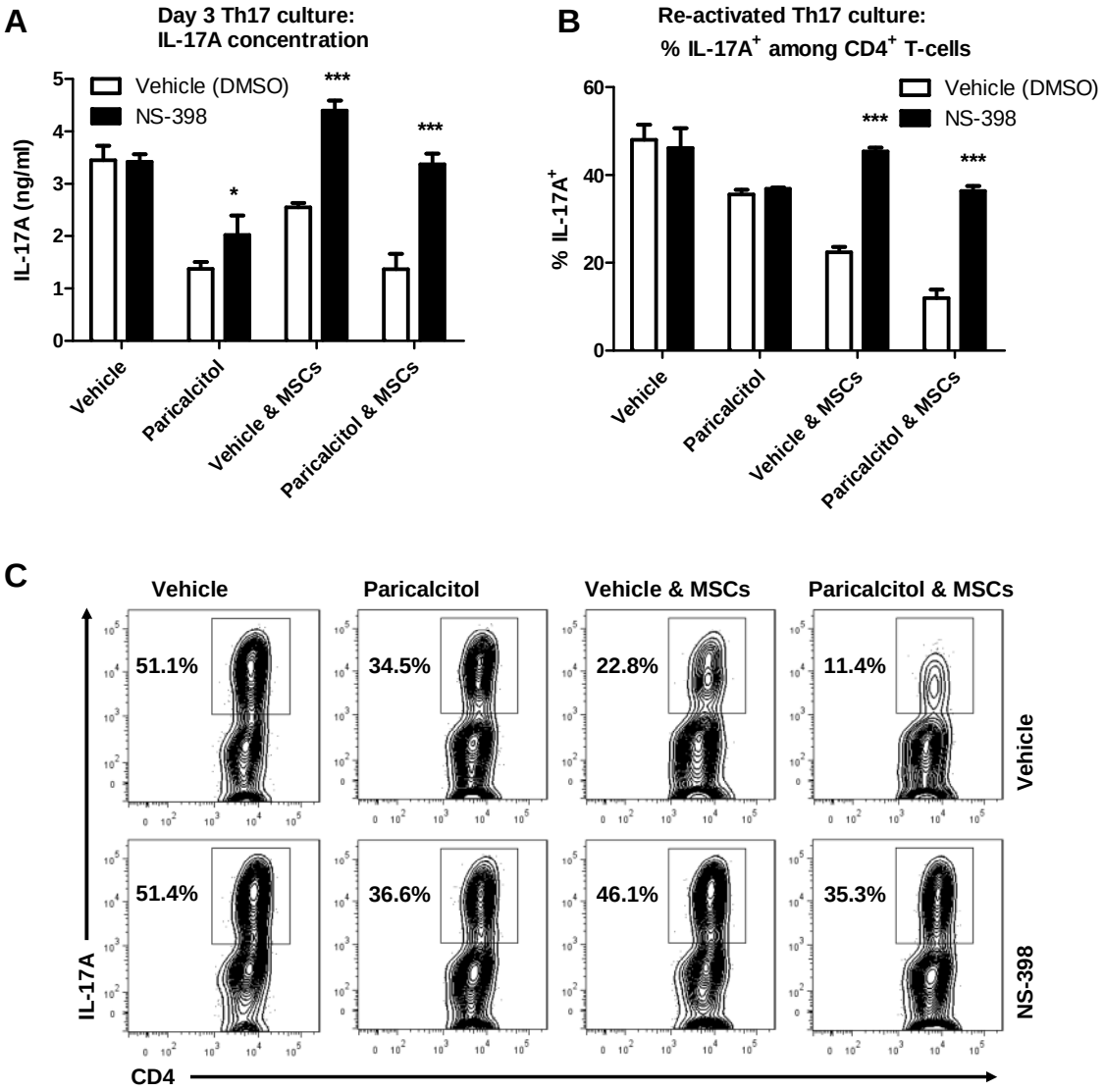

Figure 4.8 Paricalcitol-mediated inhibition of primary Th17 differentiation does not require COX2 signaling: $CD4^+$ T-cells were MACS-enriched and cultured for 3 days under Th17-skewed conditions in the presence of APCs with or without MSCs and/or paricalcitol. NS-398 (1 μM) was added to the primary culture or equivalent volume of DMSO vehicle. (**A**) Concentration of IL-17A in supernatant at day 3. (**B**) Graphical representation showing the frequency of IL-$17A^+$ cells among cells gated on $CD4^+$. (**C**) Representative contour plots of intracellular IL-17A staining following re-stimulation for 8 hours. Data are represented as mean +/-standard deviations and are representative of 2 individual experiments (* p = <0.05, *** p = <0.001 compared with equivalent vehicle (DMSO) control, Bonferroni posttest).

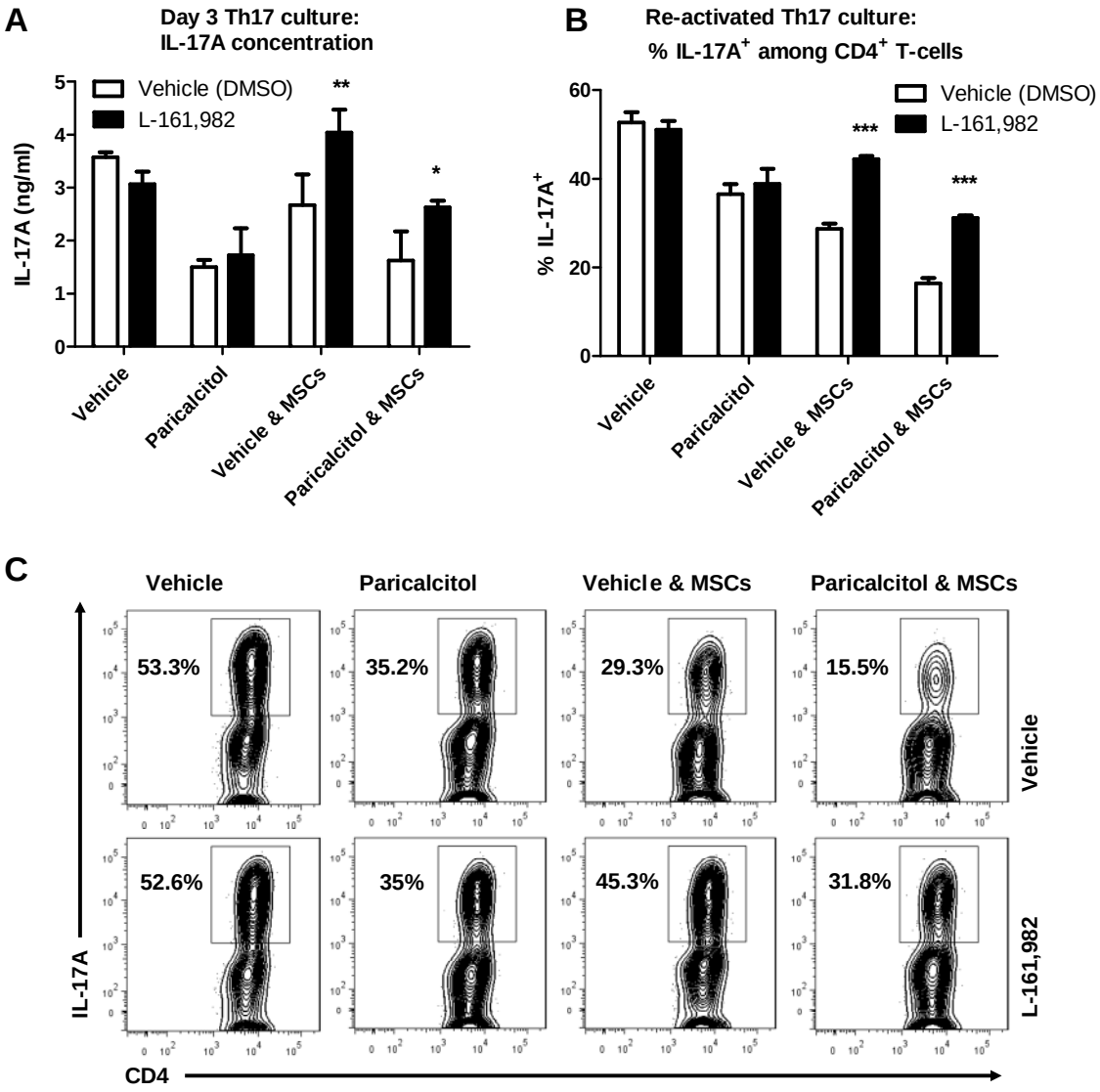

Figure 4.9 Paricalcitol-mediated inhibition of primary Th17 differentiation does not require EP4 activation: $CD4^+$ T-cells were MACS-enriched and cultured for 3 days under Th17-skewed conditions in the presence of APCs with or without MSCs and/or paricalcitol. L-161,982 (1 μM) was added to the primary culture or equivalent volume of DMSO vehicle. (**A**) Concentration of IL-17A in supernatant at day 3. (**B**) Graphical representation showing the frequency of $IL\text{-}17A^+$ cells among cells gated on $CD4^+$. (**C**) Representative contour plots of intracellular IL-17A staining following re-stimulation for 8 hours. Data are represented as mean +/-standard deviations and are representative of triplicate samples from one experiment (* p = <0.05, ** p = <0.01, *** p = <0.001 compared with equivalent vehicle (DMSO) control, Bonferroni posttest).

4.3.8 INDUCTION OF THE VITAMIN D RECEPTOR BY PARICALCITOL

As an immunomodulatory agent, vitamin D is reported to act directly through the VDR by modulating transcription of individual genes and signaling pathways including the essential T-cell activation pathways NF-κB, NFAT, MAPK and PI3-K (Griffin et al., 2003). The phenomenon whereby VDR agonists up-regulate expression of the VDR, which may act as a positive feedback loop to further enhance their effects, has been well reported (Naveh-Many et al., 1990, Pan and Price, 1987). In order to determine whether paricalcitol treatment affected VDR expression by T-cells, $CD4^+$ T-cells were co-cultured for 3 days in the presence of APCs under Th17-skewed conditions with or without MSCs (1:400) and/or paricalcitol (10 nM). $CD4^+$ T-cells were re-purified by MACS and subjected to Western Blot. Relevant vehicle control conditions, MSCs and fresh naïve non-activated $CD4^+$ T-cells were also examined for VDR expression. The VDR is both nuclear and cytoplasmic thus lysed whole cell extracts were analyzed (Campbell et al., 2010). Thorough attention was given to equal protein loading using a Bradford® protein determination assay which was verified by Ponceau S staining of the membrane post electro-transfer (data not shown) and target bands were normalized to their respective β-actin bands. Spot densitometry was performed on a Fluorochem™ chemiluminescent imaging system. All samples were compared relative to the Th17 vehicle control (lane 3) which was appointed a spot densitometry value of one.

As shown in **Figure 4.10**, MSCs constitutively expressed VDR (lane 1). In contrast primary $CD4^+$ T-cells (lane 2) freshly lysed following preparation of a single cell suspension and CD4 MACS-enrichment did not express VDR. Upon activation of $CD4^+$ T-cells by APCs and anti-CD3ε (0.1 μg/ml) under Th17-skewed culture conditions, VDR was induced in the presence or absence of MSCs (lanes 3/5). Paricalcitol treatment was associated with a strong induction of VDR (lanes 4/6).

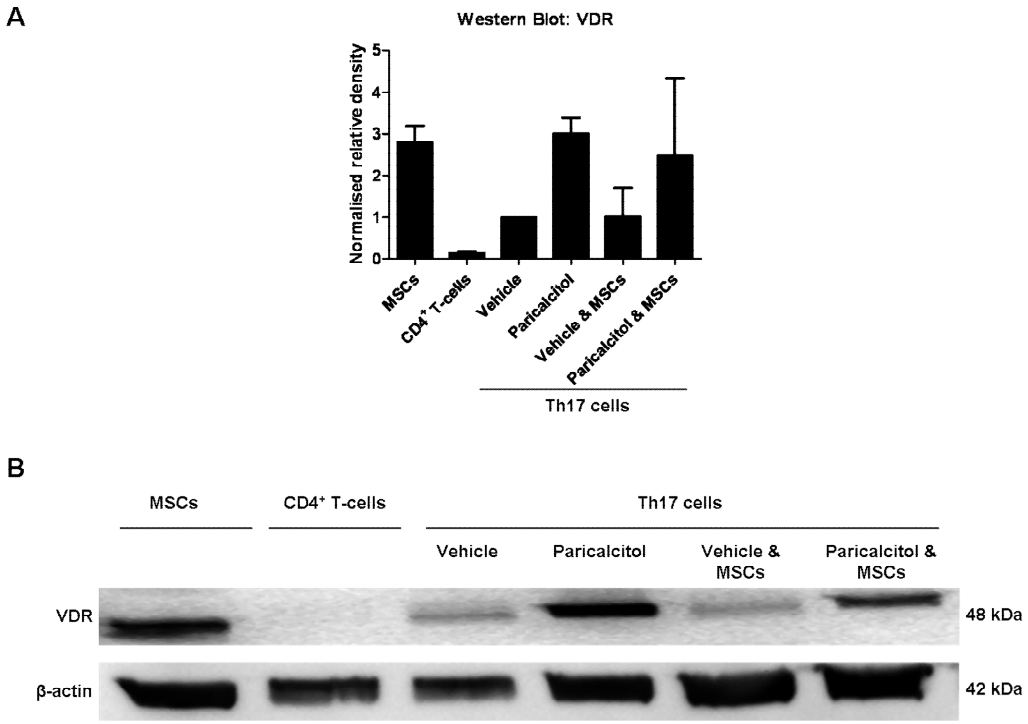

Figure 4.10 Paricalcitol induces upregulation of VDR: $CD4^+$ T-cells were cultured with APCs in the presence or absence of MSCs and/or paricalcitol/ethanol vehicle for 3 days under Th17-skewed conditions. $CD4^+$ T-cells were re-purified by MACS and subjected to Western Blot for VDR. MSCs cultured alone for 3 days and primary $CD4^+$ splenic T-cells were also analyzed. Data is representative of 2 individual Western Blots in which protein from 2 individual culture experiments were examined.

4.3.9 Differential effects on intracellular mediators of the Th17 differentiation pathway by paricalcitol and MSCs

Due to reported transcriptional modulation of target genes by VDR signaling (Griffin et al., 2003), I elected to examine the effects of MSCs and paricalcitol on specific signaling pathways, transcription factors, and negative regulators associated with primary Th17 differentiation including STAT3, RORγt, Runx1, IRF4 and FOXP3 (O'Shea et al., 2009).

Phosphorylation of the IL-6R following engagement with IL-6 and subsequent activation of Jak1 and Jak2 leads to the recruitment of STAT3 to the receptor complex (O'Shea et al., 2009). Phosphorylation of STAT3 induces dimerization, translocation to the nucleus, DNA binding and ultimately results in the activation of RORγt (Hermann-Kleiter and Baier, 2010). Thus, STAT3 signaling is essential for optimal Th17 responses.

In this experiment, total STAT3 bands were normalized to their respective β-actin bands and then phosphorylated STAT3 bands were normalized to their respective total STAT3 bands. As shown in **Figure 4.11**, STAT3 was minimally phosphorylated in MSCs (lane 1) and in primary $CD4^+$ T-cells (lane 2). Upon activation of T-cells (lane 3) under Th17-skewed conditions, STAT3 was highly phosphorylated. Neither paricalcitol nor MSCs affected the status of STAT3 phosphorylation (lanes 4-5).

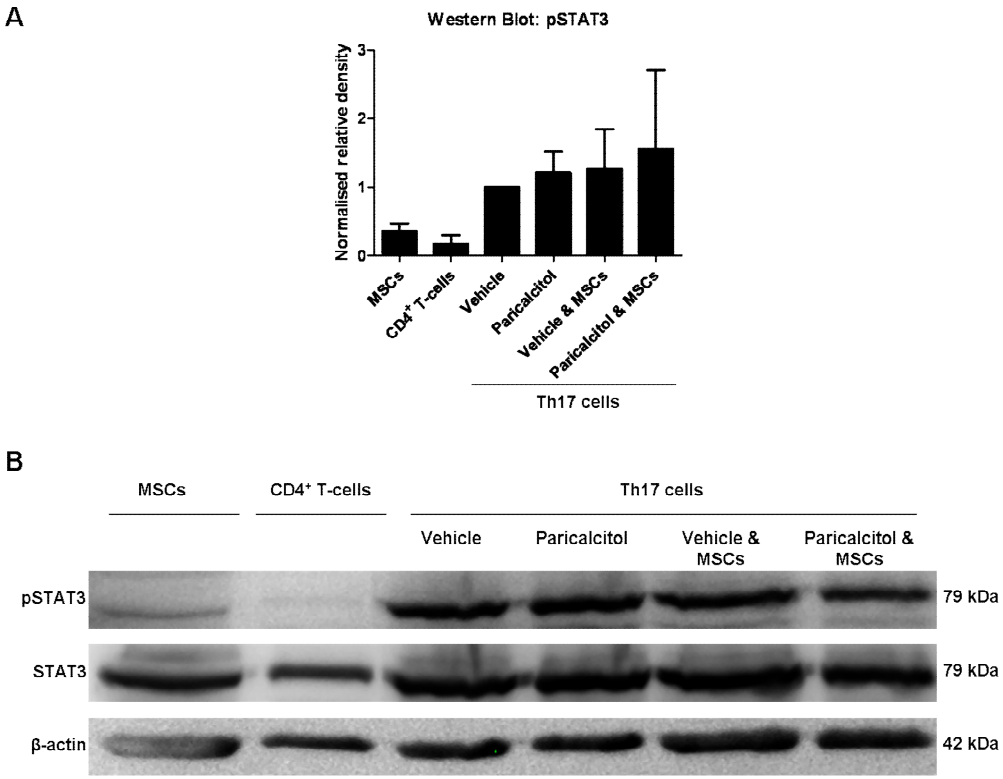

Figure 4.11 Paricalcitol and MSCs do not target STAT3 signaling: $CD4^+$ T-cells were cultured with APCs in the presence or absence of MSCs and/or paricalcitol/ethanol vehicle for 3 days under Th17-skewed conditions. $CD4^+$ T-cells were re-purified by MACS and subjected to Western Blot for phosphorylated and total STAT3. MSCs cultured alone for 3 days and primary $CD4^+$ splenic T-cells were also analyzed. Data is representative of 2 individual Western Blots in which protein from 2 individual culture experiments were examined.

RORγt is an isoform of RORγ which, together with RORα and RORβ, make up the ROR family of intracellular ligand-dependent hormone receptors. RORγt, encoded by *RORC*, is the master regulator of Th17 differentiation (O'Shea et al., 2009).

As shown in **Figure 4.12**, neither MSCs nor non-activated $CD4^+$ T-cells expressed RORγt (lanes 1/2) while Th17 differentiation was associated with strong expression of RORγt. Paricalcitol did not affect RORγt expression (lane 4) compared to vehicle-

treated Th17 cells. In contrast, RORγt expression by Th17 cells was moderately reduced by MSCs with or without paricalcitol (lanes 5/6) compared to vehicle control.

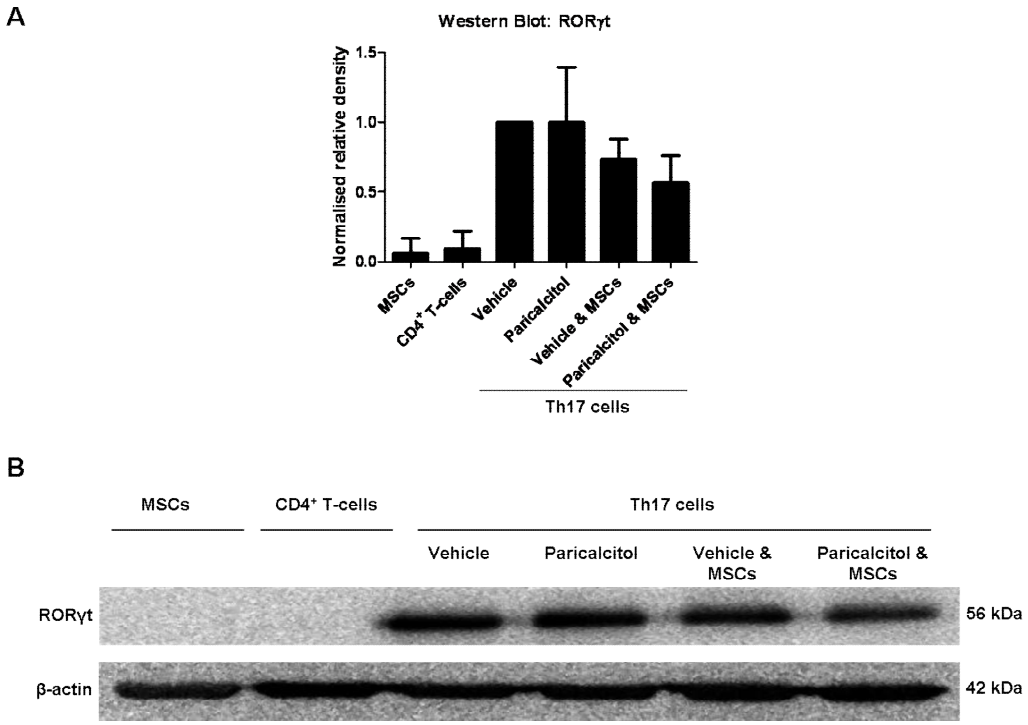

Figure 4.12 MSCs target the key Th17-associated transcription factor, RORγt: $CD4^+$ T-cells were cultured with APCs in the presence or absence of MSCs and/or paricalcitol/ethanol vehicle for 3 days under Th17-skewed conditions. $CD4^+$ T-cells were re-purified by MACS and subjected to Western Blot for RORγt. MSCs cultured alone for 3 days and primary $CD4^+$ splenic T-cells were also analyzed. Data is representative of 3 individual Western Blots for RORγt in which protein from 3 individual culture experiments were examined.

IRF4 and Runx1 are reported to play important roles in co-activating RORγt and IL-17A transcription, respectively (Hwang, 2010, O'Shea et al., 2009). IRF4 was not expressed by MSCs or primary $CD4^+$ T-cells while very low levels of Runx1 were expressed by both of these cell types (lanes 1-2) (**Figure 4.13**). Activation of $CD4^+$ T-cells by APCs and anti-CD3ε under Th17-skewed conditions resulted in the upregulation of IRF4 and Runx1 (lane 3). Paricalcitol did not affect IRF4 expression (lane 4) compared with vehicle-treated Th17 cells while Runx1 expression was moderately induced by paricalcitol. The presence of MSCs in Th17 cultures without (lane 5) or with paricalcitol (lane 6) resulted in reduced expression of IRF4 and Runx1.

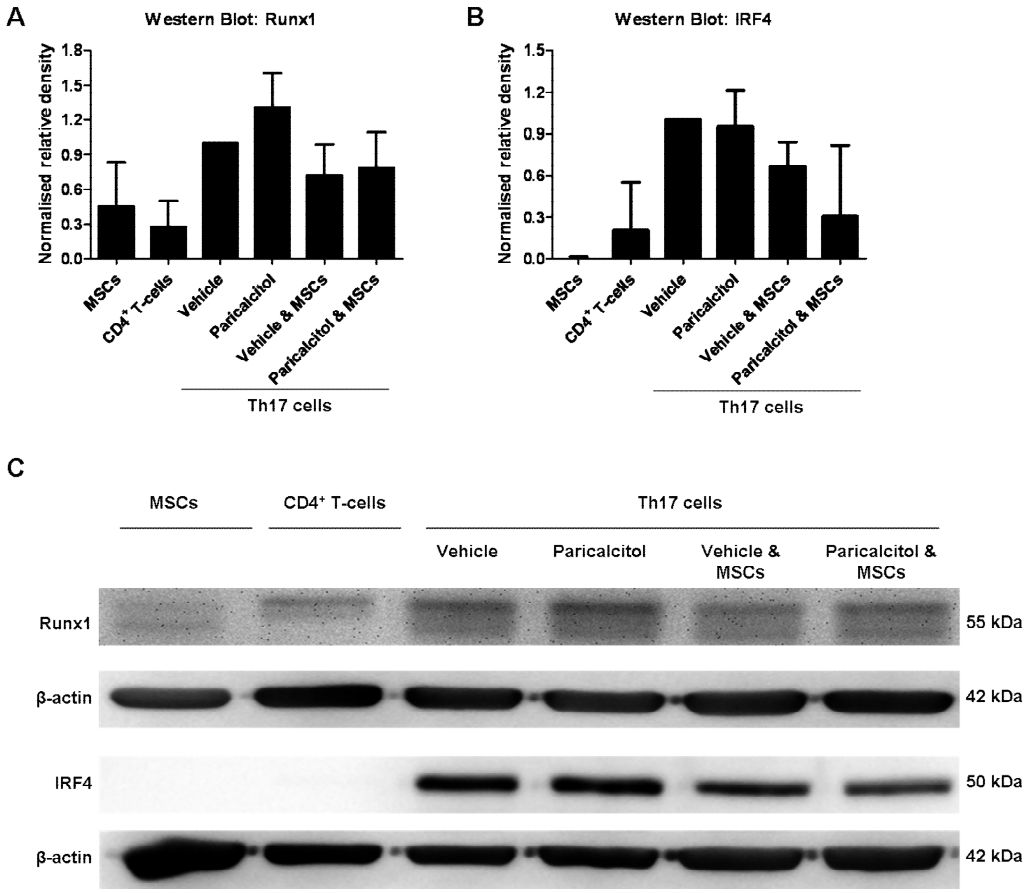

Figure 4.13 Paricalcitol does not affect IRF4 or Runx1 expression: $CD4^+$ T-cells were cultured with APCs in the presence or absence of MSCs and/or paricalcitol/ethanol vehicle for 3 days under Th17-skewed conditions. $CD4^+$ T-cells were re-purified by MACS and subjected to Western Blot for IRF4 and Runx1. MSCs cultured alone for 3 days and primary $CD4^+$ splenic T-cells were also analyzed. Data is representative of 3 individual Western Blots each for IRF4 and Runx1 in which protein from 3 individual culture experiments were examined.

Vitamin D agonists have been reported to induce T_{regs} (Mora et al., 2008). Furthermore, Ghannam et al. reported that MSCs inhibit human Th17 differentiation *via* PGE2 and that this was characterized by a concomitant increase in FOXP3-expressing T-cells (Ghannam et al., 2010). In multiple experiments, I was unable to detect induction of T_{regs} in Th17 differentiation cultures employing intracellular FOXP3 flow cytometry (data not shown). Nonetheless, I elected to determine whether MSCs or paricalcitol suppressed primary Th17 differentiation *via* induction of T_{regs} by performing a Western Blot for FOXP3. TGF-β1 signaling results in the induction of FOXP3 however TGF-β1 together with IL-6 induces RORγt expression by T-cells. FOXP3 is a negative regulator of RORγt (Hwang, 2010).

Protein for FOXP3 was not detected in MSC samples (lane 1) (**Figure 4.14**). Low levels of FOXP3 were detected in naïve, non-activated $CD4^+$ T-cells (lane 2).

Surprisingly, mouse Th17 cells expressed higher levels of FOXP3 than primary $CD4^+$ T-cells however, levels of FOXP3 were reduced in the presence of MSCs (lane 5) and paricalcitol (lane 4) suggesting that neither MSCs non paricalcitol actively promote T_{reg} expansion in this culture system.

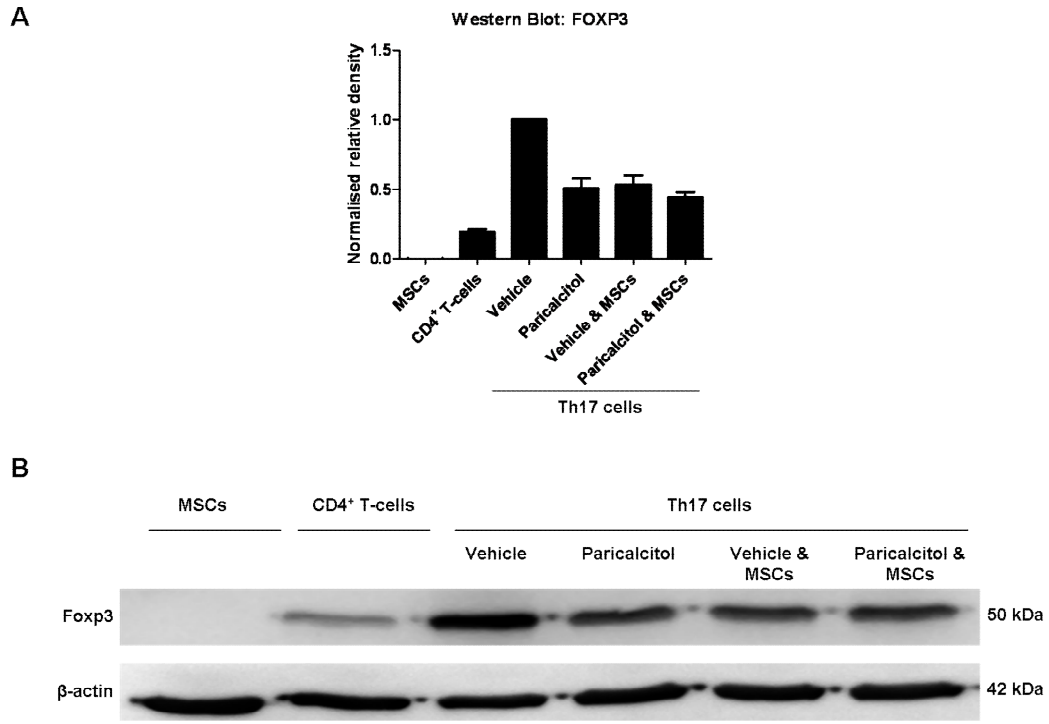

Figure 4.14 Neither MSCs nor paricalcitol induce FOXP3 expression: $CD4^+$ T-cells were cultured with APCs in the presence or absence of MSCs and/or paricalcitol/ethanol vehicle for 3 days under Th17-skewed conditions. $CD4^+$ T-cells were re-purified by MACS and subjected to Western Blot for FOXP3. MSCs cultured alone for 3 days and primary $CD4^+$ splenic T-cells were also analyzed. Data is representative of 2 individual Western Blots in which protein from 2 individual culture experiments were examined.

Overall, chapter 4 has demonstrated dose-dependent inhibition of IL-17A in primary Th17 cultures as well as in re-stimulated cultures by paricalcitol. This was associated with a mild anti-proliferative effect and without reduction in CD25 surface expression. At the optimal concentration (10 nM), paricalcitol augmented MSC-mediated inhibition of primary Th17 differentiation. These effects of paricalcitol were quite potent for naïve-phenotype responders but less so for memory-phenotype responders. Paricalcitol did not inhibit anti-CD3ε-induced IL-17 production by *in-vivo*-derived $CD45^+$ leukocytes from a site of sterile inflammation and also did not prevent MSC-mediated enhancement of IL-1α- and IL-23-induced IL-17A production by fully differentiated Th17 cells. Inhibition of primary Th17 differentiation by

paricalcitol was independent of APCs and did not involve PGE2/EP4 signaling. Th17 cells cultured in the presence of MSCs had lower expression of the key Th17-associated transcription factors RORγt, IRF4 and Runx1 while paricalcitol had no suppressive effect on expression of these proteins or in the case of Runx1 was associated with a modest increase in expression.

4.4 Discussion

4.4.1 Effects of VDR agonists on Th17 responses

In chapter 4 the effects of paricalcitol on the primary differentiation of Th17 cells were investigated. I clearly demonstrated for the first time, dose-dependent inhibition of IL-17A production by $CD4^+$ T-cells undergoing primary Th17 induction in the presence of paricalcitol (**Figure 4.1A/B/C**). Inhibition of primary Th17 differentiation in mice by calcitriol or analogues of calcitriol has been confirmed by a number of laboratories during the course of this thesis (Bruce et al., 2011, Joshi et al., 2011, Palmer et al., 2011, Lossius et al., 2011, van Hamburg et al., 2012). Specifically, Palmer and colleagues demonstrated dose-dependent inhibition of IL-17A by OVA-stimulated naïve $CD4^+$ T-cells from DO11.10 mice undergoing primary Th17 differentiation in the presence of graded concentrations of calcitriol. In humans, Joshi et al. showed dose-dependent suppression of the frequency of IL-17A-producing $CD4^+$ T-cells from anti-CD3/anti-CD28-activated PBMCs under Th17-skewed conditions (Joshi et al., 2011).

The therapeutic potential of calcitriol has been further strengthened by the development of new analogues of this compound, including paricalcitol, which have come to the fore in recent years. In a joint venture by Eli Lilly and Merck, a new VDR modulator (VDRM) was shown to enhance IL-4, IL-5, IL-10 and GATA3 expression and reduce proinflammatory IFN-γ, IL-2 and TNF-α production by PBMCs from healthy volunteers (Na et al., 2011). In this study, IL-17A and IL-22 production was inhibited by naïve $CD4^+$ mouse T-cells undergoing primary Th17 differentiation in the presence of the VDRM. The compound was also shown to be more efficacious and less calcemic than calcitriol in MOG-induced EAE (Na et al., 2011).

In additional experiments I showed that paricalcitol has mild anti-proliferative effects on $CD4^+$ T-cells undergoing primary Th17 differentiation at high concentrations (**Figure 4.1D**). This was also the case for calcitriol (Palmer et al., 2011). CCR6 expression by Th17 cells was also reduced in the presence of paricalcitol (**Figure 4.2F**). Chang and colleagues confirmed this result using both OVA-specific and MOG-specific $CD4^+$ T-cells. Furthermore, the same group went on to demonstrate the functional relevance of calcitriol-induced inhibition of CCR6 expression which

resulted in reduced migration of Th17 cells in response to MIP-3α/CCL20 using a chemotaxis assay (Chang et al., 2010a). This may be of clinical relevance in Th17-mediated diseases as Th17 cells require CCR6 for recruitment to sites of inflammation (Kitching and Holdsworth, 2011).

4.4.2 Combined effects of VDR agonists and other agents

A number of studies demonstrated the potential of calcitriol and paricalcitol to synergise with other immune modulating reagents including all-trans retinoic acid, dexamethasone and angiotensin inhibitors (Deb et al., 2010, Ikeda et al., 2010, Daniel et al., 2008, Tan et al., 2009). My work is novel in that it is the first study to investigate the combined effects of paricalcitol and a cell based therapy. In this regard I demonstrated that paricalcitol and MSC-mediated inhibition of Th17 differentiation was additive (**Figure 4.2**).

4.4.3 Effects of VDR agonists on naïve versus memory Th17 cells

The VDR is expressed by activated T-cells including Th17 cells but not by naïve T-cells (Chang et al., 2010b). Therefore, I hypothesized that paricalcitol would potently inhibit memory-phenotype T-cells. I detected minimal expression of VDR by primary naïve $CD4^+$ T-cells and increased expression by activated Th17 cells following 3 days in culture under Th17-polarized conditions (**Figure 4.10**). IL-17A production by both naïve- and memory-phenotype responders was inhibited by paricalcitol although the effect was less potent for memory cells (**Figure 4.4**). Nonetheless, the combination of paricalcitol and MSCs had an additive inhibitory effect on both naïve- and memory-phenotype responders (**Figure 4.4**). Furthermore, fully differentiated Th17 cells that underwent three induction/expansion cycles produced significantly less IL-17A in the presence of paricalcitol even when IL-1α was added (Figure **4.6**).

Suppression of both naïve and memory $CD4^+$ T-cells was confirmed by Joshi et al. who showed that 0.5 nM calcitriol is required to significantly ($p = <0.01$) inhibit anti-CD3/anti-CD28-induced IL-17A production by naïve T-cells from 2D2 mice, while 2 nM calcitriol was required to inhibit memory T-cells to the same extent (Joshi et al., 2011). Furthermore, memory-phenotype $CCR6^+$ Th17 cells that were isolated from PBMCs of untreated rheumatoid arthritis patients and activated for 3 days with anti-CD3/anti-CD28 in the presence of calcitriol produced significantly less IL-17A, IL-22

and TNF-α (van Hamburg et al., 2012). Lossius and colleagues generated Epstein-Barr virus nuclear antigen-1 (EBNA)-specific T-cell lines and clones from cerebrospinal fluid and blood of patients with multiple sclerosis. Each clone produced varying degrees of IFN-γ, IL-17A and IL-4. When activated with anti-CD3/anti-CD28 or EBNA in the presence of calcitriol, EBNA-reactive T-cells produced significantly less IL-17A than vehicle-treated controls (Lossius et al., 2011).

MSCs significantly inhibited IL-17A production *ex-vivo* by anti-CD3ε-activated $CD45^+$ leukocytes isolated from obstructed kidneys (**Figure 4.5**). In contrast however, paricalcitol did not suppress IL-17A production in a total of three experiments. This may reflect the presence of Th17-enhancing factors in cultures of obstructed kidneys which override the inhibitory effects of paricalcitol. Pindjakova et al. demonstrated that both $CD45^+$ and $CD45^-$ cells in the obstructed kidney produce high levels of IL-1α, IL-1β, IL-6 and IL-23 (Pindjakova et al., 2012), all of which are known to facilitate Th17 differentiation and/or expansion (Mills, 2008). Th17 cells that accumulate in the kidney are believed to be effector memory cells (Dong et al., 2008). I showed in **Figure 4.6** that paricalcitol inhibited IL-17A production by tertiary activated Th17 cells however, paricalcitol did not inhibit IL-17A production in the presence of IL-23. The less potent inhibitory effect of paricalcitol on memory-phenotype responders and the lack of inhibition towards effector memory Th17 cells from an obstructed kidney may be due to the Th17-enhancing factor IL-23. Overall these results suggest that there are limitations to the degree to which VDR agonists may modulate Th17 cells *in-vivo*.

Despite of the presence of effector memory Th17 cells and Th17-enhancing factors in obstructed kidney cultures, MSCs did significantly inhibit IL-17A production in these experiments (**Figure 4.5**). In contrast, MSCs enhanced IL-1α- and/or IL-23-mediated induction of IL-17A by fully differentiated Th17 cells *in-vitro* (**Figure 4.6**). These experiments suggest that MSCs may also have indirect effects *via* ancillary cells on tissue-activated Th17 cells. Addition of paricalcitol to these cultures did not additively inhibit IL-17A production by Th17 cells from obstructed kidneys nor did it protect from or reverse MSC-mediated enhancement of IL-17A by tertiary activated Th17 cells in the presence of IL-1α and IL-23.

4.4.4 DIRECT EFFECTS OF VDR AGONISTS ON TH17 CELLS

In other experiments, I demonstrated that paricalcitol directly inhibits Th17 responses *in-vitro* in APC-free cultures (**Figure 4.3**). This finding was confirmed by Chang et al. in experiments employing VDR KO mice. Calcitriol suppressed Th17 differentiation when WT $CD4^+$ T-cells and WT APCs were co-cultured under Th17-skewed conditions (Chang et al., 2010a). The suppressive effect persisted when WT APCs were replaced by VDR KO APCs and co-cultured with WT $CD4^+$ T-cells however; inhibition of Th17 differentiation was not evident when WT $CD4^+$ T-cells were replaced by VDR KO $CD4^+$ T-cells and co-cultured with WT APCs (Chang et al., 2010a). Palmer et al. also showed that APCs were redundant in calcitriol-mediated inhibition of Th17 differentiation by employing anti-CD3/anti-CD28 T-cell expander beads instead of APCs (Palmer et al., 2011).

4.4.5 MECHANISM OF VDR AGONIST-MEDIATED TH17 INHIBITION

I have shown that MSCs inhibit primary Th17 differentiation *via* PGE2/EP4 signaling but paricalcitol-mediated suppression of Th17 responses proved to be independent of this signaling pathway (**Figures 4.7, 4.8 & 4.9**) indicating that paricalcitol does not induce endogenous PGE2 by T-cells or by ancillary cells such as DCs or macrophages. Other groups have similarly ruled out a role for IL-2, STAT1, IL-10 (Chang et al., 2010a), apoptosis (Lossius et al., 2011), STAT4, IL-21 and T-bet (Palmer et al., 2011) in vitamin D-mediated inhibition of primary Th17 responses.

4.4.6 VDR EXPRESSION

What is evident however throughout the literature is that vitamin D-mediated suppression of primary Th17 induction is dependent upon VDR expression by T-cells (Chang et al., 2010b, Chang et al., 2010a, Palmer et al., 2011). The importance of the VDR in regulating Th17 responses and the physiological relevance of the VDR itself was highlighted in a study by Bruce and colleagues. The authors found that VDR KO $CD4^+$ T-cells cultured under Th17-skewed conditions produced more IL-17A, IL-17F and IL-21 than their WT counterparts (Bruce et al., 2011). Furthermore, when WT $CD4^+$ T-cells were transferred to Rag KO or Rag-VDR KO mice, more severe inflammatory bowel disease developed in the absence of VDR which was characterized by enhanced Th17 responses (Bruce et al., 2011). A recent study by Khoo et al. also highlighted the importance of the interactions between vitamin D and

Th17 differentiation. The authors showed that during the summer months in which serum calcitriol levels were increased in healthy subjects, IL-17A production by PBMCs was reduced (Khoo et al., 2012). I found increased expression of VDR by Th17 cells cultured in the presence of paricalcitol suggesting that classical VDR-mediated signaling is active in these cells (**Figure 4.10**). Of interest, MSCs also expressed high levels of VDR suggesting that they too may also be amenable to modulation by paricalcitol.

4.4.7 T_{REG} INDUCTION BY VDR AGONISTS

A number of studies reported induction of FOXP3 and T_{reg} cells following treatment with calcitriol (Joshi et al., 2011, Mora et al., 2008, Daniel et al., 2008). Not only do T_{regs} have the potential to suppress T-cell activation and proliferation (Joshi et al., 2011) but FOXP3 also negatively regulates Th17 differentiation at the mRNA level (O'Shea et al., 2009). Joshi et al. reported that FOXP3-expressing cells were induced in spleens at day 7 and in spinal cords at day 15 in MOG-induced EAE following administration of calcitriol. The authors also showed induction of double positive $FOXP3^+/CTLA4^+$ cells in human $CD4^+CD25^-$ T-cell cultures activated for 6 days in the presence of IL-2 and calcitriol (Joshi et al., 2011). Mechanistically, VDR/RXR was shown to bind to a VDRE in the FOXP3 promoter (Joshi et al., 2011). Daniel et al. found increased expression of TGF-β1, IL-10 and FOXP3 in colonic extracts from mice with TNBS-induced colitis that were treated with calcitriol (Daniel et al., 2008). I detected expression of FOXP3 in *in-vitro* differentiated Th17 cells by Western Blot (**Figure 4.14**) but in the presence of either paricalcitol or MSCs, FOXP3 expression was >2-fold lower than control Th17 cultures. In keeping with this, Chang and colleagues found that calcitriol inhibited FOXP3 expression under T_{reg}-skewed culture conditions in a VDR-dependent manner and that this effect was reversible by addition of exogenous IL-2 (Chang et al., 2010a). In another study, FOXP3 expression did not change following addition of calcitriol under Th17-skewed culture conditions (Tang et al., 2009). Furthermore, Palmer et al. did show induction of IL-10-expressing cells following addition of calcitriol to Th17 differentiation cultures however, using IL-10 and IL-10R neutralization antibodies, the authors demonstrated that calcitriol-mediated inhibition of Th17 differentiation was independent of IL-10 (Palmer et al., 2011). Therefore, the nature of the relationship between FOXP3 and the VDR is

complex although there may be potential for VDR agonists to induce T_{regs} under specific conditions.

4.4.8 Effects of VDR agonists on intracellular Th17-associated factors

In addition to the requirement for the VDR, another aspect of calcitriol-induced inhibition of Th17 differentiation is direct suppression of IL-17A and other Th17-associated cytokines. Consistent with my findings, protein levels of IL-17A were consistently suppressed in the presence of calcitriol or analogues of calcitriol in multiple studies (Chang et al., 2010a, Ikeda et al., 2010, Joshi et al., 2011, Chang et al., 2010b, Palmer et al., 2011, Tang et al., 2009). The majority of these studies also reported transcriptional inhibition of IL-17A (Palmer et al., 2011, Chang et al., 2010a, Ikeda et al., 2010, Joshi et al., 2011). One study reported that mRNA levels of IL-17A were not affected by calcitriol suggesting that inhibition of IL-17A occurred at the protein translation level (Chang et al., 2010b). Although I did not examine transcript levels of IL-17A in my study, the number of high quality studies reporting this finding suggests that calcitriol and its analogues do induce transcriptional repression of IL-17A.

As shown in **Figure 4.11**, paricalcitol did not alter the level of pSTAT3, expression of IRF4 or expression of the key transcription factor RORγt (**Figure 4.12**). This is consistent with the findings of Tang et al. who also found that RORγt mRNA and pSTAT3 were unaffected by calcitriol (Tang et al., 2009). Similarly, Chang et al. observed similar levels of RORγt mRNA in the presence or absence of calcitriol (Chang et al., 2010b). In contrast however, Ikeda et al. and Palmer et al. reported reduced transcript levels of RORγt in human and mouse $CD4^+$ T-cells undergoing primary Th17 differentiation (Ikeda et al., 2010, Palmer et al., 2011). In my study, STAT3 and RORγt do not appear to be targets of paricalcitol. RORα and AhR are co-factors involved in enhancing Th17 differentiation (O'Shea et al., 2009). Transcript levels of RORα were not affected by calcitriol (Chang et al., 2010b, Palmer et al., 2011). In contrast, suppression of AhR by calcitriol was reported at the transcript level (Ikeda et al., 2010), suggesting that AhR may be a target of calcitriol. Despite the lack of suppressive effects on intracellular levels of some Th17-enhancing transcription factors by paricalcitol, it is also possible that paricalcitol may physically interact with

these proteins thus preventing them from binding to the IL-17A promoter as was the case with Runx1 (Joshi et al., 2011).

Runx1 is a co-activator of IL-17A transcription. Paricalictol did not suppress protein levels of Runx1 in my study (**Figure 4.13**). This is consistent with the intricate report of Joshi and colleagues in which calcitriol dose-dependently inhibited IL-17A transcription as measured by luciferase activity in Jurkat cells that were transfected with the mouse IL-17A promoter. Calcitriol did not affect the expression of Runx1 although over-expression of Runx1 reversed calcitriol-mediated IL-17A repression and siRNA knockdown of Runx1 suppressed IL-17A transcription (Joshi et al., 2011). In elaborate experiments using mouse $CD4^+$ T-cells undergoing primary Th17 differentiation, Runx1 and VDR immunoprecipitated together indicating a physical interaction between these 2 proteins (Joshi et al., 2011). Indeed chromatin immunoprecipitation (ChIP) assays revealed that, in the presence of calcitriol, significantly lower levels of Runx1 bound to the IL-17A promoter. The findings of this study indicated that Runx1 is sequestered by the VDR and prevented Runx1 from binding as a co-activator to the IL-17A promoter (Joshi et al., 2011).

In human cells, NFAT was also found to be implicated in calcitriol-mediated repression of IL-17A as VDR/RXR was shown to compete with NFAT for a binding site on the IL-17A promoter (Joshi et al., 2011). This is consistent with an earlier report in which VDR/RXR heterodimers not only competed with NFAT for binding sites on the IL-2 promoter but also prevented NFAT from forming complexes with AP-1 thereby suppressing IL-2 gene transcription (Alroy et al., 1995).

4.4.9 Effects of MSCs on intracellular Th17-associated factors

In the case of MSC-mediated inhibition of primary Th17 differentiation, I found that protein levels of IRF4, RORγt and Runx1 were reduced in Th17 cells in the presence of MSCs (**Figures 4.12 & 4.13**) suggesting that PGE2/EP4 signaling is associated with suppression of multiple key transcription factors. IRF4 is induced upon IL-1/IL-1R1 signaling and, together with STAT3, co-induces RORγt expression (Hirahara et al., 2010). This is consistent with the report of Valdez et al. who demonstrated suppression of mRNA levels of IRF4 and downstream RORγt and IL-17A in mouse $CD4^+$ T-cells undergoing primary Th17 differentiation in the presence of PGE2. The

authors also reported suppression of RORα and AhR transcripts (Valdez et al., 2012). Also in keeping with my experimental results, PGE2 did not affect STAT3 phosphorylation (**Figure 4.11**). In RORC KO mice and IRF4 KO mice, IL-17A expression was inhibited compared to WT mice, highlighting the importance of these transcription factors in Th17 differentiation. RORγt was inhibited in IRF4 KO mice however; IRF4 expression was not suppressed in RORC KO mice suggesting that suppression of IRF4 could be a pivotal factor in PGE2-mediated Th17 regulation (Valdez et al., 2012).

4.4.10 SUMMARY

Overall, chapter 4 has demonstrated potent inhibition of primary Th17 responses by paricalcitol. It has also confirmed that paricalcitol and MSC-mediated inhibition of primary Th17 differentiation from naïve- and memory-phenotype responders are additive and independent of APCs. Furthermore, the VDR was upregulated in response to paricalcitol suggesting that paricalcitol may potentiate its own suppressive effects through the VDR. At the level of interrogation that was achievable in 6 months, I made some interesting observations regarding paricalcitol-mediated inhibition of Th17 differentiation, much of which was consistent with other reported results. However, other levels of complexity that were beyond the scope of this thesis remain, including transcriptional repression or post-transcriptional modification of Th17-associated transcription factors in addition to protein-protein interactions. MSCs employed PGE2/EP4 signaling to inhibit Th17 differentiation which resulted in inhibition of key Th17 transcription factors RORγt, IRF4 and Runx1. A summary of my results along with other recently reported findings related to calcitriol- and MSC-mediated inhibition of primary Th17 differentiation are illustrated in **Tables 4.4** and **4.5**.

Table 4.4 Effects of VDR agonists on Th17-associated factors during primary Th17 differentiation *in-vitro*

Th17-associated factor	Reduced at mRNA level	Unaffected at mRNA level	Increased at mRNA level	Reduced at Protein level	Unaffected at protein level	Increased at protein level	Comments
IL-17A	2, 3, 4 & 5	6		**1,** 2, 3, 4, 5, 6, 7, 8 & 9			
IL-17F	5	6		6			
IL-21	3						
IL-22		6		6 & 9			
pSTAT3					**1** & 7		
RORγt	3 & 5	6 & 7			**1**		
RORα	5 & 6						
AhR	3						
IRF4					**1**		
Runx1					4	**1**	Sequestered by VDR preventing it from binding to IL-17 promoter (4)
NFAT							Competition between VDR and NFAT for binding site on IL-17 promoter (4)
FOXP3			4	**1**	7	4	

1 (This thesis), 2 (Chang et al., 2010a), 3 (Ikeda et al., 2010), 4 (Joshi et al., 2011), 5 (Palmer et al., 2011), 6 (Chang et al., 2010b), 7 (Tang et al., 2009), 8 (Lossius et al., 2011), 9 (Na et al., 2011).

Table 4.5 Effects of MSCs or PGE2 on Th17-associated factors during primary Th17 differentiation *in-vitro*

Th17-associated factor	Reduced at mRNA level	Reduced at Protein level	Unaffected at protein level	Increased at protein level
IL-17A	*13*	**1,** 10, 11, 12, ***1,*** *13 & 14*		
IL-17F		12		
IL-22		10		
pSTAT3			**1** & *13*	
RORγt	12, *13 & 14*	**1** & 10		
RORα	*13*			
AhR	*13*			
IRF4	*13*	**1**		
Runx1		**1**		
FOXP3		**1**		10

MSCs : **1 (This thesis),** 10 (Ghannam et al., 2010), 11 (Tatara et al., 2011), 12 (Qu et al., 2012), *PGE2 :* ***1 (This thesis),*** *13 (Valdez et al., 2012), 14 (Chen et al., 2009).*

CHAPTER FIVE

IN-VIVO EFFECTS OF MSCS AND PARICALCITOL IN OBSTRUCTIVE NEPHROPATHY

5.1 INTRODUCTION

Efficient renal function is vital for life. In terms of basic biology, the kidneys are responsible for excretion and homeostasis by removing waste and excess water from the blood, regulating water and mineral balance and releasing specific homeostatic hormones. Kidneys are composed of the more superficial cortex and deeper medulla and contain functional units termed nephrons (**Figure 5.1**). Within each nephron, capillaries of the glomerulus are closely associated with tubules. Proximal tubules collect filtrate from the blood from where it passes through the loop of Henle to the distal tubules and then to the ureters and eventually to the bladder *via* collecting ducts. Healthy kidneys receive approximately one quarter of the cardiac output and generate about 100 ml of filtrate each minute (Campbell and Reece, 2008).

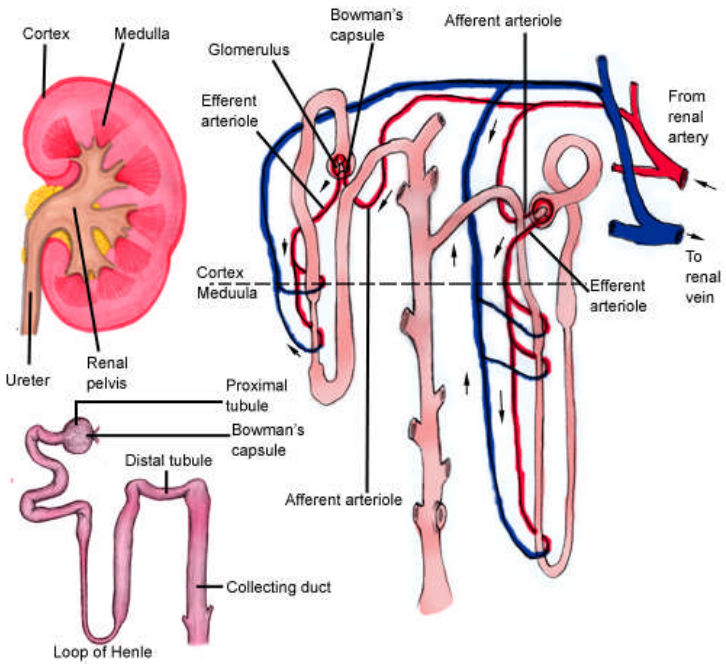

Figure 5.1 Composition of the kidney (From: Hoenig et al., Kidney Anatomy - www.emedicine.medscape.com).

Kidney disease can be broadly characterized into acute kidney injury (AKI) and chronic kidney disease (CKD). The UUO model of obstructive nephropathy employed in this thesis evolves as an acute form which progresses to a form of chronic injury characterized by renal fibrosis (Chevalier et al., 2009). Obstructive nephropathy, whether congenital or acquired, is the most common reason for renal failure in children and also represents a frequent cause of renal failure in adults (Grande et al.,

2010). AKI may be reversible while CKD is typically irreversible although its progression may be slowed by medical therapy. End stage renal disease requires dialysis or renal transplantation (Liu, 2004).

Acute urinary obstruction is characterized by multiple pathological changes including vasoconstriction, interstitial infiltration of inflammatory cells, tubular dilation and atrophy and tubulointerstitial fibrosis as illustrated in **Figure 5.2** (Misseri et al., 2004).

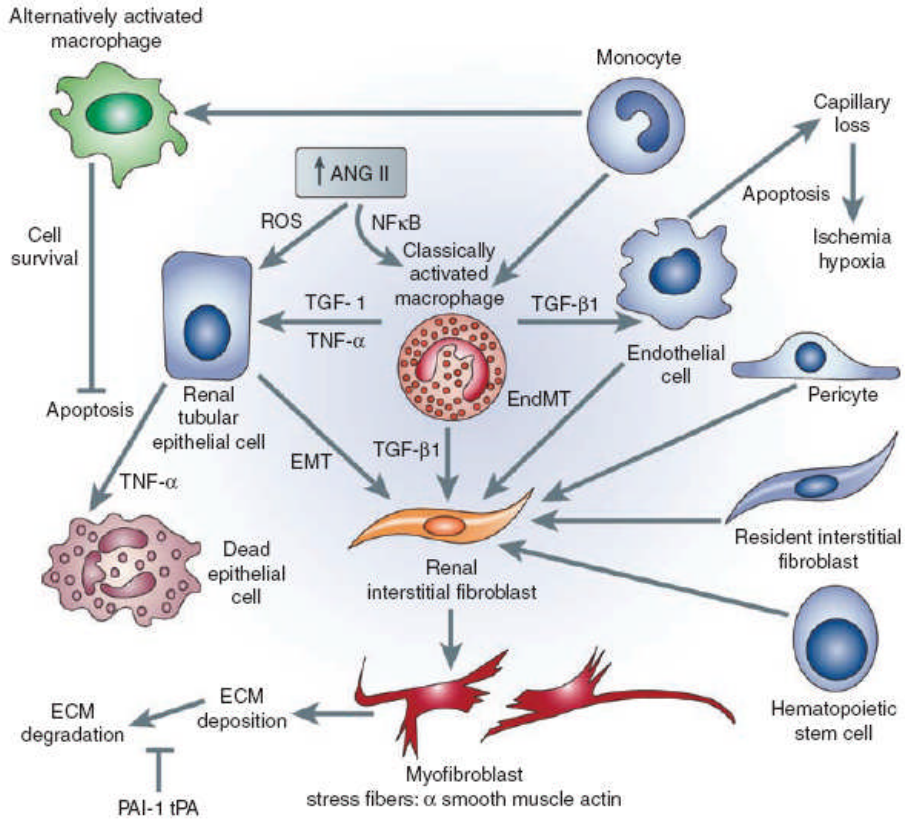

Figure 5.2 Pathological changes and cellular interactions between resident renal cells and infiltrating immune cells following UUO (From: Chevalier et al., 2009).

The UUO model has been employed to demonstrate that acute urinary obstruction activates the renin-angiotensin hormone system (RAS), reactive oxygen species and NF-κB signaling. Vasoconstriction following UUO is initiated by RAS activation and is characterized by reduced blood flow through the kidneys and glomerular filtration rate within 24 hours.

Macrophages are the most prominent inflammatory cell population that infiltrate the kidney following UUO (Grande et al., 2010). Macrophages can be broadly divided into classically activated pro-inflammatory 'M1' macrophages and alternatively activated anti-inflammatory 'M2' macrophages *in-vitro*. Nomenclature *in-vivo* is more complex as highlighted by Weidenbusch et al. due to the presence of pro-fibrotic fibroblasts (Weidenbusch and Anders, 2012). Nonetheless, a number of reports have demonstrated that pro-inflammatory macrophages are responsible for tissue damage *via* production of inflammatory mediators and growth factors including TNF-α, IL-1, IL-6, FGF, PDGF and TGF-β1 while anti-inflammatory macrophages promote cell survival in kidney disease (Weidenbusch and Anders, 2012, Kushiyama et al., 2011, Misseri et al., 2004).

T-cells also accumulate in the obstructed kidney and contribute to tissue damage by producing pro-inflammatory cytokines and chemokines resulting in the recruitment of other tissue destructive leukocytes. Th17 cells recruit neutrophils in particular to sites of inflammation (Turner et al., 2010a). $CD4^+$ T-cells accumulate in the kidney as early as 24 hours post UUO and a proportion of these are IL-$17^+CD44^+CD25^+$ effector memory-phenotype Th17 cells (Dong et al., 2008). Monocyte-derived IL-1 enhances $CCR6^+$ Th17 cells accumulation in the obstructed kidney (Pindjakova et al., 2012).

A prominent feature of UUO is tubular atrophy. This is associated with tubular epithelial cell apoptosis and tubular dilation within a micro-environment which is pro-inflammatory, ischemic, hypoxic and oxidative. Apoptosis is followed by basement membrane disruption and subsequent atrophy resulting in atubular glomeruli (Chevalier et al., 2009).

Over the course of 1-2 weeks, progressive loss of parenchyma and tubulointerstitial fibrosis occurs in the UUO model (Chevalier et al., 2009). Fibrosis is the net result of extracellular matrix (ECM) deposition at a rate that is greater than its degradation by MMPs. ECM is composed of multiple substances including collagen type I, III and IV, fibronectin and heparin sulfate proteoglycans. Fibrosis occurs due to epithelial to mesenchymal transition (EMT) of tubular epithelial cells, endothelial cells and/or pericytes into interstitial fibroblasts which become activated by tubular epithelium-

and macrophage- produced TGF-β1. TGF-β1 induces proliferation and myofibroblast activation (Chevalier et al., 2009). EMT is characterized by loss of adhesion molecules, including e-cadherin, by tubular epithelial cells, induced expression of α-smooth muscle actin (α-SMA) and by increased migration potential (Liu, 2004).

Altogether, renal vasoconstriction, cellular infiltrate, tubular atrophy and interstitial fibrosis lead to functional loss of nephrons.

The UUO model of obstructive nephropathy is interesting in that the development of kidney injury in this model encompasses many characteristics of other interstitial kidney diseases including polycystic kidney disease, acute renal failure and transplantation, while the progressive fibrotic features are shared by multiple chronic kidney diseases such as diabetic nephropathy and glomerulonephritis. UUO is advantageous in that it is induced in the absence of exogenous antigens or toxins and it is non-life threatening to the animal with the potential use of the contra-lateral kidney as a non-obstructed control.

At the onset of this thesis there were no publications in relation to MSC administration in UUO. More recently, Asanuma et al. reported that human MSCs delivered *via* the renal artery were detectable in the interstitium up to 4 weeks post UUO. This was associated with reduced α-SMA, fibroblast-specific protein positive cells and collagen deposition with preserved e-cadherin expression (Asanuma et al., 2011). In another study, Male MSCs administered intravenously to female rats were detected in tubules and reduced α-SMA expression. This was further enhanced by HGF adenovirus transfected-MSCs (Liu et al., 2011). Allogeneic MSCs delivered *via* the vena cava in rats also reduced collagen deposition as detected by Trichrome staining and $ED1^+$ macrophage infiltration 3 and 7 days post UUO (Liu et al., 2012). Of interest, Nakagawa et al. reported that an EP4 specific agonist attenuated interstitial fibrosis, macrophage infiltration and α-SMA myofibroblast proliferation following administration to WT mice with UUO. WT mice with UUO had increased expression of COX2 in tubular epithelial cells which co-localized with MCP-1 expression (Nakagawa et al., 2012). EP4 KO mice developed more severe UUO, suggesting that endogenous PGE2-EP4 signaling protects from interstitial fibrosis and macrophage infiltration (Nakagawa et al., 2012).

The number of studies examining the effect of paricalcitol in UUO was also limited at the initiation of this thesis. Subsequently, one group has extensively investigated the effects of paricalcitol on interstitial fibrosis and cellular infiltrate in mouse UUO (Tan et al., 2006, Tan et al., 2008, Tan et al., 2009). In these studies, paricalcitol was administered subcutaneously to male CD-1 out-bred mice (0.1-0.3 μg/kg/day) until day 7 following UUO. The authors found dose-dependent reduction in interstitial volume, tubular atrophy and apoptosis and collagen deposition with paricalcitol treatment. Expression of fibronectin, collagens I and III and α-SMA was reduced with preservation of e-cadherin by paricalcitol (Tan et al., 2006). Mechanistically, UUO was associated with increased TGF-βR1 expression which was suppressed by paricalcitol. *In-vitro*, TGF-β induced-snail expression and EMT in tubular epithelial cells were suppressed by paricalcitol. The snail transcription factor initiates EMT by repression of e-cadherin. The authors found that paricalcitol reduced snail expression following UUO (Tan et al., 2006). Cellular infiltration ($CD3^+$ T-cells and $F4/80^+$ myeloid cells) was also suppressed by paricalcitol. The authors demonstrated by *in-vitro* chemotaxis assays that this may be due to suppression of TNF-α-induced RANTES expression by tubular epithelial cells (Tan et al., 2008). TNF-α-induced RANTES expression was dependent on NF-κB signaling. Paricalcitol treatment did not affect TNF-α-induced phosphorylation of p65 NF-κB but rather induced VDR sequestration of p65 NF-κB which prevented it from binding to the RANTES promoter (Tan et al., 2008).

Following UUO, VDR expression was inhibited as early as 24 hours (Tan et al., 2008, Xiong et al., 2012). Paricalclitol and calcitriol restored VDR expression and this was associated with EMT inhibition (Tan et al., 2008, Xiong et al., 2012). Loss of VDR *in-vitro* by tubular epithelial cells was associated with increased TNF-α expression (Xiong et al., 2012). TNF-α also synergized with TGF-β1 to induce EMT – an effect which was prevented by over-expression of VDR. The effect of TNF-α-induced EMT was mirrored by knockdown of VDR. The importance of VDR expression was demonstrated in VDR KO mice which developed more severe fibrosis characterized by enhanced expression of fibronectin, collagen I, TGF-β, α-SMA, snail, renin and angiotensin I and II but reduced e-cadherin expression (Zhang et al., 2010b). Administration of an angiotensin I inhibitor partially reversed the enhanced fibrosis

observed in VDR KO mice suggesting that VDR suppressed RAS to attenuate interstitial fibrosis (Zhang et al., 2010b).

Based on the above publications, it was clear that MSC and paricalcitol mono-therapies mediate some individual beneficial effects in UUO. Mechanistically, the effects of paricalcitol in particular were well examined by Tan and colleagues. However, the effects of MSCs and paricalcitol individually and in combination on certain basic aspects of the model were unknown. Specifically, effects on the relative frequency and functionality of T-cell and macrophage subtypes were not clear. Of specific relevance to my work, the influence of MSCs and/or paricalcitol on IL-17-producing T-cells *in-vivo* in this model had not been previously examined. Indeed combination therapy with MSCs and paricalcitol had never been investigated in any model or *in-vitro* scenario. The UUO model has been extensively used by my laboratory to examine Th17 responses post acute urinary obstruction (Dong et al., 2008, Pindjakova et al., 2012). This model allowed me to investigate the effects of MSCs and/or paricalcitol on Th17 activation *in-vivo* as well as providing the opportunity to examine other aspects of MSC- and/or paricalcitol-mediated immunosuppression.

Therefore, specific aims for charter 5 were to:

1. Determine the effects of paricalcitol and MSCs alone and in combination on IL-17-producing Th17 cells and other infiltrating immune cells in the kidney following acute urinary obstruction.
2. Determine the effects of paricalcitol and MSCs alone and in combination on renal structural damage following acute urinary obstruction.

5.2 MATERIALS AND METHODS

5.2.1 INTRAVENOUS ADMINISTRATION OF MSCS

Mice were placed in a restrainer while a heat lamp was used to warm the tail for 30 seconds prior to administration of MSCs at 18 and 48 hours relative to ureteral ligation in the UUO model. Autologous MSCs (2.5 x 10^6/ml) were slowly administered in 200 µl of sterile saline *via* tail vein injection using a sterile 27G needle attached to a 1 ml insulin syringe.

5.2.2 SUBCUTANEOUS ADMINISTRATION OF PARICALCITOL

Paricalcitol (0.3 µg/kg/day) was administered subcutaneously in a volume of 100 µl of saline daily starting on day 0 relative to UUO until day 7. The mice were scruffed and restrained in one hand while the other hand adminsitered the paricalcitol subcutaneously to the loose skin on the back of the neck.

5.2.3 PROCESSING OF KIDNEY TISSUE FOR HISTOLOGY AND IMMUNOHISTOCHEMISTRY

Kidneys were dissected from mice and placed in 10% neutral buffered formalin for < 24 hours prior to processing in a Leica ASP 300 tissue processor (Wetzlar, Germany). Tissues were wax embedded in a Leica EG1150H wax embedder and 2 µm sections were cut using a Leica RM2235 microtome. The sections were transferred to Superfrost Plus® microscope slides (Fisher Scientific Ireland) and incubated overnight at 55°C to dry.

5.2.4 HEMATOXYLIN AND EOSIN (H & E) STAINING

Sections were de-waxed in xylene (2 changes of 10 minutes each). Xylene was removed in absolute alcohol for 5 minutes. The sections were brought to tap water through 95% and 70% alcohols for 5 minutes each. The alcohol was removed in running tap water for 2 minutes. Sections were stained in Mayer's Hematoxylin for 40 seconds and washed in running tap water for 5 minutes followed by staining in Eosin for 5 minutes. The sections were rinsed in tap water quickly and dehydrated through graded alcohols (70%, 95% and 100% for 3 minutes each). Sections were cleared in xylene (two changes of 10 minutes each) and covered with DPX mounting medium

and cover slips applied. Ten non-overlapping fields throughout the superficial and deep cortex were examined. Blinded scoring was carried out at 20 X magnification jointly with Dr. Bairbre McNicholas, Specialist Registrar in Nephrology, Galway University Hospitals/NUIG.

5.2.5 Masson's Trichrome staining with Gomori's Aldehyde Fuchsin

Sections were de-waxed in xylene (2 changes of 10 minutes each). Xylene was removed in 2 changes of absolute alcohol for 2 minutes each. The sections were brought to tap water through 95%, 70% and 50% alcohols for 1 minute each. The alcohol was removed in running tap water for 2 minutes. The sections were oxidized in equal parts 0.5% potassium permanganate/0.5% sulfuric acid for 2 minutes, rinsed in tap water and bleached in 2% sodium metabisulphite for 2 minutes. The sections were washed in water for 30 seconds followed by 70% alcohol for 1 minute and then stained in Gomori's Aldehyde Fuchsin for 1 minute. This was followed by rinsing in water, 95% alcohol and water again for 10 seconds each. The sections were stained in Celestine blue for 4 minutes, rinsed in water for 30 seconds followed by staining in Mayer's Hematoxylin for 4 minutes. The sections were washed in water for 30 seconds and differentiated in acid alcohol for 20 seconds. The sections were washed in running tap water for 4 minutes, stained in Masson's cytoplasmic stain for 1 minute, rinsed in water and then differentiated in 1% dodeca-molybdophosphoric acid for 2 minutes. The sections were rinsed in water, counterstained in fastgreen for 1 minute, differentiated in 1% acetic acid for another minute and then dehydrated through 50%, 70%, 95% and absolute alcohols for 1 minute each. The sections were cleared in xylene (2 changes of 10 minutes each) and mounted in DPX medium. Ten non-overlapping fields throughout the superficial and deep cortex were examined and scored blinded at 20 X magnification.

5.2.6 Periodic Acid-Schiff (PAS) staining

Sections were de-waxed in xylene (2 changes of 5 minutes each). Xylene was removed in 3 changes of absolute alcohol for 2 minutes each. The sections were brought through 2 washes in 95% alcohol and 1 wash in 70% alcohol for 2 minutes each. The sections were washed in PBS for 7 minutes twice followed by oxidation in 2% periodic acid solution for 5 minutes in the dark. Sections were washed in distilled water for 5 minutes followed by incubation in Schiff reagent for 20 minutes. Sections

were washed in warm water for 7 minutes and counterstained in Mayer's Hematoxylin for 2 minutes. Sections were washed in tap water for 5 minutes followed by dehydration in 70%, 95% and absolute alcohols for 1 minute each. The sections were cleared in xylene (2 changes of 10 minutes each) and mounted in DPX medium. Ten non-overlapping fields throughout the superficial and deep cortex were examined and scored blinded at 20 X magnification.

5.2.7 IMMUNOHISTOCHEMISTRY (IHC)

Sections were de-waxed in xylene (2 changes of 5 minutes each). Xylene was removed in 3 changes of absolute alcohol for 2 minutes each. Slides were brought through 2 washes in 95% alcohol and 1 wash in 70% alcohol for 2 minutes each prior to washing in PBS for 7 minutes. Endogenous peroxidase was blocked by incubation of sections in 30% hydrogen peroxide:methanol (1:10) for 20 minutes in the dark followed by a 7 minute PBS wash. The autoclave method of antigen unmasking was employed. Slides were placed in boiling 1% antigen unmasking solution:distilled water for 5 minutes at 121°C. Once cooled, slides were washed in PBS for 7 minutes. Slides were marked with liquid repellent slide marker pen and 1 drop of avidin blocking solution was applied for 15 minutes to block endogenous biotin. Slides were washed in PBS for 7 minutes followed by application of 1 drop of biotin solution for 15 minutes. Slides were washed in PBS for 7 minutes followed by addition of 100 µl of diluted primary antibody for 1 hour at room temperature according to **Table 5.1**. Slides were washed in PBS for 7 minutes followed by addition of 100 µl of diluted secondary antibody for 30 minutes at room temperature. Slides were washed in PBS for 7 minutes followed by addition of 100 µl of avidin-biotin complex (ABC) reagent for 30 minutes. Slides were washed in PBS for 5 minutes and TRIS-HCL pH 7.6 for 5 minutes. Slides were incubated in 3,3-diaminobenzidine (DAB) substrate solution for 2 minutes followed by counterstaining in methylgreen for 2 minutes. Slides were incubated in 95% alcohol twice for 10 seconds followed by 3 X 10 second incubations in absolute alcohol then 2 X 10 second incubations in xylene. Slides were mounted in DPX medium. Ten non-overlapping fields throughout the superficial and deep cortex were photographed at 20 X magnification and subjected to image analysis and aerial measurements using Adobe Photoshop CS6.

Table 5.1 IHC antibody preparation

Name	Dilution	Diluent	Secondary
Anti-CD3 polyclonal	1/200	(10% w/v milk powder/PBS)	Goat anti-rabbit (1/300)

5.2.8 RNA ISOLATION FROM KIDNEY TISSUE AND QUANTITATIVE REAL TIME POLYMERASE CHAIN REACTION (QRT-PCR)

Tissue samples were stored in RNAlater® solution following dissection from mice and placed in a -80°C freezer. Tissues were allowed to defrost and were placed into new RNase-free eppendorfs. Samples were homogenized for 1 minute using a pestle cleaned with RNaseZap® solution. Samples were re-suspended in 1 ml of Trizol® solution and pipetted up and down to dissolve the tissue. The solution was left to stand for 5 minutes. Chloroform (200 µl) was added and the tubes were shaken vigorously for 30 seconds. Samples were left to stand for 2 minutes followed by centrifugation at 12,000 RCF for 15 minutes at 4°C. The upper aqueous layer (RNA) was removed carefully so as not to disrupt the bottom two layers (phenol (pink) and DNA/protein). The solution was placed into clean RNase-free eppendorfs and 500 µl of isopropanol was added. The tubes were gently inverted 3-4 times, left at room temperature for 10 minutes and centrifuged at 12,000 RCF for 10 minutes at 4°C. The eppendorfs were placed on ice. The isopropanol was removed and 1 ml of 75% ethanol was added. The tubes were inverted 3-4 times and centrifuged at 7,500 RCF for 5 minutes at 4°C. Ethanol was removed and the samples left to air dry for 10 minutes. Pellets were re-suspended in 50ul of RNase-free water and dissolved in a heat block at 55°C for 10 minutes. RNA was measured using a Nanodrop ND-1000 spectrophotometer. Equal quantities of RNA were DNase-treated by adding 10 X TURBO DNase buffer (10% of final volume) and 1 µl of TURBO DNase to the RNA followed by gentle mixing. Samples were incubated at 37°C for 20 minutes. DNase inactivation reagent was added (10% of final volume) and mixed thoroughly. Samples were incubated for 2 minutes at room temperature. Centrifugation was performed at 10,000 RCF for 90 seconds and the RNA was transferred to fresh tubes prior to measurement of RNA content.

Complementary DNA (cDNA) was synthesized using a High Capacity cDNA Reverse Transcription Kit with RNase Inhibitor® and a GeneAmp 9700 A Thermal Cycler from Applied Biosystems. cDNA was equalized between samples and subjected to

qRT-PCR using inventoried TaqMan® gene expression assays and reagents and a StepOne Plus Real Time PCR System (Applied Biosystems). The comparative C_T method was employed to determine relative quantification. Target genes were normalized to GAPDH and expressed as fold change relative to an appropriate reference sample.

All other methods for this chapter are as described in sections 2.2, 3.2 and 4.2.

5.3 RESULTS

To date, all experiments were performed using *in-vitro* generated Th17 cells or *in-vivo*-derived Th17 which were cultured *ex-vivo* in the presence of paricalcitol and/or MSCs. In order to determine the combined effect of MSCs and paricalcitol to suppress Th17 immune responses *in-vivo*, I elected to use a mouse model of kidney disease characterised by abnormal Th17 responses.

UUO was performed on female B6 mice (19.2 g-24.2 g) followed by random assignment into 4 groups (**Figure 5.3B**). Daily subcutaneous administration of paricalcitol (0.3 µg/kg)/vehicle and/or intravenous administration of MSCs (0.5 x 10^6)/saline control the morning after UUO and again at day 2 were performed according to **Figure 5.3**. The combination of paricalcitol and MSCs together was compared to vehicles alone (no treatment), paricalcitol alone and MSCs alone. Animals were euthanized by carbon dioxide asphyxiation at day 3 (n = 20) or day 8 (n = 19) and control and obstructed kidneys were dissected.

A

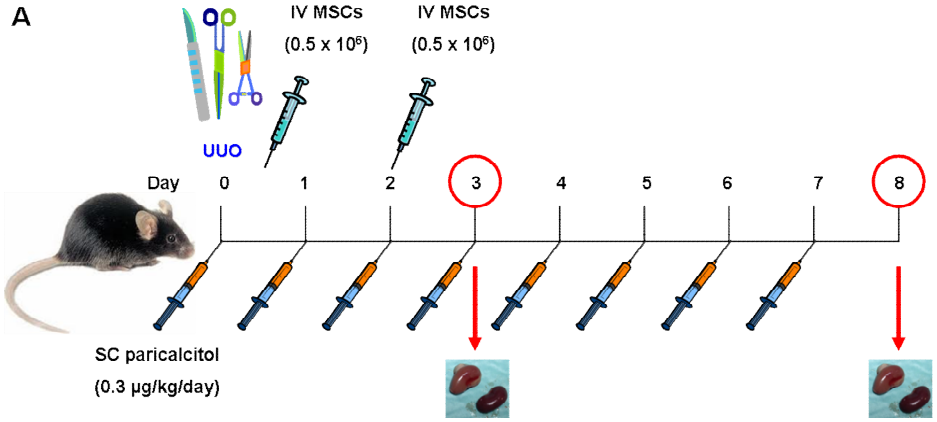

B

Group	Treatment regime and frequency
No treatment (n = 5)	Vehicle control daily (100 µl SC) & saline control at 18 & 48 hours (200 µl IV)
MSCs alone (n = 5)	Vehicle control daily (100 µl SC) & MSCs at 18 & 48 hours (0.5×10^6 cells in 200 µl IV)
Paricalcitol alone (n = 5)	Paricalcitol daily (0.3 µg/kg in 100 µl SC) & saline control at 18 & 48 hours (200 µl IV)
MSCs and paricalcitol (n = 5)	Paricalcitol daily (0.3 µg/kg in 100 µl SC) & MSCs at 18 & 48 hours (0.5×10^6 cells in 200 µl IV)

Figure 5.3 (A) Schematic highlighting the timeline of UUO, administration of immune modulating agents and termination of study with organ harvest. (B) Study design showing number of animals per group and treatment regime.

The control and obstructed kidneys were cut along the long axis. Half of each kidney was stored in 10% formalin solution for histological/IHC staining, one quarter was kept aside for digestion for flow cytometry while the remaining tissue was snap frozen and stored at -80°C for protein detection and stored in RNAlater® for RT-PCR.

In order to determine the effects of combined MSC and paricalcitol administration in UUO, a number of experimental read-outs were employed including analysis of the frequency of multiple immune populations in the kidneys by multi-colour flow-cytometry, cytokine production by intracellular flow cytometric staining and RT-PCR, tubular atrophy and dilation by H & E histological staining, interstitial fibrosis by Masson's Trichrome histological staining and cellular infiltrate by PAS histological staining and IHC.

The primary experimental read-out at day 3 of UUO was analysis of T-cell populations with particular emphasis on IL-17-producing $CD4^+$ T-cells. Secondary read-outs included examination of myeloid cell populations in the kidneys following UUO. Primary experimental read-outs at day 8 of UUO included histological analysis of kidney damage; tubular atrophy and dilation, cellular infiltration and collagen deposition. Secondary read-outs included analysis of T-cell and myeloid cell populations by flow cytometry and IHC.

In order to examine T-cell accumulation in the kidneys at days 3 and 8 following UUO, control and obstructed kidneys were dissected, digested and single cell suspensions prepared prior to multi-colour flow cytometry. As shown in **Figure 5.4**, cells were gated on viable cells only with doublets being excluded. The pan leukocyte marker, CD45 was used to discriminate immune cells followed by analysis of $CD4^+$ and $CD8^+$ T-cell populations within the TCR-β compartment. Data are represented as percent positive of total viable cells.

Figure 5.4 (overleaf) (A) Representative gating strategies of T-cell populations in control and obstructed kidneys following UUO and **(B)** representative examples of dot plots for $CD45^+$, TCR-β^+, $CD4^+$, $CD8^+$ and $CCR6^+$ populations in obstructed kidneys for each of the treatment groups.

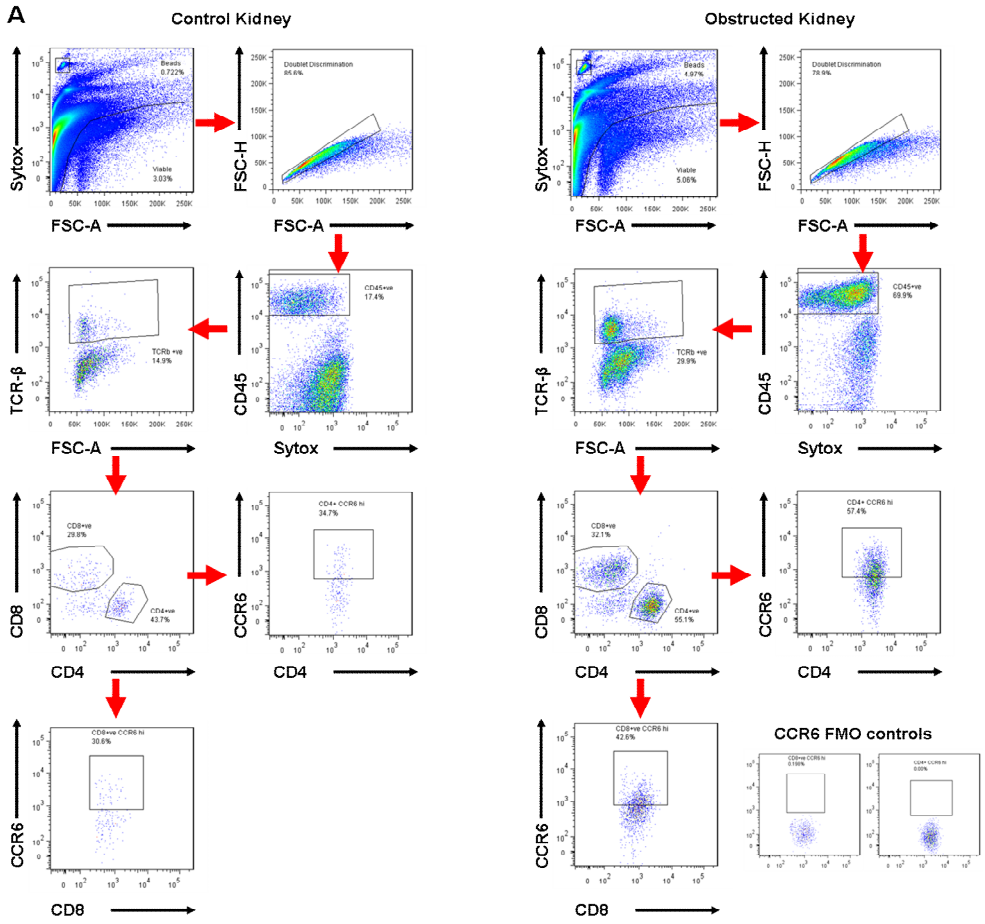
A
Control Kidney
Obstructed Kidney
Sytox
FSC-A
FSC-H
TCR-β
CD45
CD8
CD4
CCR6
CCR6 FMO controls

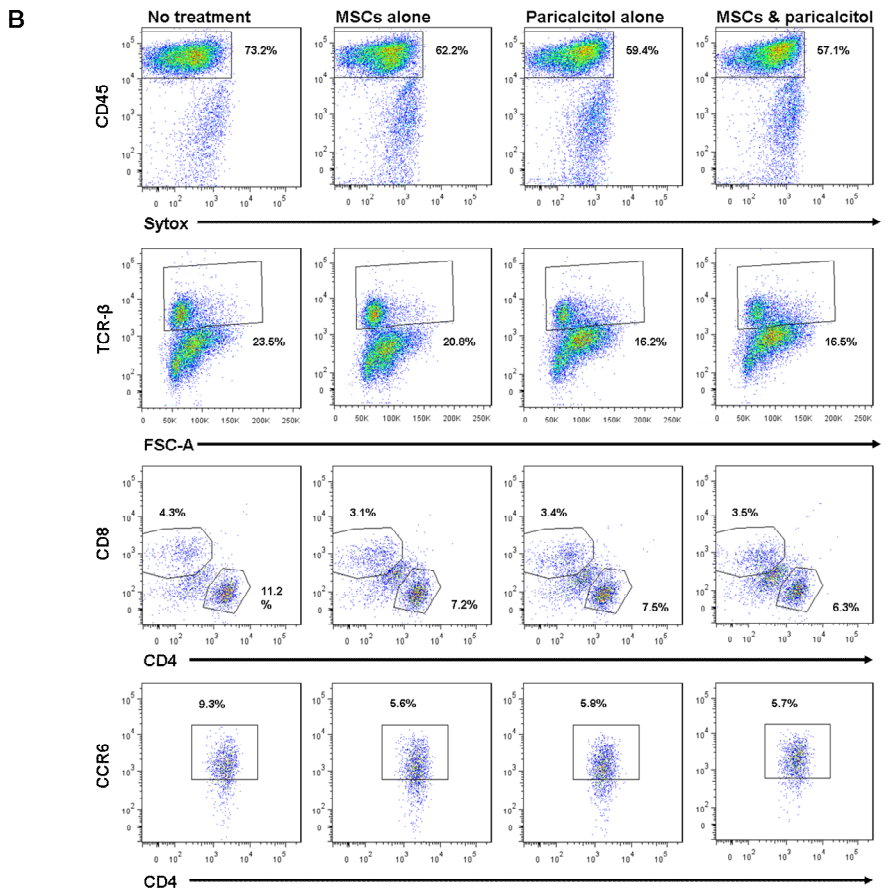
B
No treatment
MSCs alone
Paricalcitol alone
MSCs & paricalcitol
CD45
Sytox
TCR-β
FSC-A
CD8
CD4
CCR6
73.2%
62.2%
59.4%
57.1%
23.5%
20.8%
16.2%
16.5%
4.3%
11.2 %
3.1%
7.2%
3.4%
7.5%
3.5%
6.3%
9.3%
5.6%
5.8%
5.7%

Total leukocytes were significantly reduced (p = <0.01) in obstructed kidneys of MSC and paricalcitol double-treated mice at day 3 of analysis based on CD45 flow cytometric staining as compared with the no treatment group (**Figure 5.5A**). There was also a trend towards reduced $CD45^+$ cell accumulation in the obstructed kidneys of MSCs alone and paricalcitol alone groups albeit not significant. At day 8, paricalcitol treated mice had significantly less (p = <0.01) $CD45^+$ cell accumulation in obstructed kidneys than those receiving no treatment.

A similar trend occurred with TCR-β^+, $CD4^+$ and $CD8^+$ T-cells at day 3 following UUO in that each of these populations was significantly lower (p = 0.01, 0.01 and 0.05, respectively) in the obstructed kidneys of double-treated mice compared with the no treatment group (**Figure 5.5B, C & E**).

In a similar fashion, at day 8, TCR-β^+ and $CD4^+$ T-cells were significantly reduced (p = 0.05 and 0.01, respectively) in obstructed kidneys of paricalcitol treated mice compared to mice receiving no treatment. $CD8^+$ T-cells were unaffected at day 8.

CCR6 is a surrogate marker for Th17 cells (Chang et al., 2010a, Esplugues et al., 2011, Pindjakova et al., 2012). It is however, also expressed by T_{regs} (Turner et al., 2010b). At day 3 following UUO, the frequency of $CCR6^+$ $CD4^+$ T-cells was significantly lower (p = 0.01) in obstructed kidneys of double-treated mice compared to the no treatment group (**Figure 5.5D**). This was the first indication that Th17 cell accumulation may be modulated *in-vivo* in this model by MSCs and paricalcitol.

Figure 5.5 (overleaf) Flow cytometric analysis of T-cell populations following UUO: Non-treated, MSC-treated, paricalcitol-treated and double-treated B6 mice underwent UUO for 3 or 8 days after which time, control and obstructed kidneys were digested, single cell suspensions prepared and subjected to flow cytometry. Graphical representation of the percent of (**A**) $CD45^+$ cells, (**B**) TCR-β^+ cells, (**C**) $CD4^+$ cells, (**D**) $CD8^+$ cells and (**E**) $CCR6^+$ cells among viable cells (cells gated on $CD4^+$) (left: 3 days, right 8 days). Data are represented as control (○) and obstructed kidneys (□) from individual animals with n = 5 per group (Bonferroni posttest, * compared with equivalent control kidney group, ***** compared with equivalent no treatment group, * p = <0.05, ** p = <0.01, *** p = <0.001).

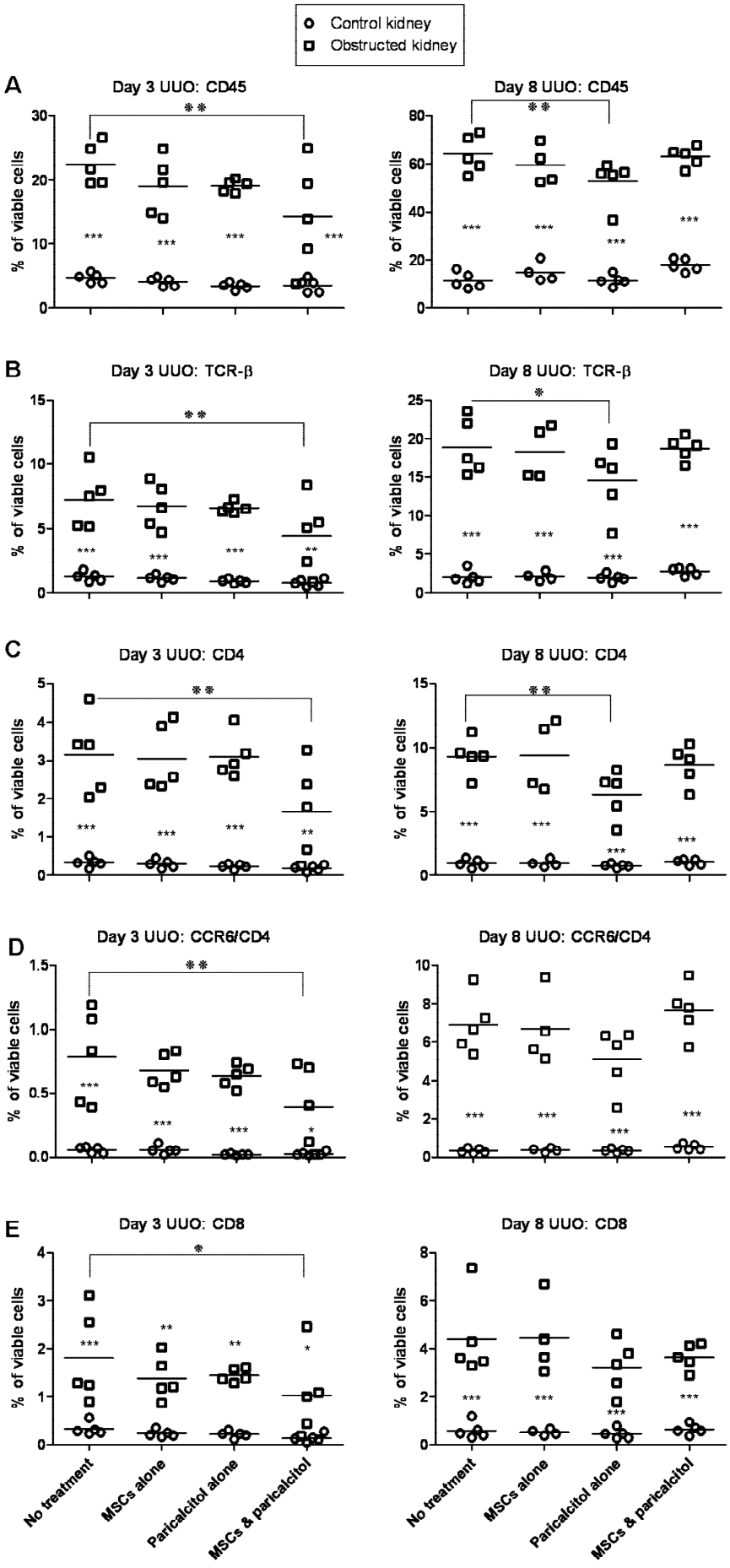
Control kidney
Obstructed kidney
A
Day 3 UUO: CD45
Day 8 UUO: CD45
B
Day 3 UUO: TCR-β
Day 8 UUO: TCR-β
C
Day 3 UUO: CD4
Day 8 UUO: CD4
D
Day 3 UUO: CCR6/CD4
Day 8 UUO: CCR6/CD4
E
Day 3 UUO: CD8
Day 8 UUO: CD8
% of viable cells
No treatment
MSCs alone
Paricalcitol alone
MSCs & paricalcitol

In order to quantify the proportion of T-cells that accumulated in the kidneys following UUO, IHC was employed. Analysis at day 8 following UUO showed that there were no significant differences between obstructed kidneys in any of the treatment groups compared to the no treatment group. However, the statistical significance ($p = <0.05$) detected in T-cell infiltrate between control and obstructed kidneys of untreated mice was lost in all treated groups (**Figure 5.6).**

Figure 5.6 (overleaf) $CD3^+$ cell accumulation in the kidney following UUO: Non-treated, MSC-treated, paricalcitol-treated and double-treated B6 mice underwent UUO for 8 days after which time, control and obstructed kidneys were subjected to anti-CD3 IHC. Ten non-overlapping fields throughout the superficial and deep cortex were examined blinded in sections stained with anti-CD3 at 20 X magnification. (**A**) Graphical representation of CD3 accumulation on day 8 based on Adobe Photoshop CS6 analysis (20 X). (**B**) Representative images of anti-CD3-stained kidney sections from control (left) and obstructed (right) kidneys on day 8 (20 X). Data are represented as control (○) and obstructed kidneys (□) from individual animals with n = 5 per group ((**B/C**) compared with equivalent control kidney group, Bonferroni posttest, * $p = <0.05$).

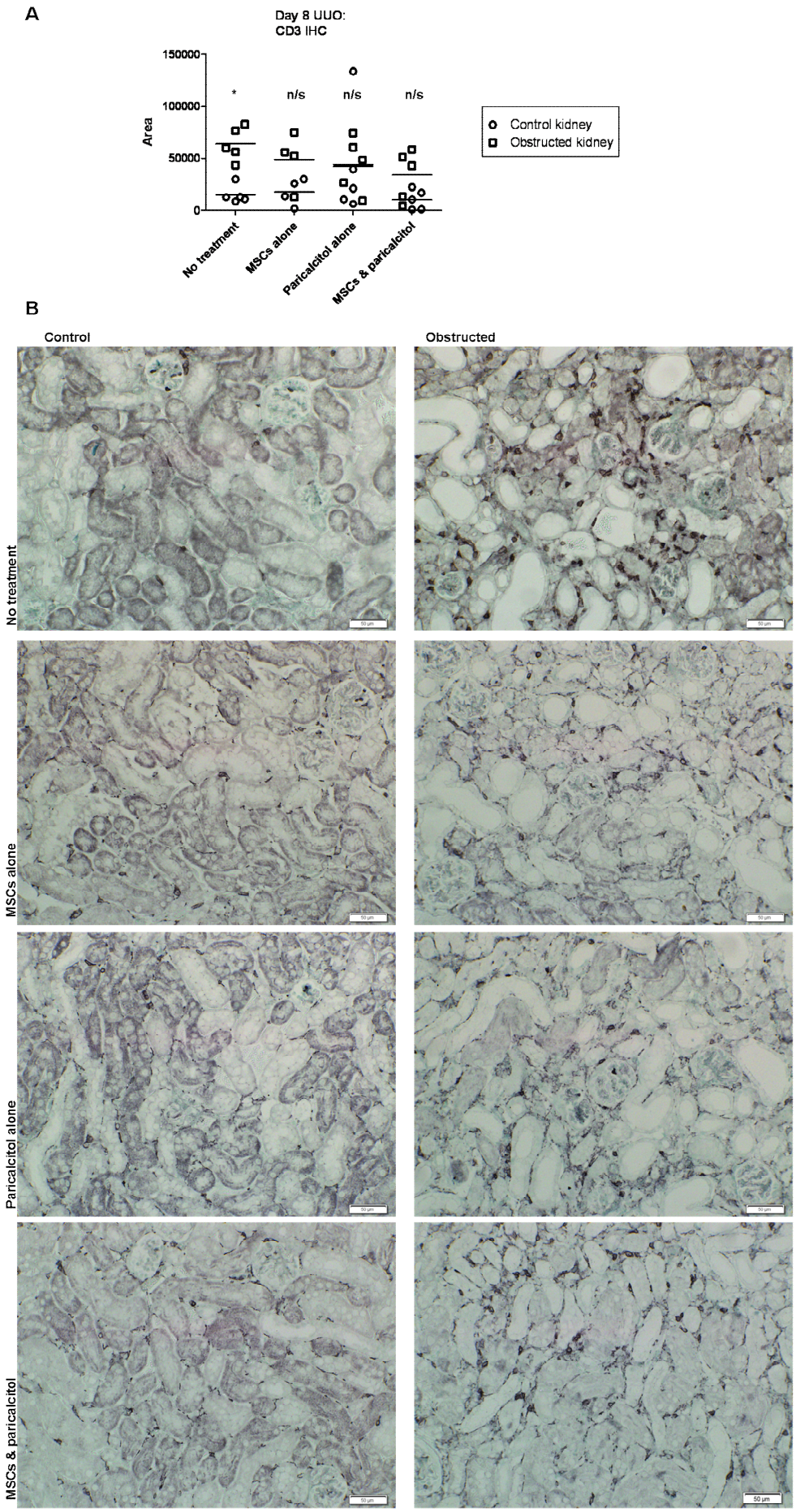
A
Day 8 UUO:
CD3 IHC
Area
150000
100000
50000
0
*
n/s
n/s
n/s
No treatment
MSCs alone
Paricalcitol alone
MSCs & paricalcitol
Control kidney
Obstructed kidney
B
Control
Obstructed
No treatment
MSCs alone
Paricalcitol alone
MSCs & paricalcitol

To examine the effects of MSCs and/or paricalcitol on Th17 cells *in-vivo* in this model, I elected to use qRT-PCR to measure IL-17A transcripts in control and obstructed kidneys at 3 and 8 days post UUO. Samples were normalized to GAPDH and expressed as fold change relative to a control kidney in which low levels of IL-17A were detectable.

Mice that received both MSCs and paricalcitol had a significant reduction ($p = <0.05$) in detectable IL-17A in obstructed kidneys compared to the no treatment group at the same time-point (**Figure 5.7A**). Obstructed kidneys from mice that were administered paricalcitol alone or a combination of paricalcitol and MSCs did not express significantly different levels of IL-17A compared to their respective control kidneys. IL-17A was not detectable at the 8 day time-point (data not shown).

In a similar manner, FOXP3 expression was significantly reduced in obstructed kidneys of paricalcitol alone and MSC and paricalcitol double-treated mice compared to the no treatment group at 3 ($p = <0.001$) and 8 ($p = <0.01$) days post UUO (**Figure 5.7B/C**). There was a non-significant trend towards reduced FOXP3 expression in obstructed kidneys of MSC alone treated mice at day 8.

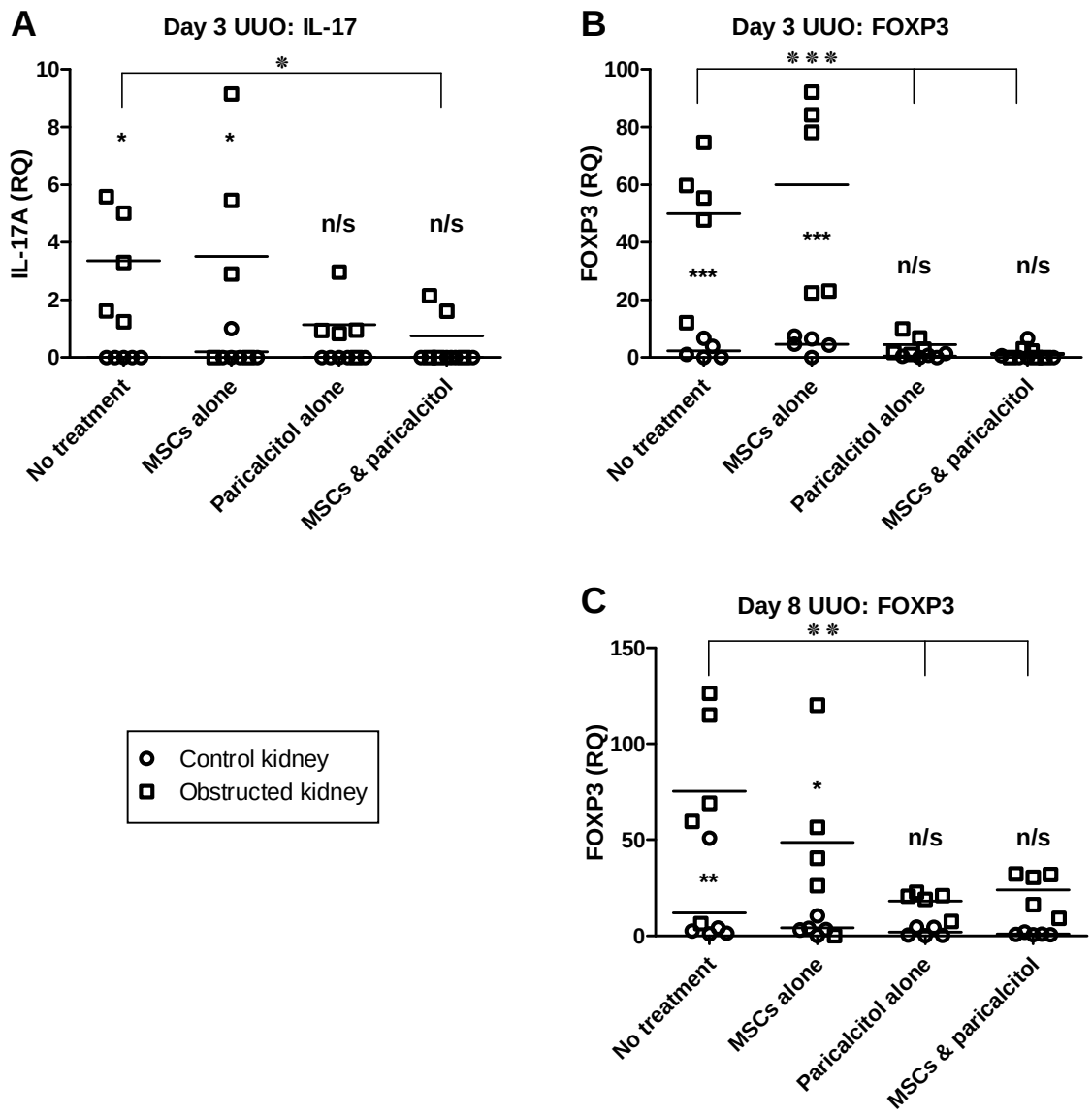

Figure 5.7 IL-17A and FOXP3 expression following UUO: Non-treated, MSC-treated, paricalcitol-treated and double-treated B6 mice underwent UUO for 3 days after which time, RNA was extracted from control and obstructed kidney tissue, cDNA was synthesized and samples subjected to qRT-PCR. (**A**) Relative quantification of IL-17A in control and obstructed kidneys at day 3. (**B**) Relative quantification of FOXP3 in control and obstructed kidneys at day 3. (**C**) Relative quantification of FOXP3 in control and obstructed kidneys at day 8. Data are represented as control (○) and obstructed kidneys (□) from individual animals with n = 5 per group. (Bonferroni posttest, * compared with no treatment group, * compared with equivalent control kidney group, * p = <0.05, ** p = <0.01, *** p = <0.001).

Intracellular IL-17A flow cytometric staining was also performed at day 3 to confirm the effect of MSCs and/or paricalcitol on Th17 cell accumulation in the obstructed kidneys at this time-point. Obstructed kidneys were dissected at day 3 following UUO, digested and single cell suspensions prepared. Cells were CD45 MACS-enriched and control or obstructed kidneys from individual mice from each group were pooled together in order to have enough cells for this technique. $CD45^+$ cells were stimulated for 8 hours with brefeldin A and low dose anti-CD3ε (0.1 μg/ml) prior to intracellular staining for IL-17A and IFN-γ.

The frequency of IL-17A-producing $CD4^+$ T-cells was significantly lower in all treatment groups compared to the no treatment group (MSCs alone $p = <0.001$, paricalcitol alone $p = <0.01$, MSCs and paricalcitol $p = <0.05$) however, there were no significant differences detected between the 3 treatment groups (**Figure 5.8A/B**). The frequency of IFN-γ-producing cells was not significantly affected by MSCs or paricalcitol at 3 days following UUO (**Figure 5.8C/D**).

Based on the above T-cell experiments, I concluded that double administration of MSCs and paricalcitol attenuated overall early (day 3) T-cell accumulation in the obstructed kidney following UUO and was associated with reduced Th17 activity within the kidney at the same time point. Administration of either MSCs or paricalcitol alone may also suppress intra-renal Th17 activity in UUO although these findings were less convincing.

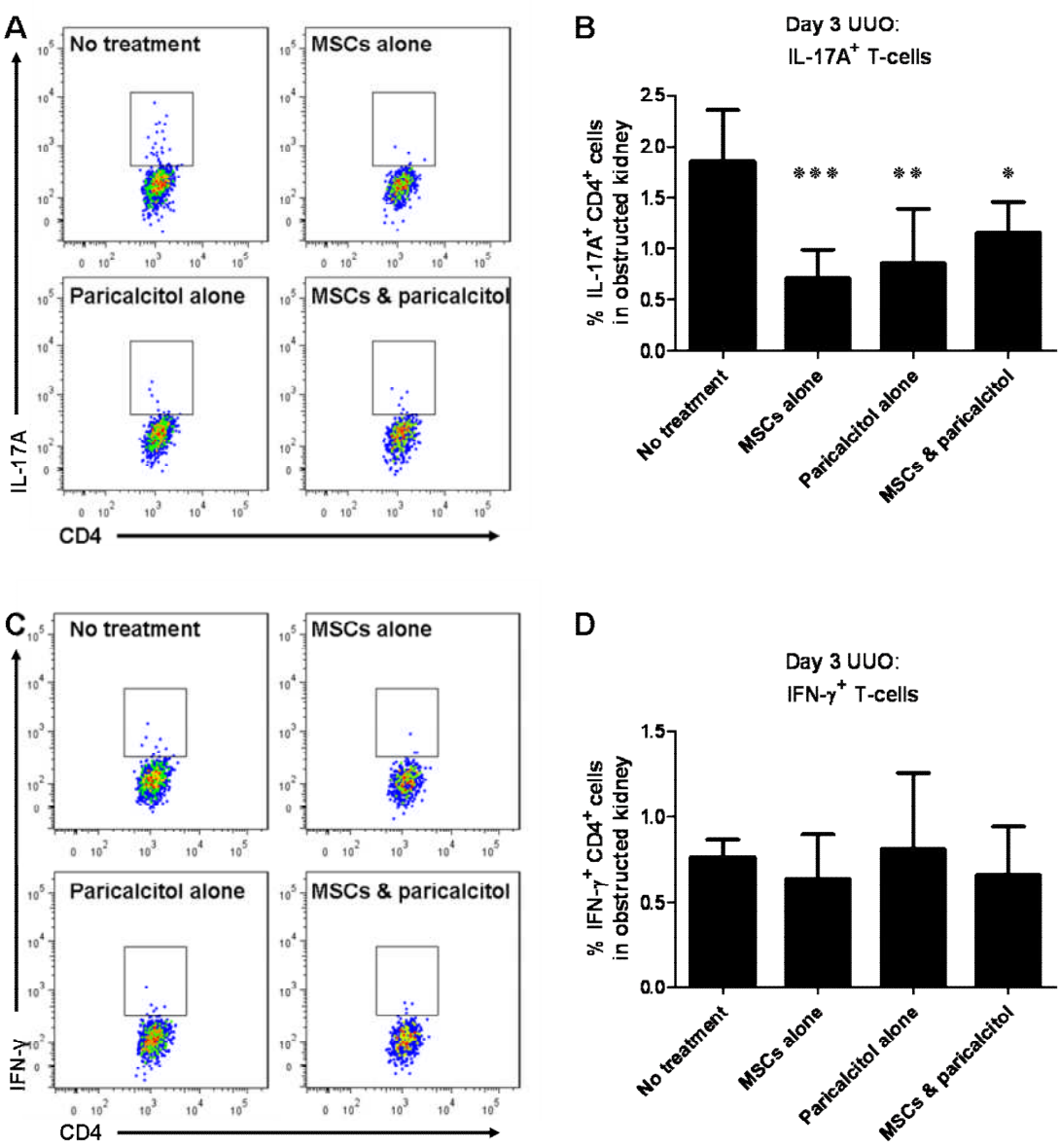

Figure 5.8 IL-17A- and IFN-γ-producing T-cell accumulation in the kidney following UUO: Non-treated, MSC-treated, paricalcitol-treated and double-treated B6 mice underwent UUO for 3 days after which time, obstructed kidneys were digested, single cell suspensions prepared and subjected to intracellular cytokine analysis by flow cytometry (**A**) Representative dot plots of IL-17A$^+$ cells among cells gated on CD4$^+$ (**B**) Graphical representation of the percent of IL-17A$^+$ cells. (**C**) Representative dot plots of IFN-γ$^+$ cells among cells gated on CD4$^+$. (**D**) Graphical representation of the percent of IFN-γ$^+$ cells. Data are represented as mean +/- standard deviations from 6-9 pooled replicates. (Bonferroni posttest, * p = <0.05, ** p = <0.01, *** p = <0.001 compared with no treatment group).

In addition to T-cell populations, I also examined myeloid cell distribution in the kidneys following UUO by multi-colour flow cytometry given that both MSCs and calcitriol have been reported to inhibit APC maturation, cytokine production and antigen presentation (Griffin et al., 2003, Griffin et al., 2010, Mora et al., 2008). As shown in **Figure 5.9**, initial gating on viable cells alone was followed by doublet discrimination. The pan myeloid marker, CD11b was then used to discriminate myeloid cells followed by analysis of neutrophils ($Ly6G^+$), DCs ($CD11c^+$), inflammatory monocytes ($Ly6C^+$ $F4/80^+$) and macrophages ($Ly6C^-$ $F4/80^+$). At day 8 post UUO, macrophages were further categorized into M1 pro-inflammatory or M2 anti-inflammatory macrophages using CD206 to discriminate between the two phenotypes (Kushiyama et al., 2011). Data are represented as percent positive of total viable cells.

Figure 5.9 (overleaf) (A) Representative gating strategies of myeloid cell populations in control and obstructed kidneys following UUO and **(B)** representative examples of dot plots for $CD11b^+$ myeloid cells, $Ly6G^+$ neutrophils, $CD11c^+$ DCs, $Ly6C^+$ inflammatory monocytes and $Ly6C^-$ macrophage populations in obstructed kidneys for each of the treatment groups.

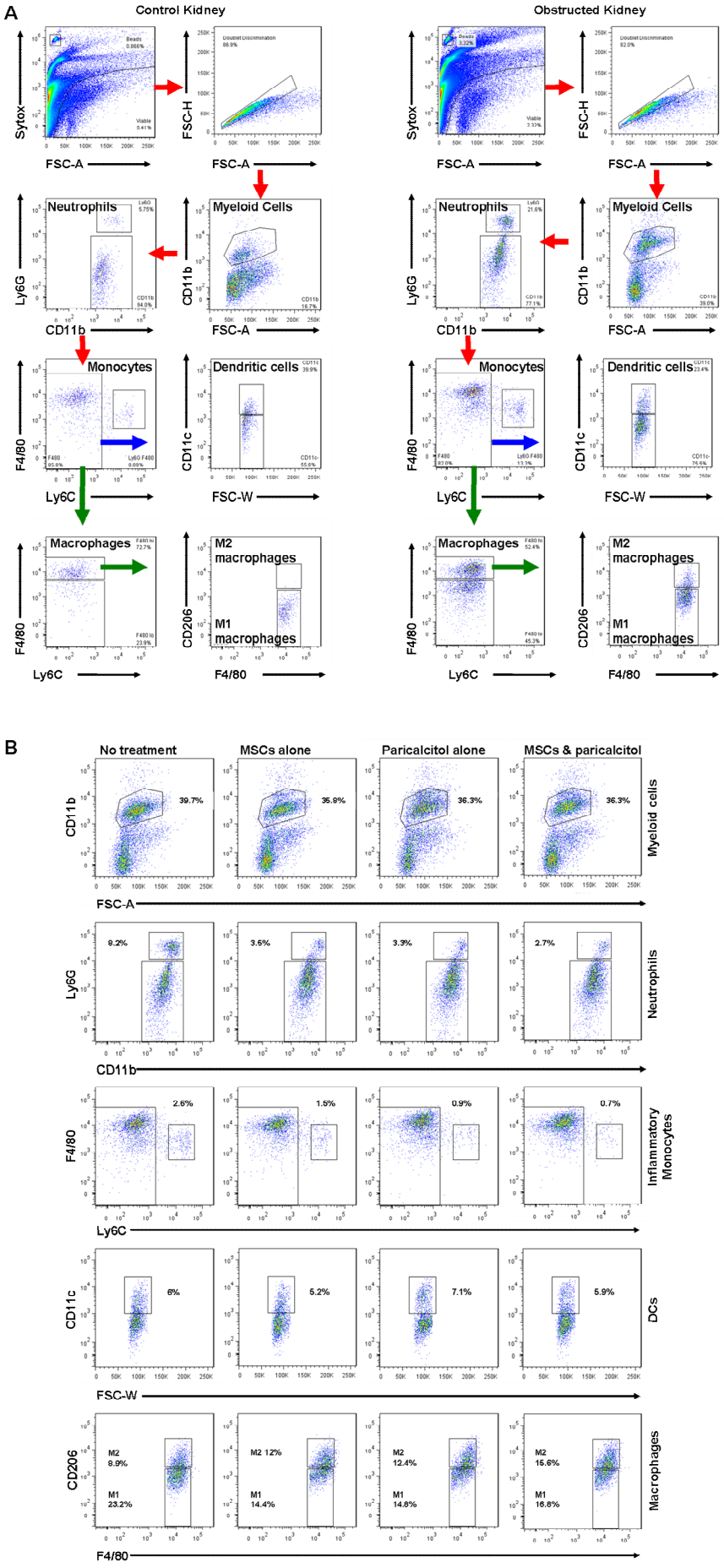
A
Control Kidney
Obstructed Kidney
Sytox
FSC-A
FSC-H
Neutrophils
Myeloid Cells
Ly6G
CD11b
Monocytes
Dendritic cells
F4/80
Ly6C
CD11c
FSC-W
Macrophages
M2 macrophages
M1 macrophages
CD206
B
No treatment
MSCs alone
Paricalcitol alone
MSCs & paricalcitol
39.7%
35.8%
36.3%
36.3%
Myeloid cells
9.2%
3.6%
3.3%
2.7%
Neutrophils
2.6%
1.5%
0.9%
0.7%
Inflammatory Monocytes
6%
5.2%
7.1%
5.9%
DCs
M2 9.9%
M1 23.2%
M2 12%
M1 14.4%
M2 12.4%
M1 14.8%
M2 15.6%
M1 16.8%
Macrophages

As shown in **Figure 5.10A**, the overall frequency of myeloid cells was significantly reduced ($p = <0.01$) in obstructed kidneys of double-treated mice compared to the no treatment group. However, by day 8 post UUO, there were no significant differences between the groups.

Looking at individual populations more specifically, I detected significantly less ($p = 0.05$) neutrophils in the obstructed kidneys of double-treated mice compared to mice that received no treatment (**Figure 5.10B**). At day 8, all three treatment groups had significantly lower frequencies of neutrophils than the no treatment group (MSCs alone $p = <0.01$, paricalcitol alone $p = <0.05$, MSCs and paricalcitol $p = <0.001$). This may be a result of reduced Th17 accumulation in the obstructed kidneys following administration of MSCs and/or paricalcitol as Th17 cells are reported to recruit neutrophils to injured kidneys (Kitching and Holdsworth, 2011).

The proportion of DCs was unaffected by MSCs and/or paricalcitol in obstructed kidneys at day 3 post UUO (**Figure 5.10C**). By day 8, the frequency of DCs in obstructed kidneys was significantly greater ($p = <0.05$) in paricalcitol treated mice than the no treatment group.

The frequency of inflammatory monocytes was significantly lower ($p = 0.01$) in double-treated mice compared to mice receiving no treatment at both day 3 and day 8 (**Figure 5.10D**). I observed a non-significant trend towards reduced inflammatory monocyte accumulation in MSC single treated and paricalcitol single treated obstructed kidneys at both time-points.

Overall macrophage accumulation was not significantly affected by MSCs or paricalcitol (**Figure 5.10E**) however, in examining macrophage phenotypes at day 8, I detected a significantly lower proportion ($p = <0.01$) of M1 macrophages ($CD206^-/F4/80^+/CD11b^+Ly6C^-$) in obstructed kidneys of paricalcitol treated mice with a trend towards reduced M1 macrophages in MSC single treated and MSC and paricalcitol double-treated mice compared with the no treatment group (**Figure 5.10F**). The reduction of M1 macrophages was paralleled by a significant increase ($p = <0.01$) in M2 macrophage ($CD206^+/F4/80^+/CD11b^+Ly6C^-$) accumulation in obstructed kidneys of double-treated mice compared to the no treatment group.

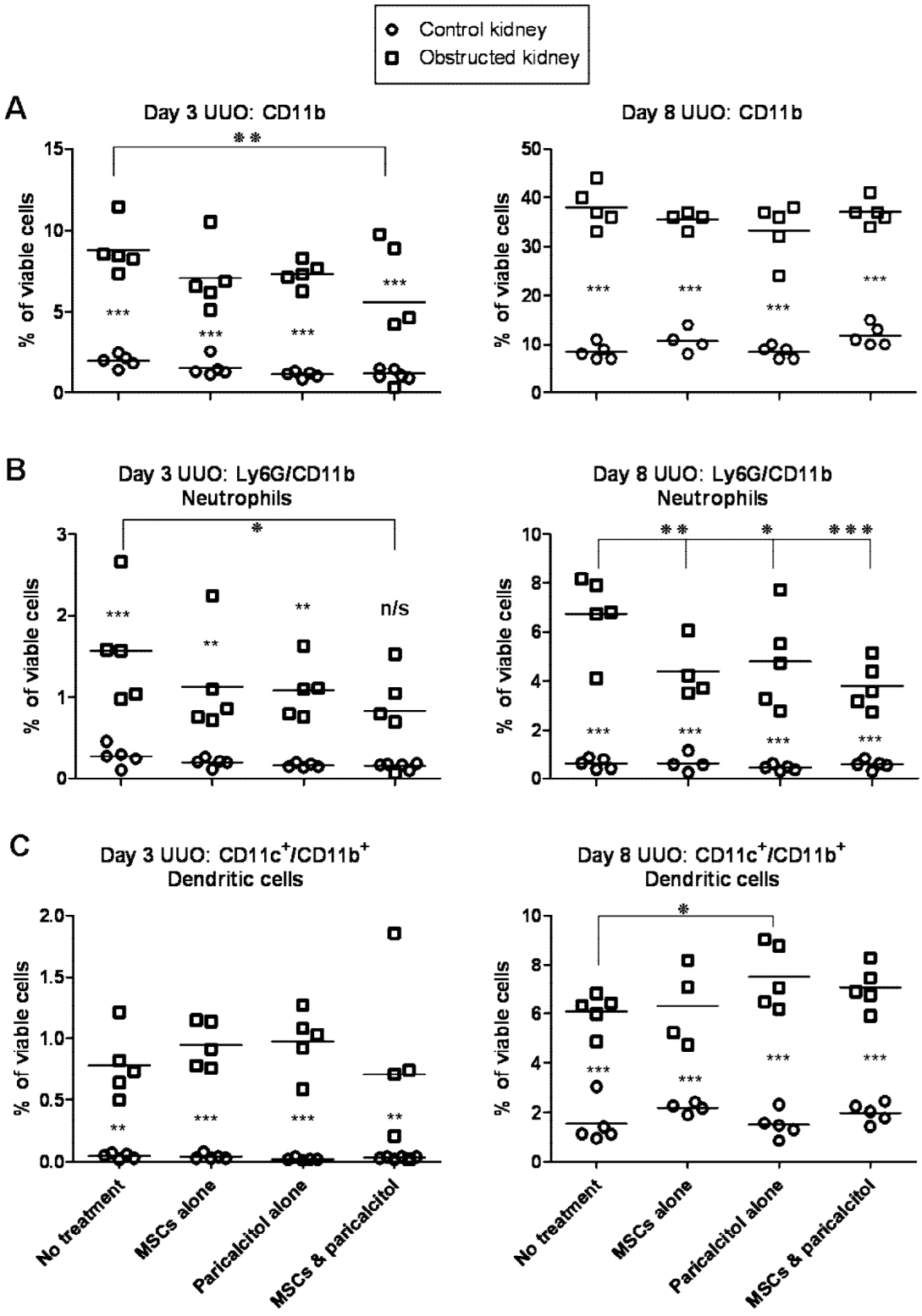
Control kidney
Obstructed kidney
A
Day 3 UUO: CD11b
Day 8 UUO: CD11b
% of viable cells
B
Day 3 UUO: Ly6G/CD11b
Neutrophils
Day 8 UUO: Ly6G/CD11b
Neutrophils
n/s
C
Day 3 UUO: CD11c+/CD11b+
Dendritic cells
Day 8 UUO: CD11c+/CD11b+
Dendritic cells
No treatment
MSCs alone
Paricalcitol alone
MSCs & paricalcitol

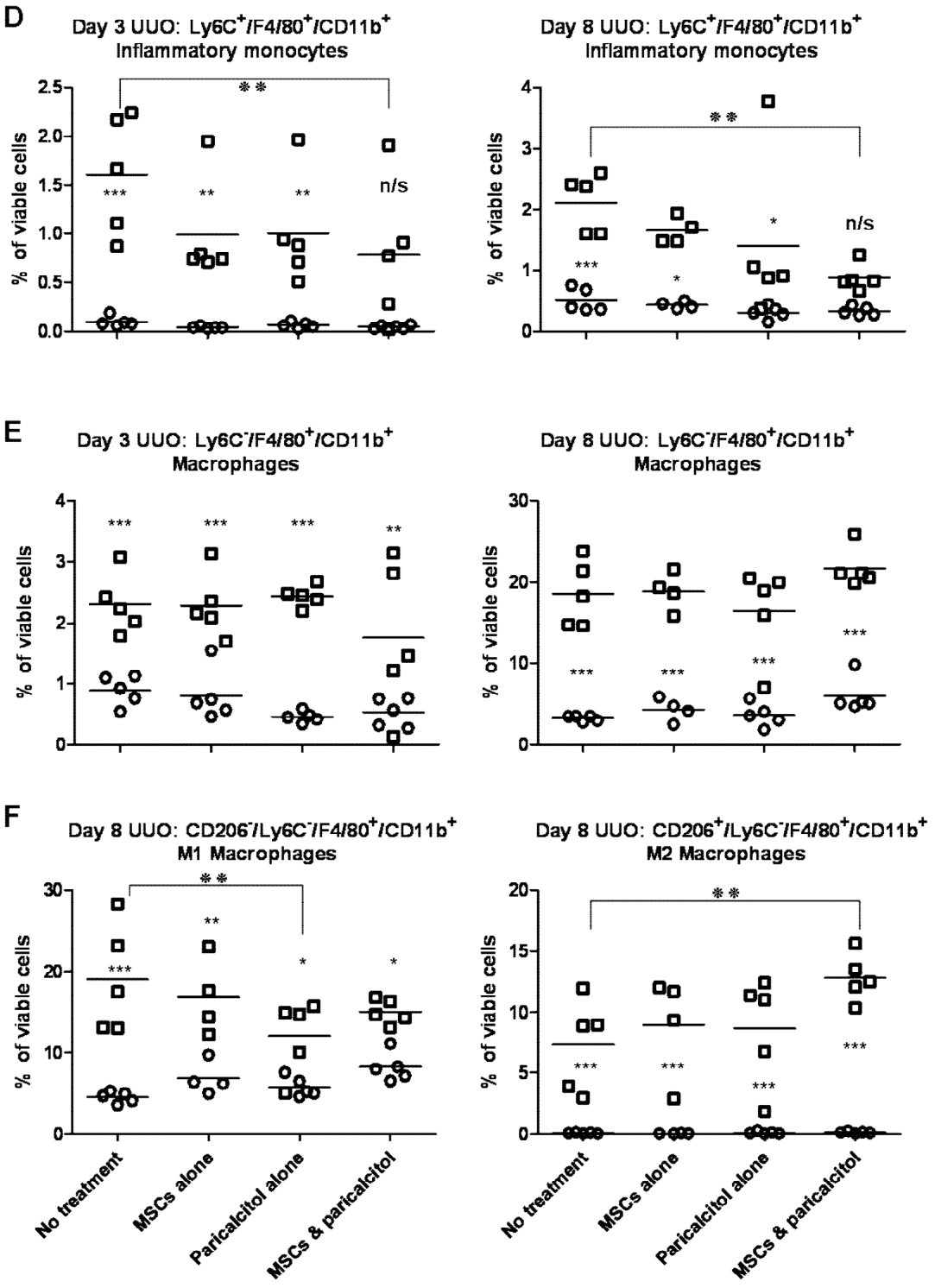

Figure 5.10 Flow cytometric analysis of myeloid populations following UUO: Non-treated, MSC-treated, paricalcitol-treated and double-treated B6 mice underwent UUO for 3 or 8 days after which, control and obstructed kidneys were digested, single cell suspensions prepared and subjected to flow cytometry. Graphical representation of the percent of (**A**) myeloid cells, (**B**) neutrophils, (**C**) inflammatory monocytes, (**D**) DCs, (**E**) macrophages (left: 3 days, right 8 days) and (**F**) M1 (left) and M2 (right) macrophages among viable cells on day 8. Data are represented as control (○) and obstructed kidneys (□) from individual animals with n = 5 per group (Bonferroni posttest, * compared with equivalent control kidney group, * compared with equivalent no treatment group, * p = <0.05, ** p = <0.01, *** p = <0.001).

Thus, from this series of experiments I concluded that, although MSC and/or paricalcitol administration did not have a dramatic effect overall on the proportion of myeloid cell accumulation following UUO, both MSCs and paricalcitol significantly affected the ratio of myeloid cell phenotypes within the $CD11b^+$ population. Potentially tissue destructive populations including neutrophils, inflammatory monocytes and M1 macrophages were reduced while anti-inflammatory M2 macrophages were increased following administration of MSCs or paricalcitol to mice that underwent UUO. This effect was particularly evident in MSC and paricalcitol double-treated mice.

In order to examine the impact of MSCs and/or paricalcitol on overall kidney structure at day 8, a number of histological staining techniques were performed on sections of control and obstructed kidneys with analyses by semi-quantitative, blinded scoring of stained tissue sections.

Analysis of PAS-stained kidney sections revealed that total cellular infiltrate at a gross histological level was not suppressed in obstructed kidneys by MSC and/or paricalcitol administration at day 8 post UUO (**Figure 5.11**).

Figure 5.11 (overleaf) Cellular infiltrate following UUO: Non-treated, MSC-treated, paricalcitol-treated and double-treated B6 mice underwent UUO for 8 days after which time, control and obstructed kidneys were subjected to PAS staining. Ten non-overlapping fields throughout the superficial and deep cortex were examined blinded at 20 X magnification for symptoms of cellular infiltration according to (**A**). (**B**) Graphical representation of cellular infiltration scores on day 8 (20 X). (**C**) Representative images of PAS-stained kidney sections from control (left) and obstructed (right) kidneys on day 8 (20 X). Data are represented as control (○) and obstructed kidneys (□) from individual animals with n = 5 per group (Bonferroni posttest, * compared with equivalent control kidney group, * compared with no treatment group, * p = <0.05, ** p = <0.01,*** p = <0.001).

A

Percent of field	Score
<3 %	1
3-10 %	2
10-25 %	3
>25 %	4

B

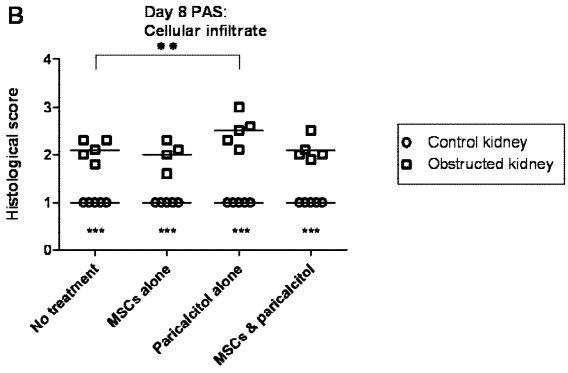

C

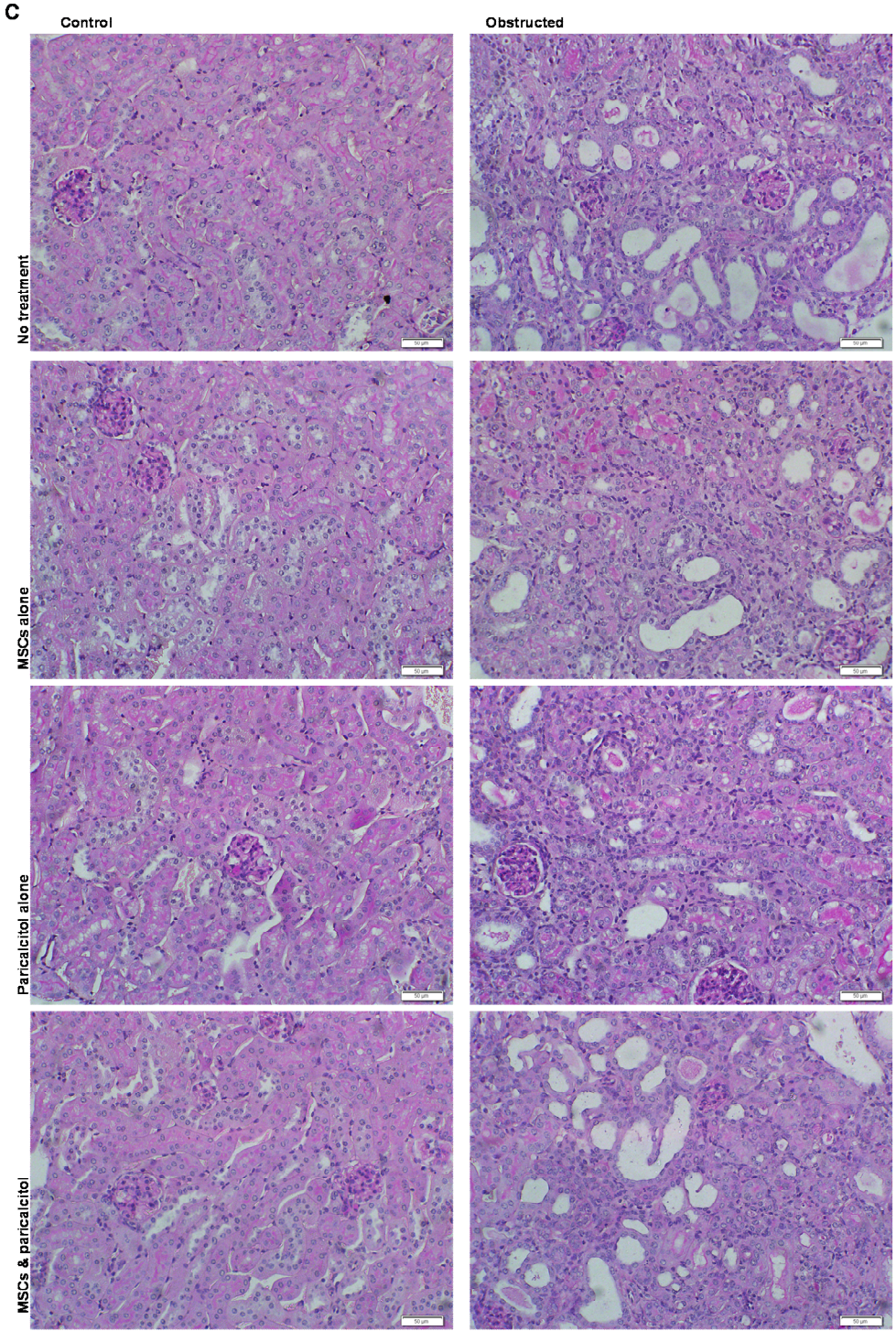

Examination of tubular atrophy and dilation in obstructed kidneys by H & E staining at day 8 revealed that obstructed kidneys from double-treated mice displayed significantly lower scores ($p = <0.05$) for atrophy and dilation than equivalent no treatment mice (**Figure 5.12**) suggesting that MSC and paricalcitol administration attenuated kidney damage. A non-significant trend towards reduced tubular atrophy and dilation was observed with both single agent treatments.

Figure 5.12 (overleaf) Dilation and atrophy of tubules following UUO: Non-treated, MSC-treated, paricalcitol-treated and double-treated B6 mice underwent UUO for 8 days after which, control and obstructed kidneys were formalin fixed, processed, wax embedded, sectioned and subjected to H & E staining. Ten non-overlapping fields throughout the superficial and deep cortex were examined blinded at 20 X magnification for symptoms of atrophy and dilation according to (**A**). (**B**) Graphical representation of atrophy and dilation scores on day 8 (20 X). (**C**) Representative images of H & E-stained kidney sections from control (left) and obstructed (right) kidneys (20 X). Data are represented as control (○) and obstructed kidneys (□) from individual animals with n = 5 per group (Bonferroni posttest, * compared with equivalent control kidney group, ⁕ compared with no treatment group, * $p = <0.05$, ** $p = <0.01$,*** $p = <0.001$).

A

Percent of field	Score
< 10%	1
10-25 %	2
25-50 %	3
> 50%	4

B

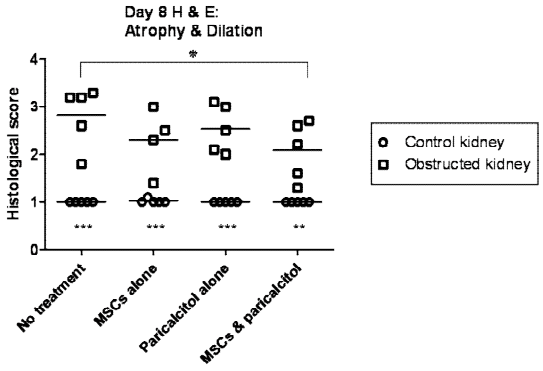

C

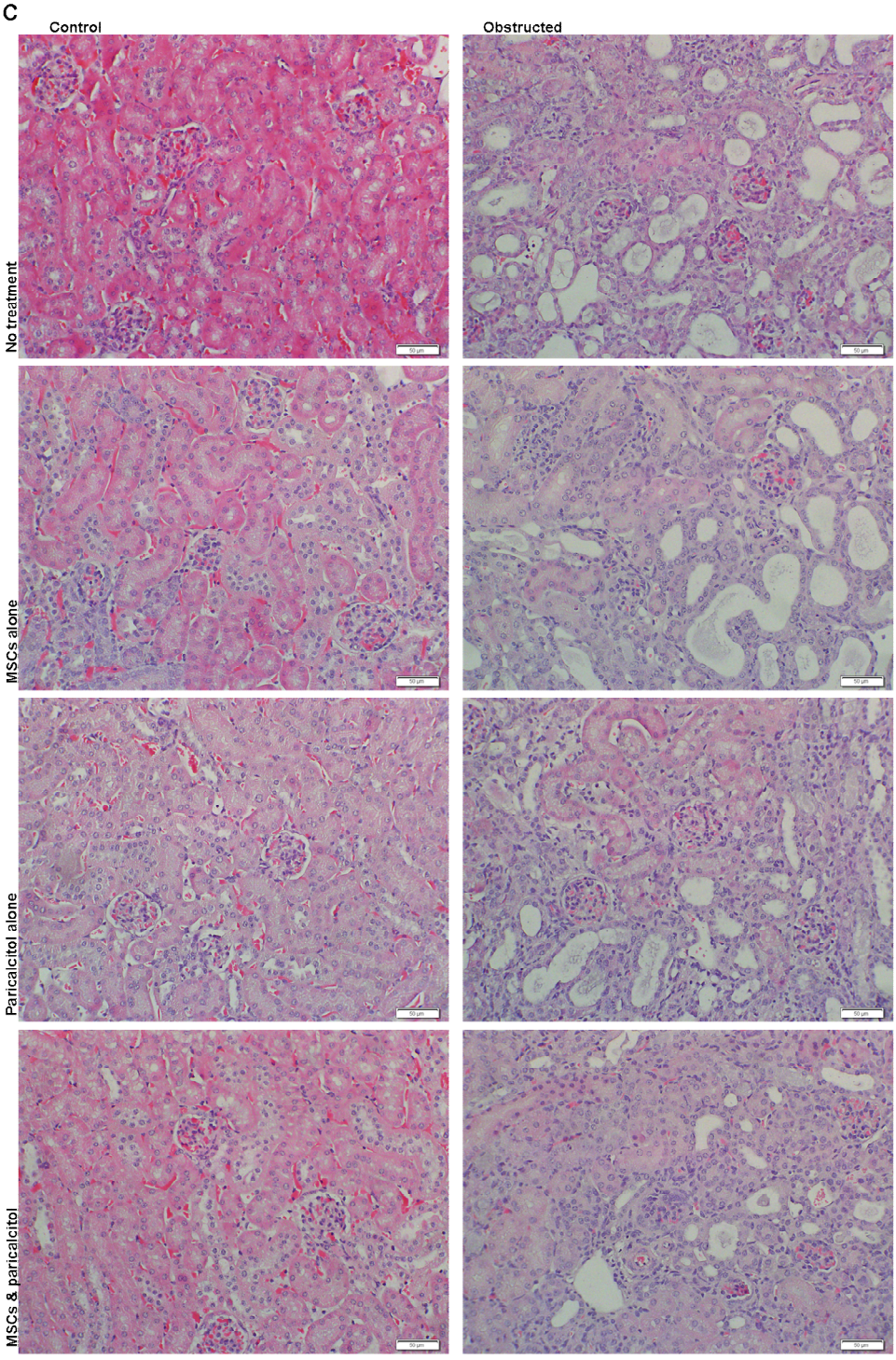

Late stage UUO is characterized by induction of fibrosis. For this reason I elected to determine the effect of MSCs and/or paricalcitol on collagen deposition in this model using Masson's Trichrome staining of day 8 control and obstructed kidneys.

Mice treated with both MSCs and paricalcitol had significantly lower ($p = <0.01$) interstitial fibrosis scores in obstructed kidneys than those in the no treatment group (**Figure 5.13**). Furthermore, obstructed kidneys in the no treatment group had significantly greater ($p = <0.001$) interstitial fibrosis compared to equivalent control kidneys however control and obstructed kidneys from all three treatment groups were not significantly different from each other.

This series of histological analyses led me to conclude that co-administeration of MSCs and paricalcitol protected from kidney damage in terms of tubular atrophy and dilation and interstitial fibrosis.

Figure 5.13 (overleaf) Interstitial fibrosis following UUO: Non-treated, MSC-treated, paricalcitol-treated and double-treated B6 mice underwent UUO for 8 days which, control and obstructed kidneys were subjected to Masson's Trichrome staining. Ten non-overlapping fields throughout the superficial and deep cortex were examined in sections stained with Masson's Trichrome at 20 X magnification according to (**A**). (**B**) Graphical representation of interstitial fibrosis scores based on Masson's Trichrome staining (20 X). (**C**) Representative images of Masson's Trichrome-stained kidney sections from control (left) and obstructed (right) kidneys (20 X). Data are represented as control (○) and obstructed kidneys (□) from individual animals with n = 5 per group (Bonferroni posttest, * compared with equivalent control kidney group, * compared with no treatment group, * p = <0.05, ** p = <0.01,*** p = <0.001).

A

Percent of field	Score
<3 %	1
3-10 %	2
10-25 %	3
>25 %	4

B

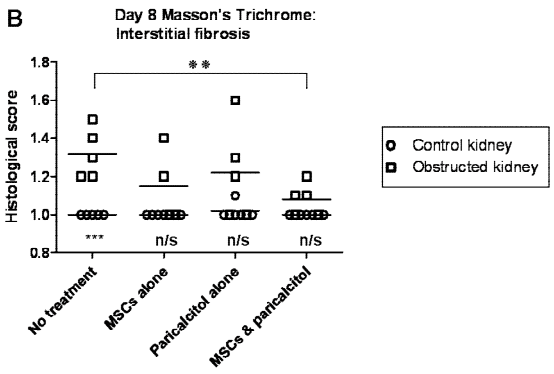

C

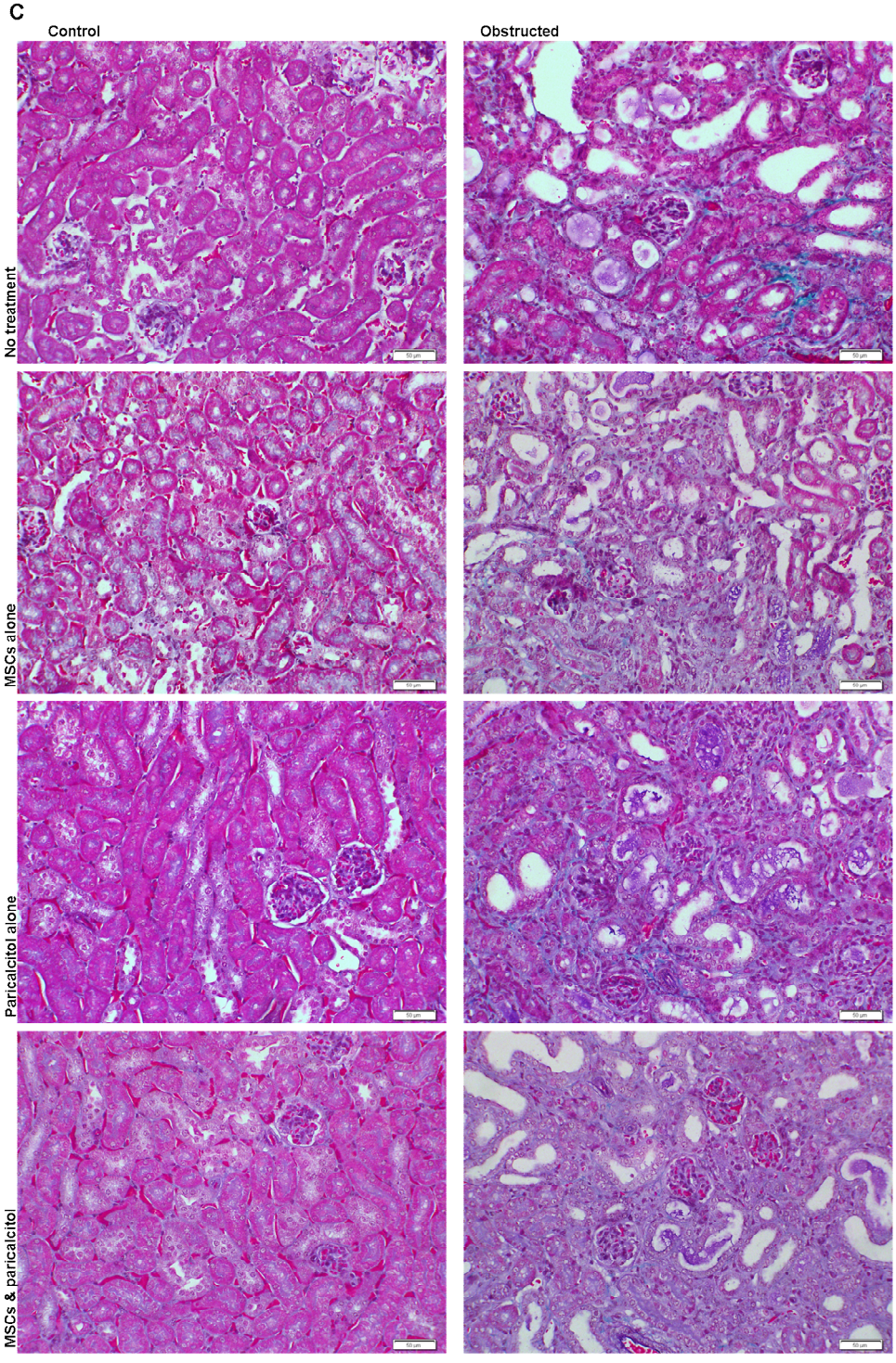

Overall histological scores on day 8 (cellular infiltrate, atrophy/dilation and collagen deposition) were significantly reduced (p = <0.01) in MSC and paricalcitol double-treated mice (**Figure 5.14B**). This was largely attributable to reduced tubular atrophy and dilation in this group of animals.

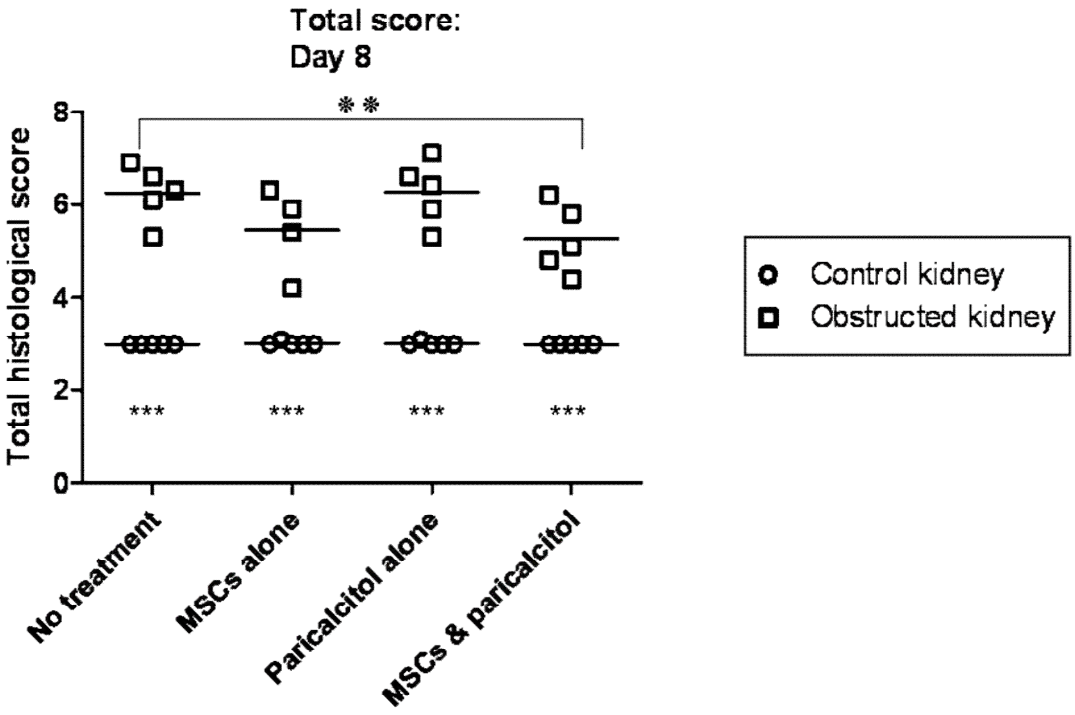

Figure 5.14 Total histological scores following UUO: Graphical representation of total histological scores at day 8 based on H & E, PAS and Masson's Trichrome staining (20 X). Data are represented as control (○) and obstructed kidneys (□) from individual animals with n = 5 per group (Bonferroni posttest, * compared with equivalent control kidney group, * compared with equivalent no treatment group, ** p = <0.01, *** p = <0.001).

In conclusion, MSC and/or paricalcitol treatment of mice with UUO did not have a dramatic effect on total cellular infiltrate however double-treated mice displayed significantly lower proportions of T-cells including IL-17-producing $CD4^+$ T-cells, inflammatory monocytes, neutrophils and M1 macrophages with a concomitant increase in M2 macrophages. This was associated with reduced interstitial fibrosis and tubular atrophy and dilation.

Table 5.2 Summary of *in-vivo* results

	Versus no treatment obstructed kidneys.			*Versus equivalent control kidneys.*			
Day 3 UUO	**MSCs**	**Paricalcitol**	**MSCs and paricalcitol**	**No treatment**	**MSCs**	**Paricalcitol**	**MSCs and paricalcitol**
Flow Cytometry							
$CD45^+$ cells	n/s	n/s	**	***	***	***	***
TCR-β^+ cells	n/s	n/s	**	***	***	***	**
$CD4^+$ cells	n/s	n/s	**	***	***	***	**
$CCR6^+$ $CD4^+$ cells	n/s	n/s	**	***	***	***	*
$CD8^+$ cells	n/s	n/s	*	***	**	**	*
Myeloid cells	n/s	n/s	**	***	***	***	***
Neutrophils	n/s	n/s	*	***	**	**	*n/s*
DCs	n/s	n/s		**	***	***	**
Inflammatory monocytes	n/s	n/s	**	***	**	**	*n/s*
Macrophages	n/s	n/s	n/s	***	***	***	**
qRT-PCR							
IL-17A	n/s	n/s	*	ND	ND	ND	ND
FOXP3	n/s	***	***	ND	ND	ND	ND
Intracellular Flow Cytometry							
IL-17A	***	**	*	*	*	*n/s*	*n/s*
IFN-γ	n/s	n/s	n/s	***	***	*n/s*	*n/s*

Day 8 UUO	**MSCs**	**Paricalcitol**	**MSCs and paricalcitol**	**No treatment**	**MSCs**	**Paricalcitol**	**MSCs and paricalcitol**
Flow Cytometry							
$CD45^+$ cells	n/s	**	n/s	***	***	***	***
TCR-β^+ cells	n/s	*	n/s	***	***	***	***
$CD4^+$ cells	n/s	**	n/s	***	***	***	***
$CCR6^+$ $CD4^+$ cells	n/s	n/s	n/s	***	***	***	***
$CD8^+$ cells	n/s	n/s	n/s	***	***	***	***
Myeloid cells	n/s	n/s	n/s	***	***	***	***
Neutrophils	**	*	***	***	***	***	***
DCs	n/s	*	n/s	***	***	***	***
Inflammatory monocytes	n/s	n/s	**	***	*	*	*n/s*
Macrophages	n/s	n/s	n/s	***	***	***	***
M1 macrophages	n/s	**	n/s	***	**	*	*
M2 macrophages	n/s	n/s	**	***	***	***	***
IHC							
$CD3^+$	n/s	n/s	n/s	*	*n/s*	*n/s*	*n/s*
Histology							
Cellular infiltrate	n/s	**	n/s	***	***	***	***
Atrophy and dilation	n/s	n/s	*	***	***	***	**
Collagen deposition	n/s	n/s	**	***	*n/s*	*n/s*	*n/s*
Total score	n/s	n/s	**	***	***	***	***

All significant differences represent a reduction compared to reference sample unless otherwise illustrated in red.

p = <0.05 */*, p = <0.01 **/**, p = <0.001 ***/***.

5.4 DISCUSSION

This study represents the first time that the combined effects of a VDR agonist and MSCs have been examined for combined immunomodulatory effects in an *in-vivo* setting. The extensive multi-colour flow cytometric analysis of infiltrating inflammatory cells was also novel to the fields of MSC and paricalcitol therapy for obstructive nephropathy in UUO.

5.4.1 EFFECTS OF MSCS AND PARICALCITOL ON TH17 RESPONSES

As highlighted in **Table 5.2**, MSC monotherapy was associated with reduced IL-17A expression and neutrophil recruitment in the obstructed kidney at day 3. Paricalcitol monotherapy also had suppressive effects on IL-17A expression as well as on T-cell, monocyte and M1 macrophage recruitment. However, the combination of MSCs and paricalcitol more clearly modulated all early inflammatory cell parameters measured and this was associated with evidence of reduced kidney damage at day 8.

5.4.2 EFFECTS OF MSCS IN UUO

This was the first study to examine the effects of MSCs in a mouse model of UUO. In contrast to the studies of UUO in rats by Liu et al. and Asanuma et al., I did not detect significant differences in interstitial fibrosis at day 8 following UUO with MSC mono-therapy (**Figure 5.13**). This may relate to species differences or to the delivery route of MSCs as, in the other reported studies, MSCs were administered *via* the inferior vena cava and directly *via* the renal artery respectively (Liu et al., 2012, Asanuma et al., 2011). Liu et al. reported that by day 14 following UUO, MSCs did not have a significant suppressive effect on collagen deposition (Liu et al., 2012) highlighting the potential for combination therapies to complement the effects of MSCs in this model.

Macrophage recruitment to the obstructed kidney was inhibited following administration of MSCs in rat UUO (Liu et al., 2012) however I did not detect a significant reduction in the overall proportion of macrophages (**Figure 5.10E**). However, $Ly6G^{+}$ neutrophils were significantly reduced following MSC mono-therapy (**Figure 5.10B**) which may be a result of suppressed Th17 responses (**Figures 5.7** and **5.8**) in this model.

In terms of EMT, HGF and bone morphogenic protein (BMP)-7 are potent inhibitors of this process (Liu, 2004). MSCs constitutively produce low levels of HGF (English et al., 2007) but when transfected with HGF, further reduce α-SMA expression in UUO compared with non-transfected MSCs (Liu et al., 2011). Furthermore, Rat MSCs administered following nephrectomy suppressed ED-1^+ macrophage infiltration and α-SMA expression. This was associated with enhanced BMP-7 expression (Villanueva et al., 2011).

5.4.3 Effects of paricalcitol in UUO

Paricalcitol administration also suppressed Th17 responses in UUO (**Figures 5.7** and **5.8**). Tan et al. found reduced $CD3^+$ T-cell recruitment following paricalcitol administration in UUO (Tan et al., 2008). In my study, $CD3^+$ T-cell recruitment was not significantly different between the treated and non-treated obstructed kidneys, however, I did observe that the no treatment obstructed kidneys contained significantly more $CD3^+$ T-cells than their control contra-lateral kidneys (**Figure 5.6**). In contrast, obstructed kidneys from all three treatment groups were not significantly different to their contra-lateral control kidneys suggesting that MSCs and paricalcitol alone and in combination suppress T-cell recruitment following UUO. Furthermore, I found reduced frequencies of TCR-β^+, $CD4^+$, $CCR6^+/CD4^+$, and $CD8^+$ T-cells in the obstructed kidneys of double-treated mice at day 3 (**Figure 5.5**).

5.4.4 Effects of MSCs and paricalcitol on cellular infiltrate

Reduced T-cell infiltration following administration of MSCs and/or paricalcitol may be associated with suppressed chemokine expression. UUO is associated with induced expression of MCP-1/CCL2, MIP-1α/CCL3, MIP-1β/CCL4, RANTES/CCL5, eotaxin/CCL11, MIP-2/CXCL2 and IFN-γ-induced protein 10 (IP-10)/CXCL10 (Vielhauer et al., 2001). Chemokine receptors CCR1, CCR2 and CCR5 are also found in abundance in obstructed kidneys post UUO (Anders et al., 2002). CCR1, whose ligands include MIP-1α and RANTES, was detected on $F4/80^+$ myeloid cells (Eis et al., 2004). CCR2 is the receptor for MCP-1 and was detected on $CD11b^+$ myeloid cells while CCR5 was highly expressed by $CD4^+$ and $CD8^+$ T-cells (Vielhauer et al., 2001). The ligands for CCR5 include MCP-1, MIP-1α, MIP-1β, and RANTES. CCR1 is believed to be particularly important for myeloid and T-cell infiltration and fibrosis following UUO (Anders et al., 2002, Eis et al., 2004).

In chapter 2, I demonstrated that in the presence of MSCs, memory $CD4^+$ T-cells activated with anti-CD3ε and APCs produced significantly less MIP-1α, MIP-1β and RANTES (**Figure 2.8**). Furthermore, Tan et al. showed that paricalcitol administration in UUO significantly reduced RANTES expression by tubular epithelial cells. This was associated with VDR sequestration of NF-κB p65 which prevented it from binding to the RANTES promoter (Tan et al., 2008).

The overall proportion of $F4/80^+/CD11b^+/Ly6C^-$ macrophages was not affected by paricalcitol as was reported by Tan et al. who detected reduced $F4/80^+$ myeloid cell infiltration following administration of paricalcitol to mice with UUO (Tan et al., 2008). However, I did observe a reduced frequency of $CD206^-/F4/80^+/CD11b^+/Ly6C^-$ M1 macrophages in obstructed kidneys of paricalcitol treated mice compared to the no treatment group (**Figure 5.10F**). Furthermore, in double-treated mice, $CD206^+/F4/80^+/CD11b^+/Ly6C^-$ M2 macrophages were significantly increased (**Figure 5.10F**). M2 macrophages have been reported to play a protective role in UUO (Kushiyama et al., 2011). Following reversal of 10 day UUO, collagen deposition and α-SMA expression reduced over time in association with increased ratios of CD206 and CD204 to CD68 (Kushiyama et al., 2011).

5.4.5 MACROPHAGE RE-PROGRAMMING

Re-programming of pro-inflammatory M1 macrophages to anti-inflammatory M2 macrophages by MSCs and PGE2 is well reported (Nemeth et al., 2009, Zhang et al., 2010a, Ylostalo et al., 2012, Takayama et al., 2002, Anderson et al., 2012). Nemeth et al. showed that MSC-derived PGE2 induced macrophages to produce IL-10 *via* EP2/EP4 which enhanced survival in a cecal ligation and puncture model of sepsis (Nemeth et al., 2009). Mouse AT-MSCs co-cultured with BM-macrophages induced phenotypically different regulatory macrophages from those of IL-4-alternatively-activated macrophages (Anderson et al., 2012). In addition to the AT-MSCs themselves, the regulatory macrophages also attenuated DSS- and TNBS-induced colitis (Anderson et al., 2012). Human gingiva-derived MSCs co-cultured with $CD14^+$ monocytes isolated from PBMCs had higher expression of CD206 and produced increased levels of IL-10 but reduced levels TNF-α. Furthermore, these anti-inflammatory cells displayed reduced ability to activate Th17 cells (Zhang et al.,

2010a). Human MSCs cultured as spheroid drops had increased ability to inhibit TNF-α, IL-23, IL-12p40 and MIP-2/CXCL2 production by LPS-stimulated macrophages in a PGE2/EP4-dependent manner (Ylostalo et al., 2012). Exogenous PGE2 suppressed LPS-mediated production of MCP-1, MIP-1β and IP-10 by human macrophages in addition to IFN-γ-, TNF-α- and IL-1β-induced production of MCP-1 and MIP-1β (Takayama et al., 2002). Endogenous PGE2 produced by smooth muscle cells in co-culture with macrophages suppressed LPS-induced MIP-1β production (Takayama et al., 2002). In UUO, administration of an EP4 agonist reduced renal expression of TGF-β1, MCP-1 and RANTES and this effect was associated with reduced macrophage infiltration and interstitial fibrosis (Nakagawa et al., 2012). Indeed, EP4 KO mice developed more severe obstructive nephropathy (Nakagawa et al., 2012). Thus, MSC-derived PGE2 may also confer additional beneficial effects in UUO in addition to suppression of Th17 responses.

5.4.6 SUMMARY

In conclusion, I have demonstrated, for the first time, suppressed Th17 responses by MSCs and paricalcitol alone and in combination *in-vivo* in the UUO model of obstructive nephropathy. This was characterised by a reduction in IL-17-producing $CD4^+$ T-cells and neutrophils in all three treatment groups and early reduction of $CCR6^+$ $CD4^+$ T-cells in double-treated animals. Furthermore, administration of the combination of MSCs and paricalcitol was associated with reduced inflammatory monocytes and M1 macrophages and increased M2 anti-inflammatory macrophages in obstructed kidneys. MSC and paricalcitol treatment also resulted in less kidney damage at day 8 as determined by analysis of tubular atrophy and dilation and interstitial fibrosis.

Given more time, I would be interested in investigating the functional relevance of the M1-M2 macrophage conversion observed in this study and the role of neutrophils in UUO. Kidney tissues were banked away for future protein analysis of EMT markers including α-SMA, snail, e-cadherin, collagens and fibronectin. Indeed, it would be interesting to investigate the effects of MSCs and/or paricalcitol on other aspects of obstruction-induced histological alterations including tubular cell apoptosis/necrosis using TUNEL staining, interstitial volume using silver staining or anti-laminin IHC and microvessel density using anti-platelet endothelial cell adhesion molecule

(PECAM)-1 IHC. Additionally, I would like to confirm my flow cytometry data of reduced neutrophil and M1 macrophage and increased M2 macrophage recruitment using IHC antibodies specific for Ly6G, F4/80 and CD206.

CHAPTER SIX

OVERALL DISCUSSION

The immune suppressive and anti-inflammatory properties of MSCs are now very well established and clearly encompass potent modulatory influences on the generation and disease-associated activity of multiple T-cell effector phenotypes including Th17 cells (Duffy et al., 2011, Caplan, 2009, Griffin et al., 2010). Furthermore, VDR agonists are now known to mediate immunomodulatory effects which, together with other agents, produce additive or synergistic immune suppressive effects (Daniel et al., 2008, Deb et al., 2010, Tan et al., 2009, Ikeda et al., 2010).

The discussions in the preceeding individual chapters have dealt with specific topics related to my findings. In this chapter I would like to develop some broader themes related to my results and discuss the potential translation of MSCs to clinical studies based on my findings.

6.1 THE COMPLEXITY OF MSC- AND PARICALCITOL-MEDIATED EFFECTS ON NAÏVE, MEMORY AND TISSUE-ACTIVATED T-CELLS

One of the interesting findings from my work which, perhaps, requires further elucidation was that MSCs potently inhibited Th17 differentiation from naïve $CD4^+$ T-cell precursors but were less inhibitory towards memory-phenotype responders. Furthermore, they did not suppress $CCR6^+$ memory T-cells and even enhanced IL-17 production by fully differentiated Th17 cells in the presence of IL-1α and IL-23. This is in line with multiple studies which also reported that MSCs (Bouffi et al., 2010, Ghannam et al., 2010, Rafei et al., 2009, Kong et al., 2009, Wang et al., 2008a, Zhang et al., 2011, Zhao et al., 2008, Zhou et al., 2011) and PGE2 (Chen et al., 2009, Valdez et al., 2012) suppress Th17 differentiation and function. My findings may explain the discrepancies with reports of enhanced Th17 responses under certain pro-inflammatory conditions by MSCs (Carrion et al., 2010, Darlington et al., 2010, Guo et al., 2009) and PGE2 (Boniface et al., 2009, Khayrullina et al., 2008, Yao et al., 2009). It appears that MSCs consistently suppress primary Th17 differentiation from naïve precursors but may also indirectly enhance Th17 responses by fully differentiated Th17 cells, *via* PGE2-induced production of the Th17-enhancing factor IL-23 (Schirmer et al., 2010, Yao et al., 2009).

The effects of MSCs *in-vivo* are far more complex due to their combined effects on other ancillary cells. Th17 cells of an effector memory phenotype accumulate in the obstructed kidney (Dong et al., 2008). Surprisingly, despite having no effects on splenic memory $CCR6^+$ T-cells *in-vitro* and the abundance of Th17-enhancing factors IL-1α, IL-1β, IL-6 and IL-23 in this model (Pindjakova et al., 2012), MSCs suppressed IL-17 production by effector memory Th17 cells *in-vivo* in UUO and also *ex-vivo* when co-cultured with anti-CD3ε-stimulated leukocytes isolated from obstructed kidneys. A possible explanation for this discrepancy is that MSCs exert additional inhibitory effects on other leukocyte populations (e.g. monocytes/macrophages or DCs (Wang et al., 2008b, Cutler et al., 2010)) present in the obstructed kidney which indirectly suppress Th17 activation.

In a similar manner, paricalcitol was associated with potent inhibition of Th17 differentiation from naïve-phenotype precursors but had limited effects on memory-phenotype responders. Paricalcitol did not affect IL-17 production *ex-vivo* by anti-CD3ε-stimulated CD45 MACS-enriched cells from obstructed kidneys however, when administered *in-vivo* at the initiation of UUO, was associated with reduced Th17 responses. This suggests that paricalcitol attenuates Th17 responses when administered early but may have limited effects when UUO is established. Additional experiments would be necessary to confirm this hypothesis. Furthermore, mice in which a suppressive effect on Th17 accumulation was observed, received multiple daily doses of paricalcitol over a longer period of time. Paricalcitol monotherapy has been reported to attenuate EAE, rheumatoid arthritis, experimental colitis and prostatitis (Chang et al., 2010a, Colin et al., 2010, Daniel et al., 2008, Penna et al., 2006) while MSCs also exerted beneficial effects in EAE and experimental colitis and arthritis (Bouffi et al., 2010, Rafei et al., 2009, Anderson et al., 2012). It would be interesting to examine the combined effects of paricalcitol and MSCs in such antigen-specific models.

6.2 DIVERSITY OF MEDIATORS AND MECHANISMS OF ACTION OF MSC IMMUNOSUPPRESSION

The diversity of soluble mediators and mechanisms of action reported for MSC immunosuppression may relate to varying MSC culture conditions and the

heterogeneous nature of the cells. I found that upregulation of COX2 and induced expression of PGE2 by MSCs following co-culture with activated $CD4^+$ T-cells suppressed Th17 differentiation *via* the EP4 receptor. *In-vivo*, multiple MSC mediators have been reported for Th17-mediated diseases including PGE2, TGF-β1, IDO, IL-27 and CCL2 (Ghannam et al., 2010, Kong et al., 2009, Rafei et al., 2009, Wang et al., 2008a, Zhao et al., 2008). Immunosuppressive potency, mechanism of action and fate *in-vivo* may vary among the individual cells within heterogeneous MSC cultures. Lack of standardization in isolation and culture protocols may result in selective expansion of specific cells under diverse conditions (Park et al., 2012). In addition to *ex-vivo* culture conditions, diverse mediators may be at play in different diseases depending on pathogenesis and the cytokine milieu present during the course of disease which may influence MSC fate (Papadopoulou et al., 2012).

These factors could also explain why, in a number of studies, MSC-induced expansion of T_{reg} has been reported while others including myself did not detect this phenomenon. Additionally, species differences may account for observed T_{reg} expansion in human cell cultures but not in mouse (Ghannam et al., 2010). Expansion of T_{reg} by MSCs or other MSC-mediated immune effects may not always confer benefit. It is important to note that MSC-associated immune modulation has been suggested to have detrimental effects in the setting of cancer. In a recent study by Patel and colleagues, the addition of MSCs to co-cultures of breast cancer cells and peripheral blood leukocytes resulted in enhanced T_{reg} numbers and Th2 cell-related cytokines as well as inhibited proliferation and release of granzyme B by CTLs, all of which resulted in protection of cancer cells from immune-mediated lysis (Patel et al., 2010). Kim et al. showed that addition of BM-derived macrophages and/or MSCs enhanced proliferation and reduced apoptosis of multiple myeloma cell lines (Kim et al., 2012). *In vivo* studies to examine this phenomenon are essential to fully understand the complex interaction between MSCs, immune cells, and cancer cells and to ensure that MSC administration is not associated with recurrence or rapid metastasis of cancer in some patient groups.

Another concern that requires further investigation regarding MSC-induced T_{reg} relates to the potential for phenotypic plasticity of pro- and anti-inflammatory $CD4^+$ T-cell subsets under varying *in vivo* conditions. For example, as highlighted in a

review by Afzali and colleagues, T_{reg} may be converted to a Th17 cell phenotype when exposed to inflammatory stimuli. In such circumstances, MSC-induced T_{reg} may exacerbate the disease state. Further human studies will be essential to fully elucidate the clinical relevance and robustness of MSC-induced T_{reg} *in vivo*. Indeed, MSC cloning may be used in the future to selectively expand specific populations of MSCs following extensive characterization of their immunosuppressive and differentiation potential.

6.3 *IN-VIVO* EFFICACY OF PARICALCITOL AND MSCS

Paricalcitol was chosen as the vitamin D intervention for this study due to its reduced hypercalcemic properties (Brown et al., 2002). This finding was confirmed by Tan et al. who showed that administration of 0.3 μg/kg/day of paricalcitol for 7 days was not associated with adverse calcium deposition in the obstructed kidney (Tan et al., 2006). Paricalcitol monotherapy was reported to attenuate interstitial fibrosis and tubular damage in UUO (Tan et al., 2006, Tan et al., 2009). Despite similar dosing regimens, I did not detect reduced interstitial fibrosis in this thesis using paricalcitol alone. This may relate to the use of out-bred mice by Tan et al. or to the timing of administration on day -1 prior to UUO used in one of the studies (Tan et al., 2009). Paricalcitol also reduced interstitial fibrosis in diabetic nephropathy in rats and db/db mice however, in these studies much higher doses were required (0.75 μg/kg - 3 times per week for 4 months and 0.4 μg/kg - 3 times per week for 3 months, respectively) and a different route of administration was employed (intraperitoneal) (Deb et al., 2010, Sanchez-Nino et al., 2012). Low overall interstitial fibrosis scores were observed in my study suggesting that the 8 day time-point chosen may have been too early to detect differences between the groups. Given more time, experiments could be extended to 14 days when higher interstitial fibrosis scores would be expected (Liu et al., 2012).

Paricalcitol is currently employed to treat hyperparathyroidism associated with chronic kidney disease. As described in this thesis, paricalcitol also potently inhibits primary Th17 differentiation and was associated with reduced Th17 responses *in-vivo* in UUO. Re-purposing of currently approved drugs holds many advantages over *de novo* development of drugs including reduced costs, development time and risks associated with new drug discovery (Ashburn and Thor, 2004). Based on my findings,

I believe that paricalcitol could be repositioned for the treatment of autoimmune and inflammatory diseases associated with maladaptive Th17 responses including multiple sclerosis, Crohn's disease, psoriasis and kidney disease.

Similar to paricalcitol, I did not detect reduced interstitial fibrosis by administering MSCs alone in UUO in contrast to a number of studies in the rat model of UUO (Asanuma et al., 2011, Liu et al., 2011, Liu et al., 2012). In addition to the difference in species in which UUO was performed, these studies differed to mine in that human MSCs were administered (Asanuma et al., 2011), the route of administration was *via* the renal artery (Asanuma et al., 2011) or vena cava (Liu et al., 2012), the MSCs were administered only once (Asanuma et al., 2011, Liu et al., 2011, Liu et al., 2012), MSCs were administered prior to UUO (Asanuma et al., 2011), directly after UUO (Liu et al., 2012) or 6 hours post UUO (Liu et al., 2011) and much lower numbers of MSCs were administered. I administered 0.5 x 10^6 twice into ~ 22 g mice while 1-2 x 10^6 MSCs were administered into 150-300 g rats (Asanuma et al., 2011, Liu et al., 2011, Liu et al., 2012). Given more time, I think it would be interesting to titrate down the number of MSCs used in this thesis to 1 x 10^6/kg which is currently used clinically in human studies (Moll et al., 2012).

6.4 CHALLENGES OF PRE-CLINICAL TO CLINICAL TRANSLATION OF MSC THERAPY

This thesis was carried out in the Regenerative Medicine Institute in NUI, Galway which has a strong focus on the translation of MSC therapy to the clinic for multiple diseases. Indeed, pre-clinical models have provided a strong impetus for translating MSC therapy as well as vitamin D intervention to widespread clinical use for a range of common, Th17-mediated autoimmune and inflammatory diseases and for prevention or treatment of transplant complications such as rejection and GvHD (English et al., 2010, Griffin et al., 2010). However, limitations in the process of pre-clinical to clinical translation may explain some of the recent mixed outcomes of MSC clinical trials (Ankrum and Karp, 2010).

Serial passaging and *ex-vivo* expansion of MSCs, which is necessary to generate sufficient numbers, affects differentiation and clonogenic potential as well as senescence (Gruber et al., 2012). In mice, sequential passaging is required to generate

a pure population of non-hematopoietic cells. Thus, it is common to use P4-P8 MSCs for experimentation. In contrast, in the human system, P1-P4 MSCs are typically employed. Passaging did not affect cell surface marker expression (Lo Surdo and Bauer, 2012) however, in a comparative study of P3 versus P7 human MSCs, extended *ex-vivo* passaging resulted in increased cell size, granularity and proliferation and also affected protein expression (Madeira et al., 2012). MSC population doublings, as assessed by colony formation units, were significantly reduced after P5. To make better comparisons with human MSCs, it may be more appropriate to use early passage MSCs in mouse studies, although this will require optimisation of culture and isolation conditions to remove hematopoietic contaminants from early passage mouse MSCs.

Moll and colleagues also described increased immunogenicity of MSCs with extended passaging. The authors found that, within one hour of exposure to blood *in-vitro*, MSCs were associated with reduced numbers of free platelets and increased expression of thrombin. MSC-induced elicitation of an innate immune response was increased with dose and passaging. *In-vivo* MSC responses were measured in patients who received hematopoietic stem cell transplantation. The authors found that P1-P4 MSC doses (1-3 x 10^6/kg) commonly used in the clinic, were associated with weak blood responses however, based on *in-vitro* findings, the authors hypothesized that higher passage MSCs administered in higher doses may cause adverse affects.

Another issue with human MSCs is donor to donor variability in terms of differentiation, clonogenic and immunosuppressive potential. Although the effects of autologous verus allogeneic MSCs have been well examined, the issue of donor variability has not been effectively addressed in animal model experiments using inbred strains. The clonogenic potential of unsorted mouse BM is ~1/1 x 10^6 cells (Park et al., 2012). MSC subpopulations with enhanced clonogenic potential are now being isolated and characterized from heterogeneous BM, based on *in-vivo* function in their natural site of residence (Morikawa et al., 2009, Park et al., 2012). In the future, this may facilitate tailoring MSC therapy to specific diseases.

Time of administration of MSCs is also a critical parameter for successful treatment of certain diseases. In a study by Zappia et al. using the EAE model, MSC

administration prior to or during the early disease course was effective whereas MSC benefit was lost once central nervous system inflammation (Zappia et al., 2005). Similarly, in experimental arthritis, the timing of MSC administration, the relative effects of MSCs on different T-cell subsets, and the local joint conditions have been reported to critically determine the balance between therapeutic efficacy, lack of benefit, and detrimental effects (Bouffi et al., 2010, Carrion et al., 2010, Chen et al., 2010a, Tso et al., 2010).

These studies highlight the complexity of the interactions that occur between stromal cells and cells of the immune system and the wealth of basic and therapeutic insights that can be gained from continued investigation of these interactions. It also raises the interesting question of how long-lasting MSC modulation of T-cell effectors occurs following single or multiple *in vivo* administrations.

In-vitro, we addressed the topic of duration of MSC suppressive phenotype following co-culture with activated $CD4^+$ T-cells. As part of my Ph.D. in REMEDI, I had the opportunity to mentor a summer medical student, Ms. Cliona Small. The aim of this project was to determine the duration of the MSC immunosuppressive phenotype *in-vitro*. The rate of proliferation of CFSE-labeled $CD4^+$ T-cells activated with anti-CD3/anti-CD28 beads in the presence of various conditioned media from multiple time-points was measured. Conditioned media generated from MSCs alone or from MSCs that were cultured in the presence of inactivated $CD4^+$ T-cells were not suppressive at any time-point. In comparison, conditioned media generated from MSCs cultured in the presence of activated $CD4^+$ T-cells were potently suppressive as early as 12 hours and remained suppressive up to 72 hours. Conditioned media from the 24 hour time-point displayed maximum suppressive potential suggesting that optimal suppression occurs early following cellular contact between MSCs and activated $CD4^+$ T-cells. This topic certainly requires attention in the future and should to be better addressed *in-vivo* for the full therapeutic potential of MSCs to be realized.

6.5 CONCLUSIONS

In conclusion, this thesis has added to existing knowledge by describing a novel mechanism of MSC-mediated Th17 inhibition *via* EP4 receptor activation. Following cell-cell cross talk with activated $CD4^+$ T-cells, COX2 upregulation resulted in PGE2 production by the MSCs. PGE2 interaction with EP4 suppressed primary Th17 differentiation. Furthermore, $CD4^+$ T-cells co-cultured with MSCs under Th17-skewed conditions expressed lower levels of multiple key Th17 differentiation pathway transcription factors including RORγt, IRF4 and Runx1. Paricalcitol-mediated suppression of Th17 differentiation was associated with upregulation of the VDR but not with detectable suppression of the Th17 differentiation pathway transcription factors or signalling pathways tested. I propose that further characterization of the interactions between Th17 cells, MSCs and paricalcitol, including determination of the nature of the contact-dependent signal responsible for COX2 up-regulation in MSCs and the mechanism of paricalcitol-mediated Th17 suppression, will identify additional opportunities for manipulation of the Th17 differentiation program.

In an *in-vivo* setting, MSCs and paricalcitol, alone and, for the first time, in combination suppressed Th17 responses. This was associated with evidence of an alteration in the balance between pro- and anti-inflammatory macrophages in UUO in addition to reduced interstitial fibrosis and tubular atrophy and dilation. This indicates the potential for MSCs to ameliorate tissue damage associated with maladaptive acute or chronic Th17 activation in autoimmune and inflammatory diseases if delivered in the correct context. It also suggests that adjunctive therapy with VDR agonists may represent a strategy for enhancing the immunosuppressive properties of MSCs.

APPENDICES

APPENDIX ONE: PUBLICATIONS, PRESENTATIONS AND ACHIEVEMENTS

Publications:

1. Duffy, M.M., Ritter, T., Ceredig, R. & Griffin, M.D. (2011) Mesenchymal stem cell effects on T-cell effector pathways. *Stem Cell Research & Therapy*, 2**,** 34.

2. Duffy, M.M., Pindjakova, J., Hanley, S.A., McCarthy, C., Weidhofer, G.A., Sweeney, E.M., English, K., Shaw, G., Murphy, J.M., Barry, F.P., Mahon, B., Belton, O., Ceredig, R. & Griffin, M.D. (2011) Mesenchymal stem cell inhibition of T-helper 17 cell-differentiation is triggered by cell-cell contact and mediated by prostaglandin E2 *via* the EP4 receptor. *European Journal of Immunology*, 41**,** 2840-51.

3. Pindjakova, J., Hanley, S.A., Duffy, M.M., Sutton C.E., Weidhofer, G.A., Miller, M.N., Nath, K.A., Mills, K.H, Ceredig, R. & Griffin, M.D. (2012) Interleukin-1 accounts for intrarenal Th17 cell activation during ureteral obstruction. *Kidney International*, 81, 379-90.

4. McCarthy, C., Duffy, M.M., Mooney, D., James, W.G., Griffin, M.D., Fitzgerald, D.J. & Belton, O. (2012). Interleukin-10 mediates the immunoregulatory response in CLA-induced regression of atherosclerosis. *FASEB Journal*, epub ahead of print.

5. In preparation: Prado Lopez, S., Duffy, M.M., Baustian, C., Alagesan, S., Hanley, S.A., Griffin, M.D. & Ceredig, R. (2012). The influence of hypoxia on the differentiation capacities and immunosuppressive properties of clonal mouse mesenchymal stem cell lines.

6. In preparation: Duffy, M.M., McNicholas, B., Monaghan, D.A., Alagesan, S., Fearnhead, H. & Griffin. M.D. (2012). Mesenchymal stem cells and the vitamin D analogue paricalcitol additively suppress Th17 responses *via* distinct mechanisms.

Oral presentations:

1. "Marrow stromal cells potently inhibit the primary induction of T-helper 17 cells through cell-cell contact" - Irish Cytometry Society conference 17-18 November 2009 Dublin, Ireland.

2. "Extinguishing inflammation with mesenchymal stem cells" - National Centre for Biomedical Engineering Science representative for the NUI, Galway Science Speak competition 12 April 2010.

3. "Marrow stromal cells potently inhibit the primary induction of T-helper 17 cells through cell-cell contact" - Tissue Engineering and Regenerative Medicine International Society (TERMIS) EU meeting 13-17 June 2010 Galway, Ireland.

4. "Inhibition of T-helper 17 induction by mesenchymal stromal cells is induced by cell-cell contact through prostaglandin E2 *via* EP4 receptor" - Irish Society for Immunology 25th anniversary symposium 15 October 2010 Dublin, Ireland.

Poster presentations:

1. "Marrow stromal cells potently inhibit the primary induction of T-helper 17 cells through cell-cell contact" - Irish Society for Immunology conference 10-11 September 2009 Dublin, Ireland.

2. "Characterisation of the phenotype, developmental potential & immunosuppressive properties of mouse mesenchymal progenitor cell lines and clones" - Irish Society for Immunology conference 10-11 September 2009 Dublin, Ireland.

3. "Mesenchymal stromal cells potently inhibit the primary induction of T-helper 17 cells through cell-cell contact" - American Transplant Congress 1-5 May 2010 San Diego, California, USA.

4. "Mesenchymal stromal cells suppress primary T-helper 17 (Th17) differentiation as well as re-activation of Th17 cells from injured kidney" - American Society Nephrology 16-21 November 2010 Denver, Colorado, USA.

5. "The duration of mesenchymal stem cell immunosuppressive phenotype following co-culture with activated $CD4^+$ T-cells" - Irish Society for Immunology conference 01-02 September 2011 Galway, Ireland.

6. "The influence of hypoxia on the differentiation capacities and immunosuppressive properties of clonal mouse MSC lines" – Royal Academy of Medicine in Ireland (RAMI) 14 June 2012 Galway, Ireland.

7. "Mesenchymal stem cells and the vitamin D analogue paricalcitol additively suppress Th17 induction *via* distinct mechanisms" - International Cytokine Society – The IL-17 and Related Cytokines Conference 18-21 June 2012 Dublin, Ireland.

8. "$Sca1^+$ and $Sca1^-$ mouse bone marrow stromal cells exhibit distinct responses to osteochondral stimuli in-vitro" - International Mesenchymal Stem Cell Conference 02-03 July 2012 Galway, Ireland.

9. "The influence of hypoxia on the differentiation capacities and immunosuppressive properties of clonal mouse MSC lines" – International Mesenchymal Stem Cell Conference 02-03 July 2012 Galway, Ireland.

10. "Paricalcitol and mesenchymal stem cells additively suppress primary T-helper 17 differentiation *via* distinct mechanisms" - American Society Nephrology 30 October-04 November 2012 San Diego, California, USA.

Achievements:

1. First prize for student poster presentation: Irish Society for Immunology conference 2009.

2. First prize for oral presentation: Irish Cytometry Society conference 2009.

3. Joint first prize for oral presentation: Irish Society for Immunology 25th anniversary symposium 2010.

4. First prize for oral presentation: Regenerative Medicine Institute Ph.D. research day March 2010.

5. First prize for oral presentation: Regenerative Medicine Institute Ph.D. research day September 2010.

APPENDIX TWO: REAGENTS

Reagent	Supplier	Catalogue number
0.25% trypsin/EDTA	Sigma-Aldrich	T4049
10% neutral buffered formalin	Sigma-Aldrich	HT501128
2-mercaptoethanol	Sigma-Aldrich	M3148
3,3'-diaminobenzidine (DAB) substrate	Sigma-Aldrich	D8001
30% acrylamide	Sigma-Aldrich	A3574
30% hydrogen peroxide	Sigma-Aldrich	H1009
ABC reagent	Vector Laboratories, Peterborough, UK	SP-2001
Acetic acid	Sigma-Aldrich	695092
Alpha-MEM	Gibco-Invitrogen	32561
Ammonium chloride	Sigma-Aldrich	A0171
Ammonium persulfate	Sigma-Aldrich	A3678
Antigen unmasking solution	Vector Laboratories	H-3301
Anti-mouse CD4 microbeads	Miltenyi Biotec Inc.	130-049-201
Anti-mouse CD45 microbeads	Miltenyi Biotec Inc.	130-052-301
Anti-mouse CD90.2 microbeads	Miltenyi Biotec Inc.	130-049-101
Pierce® BCA protein assay kit	Fisher Scientific Ireland	23225
Biorad cytokine reagent kit	Biorad	10008294
Biorad murine cytokine kit, 23 plex	Biorad	171-F11241
Bovine serum albumin	Sigma-Aldrich	A2153
Bradford® reagent	Sigma-Aldrich	B6916
Bromophenol blue	Sigma-Aldrich	B8026
Calcium chloride	Sigma-Aldrich	C8106
Capacity cDNA reverse transcription kit with RNase inhibitor®	Applied Biosystems	4374966
CD3/CD28 T-cell expander beads-Dynabeads®	Invitrogen	114.52D
Celestine blue	Sigma-Aldrich	206342
CellTrace CFSE cell proliferation kit®	Molecular Probes-Invitrogen	C34554
CHAPS	Sigma-Aldrich	C9426
Chloroform	Sigma-Aldrich	496189
CLAP protease inhibitor cocktail	Sigma-Aldrich	P8340
Collagenase I	Sigma-Aldrich	C9891
Cytofix/cytoperm® kit	BD Biosciences	555028
Dimethyl sulfoxide	Sigma-Aldrich	D2650
Disodium EDTA	Sigma-Aldrich	E5134
DL-dithiothreitol	Sigma-Aldrich	D0632
DNase I	Sigma-Aldrich	DN25
DPX mounting medium	Sigma-Aldrich	44581
Phosphomolybdic acid hydrate	Sigma-Aldrich	79560
Dulbecco's modified Eagles medium	Sigma-Aldrich	D6429
Dulbecco's PBS	Gibco-Invitrogen	14190
DuoSet® ELISA development systems	R&D Systems	DY421 (IL-17A), DY485 (IFN-γ), DY1679 (TGF-β1)
EGTA	Sigma-Aldrich	03777
Eosin	Sigma-Aldrich	HT110116
EP1 antagonist SC-51322	Cayman Chemical Company, Ann Arbor, MI, USA	10010744
EP2 antagonist AH-6809	Cayman Chemical Company	14050

EP4 agonist L-902,688	Cayman Chemical Company	10007712
EP4 antagonist L-161,982	Cayman Chemical Company	10011565
Ethanol	Sigma-Aldrich	E7023
F-12 nutrient mixture	Gibco-Invitrogen	21765
Fast green	Sigma-Aldrich	F7252
Glycerol	Sigma-Aldrich	G8773
Glycine	Sigma-Aldrich	G8898
Hank's Balanced Salt Solution	Sigma-Aldrich	H6648
Hematoxylin	Sigma-Aldrich	HHS16
HEPES	Sigma-Aldrich	H0887
Hyclone equine serum	Sigma-Aldrich	H1270
Hyclone fetal bovine serum (FBS)	Fisher Scientific Ireland	SV30143.03
Hydrochloric acid	Sigma-Aldrich	H1758
Hydrogen peroxide	Sigma-Aldrich	216763
Immobilon® Western Chemiluminescent HRP Substrate	Millipore	WBKLSO500
Indomethacin	Sigma-Aldrich	I7378
Iscove's modified Dulbecco's medium	Sigma-Aldrich	13390
Isopropanol	Sigma-Aldrich	I9516
L-glutamine	Gibco-Invitrogen	25030-024
L-NAME	Sigma-Aldrich	N5751
Magnesium chloride hexahydrate	Sigma-Aldrich	M9272
Methanol	Sigma-Aldrich	34860
Methylgreen	Sigma-Aldrich	M8884
Non-essential amino-acids	Sigma-Aldrich	M7145
NS-398	Sigma-Aldrich	N194
Parameter™ PGE2 competitive assay	R&D Systems	SKGE004B
Pararosaniline hydrochloride	Sigma-Aldrich	P1528
Paricalcitol	Abbott Laboratories	49510
Penicillin/streptomycin	Gibco-Invitrogen	15140-122
Periodic acid	Sigma-Aldrich	P7875
Phosphatase inhibitor cocktail II	Sigma-Aldrich	P5726
Phosphate buffered saline tablets	Sigma-Aldrich	P4417
Ponceau S	Sigma-Aldrich	78376
Potassium chloride	Sigma-Aldrich	P3911
Potassium hydroxide	Sigma-Aldrich	P5958
Potassium permanganate	Sigma-Aldrich	223468
Precision Plus Protein™ Western C™ standards	Biorad	161-0376
Protease inhibitor cocktail tablets	Roche Diagnostics GmbH, Mannheim, Germany	11 836 170 001
Purified PGE2	Cayman Chemical Company	14010
Recombinant human TGF-β1	Peprotech Inc., Rocky Hill, NJ, USA	100-21
Recombinant mouse IL-1α	Peprotech Inc.	211-11A
Recombinant murine IL-23	R&D Systems	1887-ML-010
Recombinant murine IL-6	Peprotech Inc.	216-16
RNA Later® solution	Applied Biosystems	AM7020
RNA zap	Applied Biosystems	AM9780
RPMI-1640	Sigma-Aldrich	R0833
Sodium Chloride 0.9% w/v intravenous infusion	B. Braun Melsungen, Germany	630137

Schiff reagent	Sigma-Aldrich	3952016
Sodium azide	Sigma-Aldrich	A2152
Sodium bicarbonate	Sigma-Aldrich	S7277
Sodium chloride	Sigma-Aldrich	S5886
Sodium dodecyl sulfate	Sigma-Aldrich	L4390
Sodium fluoride	Sigma-Aldrich	S7920
Sodium hydroxide	Sigma-Aldrich	S5881
Sodium metabisulphite	Sigma-Aldrich	S9000
StrepTactin-HRP conjugate	Biorad	161-0380
Sulfuric acid	Sigma-Aldrich	339741
Sytox® Blue	Invitrogen	S10349
TaqMan® gene expression assay GAPDH	Applied Biosystems	Mm99999915_g1
TaqMan® gene expression assay IL-17A	Applied Biosystems	Mm00439618_m1
TaqMan® Universal Master Mix II, no UNG	Applied Biosystems	4440047
TEMED	Sigma-Aldrich	T9281
TMB/E ELISA substrate	Millipore	ES001
Trizma® base	Sigma-Aldrich	T6066
Trizol®	Invitrogen	15596018
TURBO DNase	Applied Biosystems	AM1907
Tween-20®	Sigma-Aldrich	P1379
Xylene	Sigma-Aldrich	534056

APPENDIX THREE: ANTIBODY PREPARATIONS

Antibody Preparation	Species/Isotype	Clone	Supplier
Purified			
Purified anti-mouse IFN-γ	Rat IgG1	XMG1.2	BD Biosciences
Purified anti-mouse IL-4	Rat IgG1	11B11	BD Biosciences
Purified anti-mouse CD3ε	Armenian Hamster IgG	145-2C11	eBioscience Inc., San Diego, CA, USA
Anti-mouse CCL2 neutralization antibody	Rat IgG2b	123616	R&D Systems
FITC-conjugated			
Anti-mouse CD4	Rat IgG2b, κ	RM-4-4	BD Biosciences
Anti-mouse CD8a (Ly-2)	Rat IgG2a, κ	53-6.7	BD Biosciences
Anti-mouse CD14	Rat IgG1, κ	rmC5-3	BD Biosciences
Anti-mouse CD19	Rat IgG2a, κ	1D3	BD Biosciences
Anti-mouse CD25	Rat IgM, κ	7D4	Southern Biotech, Birmingham, AL, USA
Anti-mouse CD45	Rat IgG2b, κ	30-F11	eBioscience
Anti-mouse CD80 (B7-1)	Armenian Hamster IgG2, κ	16-10A1	BD Biosciences
Anti-mouse CD106	Rat IgG2a, κ	429	eBioscience
Anti-mouse IFN-γ	Rat IgG1, κ	XMG1.2	BD Biosciences
Anti-mouse IL-17A	Rat IgG1, κ	TC11-18H10.1	Biolegend, San Diego, CA, USA
Anti-mouse Ly6A/E (Sca-1)	Rat IgG2a, κ	D7	eBioscience
Anti-mouse Ly6C	Rat IgM, κ	AL-21	BD Biosciences
I-A^d	Mouse IgG2b, κ	AMS-32.1	BD Biosciences
Mouse monoclonal to CD90/Thy 1	IgG2b	1.BB.730	Abcam, Cambridge, UK
AF488-conjugated			
Anti-mouse/human CD11b	Rat IgG2b, κ	M1/70	Biolegend
PE-conjugated			
Anti-mMMR (CD206)	Goat IgG	IC108P	R&D Systems
Anti-mouse CCR6	Armenian Hamster IgG	29-2L17	Biolegend
Anti-mouse CD4	Rat IgG2b, κ	GK1.5	BD Biosciences
Anti-mouse CD11b	Rat IgG2b, k	M1/70	BD Biosciences
Anti-mouse CD11c	Armenian Hamster IgG, λ2	HL3	BD Biosciences
Anti-mouse CD25	Rat IgG1, λ	PC61	BD Biosciences
Anti-mouse CD31	Rat IgG2a, κ	390	eBioscience
Anti-mouse/human CD44 (Pgp-1, Ly-24)	IgG2b, κ	IM7	eBioscience
Anti-mouse CD54 (ICAM-1)	Armenian Hamster IgG1, κ	3E2	BD Biosciences
Anti-mouse CD62L	Rat IgG2a, κ	MEL-14	eBioscience
Anti-mouse CD73	Rat IgG1	eBioTY/11.8 (TY/11.8)	eBioscience
Anti-mouse CD80	Armenian Hamster IgG2,κ	16-10A1	BD Biosciences
Anti-Mouse CD86	Rat IgG2a, κ	GL1	BD Biosciences
Anti-mouse CD90.2 (Thy-1.2)	Rat IgG2a, κ	53-2.1	BD Biosciences
Anti-mouse CD105	Rat IgG2a, κ	MJ7/18	eBioscience
Anti-mouse CD137 ligand	Rat IgG2a, κ	TKS-1	eBioscience
Anti-mouse CD252	Rat IgG2b, κ	RM134L	eBioscience
Anti-mouse CD273	Rat IgG2a, κ	122	eBioscience
Anti-mouse CD275	Rat IgG2a, κ	HK5.3	eBioscience
Anti-mouse IL-17	Rat IgG1, κ	TC11-18H10.1	Biolegend
Anti-mouse/rat I-E^k	IgG2a, κ	14-4-4S	eBioscience
Anti-mouse TCR-β chain	Armenian Hamster IgG2, λ	H57-597	BD Biosciences

Anti-TER-119	Rat IgG2b, κ	TER-119	eBioscience
I-A^b	Mouse IgG2a, κ	AF6-120.1	BD Biosciences
PerCP-Cy5.5-conjugated			
Anti-mouse CD4	Rat IgG2a, κ	RM4-5	BD Biosciences
Ly6C	Rat IgM, κ	AL-21	BD Biosciences
PE-Cy7-conjugated			
Anti-mouse CD45	Rat IgG2b, κ	30-F11	BD Biosciences
Anti-mouse Ly6G	Rat IgG2a, κ	1A8	Biolegend
APC-conjugated			
Anti-mouse/Rat CD29	Armenian Hamster IgG	HMb1-1	eBioscience
Anti-mouse CD31	Rat IgG2a, κ	390	eBioscience
Anti-mouse CD44	Rat IgG2b, κ	IM7	BD Biosciences
Anti-mouse CCR6	Armenian Hamster IgG	29-2L17	Biolegend
Anti-mouse F4/80	Rat IgG2a, κ	BM8	eBioscience
AF647-conjugated			
Anti-mouse CCR6	Armenian Hamster IgG	29-2L17	Biolegend
Anti-mouse FOXP3	Rat IgG2b	MF23	BD Biosciences
Anti-mouse IL-17	Rat IgG2a, κ	eBio17B7	eBioscience
Western Blot			
AML1 (Runx1) rabbit polyclonal	Goat anti-rabbit		Cell Signaling Technology Inc., Beverly, MA, USA
Anti-mouse/rat FOXP3 purified	Goat anti-rat	FJK-16s	eBioscience
Anti-mouse RORγt purified	Goat anti-rat	B2D	eBioscience
Anti-vitamin D receptor monoclonal antibody	Goat anti-rabbit	EPR4552	Abcam
CHOP-10/ GADD 153	Goat anti-rabbit	R-20	Santa Cruz Biotechnology Inc., CA, USA
Monoclonal anti-β-actin	Goat anti-mouse	AC-15	Sigma-Aldrich
Phospho-STAT3 (Tyr705) rabbit polyclonal	Goat anti-rabbit		Cell Signaling Technology Inc.
STAT3 rabbit polyclonal	Goat anti-rabbit		Cell Signaling Technology Inc.
Polyclonal rabbit anti-IRF4	Goat anti-rabbit		Cell Signaling Technology Inc.
Polyclonal rabbit anti-mouse COX1	Goat anti-rabbit		Cayman Chemical Company
Polyclonal rabbit anti-mouse COX2	Goat anti-rabbit		Cayman Chemical Company
IHC			
Anti-CD3 polyclonal	Goat anti-rabbit		Abcam

APPENDIX FOUR: MEDIA/BUFFER FORMULATIONS

Complete isolation media (CIM):
RPMI-1640
Fetal bovine serum (FBS) (10%)
Equine serum (10%)
Penicillin-streptomycin (1%)
L-glutamine (1%)

Complete expansion media (CEM):
Alpha-MEM
FBS (10%)
Equine serum (10%)
Penicillin-streptomycin (1%)
L-glutamine (1%)

MSC culture media:
IMDM
FBS (9%)
Equine serum (9%)
Penicillin-streptomycin (1%)
L-glutamine (1%)

Freezing media:
FBS
DMSO (10%)

Th17 culture media:
DMEM
FBS (10%)
Penicillin-streptomycin (1%)
L-glutamine (1%)
HEPES (1%)
Non-essential amino acids (1%)
2-mercaptoethanol (0.1%)

Fibroblast media:
DMEM
F-12 Nutrient mixture (50%)
FBS (10%)
Penicillin-streptomycin (1%)
L-glutamine (1%)
HEPES (1%)
Non-essential amino acids (1%)

Ammonium chloride lysis buffer (10 x):
Ammoniun chloride (1.5 M)
Sodium bicarbonate (100 mM)
Disodium EDTA (10 mM)
Adjusted to pH 7.4

FACS sorting buffer:
Calcium- and magnesium-free D-PBS
FBS (1%)
HEPES (25 mM)
Disodium EDTA (2 mM)

MACS buffer:
D-PBS
Bovine serum albumin (0.5%)
Disodium EDTA (0.2 mM)

FACS buffer:
D-PBS
FBS (2%)
Sodium azide (0.05%)

Western Blot complete lysis buffer A (pH 7.4):
Tris (50 mM)
Sodium Chloride (150 mM)
Magnesium Chloride (1 mM)
Calcium Chloride (1 mM)
Sodium Fluoride (25 mM)
Potassium Chloride (1 mM)
NP-40 (0.5%)
Glycerol (10%)
Protease inhibitor cocktail tablets

Western Blot complete lysis buffer B:
HEPES-KOH pH 7.2 (50 mM)
EGTA (5 mM)
Potassium Chloride (10 mM)
Magnesium Chloride (2 mM)
CHAPS (1% w/v)
CLAP (0.1% v/v)
DL-Dithiothreitol (2 mM)
Phosphatase inhibitor II (1% v/v)

10 X TBS pH 7.4:
Tris (250 mM)
Sodium Chloride (1.5 M)
Potassium Chloride (20 mM)

1 X TBST:
10 X TBS
Distilled H_20
Tween® 20 (0.05% v/v)

2 X Laemmli/loading buffer:
Sodium Dodecyl Sulfate (4% w/v)
Glycerol (10% v/v)
Tris-HCL pH6.8 (80 mM)
Bromophenol blue (0.05% w/v)
DL-Dithiothreitol (100 mM)

10 X Running buffer:
Tris (250 mM)
Glycine (1.92 mM)
Sodium Dodecyl Sulfate (1% w/v)

10 X Transfer buffer:
Tris (250 mM)
Glycine (1.92 mM)
Methanol (10% v/v)

Ponceau S solution:
Ponceau S (0.1%)
Acetic acid (5%)

REFERENCES

ABRAHAM, C. & CHO, J. (2009) Interleukin-23/Th17 pathways and inflammatory bowel disease. *Inflamm Bowel Dis,* 15**,** 1090-100.

AGGARWAL, S. & GURNEY, A. L. (2002) IL-17: prototype member of an emerging cytokine family. *J Leukoc Biol,* 71**,** 1-8.

AKSU, A. E., HORIBE, E., SACKS, J., IKEGUCHI, R., BREITINGER, J., SCOZIO, M., UNADKAT, J. & FEILI-HARIRI, M. (2008) Co-infusion of donor bone marrow with host mesenchymal stem cells treats GVHD and promotes vascularized skin allograft survival in rats. *Clin Immunol,* 127**,** 348-58.

ALROY, I., TOWERS, T. L. & FREEDMAN, L. P. (1995) Transcriptional repression of the interleukin-2 gene by vitamin D3: direct inhibition of NFATp/AP-1 complex formation by a nuclear hormone receptor. *Mol Cell Biol,* 15**,** 5789-99.

ALVAREZ, R. J., SUN, M. J., HAVERTY, T. P., IOZZO, R. V., MYERS, J. C. & NEILSON, E. G. (1992) Biosynthetic and proliferative characteristics of tubulointerstitial fibroblasts probed with paracrine cytokines. *Kidney Int,* 41**,** 14-23.

ANDERS, H. J., VIELHAUER, V., FRINK, M., LINDE, Y., COHEN, C. D., BLATTNER, S. M., KRETZLER, M., STRUTZ, F., MACK, M., GRONE, H. J., ONUFFER, J., HORUK, R., NELSON, P. J. & SCHLONDORFF, D. (2002) A chemokine receptor CCR-1 antagonist reduces renal fibrosis after unilateral ureter ligation. *J Clin Invest,* 109**,** 251-9.

ANDERSON, P., SOUZA-MOREIRA, L., MORELL, M., CARO, M., O'VALLE, F., GONZALEZ-REY, E. & DELGADO, M. (2012) Adipose-derived mesenchymal stromal cells induce immunomodulatory macrophages which protect from experimental colitis and sepsis. *Gut.*

ANKRUM, J. & KARP, J. M. (2010) Mesenchymal stem cell therapy: Two steps forward, one step back. *Trends Mol Med,* 16**,** 203-9.

ANNUNZIATO, F. & ROMAGNANI, S. (2011) Mouse T helper 17 phenotype: not so different than in man after all. *Cytokine,* 56**,** 112-5.

ASANUMA, H., VANDERBRINK, B. A., CAMPBELL, M. T., HILE, K. L., ZHANG, H., MELDRUM, D. R. & MELDRUM, K. K. (2011) Arterially delivered mesenchymal stem cells prevent obstruction-induced renal fibrosis. *J Surg Res,* 168**,** e51-9.

ASHBURN, T. T. & THOR, K. B. (2004) Drug repositioning: identifying and developing new uses for existing drugs. *Nat Rev Drug Discov,* 3**,** 673-83.

AUGELLO, A., TASSO, R., NEGRINI, S. M., AMATEIS, A., INDIVERI, F., CANCEDDA, R. & PENNESI, G. (2005) Bone marrow mesenchymal progenitor cells inhibit lymphocyte proliferation by activation of the programmed death 1 pathway. *Eur J Immunol,* 35**,** 1482-90.

AWASTHI, A. & KUCHROO, V. K. (2009) Th17 cells: from precursors to players in inflammation and infection. *Int. Immunol.,* 21**,** 489-498.

BAI, L., LENNON, D. P., CAPLAN, A. I., DECHANT, A., HECKER, J., KRANSO, J., ZAREMBA, A. & MILLER, R. H. (2012) Hepatocyte growth factor mediates mesenchymal stem cell-induced recovery in multiple sclerosis models. *Nat Neurosci,* 15**,** 862-870.

BAI, L., LENNON, D. P., EATON, V., MAIER, K., CAPLAN, A. I., MILLER, S. D. & MILLER, R. H. (2009) Human bone marrow-derived mesenchymal stem cells induce Th2-polarized immune response and promote endogenous repair in animal models of multiple sclerosis. *Glia,* 57**,** 1192-203.

BARRY, F. P. & MURPHY, J. M. (2004) Mesenchymal stem cells: clinical applications and biological characterization. *Int J Biochem Cell Biol,* 36**,** 568-84.

BARTHOLOMEW, A., STURGEON, C., SIATSKAS, M., FERRER, K., MCINTOSH, K., PATIL, S., HARDY, W., DEVINE, S., UCKER, D., DEANS, R., MOSELEY, A. & HOFFMAN, R. (2002) Mesenchymal stem cells suppress lymphocyte proliferation in vitro and prolong skin graft survival in vivo. *Exp Hematol,* 30**,** 42-8.

BATTEN, P., SARATHCHANDRA, P., ANTONIW, J. W., TAY, S. S., LOWDELL, M. W., TAYLOR, P. M. & YACOUB, M. H. (2006) Human mesenchymal stem cells induce T cell anergy and downregulate T cell allo-responses via the TH2 pathway: relevance to tissue engineering human heart valves. *Tissue Eng,* 12**,** 2263-73.

BI, B., SCHMITT, R., ISRAILOVA, M., NISHIO, H. & CANTLEY, L. G. (2007) Stromal cells protect against acute tubular injury via an endocrine effect. *J Am Soc Nephrol,* 18**,** 2486-96.

BONIFACE, K., BAK-JENSEN, K. S., LI, Y., BLUMENSCHEIN, W. M., MCGEACHY, M. J., MCCLANAHAN, T. K., MCKENZIE, B. S., KASTELEIN, R. A., CUA, D. J. & DE WAAL

MALEFYT, R. (2009) Prostaglandin E2 regulates Th17 cell differentiation and function through cyclic AMP and EP2/EP4 receptor signaling. *J Exp Med,* 206**,** 535-48.

BOUFFI, C., BONY, C., COURTIES, G., JORGENSEN, C. & NOÃ«L, D. L. (2010) IL-6-Dependent PGE2 Secretion by Mesenchymal Stem Cells Inhibits Local Inflammation in Experimental Arthritis. *PLoS ONE,* 5**,** e14247.

BOUMAZA, I., SRINIVASAN, S., WITT, W. T., FEGHALI-BOSTWICK, C., DAI, Y., GARCIA-OCANA, A. & FEILI-HARIRI, M. (2009) Autologous bone marrow-derived rat mesenchymal stem cells promote PDX-1 and insulin expression in the islets, alter T cell cytokine pattern and preserve regulatory T cells in the periphery and induce sustained normoglycemia. *J Autoimmun,* 32**,** 33-42.

BROWN, A. J., FINCH, J. & SLATOPOLSKY, E. (2002) Differential effects of 19-nor-1,25-dihydroxyvitamin D(2) and 1,25-dihydroxyvitamin D(3) on intestinal calcium and phosphate transport. *J Lab Clin Med,* 139**,** 279-84.

BRUCE, D., YU, S., OOI, J. H. & CANTORNA, M. T. (2011) Converging pathways lead to overproduction of IL-17 in the absence of vitamin D signaling. *Int Immunol,* 23**,** 519-28.

BRUNO, S., GRANGE, C., COLLINO, F., DEREGIBUS, M. C., CANTALUPPI, V., BIANCONE, L., TETTA, C. & CAMUSSI, G. (2012) Microvesicles derived from mesenchymal stem cells enhance survival in a lethal model of acute kidney injury. *PLoS ONE,* 7**,** e33115.

BRUNO, S., GRANGE, C., DEREGIBUS, M. C., CALOGERO, R. A., SAVIOZZI, S., COLLINO, F., MORANDO, L., BUSCA, A., FALDA, M., BUSSOLATI, B., TETTA, C. & CAMUSSI, G. (2009) Mesenchymal stem cell-derived microvesicles protect against acute tubular injury. *J Am Soc Nephrol,* 20**,** 1053-67.

CAMPBELL, F. C., XU, H., EL-TANANI, M., CROWE, P. & BINGHAM, V. (2010) The yin and yang of vitamin D receptor (VDR) signaling in neoplastic progression: operational networks and tissue-specific growth control. *Biochem Pharmacol,* 79**,** 1-9.

CAMPBELL, N. A. & REECE, J. B. (Eds.) (2008) *Biology* Pearson Benjamin Cummings, 1301 Sansome Street, San Francisco, CA 94111.

CAPLAN, A. I. (2009) Why are MSCs therapeutic? New data: new insight. *J Pathol,* 217**,** 318-24.

CARLBERG, C., SEUTER, S. & HEIKKINEN, S. (2012) The first genome-wide view of vitamin D receptor locations and their mechanistic implications. *Anticancer Res,* 32**,** 271-82.

CARRION, F., NOVA, E., LUZ, P., APABLAZA, F. & FIGUEROA, F. (2010) Opposing effect of mesenchymal stem cells on Th1 and Th17 cell polarization according to the state of CD4(+) T cell activation. *Immunol Lett,* 135**,** 10-16.

CASIRAGHI, F., AZZOLLINI, N., CASSIS, P., IMBERTI, B., MORIGI, M., CUGINI, D., CAVINATO, R. A., TODESCHINI, M., SOLINI, S., SONZOGNI, A., PERICO, N., REMUZZI, G. & NORIS, M. (2008) Pretransplant infusion of mesenchymal stem cells prolongs the survival of a semiallogeneic heart transplant through the generation of regulatory T cells. *J Immunol,* 181**,** 3933-46.

CHANG, J. H., CHA, H. R., LEE, D. S., SEO, K. Y. & KWEON, M. N. (2010a) 1,25-Dihydroxyvitamin D3 inhibits the differentiation and migration of T(H)17 cells to protect against experimental autoimmune encephalomyelitis. *PLoS ONE,* 5**,** e12925.

CHANG, S. H., CHUNG, Y. & DONG, C. (2010b) Vitamin D suppresses Th17 cytokine production by inducing C/EBP homologous protein (CHOP) expression. *J Biol Chem,* 285**,** 38751-5.

CHEN, B., HU, J., LIAO, L., SUN, Z., HAN, Q., SONG, Z. & ZHAO, R. C. (2010a) Flk-1+ mesenchymal stem cells aggravate collagen-induced arthritis by up-regulating interleukin-6. *Clin Exp Immunol,* 159**,** 292-302.

CHEN, H., QIN, J., WEI, P., ZHANG, J., LI, Q., FU, L., LI, S., MA, C. & CONG, B. (2009) Effects of leukotriene B4 and prostaglandin E2 on the differentiation of murine Foxp3+ T regulatory cells and Th17 cells. *Prostaglandins Leukot Essent Fatty Acids,* 80**,** 195-200.

CHEN, Q., MURAMOTO, K., MASAAKI, N., DING, Y., YANG, H., MACKEY, M., LI, W., INOUE, Y., ACKERMANN, K., SHIROTA, H., MATSUMOTO, I., SPYVEE, M., SCHILLER, S., SUMIDA, T., GUSOVSKY, F. & LAMPHIER, M. (2010b) A novel antagonist of the prostaglandin E(2) EP(4) receptor inhibits Th1 differentiation and Th17 expansion and is orally active in arthritis models. *Br J Pharmacol,* 160**,** 292-310.

CHEVALIER, R. L., FORBES, M. S. & THORNHILL, B. A. (2009) Ureteral obstruction as a model of renal interstitial fibrosis and obstructive nephropathy. *Kidney Int,* 75**,** 1145-52.

CHIZZOLINI, C., CHICHEPORTICHE, R., ALVAREZ, M., DE RHAM, C., ROUX-LOMBARD, P., FERRARI-LACRAZ, S. & DAYER, J. M. (2008) Prostaglandin E2 synergistically with interleukin-23 favors human Th17 expansion. *Blood,* 112**,** 3696-703.

CHUNG, Y., CHANG, S. H., MARTINEZ, G. J., YANG, X. O., NURIEVA, R., KANG, H. S., MA, L., WATOWICH, S. S., JETTEN, A. M., TIAN, Q. & DONG, C. (2009) Critical regulation of early Th17 cell differentiation by interleukin-1 signaling. *Immunity,* 30**,** 576-87.

COFFMAN, R. L. (2010) The Origin of TH2 Responses. *Science,* 328**,** 1116-1117.

COLIN, E. M., ASMAWIDJAJA, P. S., VAN HAMBURG, J. P., MUS, A. M., VAN DRIEL, M., HAZES, J. M., VAN LEEUWEN, J. P. & LUBBERTS, E. (2010) 1,25-dihydroxyvitamin D3 modulates Th17 polarization and interleukin-22 expression by memory T cells from patients with early rheumatoid arthritis. *Arthritis Rheum,* 62**,** 132-42.

CUA, D. J., SHERLOCK, J., CHEN, Y., MURPHY, C. A., JOYCE, B., SEYMOUR, B., LUCIAN, L., TO, W., KWAN, S., CHURAKOVA, T., ZURAWSKI, S., WIEKOWSKI, M., LIRA, S. A., GORMAN, D., KASTELEIN, R. A. & SEDGWICK, J. D. (2003) Interleukin-23 rather than interleukin-12 is the critical cytokine for autoimmune inflammation of the brain. *Nature,* 421**,** 744-8.

CUTLER, A. J., LIMBANI, V., GIRDLESTONE, J. & NAVARRETE, C. V. (2010) Umbilical cord-derived mesenchymal stromal cells modulate monocyte function to suppress T cell proliferation. *J Immunol,* 185**,** 6617-23.

DANIEL, C., SARTORY, N. A., ZAHN, N., RADEKE, H. H. & STEIN, J. M. (2008) Immune modulatory treatment of trinitrobenzene sulfonic acid colitis with calcitriol is associated with a change of a T helper (Th) 1/Th17 to a Th2 and regulatory T cell profile. *J Pharmacol Exp Ther,* 324**,** 23-33.

DARLINGTON, P. J., BOIVIN, M. N., RENOUX, C., FRANCOIS, M., GALIPEAU, J., FREEDMAN, M. S., ATKINS, H. L., COHEN, J. A., SOLCHAGA, L. & BAR-OR, A. (2010) Reciprocal Th1 and Th17 regulation by mesenchymal stem cells: Implication for multiple sclerosis. *Ann Neurol,* 68**,** 540-5.

DEB, D. K., SUN, T., WONG, K. E., ZHANG, Z., NING, G., ZHANG, Y., KONG, J., SHI, H., CHANG, A. & LI, Y. C. (2010) Combined vitamin D analog and AT1 receptor antagonist synergistically block the development of kidney disease in a model of type 2 diabetes. *Kidney Int,* 77**,** 1000-9.

DI NICOLA, M., CARLO-STELLA, C., MAGNI, M., MILANESI, M., LONGONI, P. D., MATTEUCCI, P., GRISANTI, S. & GIANNI, A. M. (2002) Human bone marrow stromal cells suppress T-lymphocyte proliferation induced by cellular or nonspecific mitogenic stimuli. *Blood,* 99**,** 3838-43.

DONG, X., BACHMAN, L. A., MILLER, M. N., NATH, K. A. & GRIFFIN, M. D. (2008) Dendritic cells facilitate accumulation of IL-17 T cells in the kidney following acute renal obstruction. *Kidney Int,* 74**,** 1294-309.

DUFFY, M. M., RITTER, T., CEREDIG, R. & GRIFFIN, M. D. (2011) Mesenchymal stem cell effects on T-cell effector pathways. *Stem Cell Res Ther,* 2**,** 34.

DUIJVESTEIN, M., WILDENBERG, M. E., WELLING, M. M., HENNINK, S., MOLENDIJK, I., VAN ZUYLEN, V. L., BOSSE, T., VOS, A. C., DE JONGE-MULLER, E. S., ROELOFS, H., VAN DER WEERD, L., VERSPAGET, H. W., FIBBE, W. E., TE VELDE, A. A., VAN DEN BRINK, G. R. & HOMMES, D. W. (2011) Pretreatment with interferon-gamma enhances the therapeutic activity of mesenchymal stromal cells in animal models of colitis. *Stem Cells,* 29**,** 1549-58.

DURELLI, L., CONTI, L., CLERICO, M., BOSELLI, D., CONTESSA, G., RIPELLINO, P., FERRERO, B., EID, P. & NOVELLI, F. (2009) T-helper 17 cells expand in multiple sclerosis and are inhibited by interferon-beta. *Ann Neurol,* 65**,** 499-509.

EIS, V., LUCKOW, B., VIELHAUER, V., SIVEKE, J. T., LINDE, Y., SEGERER, S., PEREZ DE LEMA, G., COHEN, C. D., KRETZLER, M., MACK, M., HORUK, R., MURPHY, P. M., GAO, J. L., HUDKINS, K. L., ALPERS, C. E., GRONE, H. J., SCHLONDORFF, D. & ANDERS, H. J. (2004) Chemokine receptor CCR1 but not CCR5 mediates leukocyte recruitment and subsequent renal fibrosis after unilateral ureteral obstruction. *J Am Soc Nephrol,* 15**,** 337-47.

ENGLISH, K., BARRY, F. P., FIELD-CORBETT, C. P. & MAHON, B. P. (2007) IFN-gamma and TNF-alpha differentially regulate immunomodulation by murine mesenchymal stem cells. *Immunol Lett,* 110**,** 91-100.

ENGLISH, K., FRENCH, A. & WOOD, K. J. (2010) Mesenchymal stromal cells: facilitators of successful transplantation? *Cell Stem Cell,* 7**,** 431-42.

ENGLISH, K., RYAN, J. M., TOBIN, L., MURPHY, M. J., BARRY, F. P. & MAHON, B. P. (2009) Cell contact, prostaglandin E(2) and transforming growth factor beta 1 play non-redundant

roles in human mesenchymal stem cell induction of CD4+CD25(High) forkhead box P3+ regulatory T cells. *Clin Exp Immunol,* 156**,** 149-60.

ESAKI, Y., LI, Y., SAKATA, D., YAO, C., SEGI-NISHIDA, E., MATSUOKA, T., FUKUDA, K. & NARUMIYA, S. (2010) Dual roles of PGE2-EP4 signaling in mouse experimental autoimmune encephalomyelitis. *Proc Natl Acad Sci U S A,* 107**,** 12233-8.

ESPINOSA, V. & RIVERA, A. (2012) Cytokines and the regulation of fungus-specific CD4 T cell differentiation. *Cytokine,* 58**,** 100-6.

ESPLUGUES, E., HUBER, S., GAGLIANI, N., HAUSER, A. E., TOWN, T., WAN, Y. Y., O'CONNOR, W., JR., RONGVAUX, A., VAN ROOIJEN, N., HABERMAN, A. M., IWAKURA, Y., KUCHROO, V. K., KOLLS, J. K., BLUESTONE, J. A., HEROLD, K. C. & FLAVELL, R. A. (2011) Control of TH17 cells occurs in the small intestine. *Nature,* 475**,** 514-8.

FIORINA, P., JUREWICZ, M., AUGELLO, A., VERGANI, A., DADA, S., LA ROSA, S., SELIG, M., GODWIN, J., LAW, K., PLACIDI, C., SMITH, R. N., CAPELLA, C., RODIG, S., ADRA, C. N., ATKINSON, M., SAYEGH, M. H. & ABDI, R. (2009) Immunomodulatory function of bone marrow-derived mesenchymal stem cells in experimental autoimmune type 1 diabetes. *J Immunol,* 183**,** 993-1004.

FLANAGAN, K., FITZGERALD, K., BAKER, J., REGNSTROM, K., GARDAI, S., BARD, F., MOCCI, S., SETO, P., YOU, M., LAROCHELLE, C., PRAT, A., CHOW, S., LI, L., VANDEVERT, C., ZAGO, W., LORENZANA, C., NISHIOKA, C., HOFFMAN, J., BOTELHO, R., WILLITS, C., TANAKA, K., JOHNSTON, J. & YEDNOCK, T. (2012) Laminin-411 Is a Vascular Ligand for MCAM and Facilitates TH17 Cell Entry into the CNS. *PLoS ONE,* 7**,** e40443.

FOUDI, N., KOTELEVETS, L., LOUEDEC, L., LESECHE, G., HENIN, D., CHASTRE, E. & NOREL, X. (2008) Vasorelaxation induced by prostaglandin E2 in human pulmonary vein: role of the EP4 receptor subtype. *Br J Pharmacol,* 154**,** 1631-9.

FRIEDENSTEIN, A. J., PIATETZKY, S., II & PETRAKOVA, K. V. (1966) Osteogenesis in transplants of bone marrow cells. *J Embryol Exp Morphol,* 16**,** 381-90.

GAFFEN, S. L. (2009) Structure and signalling in the IL-17 receptor family. *Nat Rev Immunol,* 9**,** 556-67.

GE, W., JIANG, J., ARP, J., LIU, W., GARCIA, B. & WANG, H. (2010) Regulatory T-cell generation and kidney allograft tolerance induced by mesenchymal stem cells associated with indoleamine 2,3-dioxygenase expression. *Transplantation,* 90**,** 1312-20.

GHANNAM, S., PENE, J., TORCY-MOQUET, G., JORGENSEN, C. & YSSEL, H. (2010) Mesenchymal stem cells inhibit human Th17 cell differentiation and function and induce a T regulatory cell phenotype. *J Immunol,* 185**,** 302-12.

GIESEKE, F., BOHRINGER, J., BUSSOLARI, R., DOMINICI, M., HANDGRETINGER, R. & MULLER, I. (2010) Human multipotent mesenchymal stromal cells use galectin-1 to inhibit immune effector cells. *Blood,* 116**,** 3770-9.

GONZALEZ-REY, E., GONZALEZ, M. A., VARELA, N., O'VALLE, F., HERNANDEZ-CORTES, P., RICO, L., BUSCHER, D. & DELGADO, M. (2010) Human adipose-derived mesenchymal stem cells reduce inflammatory and T cell responses and induce regulatory T cells in vitro in rheumatoid arthritis. *Ann Rheum Dis,* 69**,** 241-8.

GONZALEZ, M. A., GONZALEZ-REY, E., RICO, L., BUSCHER, D. & DELGADO, M. (2009) Adipose-derived mesenchymal stem cells alleviate experimental colitis by inhibiting inflammatory and autoimmune responses. *Gastroenterology,* 136**,** 978-89.

GOODWIN, M., SUEBLINVONG, V., EISENHAUER, P., ZIATS, N. P., LECLAIR, L., POYNTER, M. E., STEELE, C., RINCON, M. & WEISS, D. J. (2011) Bone marrow-derived mesenchymal stromal cells inhibit Th2-mediated allergic airways inflammation in mice. *Stem Cells,* 29**,** 1137-48.

GRANDE, M. T., PEREZ-BARRIOCANAL, F. & LOPEZ-NOVOA, J. M. (2010) Role of inflammation in tubulo-interstitial damage associated to obstructive nephropathy. *J Inflamm (Lond),* 7**,** 19.

GRIFFIN, M. D., RITTER, T. & MAHON, B. P. (2010) Immunological aspects of allogeneic mesenchymal stem cell therapies. *Hum Gene Ther,* 21**,** 1641-55.

GRIFFIN, M. D., XING, N. & KUMAR, R. (2003) Vitamin D and its analogs as regulators of immune activation and antigen presentation. *Annu Rev Nutr,* 23**,** 117-45.

GRUBER, H. E., SOMAYAJI, S., RILEY, F., HOELSCHER, G. L., NORTON, H. J., INGRAM, J. & HANLEY, E. N., JR. (2012) Human adipose-derived mesenchymal stem cells: serial passaging, doubling time and cell senescence. *Biotech Histochem,* 87**,** 303-11.

GUO, Z., ZHENG, C., CHEN, Z., GU, D., DU, W., GE, J., HAN, Z. & YANG, R. (2009) Fetal BM-derived mesenchymal stem cells promote the expansion of human Th17 cells, but inhibit the production of Th1 cells. *Eur J Immunol,* 39**,** 2840-9.

HE, J., WANG, Y., SUN, S., YU, M., WANG, C., PEI, X., ZHU, B., WU, J. & ZHAO, W. (2012) Bone marrow stem cells-derived microvesicles protect against renal injury in the mouse remnant kidney model. *Nephrology (Carlton),* 17**,** 493-500.

HERMANN-KLEITER, N. & BAIER, G. (2010) NFAT pulls the strings during CD4+ T helper cell effector functions. *Blood,* 115**,** 2989-2997.

HERRERA, M. B., BUSSOLATI, B., BRUNO, S., MORANDO, L., MAURIELLO-ROMANAZZI, G., SANAVIO, F., STAMENKOVIC, I., BIANCONE, L. & CAMUSSI, G. (2007) Exogenous mesenchymal stem cells localize to the kidney by means of CD44 following acute tubular injury. *Kidney Int,* 72**,** 430-41.

HIRAHARA, K., GHORESCHI, K., LAURENCE, A., YANG, X. P., KANNO, Y. & O'SHEA, J. J. (2010) Signal transduction pathways and transcriptional regulation in Th17 cell differentiation. *Cytokine Growth Factor Rev,* 21**,** 425-34.

HWANG, E. S. (2010) Transcriptional regulation of T helper 17 cell differentiation. *Yonsei Med J,* 51**,** 484-91.

IKEDA, U., WAKITA, D., OHKURI, T., CHAMOTO, K., KITAMURA, H., IWAKURA, Y. & NISHIMURA, T. (2010) 1alpha,25-Dihydroxyvitamin D3 and all-trans retinoic acid synergistically inhibit the differentiation and expansion of Th17 cells. *Immunol Lett,* 134**,** 7-16.

IVANOV, II, ZHOU, L. & LITTMAN, D. R. (2007) Transcriptional regulation of Th17 cell differentiation. *Semin Immunol,* 19**,** 409-17.

JANEWAY, C. (Ed.) (2008) *Janeway's Immunobiology,* Garland Science, Taylor & Francis Group, LLC, 270 Madison Avenue, New York, NY 10016, US.

JOSHI, S., PANTALENA, L. C., LIU, X. K., GAFFEN, S. L., LIU, H., ROHOWSKY-KOCHAN, C., ICHIYAMA, K., YOSHIMURA, A., STEINMAN, L., CHRISTAKOS, S. & YOUSSEF, S. (2011) 1,25-dihydroxyvitamin D(3) ameliorates Th17 autoimmunity via transcriptional modulation of interleukin-17A. *Mol Cell Biol,* 31**,** 3653-69.

KABASHIMA, K., SAJI, T., MURATA, T., NAGAMACHI, M., MATSUOKA, T., SEGI, E., TSUBOI, K., SUGIMOTO, Y., KOBAYASHI, T., MIYACHI, Y., ICHIKAWA, A. & NARUMIYA, S. (2002) The prostaglandin receptor EP4 suppresses colitis, mucosal damage and CD4 cell activation in the gut. *J Clin Invest,* 109**,** 883-93.

KAECH, S. M., WHERRY, E. J. & AHMED, R. (2002) Effector and memory T-cell differentiation: implications for vaccine development. *Nat Rev Immunol,* 2**,** 251-262.

KALINSKI, P. (2012) Regulation of immune responses by prostaglandin E2. *J Immunol,* 188**,** 21-8.

KARLSSON, H., SAMARASINGHE, S., BALL, L. M., SUNDBERG, B., LANKESTER, A. C., DAZZI, F., UZUNEL, M., RAO, K., VEYS, P., LE BLANC, K., RINGDEN, O. & AMROLIA, P. J. (2008) Mesenchymal stem cells exert differential effects on alloantigen and virus-specific T-cell responses. *Blood,* 112**,** 532-41.

KAVANAGH, H. & MAHON, B. P. (2010) Allogeneic mesenchymal stem cells prevent allergic airway inflammation by inducing murine regulatory T cells. *Allergy,* 66**,** 523-531.

KHAYRULLINA, T., YEN, J. H., JING, H. & GANEA, D. (2008) In vitro differentiation of dendritic cells in the presence of prostaglandin E2 alters the IL-12/IL-23 balance and promotes differentiation of Th17 cells. *J Immunol,* 181**,** 721-35.

KHOO, A. L., KOENEN, H. J., CHAI, L. Y., SWEEP, F. C., NETEA, M. G., VAN DER VEN, A. J. & JOOSTEN, I. (2012) Seasonal variation in vitamin D(3) levels is paralleled by changes in the peripheral blood human T cell compartment. *PLoS ONE,* 7**,** e29250.

KIM, J., DENU, R. A., DOLLAR, B. A., ESCALANTE, L. E., KUETHER, J. P., CALLANDER, N. S., ASIMAKOPOULOS, F. & HEMATTI, P. (2012) Macrophages and mesenchymal stromal cells support survival and proliferation of multiple myeloma cells. *Br J Haematol,* 158**,** 336-46.

KITCHING, A. R. & HOLDSWORTH, S. R. (2011) The emergence of TH17 cells as effectors of renal injury. *J Am Soc Nephrol,* 22**,** 235-8.

KOLLS, J. K. & LINDEN, A. (2004) Interleukin-17 family members and inflammation. *Immunity,* 21**,** 467-76.

KONG, Q. F., SUN, B., WANG, G. Y., ZHAI, D. X., MU, L. L., WANG, D. D., WANG, J. H., LI, R. & LI, H. L. (2009) BM stromal cells ameliorate experimental autoimmune myasthenia gravis by altering the balance of Th cells through the secretion of IDO. *Eur J Immunol,* 39**,** 800-9.

KORN, T., BETTELLI, E., OUKKA, M. & KUCHROO, V. K. (2009) IL-17 and Th17 Cells. *Annu Rev Immunol,* 27**,** 485-517.

KRAMPERA, M., COSMI, L., ANGELI, R., PASINI, A., LIOTTA, F., ANDREINI, A., SANTARLASCI, V., MAZZINGHI, B., PIZZOLO, G., VINANTE, F., ROMAGNANI, P., MAGGI, E., ROMAGNANI, S. & ANNUNZIATO, F. (2006) Role for interferon-gamma in the immunomodulatory activity of human bone marrow mesenchymal stem cells. *Stem Cells,* 24**,** 386-98.

KRAMPERA, M., GLENNIE, S., DYSON, J., SCOTT, D., LAYLOR, R., SIMPSON, E. & DAZZI, F. (2003) Bone marrow mesenchymal stem cells inhibit the response of naive and memory antigen-specific T cells to their cognate peptide. *Blood,* 101**,** 3722-9.

KUSHIYAMA, T., ODA, T., YAMADA, M., HIGASHI, K., YAMAMOTO, K., SAKURAI, Y., MIURA, S. & KUMAGAI, H. (2011) Alteration in the phenotype of macrophages in the repair of renal interstitial fibrosis in mice. *Nephrology (Carlton),* 16**,** 522-35.

LANGE, C., TOGEL, F., ITTRICH, H., CLAYTON, F., NOLTE-ERNSTING, C., ZANDER, A. R. & WESTENFELDER, C. (2005) Administered mesenchymal stem cells enhance recovery from ischemia/reperfusion-induced acute renal failure in rats. *Kidney Int,* 68**,** 1613-7.

LANGRISH, C. L., CHEN, Y., BLUMENSCHEIN, W. M., MATTSON, J., BASHAM, B., SEDGWICK, J. D., MCCLANAHAN, T., KASTELEIN, R. A. & CUA, D. J. (2005) IL-23 drives a pathogenic T cell population that induces autoimmune inflammation. *J Exp Med,* 201**,** 233-40.

LAZAREVIC, V., CHEN, X., SHIM, J. H., HWANG, E. S., JANG, E., BOLM, A. N., OUKKA, M., KUCHROO, V. K. & GLIMCHER, L. H. (2011) T-bet represses T(H)17 differentiation by preventing Runx1-mediated activation of the gene encoding RORgammat. *Nat Immunol,* 12**,** 96-104.

LE BLANC, K. & MOUGIAKAKOS, D. (2012) Multipotent mesenchymal stromal cells and the innate immune system. *Nat Rev Immunol,* 12**,** 383-96.

LEE, R. H., PULIN, A. A., SEO, M. J., KOTA, D. J., YLOSTALO, J., LARSON, B. L., SEMPRUN-PRIETO, L., DELAFONTAINE, P. & PROCKOP, D. J. (2009) Intravenous hMSCs improve myocardial infarction in mice because cells embolized in lung are activated to secrete the anti-inflammatory protein TSG-6. *Cell Stem Cell,* 5**,** 54-63.

LEE, S. Y., LEE, M. Y., PARK, S. H., KIM, T. H., MOON, Y. T., HAN, J. H. & MYUNG, S. C. (2010) NS-398 (a selective cyclooxygenase-2 inhibitor) decreases agonist-induced contraction of the human ureter via calcium channel inhibition. *J Endourol,* 24**,** 1863-8.

LEONARDI, C., MATHESON, R., ZACHARIAE, C., CAMERON, G., LI, L., EDSON-HEREDIA, E., BRAUN, D. & BANERJEE, S. (2012) Anti–Interleukin-17 Monoclonal Antibody Ixekizumab in Chronic Plaque Psoriasis. *New England Journal of Medicine,* 366**,** 1190-1199.

LIANG, L., DONG, C., CHEN, X., FANG, Z., XU, J., LIU, M., ZHANG, X., GU, D. S., WANG, D., DU, W., ZHU, D. & HAN, Z. C. (2011) Human umbilical cord mesenchymal stem cells ameliorate mice trinitrobenzene sulfonic acid (TNBS)-induced colitis. *Cell Transplant,* 20**,** 1395-408.

LIM, J. H., KIM, J. S., YOON, I. H., SHIN, J. S., NAM, H. Y., YANG, S. H., KIM, S. J. & PARK, C. G. (2010) Immunomodulation of delayed-type hypersensitivity responses by mesenchymal stem cells is associated with bystander T cell apoptosis in the draining lymph node. *J Immunol,* 185**,** 4022-9.

LIU, X., SHEN, W., YANG, Y. & LIU, G. (2011) Therapeutic implications of mesenchymal stem cells transfected with hepatocyte growth factor transplanted in rat kidney with unilateral ureteral obstruction. *J Pediatr Surg,* 46**,** 537-45.

LIU, Y. (2004) Epithelial to mesenchymal transition in renal fibrogenesis: pathologic significance, molecular mechanism, and therapeutic intervention. *J Am Soc Nephrol,* 15**,** 1-12.

LIU, Y. L., WANG, Y. D., ZHUANG, F., XIAN, S. L., FANG, J. Y., SU, W. & ZHANG, W. (2012) Immunosuppression effects of bone marrow mesenchymal stem cells on renal interstitial injury in rats with unilateral ureteral obstruction. *Cell Immunol,* 276**,** 144-52.

LO SURDO, J. & BAUER, S. R. (2012) Quantitative Approaches to Detect Donor and Passage Differences in Adipogenic Potential and Clonogenicity in Human Bone Marrow-Derived Mesenchymal Stem Cells. *Tissue Eng Part C Methods,* epub.

LOSSIUS, A., VARTDAL, F. & HOLMOY, T. (2011) Vitamin D sensitive EBNA-1 specific T cells in the cerebrospinal fluid of patients with multiple sclerosis. *J Neuroimmunol,* 240**,** 87-96.

LU, L., WANG, J., ZHANG, F., CHAI, Y., BRAND, D., WANG, X., HORWITZ, D. A., SHI, W. & ZHENG, S. G. (2010) Role of SMAD and non-SMAD signals in the development of Th17 and regulatory T cells. *J Immunol,* 184**,** 4295-306.

MADEC, A. M., MALLONE, R., AFONSO, G., ABOU MRAD, E., MESNIER, A., ELJAAFARI, A. & THIVOLET, C. (2009) Mesenchymal stem cells protect NOD mice from diabetes by inducing regulatory T cells. *Diabetologia,* 52**,** 1391-9.

MADEIRA, A., DA SILVA, C. L., DOS SANTOS, F., CAMAFEITA, E., CABRAL, J. M. & SA-CORREIA, I. (2012) Human Mesenchymal Stem Cell Expression Program upon Extended Ex-Vivo Cultivation, as Revealed by 2-DE-Based Quantitative Proteomics. *PLoS ONE,* 7**,** e43523.

MAYNE, C. G., SPANIER, J. A., RELLAND, L. M., WILLIAMS, C. B. & HAYES, C. E. (2011) 1,25-Dihydroxyvitamin D3 acts directly on the T lymphocyte vitamin D receptor to inhibit experimental autoimmune encephalomyelitis. *Eur J Immunol,* 41**,** 822-32.

MCALLISTER, F., HENRY, A., KREINDLER, J. L., DUBIN, P. J., ULRICH, L., STEELE, C., FINDER, J. D., PILEWSKI, J. M., CARRENO, B. M., GOLDMAN, S. J., PIRHONEN, J. & KOLLS, J. K. (2005) Role of IL-17A, IL-17F, and the IL-17 receptor in regulating growth-related oncogene-alpha and granulocyte colony-stimulating factor in bronchial epithelium: implications for airway inflammation in cystic fibrosis. *J Immunol,* 175**,** 404-12.

MCGOVERN, J. L., NGUYEN, D. X., NOTLEY, C. A., MAURI, C., ISENBERG, D. A. & EHRENSTEIN, M. R. (2012) Th17 cells are restrained by regulatory T cells from patients responding to anti-TNF antibody therapy via inhibition of IL-6. *Arthritis Rheum,* epub.

MENDEZ-FERRER, S., MICHURINA, T. V., FERRARO, F., MAZLOOM, A. R., MACARTHUR, B. D., LIRA, S. A., SCADDEN, D. T., MA'AYAN, A., ENIKOLOPOV, G. N. & FRENETTE, P. S. (2010) Mesenchymal and haematopoietic stem cells form a unique bone marrow niche. *Nature,* 466**,** 829-34.

MILLER, S. B. (2006) Prostaglandins in health and disease: an overview. *Semin Arthritis Rheum,* 36**,** 37-49.

MILLS, K. H. (2008) Induction, function and regulation of IL-17-producing T cells. *Eur J Immunol,* 38**,** 2636-49.

MISSERI, R., RINK, R. C., MELDRUM, D. R. & MELDRUM, K. K. (2004) Inflammatory mediators and growth factors in obstructive renal injury. *J Surg Res,* 119**,** 149-59.

MOLL, G., RASMUSSON-DUPREZ, I., VON BAHR, L., CONNOLLY-ANDERSEN, A. M., ELGUE, G., FUNKE, L., HAMAD, O. A., LONNIES, H., MAGNUSSON, P. U., SANCHEZ, J., TERAMURA, Y., NILSSON-EKDAHL, K., RINGDEN, O., KORSGREN, O., NILSSON, B. & LE BLANC, K. (2012) Are therapeutic human mesenchymal stromal cells compatible with human blood? *Stem Cells,* 30**,** 1565-74.

MORA, J. R., IWATA, M. & VON ANDRIAN, U. H. (2008) Vitamin effects on the immune system: vitamins A and D take centre stage. *Nat Rev Immunol,* 8**,** 685-98.

MORIGI, M., IMBERTI, B., ZOJA, C., CORNA, D., TOMASONI, S., ABBATE, M., ROTTOLI, D., ANGIOLETTI, S., BENIGNI, A., PERICO, N., ALISON, M. & REMUZZI, G. (2004) Mesenchymal stem cells are renotropic, helping to repair the kidney and improve function in acute renal failure. *J Am Soc Nephrol,* 15**,** 1794-804.

MORIGI, M., INTRONA, M., IMBERTI, B., CORNA, D., ABBATE, M., ROTA, C., ROTTOLI, D., BENIGNI, A., PERICO, N., ZOJA, C., RAMBALDI, A., REMUZZI, A. & REMUZZI, G. (2008) Human bone marrow mesenchymal stem cells accelerate recovery of acute renal injury and prolong survival in mice. *Stem Cells,* 26**,** 2075-82.

MORIKAWA, S., MABUCHI, Y., KUBOTA, Y., NAGAI, Y., NIIBE, K., HIRATSU, E., SUZUKI, S., MIYAUCHI-HARA, C., NAGOSHI, N., SUNABORI, T., SHIMMURA, S., MIYAWAKI, A., NAKAGAWA, T., SUDA, T., OKANO, H. & MATSUZAKI, Y. (2009) Prospective identification, isolation, and systemic transplantation of multipotent mesenchymal stem cells in murine bone marrow. *J Exp Med,* 206**,** 2483-96.

MOSMANN, T. R. & COFFMAN, R. L. (1989) TH1 and TH2 cells: different patterns of lymphokine secretion lead to different functional properties. *Annu Rev Immunol,* 7**,** 145-73.

MURPHY, C. A., LANGRISH, C. L., CHEN, Y., BLUMENSCHEIN, W., MCCLANAHAN, T., KASTELEIN, R. A., SEDGWICK, J. D. & CUA, D. J. (2003) Divergent pro- and antiinflammatory roles for IL-23 and IL-12 in joint autoimmune inflammation. *J Exp Med,* 198**,** 1951-7.

NA, S., MA, Y., ZHAO, J., SCHMIDT, C., ZENG, Q. Q., CHANDRASEKHAR, S., CHIN, W. W. & NAGPAL, S. (2011) A Nonsecosteroidal Vitamin D Receptor Modulator Ameliorates Experimental Autoimmune Encephalomyelitis without Causing Hypercalcemia. *Autoimmune Dis,* 2011.

NAKAGAWA, N., YUHKI, K., KAWABE, J., FUJINO, T., TAKAHATA, O., KABARA, M., ABE, K., KOJIMA, F., KASHIWAGI, H., HASEBE, N., KIKUCHI, K., SUGIMOTO, Y.,

NARUMIYA, S. & USHIKUBI, F. (2012) The intrinsic prostaglandin E2-EP4 system of the renal tubular epithelium limits the development of tubulointerstitial fibrosis in mice. *Kidney Int,* 82**,** 158-71.

NAPOLITANI, G., ACOSTA-RODRIGUEZ, E. V., LANZAVECCHIA, A. & SALLUSTO, F. (2009) Prostaglandin E2 enhances Th17 responses via modulation of IL-17 and IFN-gamma production by memory CD4+ T cells. *Eur J Immunol,* 39**,** 1301-12.

NAVEH-MANY, T., MARX, R., KESHET, E., PIKE, J. W. & SILVER, J. (1990) Regulation of 1,25-dihydroxyvitamin D3 receptor gene expression by 1,25-dihydroxyvitamin D3 in the parathyroid in vivo. *J Clin Invest,* 86**,** 1968-75.

NEMETH, K., LEELAHAVANICHKUL, A., YUEN, P. S., MAYER, B., PARMELEE, A., DOI, K., ROBEY, P. G., LEELAHAVANICHKUL, K., KOLLER, B. H., BROWN, J. M., HU, X., JELINEK, I., STAR, R. A. & MEZEY, E. (2009) Bone marrow stromal cells attenuate sepsis via prostaglandin E(2)-dependent reprogramming of host macrophages to increase their interleukin-10 production. *Nat Med,* 15**,** 42-9.

O'CONNOR, W., JR., ZENEWICZ, L. A. & FLAVELL, R. A. (2010) The dual nature of T(H)17 cells: shifting the focus to function. *Nat Immunol,* 11**,** 471-6.

O'SHEA, J. J., STEWARD-THARP, S. M., LAURENCE, A., WATFORD, W. T., WEI, L., ADAMSON, A. S. & FAN, S. (2009) Signal transduction and Th17 cell differentiation. *Microbes Infect,* 11**,** 599-611.

OH, D. Y., CUI, P., HOSSEINI, H., MOSSE, J., TOH, B. H. & CHAN, J. (2012) Potently immunosuppressive 5-fluorouracil-resistant mesenchymal stromal cells completely remit an experimental autoimmune disease. *J Immunol,* 188**,** 2207-17.

OU-YANG, H. F., HUANG, Y., HU, X. B. & WU, C. G. (2011) Suppression of allergic airway inflammation in a mouse model of asthma by exogenous mesenchymal stem cells. *Exp Biol Med (Maywood),* 236**,** 1461-7.

OUYANG, W., KOLLS, J. K. & ZHENG, Y. (2008) The biological functions of T helper 17 cell effector cytokines in inflammation. *Immunity,* 28**,** 454-67.

OYADOMARI, S. & MORI, M. (2004) Roles of CHOP/GADD153 in endoplasmic reticulum stress. *Cell Death Differ,* 11**,** 381-9.

PALMER, M. T., LEE, Y. K., MAYNARD, C. L., OLIVER, J. R., BIKLE, D. D., JETTEN, A. M. & WEAVER, C. T. (2011) Lineage-specific effects of 1,25-dihydroxyvitamin D(3) on the development of effector CD4 T cells. *J Biol Chem,* 286**,** 997-1004.

PAN, L. C. & PRICE, P. A. (1987) Ligand-dependent regulation of the 1,25-dihydroxyvitamin D3 receptor in rat osteosarcoma cells. *J Biol Chem,* 262**,** 4670-5.

PAPADOPOULOU, A., YIANGOU, M., ATHANASIOU, E., ZOGAS, N., KALOYANNIDIS, P., BATSIS, I., FASSAS, A., ANAGNOSTOPOULOS, A. & YANNAKI, E. (2012) Mesenchymal stem cells are conditionally therapeutic in preclinical models of rheumatoid arthritis. *Ann Rheum Dis,* 71**,** 1733-1740.

PARK, D., SPENCER, J. A., KOH, B. I., KOBAYASHI, T., FUJISAKI, J., CLEMENS, T. L., LIN, C. P., KRONENBERG, H. M. & SCADDEN, D. T. (2012) Endogenous bone marrow MSCs are dynamic, fate-restricted participants in bone maintenance and regeneration. *Cell Stem Cell,* 10**,** 259-72.

PARK, J. W., BAE, E. H., KIM, I. J., MA, S. K., CHOI, C., LEE, J. & KIM, S. W. (2010a) Paricalcitol attenuates cyclosporine-induced kidney injury in rats. *Kidney Int,* 77**,** 1076-85.

PARK, J. W., BAE, E. H., KIM, I. J., MA, S. K., CHOI, C., LEE, J. & KIM, S. W. (2010b) Renoprotective effects of paricalcitol on gentamicin-induced kidney injury in rats. *Am J Physiol Renal Physiol,* 298**,** F301-13.

PARK, M. J., PARK, H. S., CHO, M. L., OH, H. J., CHO, Y. G., MIN, S. Y., CHUNG, B. H., LEE, J. W., KIM, H. Y. & CHO, S. G. (2011) Transforming growth factor beta-transduced mesenchymal stem cells ameliorate experimental autoimmune arthritis through reciprocal regulation of Treg/Th17 cells and osteoclastogenesis. *Arthritis Rheum,* 63**,** 1668-80.

PATEL, S. A., MEYER, J. R., GRECO, S. J., CORCORAN, K. E., BRYAN, M. & RAMESHWAR, P. (2010) Mesenchymal stem cells protect breast cancer cells through regulatory T cells: role of mesenchymal stem cell-derived TGF-beta. *J Immunol,* 184**,** 5885-94.

PAUST, H. J., TURNER, J. E., STEINMETZ, O. M., PETERS, A., HEYMANN, F., HOLSCHER, C., WOLF, G., KURTS, C., MITTRUCKER, H. W., STAHL, R. A. & PANZER, U. (2009) The IL-23/Th17 axis contributes to renal injury in experimental glomerulonephritis. *J Am Soc Nephrol,* 20**,** 969-79.

PEISTER, A., MELLAD, J. A., LARSON, B. L., HALL, B. M., GIBSON, L. F. & PROCKOP, D. J. (2004) Adult stem cells from bone marrow (MSCs) isolated from different strains of inbred

mice vary in surface epitopes, rates of proliferation, and differentiation potential. *Blood,* 103**,** 1662-8.

PENNA, G., AMUCHASTEGUI, S., COSSETTI, C., AQUILANO, F., MARIANI, R., SANVITO, F., DOGLIONI, C. & ADORINI, L. (2006) Treatment of experimental autoimmune prostatitis in nonobese diabetic mice by the vitamin D receptor agonist elocalcitol. *J Immunol,* 177**,** 8504-11.

PINDJAKOVA, J., HANLEY, S. A., DUFFY, M. M., SUTTON, C. E., WEIDHOFER, G. A., MILLER, M. N., NATH, K. A., MILLS, K. H., CEREDIG, R. & GRIFFIN, M. D. (2012) Interleukin-1 accounts for intrarenal Th17 cell activation during ureteral obstruction. *Kidney Int,* 81**,** 379-390.

PRADIER, A., PASSWEG, J., VILLARD, J. & KINDLER, V. (2011) Human bone marrow stromal cells and skin fibroblasts inhibit natural killer cell proliferation and cytotoxic activity. *Cell Transplant,* 20**,** 681-91.

QU, X., LIU, X., CHENG, K., YANG, R. & ZHAO, R. C. (2012) Mesenchymal stem cells inhibit Th17 cell differentiation by IL-10 secretion. *Exp Hematol,* 40**,** 761-70.

RAFEI, M., CAMPEAU, P. M., AGUILAR-MAHECHA, A., BUCHANAN, M., WILLIAMS, P., BIRMAN, E., YUAN, S., YOUNG, Y. K., BOIVIN, M.-N. L., FORNER, K., BASIK, M. & GALIPEAU, J. (2009) Mesenchymal Stromal Cells Ameliorate Experimental Autoimmune Encephalomyelitis by Inhibiting CD4 Th17 T Cells in a CC Chemokine Ligand 2-Dependent Manner. *The Journal of Immunology,* 182**,** 5994-6002.

RAFFAGHELLO, L., BIANCHI, G., BERTOLOTTO, M., MONTECUCCO, F., BUSCA, A., DALLEGRI, F., OTTONELLO, L. & PISTOIA, V. (2008) Human mesenchymal stem cells inhibit neutrophil apoptosis: a model for neutrophil preservation in the bone marrow niche. *Stem Cells,* 26**,** 151-62.

RAJAKARIAR, R., YAQOOB, M. M. & GILROY, D. W. (2006) COX-2 in inflammation and resolution. *Mol Interv,* 6**,** 199-207.

RASMUSSON, I., UHLIN, M., LE BLANC, K. & LEVITSKY, V. (2007) Mesenchymal stem cells fail to trigger effector functions of cytotoxic T lymphocytes. *J Leukoc Biol,* 82**,** 887-93.

REN, G., ZHAO, X., ZHANG, L., ZHANG, J., L'HUILLIER, A., LING, W., ROBERTS, A. I., LE, A. D., SHI, S., SHAO, C. & SHI, Y. (2010) Inflammatory cytokine-induced intercellular adhesion molecule-1 and vascular cell adhesion molecule-1 in mesenchymal stem cells are critical for immunosuppression. *J Immunol,* 184**,** 2321-8.

ROUVIER, E., LUCIANI, M. F., MATTEI, M. G., DENIZOT, F. & GOLSTEIN, P. (1993) CTLA-8, cloned from an activated T cell, bearing AU-rich messenger RNA instability sequences, and homologous to a herpesvirus saimiri gene. *J Immunol,* 150**,** 5445-56.

RYAN, J. M., BARRY, F., MURPHY, J. M. & MAHON, B. P. (2007) Interferon-gamma does not break, but promotes the immunosuppressive capacity of adult human mesenchymal stem cells. *Clin Exp Immunol,* 149**,** 353-63.

SANCHEZ-NINO, M. D., BOZIC, M., CORDOBA-LANUS, E., VALCHEVA, P., GRACIA, O., IBARZ, M., FERNANDEZ, E., NAVARRO-GONZALEZ, J. F., ORTIZ, A. & VALDIVIELSO, J. M. (2012) Beyond proteinuria: VDR activation reduces renal inflammation in experimental diabetic nephropathy. *Am J Physiol Renal Physiol,* 302**,** F647-57.

SCHIRMER, C., KLEIN, C., VON BERGEN, M., SIMON, J. C. & SAALBACH, A. (2010) Human fibroblasts support the expansion of IL-17-producing T cells via up-regulation of IL-23 production by dendritic cells. *Blood,* 116**,** 1715-25.

SCHURGERS, E., KELCHTERMANS, H., MITERA, T., GEBOES, L. & MATTHYS, P. (2010) Discrepancy between the in vitro and in vivo effects of murine mesenchymal stem cells on T-cell proliferation and collagen-induced arthritis. *Arthritis Res Ther,* 12**,** R31.

SHEIBANIE, A. F., KHAYRULLINA, T., SAFADI, F. F. & GANEA, D. (2007a) Prostaglandin E2 exacerbates collagen-induced arthritis in mice through the inflammatory interleukin-23/interleukin-17 axis. *Arthritis Rheum,* 56**,** 2608-19.

SHEIBANIE, A. F., YEN, J. H., KHAYRULLINA, T., EMIG, F., ZHANG, M., TUMA, R. & GANEA, D. (2007b) The proinflammatory effect of prostaglandin E2 in experimental inflammatory bowel disease is mediated through the IL-23-->IL-17 axis. *J Immunol,* 178**,** 8138-47.

SHENG, H., WANG, Y., JIN, Y., ZHANG, Q., ZHANG, Y., WANG, L., SHEN, B., YIN, S., LIU, W., CUI, L. & LI, N. (2008) A critical role of IFNgamma in priming MSC-mediated suppression of T cell proliferation through up-regulation of B7-H1. *Cell Res,* 18**,** 846-57.

SREERAMKUMAR, V., FRESNO, M. & CUESTA, N. (2011) Prostaglandin E(2) and T cells: friends or foes? *Immunol Cell Biol,* 90**,** 579-86.

STEINMETZ, O. M., SUMMERS, S. A., GAN, P. Y., SEMPLE, T., HOLDSWORTH, S. R. & KITCHING, A. R. (2010) The Th17-defining transcription factor RORgammat promotes glomerulonephritis. *J Am Soc Nephrol,* 22**,** 472-83.

SUN, J., HAN, Z. B., LIAO, W., YANG, S. G., YANG, Z., YU, J., MENG, L., WU, R. & HAN, Z. C. (2011) Intrapulmonary delivery of human umbilical cord mesenchymal stem cells attenuates acute lung injury by expanding CD4+CD25+ Forkhead Boxp3 (FOXP3)+ regulatory T cells and balancing anti- and pro-inflammatory factors. *Cell Physiol Biochem,* 27**,** 587-96.

SUTTON, C., BRERETON, C., KEOGH, B., MILLS, K. H. & LAVELLE, E. C. (2006) A crucial role for interleukin (IL)-1 in the induction of IL-17-producing T cells that mediate autoimmune encephalomyelitis. *J Exp Med,* 203**,** 1685-91.

SVOBODOVA, E., KRULOVA, M., ZAJICOVA, A., POKORNA, K., PROCHAZKOVA, J., TROSAN, P. & HOLAN, V. (2011) The role of mouse mesenchymal stem cells in differentiation of naive T-cells into anti-inflammatory regulatory T-cell or proinflammatory helper T-cell 17 population. *Stem Cells Dev,* 21**,** 901-10.

SZODORAY, P., NAKKEN, B., GAAL, J., JONSSON, R., SZEGEDI, A., ZOLD, E., SZEGEDI, G., BRUN, J. G., GESZTELYI, R., ZEHER, M. & BODOLAY, E. (2008) The complex role of vitamin D in autoimmune diseases. *Scand J Immunol,* 68**,** 261-9.

TAKAYAMA, K., GARCIA-CARDENA, G., SUKHOVA, G. K., COMANDER, J., GIMBRONE, M. A., JR. & LIBBY, P. (2002) Prostaglandin E2 suppresses chemokine production in human macrophages through the EP4 receptor. *J Biol Chem,* 277**,** 44147-54.

TAN, A. H. & LAM, K. P. (2010) Pharmacologic inhibition of MEK-ERK signaling enhances Th17 differentiation. *J Immunol,* 184**,** 1849-57.

TAN, X., HE, W. & LIU, Y. (2009) Combination therapy with paricalcitol and trandolapril reduces renal fibrosis in obstructive nephropathy. *Kidney Int,* 76**,** 1248-57.

TAN, X., LI, Y. & LIU, Y. (2006) Paricalcitol attenuates renal interstitial fibrosis in obstructive nephropathy. *J Am Soc Nephrol,* 17**,** 3382-93.

TAN, X., WEN, X. & LIU, Y. (2008) Paricalcitol inhibits renal inflammation by promoting vitamin D receptor-mediated sequestration of NF-kappaB signaling. *J Am Soc Nephrol,* 19**,** 1741-52.

TANG, J., ZHOU, R., LUGER, D., ZHU, W., SILVER, P. B., GRAJEWSKI, R. S., SU, S. B., CHAN, C. C., ADORINI, L. & CASPI, R. R. (2009) Calcitriol suppresses antiretinal autoimmunity through inhibitory effects on the Th17 effector response. *J Immunol,* 182**,** 4624-32.

TATARA, R., OZAKI, K., KIKUCHI, Y., HATANAKA, K., OH, I., MEGURO, A., MATSU, H., SATO, K. & OZAWA, K. (2011) Mesenchymal stromal cells inhibit Th17 but not regulatory T-cell differentiation. *Cytotherapy,* 13.

TSO, G. H., LAW, H. K., TU, W., CHAN, G. C. & LAU, Y. L. (2010) Phagocytosis of apoptotic cells modulates mesenchymal stem cells osteogenic differentiation to enhance IL-17 and RANKL expression on CD4+ T cells. *Stem Cells,* 28**,** 939-54.

TURNER, J. E., PAUST, H. J., STEINMETZ, O. M. & PANZER, U. (2010a) The Th17 immune response in renal inflammation. *Kidney Int,* 77**,** 1070-5.

TURNER, J. E., PAUST, H. J., STEINMETZ, O. M., PETERS, A., RIEDEL, J. H., ERHARDT, A., WEGSCHEID, C., VELDEN, J., FEHR, S., MITTRUCKER, H. W., TIEGS, G., STAHL, R. A. & PANZER, U. (2010b) CCR6 recruits regulatory T cells and Th17 cells to the kidney in glomerulonephritis. *J Am Soc Nephrol,* 21**,** 974-85.

UCCELLI, A., MORETTA, L. & PISTOIA, V. (2008) Mesenchymal stem cells in health and disease. *Nat Rev Immunol,* 8**,** 726-36.

VALDEZ, P. A., VITHAYATHIL, P. J., JANELSINS, B. M., SHAFFER, A. L., WILLIAMSON, P. R. & DATTA, S. K. (2012) Prostaglandin E2 suppresses antifungal immunity by inhibiting interferon regulatory factor 4 function and interleukin-17 expression in T cells. *Immunity,* 36**,** 668-79.

VAN HAMBURG, J. P., ASMAWIDJAJA, P. S., DAVELAAR, N., MUS, A. M., CORNELISSEN, F., VAN LEEUWEN, J. P., HAZES, J. M., DOLHAIN, R. J., BAKX, P. A., COLIN, E. M. & LUBBERTS, E. (2012) TNF blockade requires 1,25(OH)2D3 to control human Th17-mediated synovial inflammation. *Ann Rheum Dis,* 71**,** 606-12.

VIELHAUER, V., ANDERS, H. J., MACK, M., CIHAK, J., STRUTZ, F., STANGASSINGER, M., LUCKOW, B., GRONE, H. J. & SCHLONDORFF, D. (2001) Obstructive nephropathy in the mouse: progressive fibrosis correlates with tubulointerstitial chemokine expression and accumulation of CC chemokine receptor 2- and 5-positive leukocytes. *J Am Soc Nephrol,* 12**,** 1173-87.

VILLANUEVA, S., EWERTZ, E., CARRION, F., TAPIA, A., VERGARA, C., CESPEDES, C., SAEZ, P. J., LUZ, P., IRARRAZABAL, C., CARRENO, J. E., FIGUEROA, F. & VIO, C. P. (2011) Mesenchymal stem cell injection ameliorates chronic renal failure in a rat model. *Clin Sci (Lond),* 121**,** 489-99.

WAN, Y. Y. & FLAVELL, R. A. (2009) How Diverse--CD4 Effector T Cells and their Functions. *J Mol Cell Biol,* 1**,** 20-36.

WANG, J., WANG, G., SUN, B., LI, H., MU, L., WANG, Q., LI, G., SHI, L., JIN, L. & KOSTULAS, N. (2008a) Interleukin-27 suppresses experimental autoimmune encephalomyelitis during bone marrow stromal cell treatment. *J Autoimmun,* 30**,** 222-9.

WANG, Q., SUN, B., WANG, D., JI, Y., KONG, Q., WANG, G., WANG, J., ZHAO, W., JIN, L. & LI, H. (2008b) Murine bone marrow mesenchymal stem cells cause mature dendritic cells to promote T-cell tolerance. *Scand J Immunol,* 68**,** 607-15.

WANG, Y., ZHANG, A., YE, Z., XIE, H. & ZHENG, S. (2009) Bone marrow-derived mesenchymal stem cells inhibit acute rejection of rat liver allografts in association with regulatory T-cell expansion. *Transplant Proc,* 41**,** 4352-6.

WEIDENBUSCH, M. & ANDERS, H. J. (2012) Tissue Microenvironments Define and Get Reinforced by Macrophage Phenotypes in Homeostasis or during Inflammation, Repair and Fibrosis. *J Innate Immun,* 4**,** 463-77.

WOODWARD, D. F., PEPPERL, D. J., BURKEY, T. H. & REGAN, J. W. (1995) 6-Isopropoxy-9-oxoxanthene-2-carboxylic acid (AH 6809), a human EP2 receptor antagonist. *Biochem Pharmacol,* 50**,** 1731-3.

XIAO, C. Y., YUHKI, K., HARA, A., FUJINO, T., KURIYAMA, S., YAMADA, T., TAKAYAMA, K., TAKAHATA, O., KARIBE, H., TANIGUCHI, T., NARUMIYA, S. & USHIKUBI, F. (2004) Prostaglandin E2 protects the heart from ischemia-reperfusion injury via its receptor subtype EP4. *Circulation,* 109**,** 2462-8.

XIONG, M., GONG, J., LIU, Y., XIANG, R. & TAN, X. (2012) Loss of vitamin D receptor in chronic kidney disease: a potential mechanism linking inflammation to epithelial-to-mesenchymal transition. *Am J Physiol Renal Physiol,* epub.

YAO, C., SAKATA, D., ESAKI, Y., LI, Y., MATSUOKA, T., KUROIWA, K., SUGIMOTO, Y. & NARUMIYA, S. (2009) Prostaglandin E2-EP4 signaling promotes immune inflammation through Th1 cell differentiation and Th17 cell expansion. *Nat Med,* 15**,** 633-40.

YLOSTALO, J. H., BARTOSH, T. J., COBLE, K. & PROCKOP, D. J. (2012) Human Mesenchymal Stem/Stromal Cells (hMSCs) Cultured as Spheroids are Self-activated to Produce Prostaglandin E2 (PGE2) that Directs Stimulated Macrophages into an Anti-inflammatory Phenotype. *Stem Cells,* 30**,** 2283-2296.

YSEBAERT, D. K., DE GREEF, K. E., DE BEUF, A., VAN ROMPAY, A. R., VERCAUTEREN, S., PERSY, V. P. & DE BROE, M. E. (2004) T cells as mediators in renal ischemia/reperfusion injury. *Kidney Int,* 66**,** 491-6.

ZAPPIA, E., CASAZZA, S., PEDEMONTE, E., BENVENUTO, F., BONANNI, I., GERDONI, E., GIUNTI, D., CERAVOLO, A., CAZZANTI, F., FRASSONI, F., MANCARDI, G. & UCCELLI, A. (2005) Mesenchymal stem cells ameliorate experimental autoimmune encephalomyelitis inducing T-cell anergy. *Blood,* 106**,** 1755-61.

ZHANG, Q. Z., SU, W. R., SHI, S. H., WILDER-SMITH, P., XIANG, A. P., WONG, A., NGUYEN, A. L., KWON, C. W. & LE, A. D. (2010a) Human gingiva-derived mesenchymal stem cells elicit polarization of m2 macrophages and enhance cutaneous wound healing. *Stem Cells,* 28**,** 1856-68.

ZHANG, X., REN, X., LI, G., JIAO, C., ZHANG, L., ZHAO, S., WANG, J., HAN, Z. C. & LI, X. (2011) Mesenchymal stem cells ameliorate experimental autoimmune uveoretinitis by comprehensive modulation of systemic autoimmunity. *Invest Ophthalmol Vis Sci,* 52**,** 3143-52.

ZHANG, Y., KONG, J., DEB, D. K., CHANG, A. & LI, Y. C. (2010b) Vitamin D receptor attenuates renal fibrosis by suppressing the renin-angiotensin system. *J Am Soc Nephrol,* 21**,** 966-73.

ZHAO, W., WANG, Y., WANG, D., SUN, B., WANG, G., WANG, J., KONG, Q., WANG, Q., PENG, H., JIN, L. & LI, H. (2008) TGF-beta expression by allogeneic bone marrow stromal cells ameliorates diabetes in NOD mice through modulating the distribution of CD4+ T cell subsets. *Cell Immunol,* 253**,** 23-30.

ZHOU, B., YUAN, J., ZHOU, Y., GHAWJI JR, M., DENG, Y.-P., LEE, A. J., LEE, A. J., NAIR, U., KANG, A. H., BRAND, D. D. & YOO, T. J. (2011) Administering human adipose-derived mesenchymal stem cells to prevent and treat experimental arthritis. *Clinical Immunology,* 141**,** 328-337.

ZHOU, H., GUO, M., BIAN, C., SUN, Z., YANG, Z., ZENG, Y., AI, H. & ZHAO, R. C. (2010) Efficacy of bone marrow-derived mesenchymal stem cells in the treatment of sclerodermatous chronic graft-versus-host disease: clinical report. *Biol Blood Marrow Transplant,* 16**,** 403-12.